FACTORS AND MECHANISMS GOVERNING CtIP REGULATION IN DNA DOUBLE STRAND BREAK REPAIR

DISSERTATION

ZUR

ERLANGUNG DER NATURWISSENSCHAFTLICHEN DOKTORWÜRDE

(DR. SC. NAT.)

VORGELEGT DER

MATHEMATISCH-NATURWISSENSCHAFTLICHEN FAKULTÄT

DER

UNIVERSITÄT ZÜRICH

VON

MARTIN STEGER

AUS

ITALIEN

PROMOTIONSKOMITEE:

PROF. DR. ALESSANDRO A. SARTORI (VORSITZ UND LEITUNG DER DISSERTATION)

PROF. DR. JOSEF JIRICNY

PD DR. MANUEL STUCKI

PROF. DR. GIANNINO DEL SAL

ZÜRICH, 2012

ZUSAMMENFASSUNG

DNS Doppelstrangbrüche (DSB) sind gefährliche Schäden des Erbguts und können entweder durch Replikationsstress oder durch die Behandlung mit DNS-schädigenden Mitteln entstehen. Neben dem Zelltod können DSB auch Chromosomentranslokationen verursachen, die ihrerseits die Zelltransformation begünstigen. Translokationen zählt man daher zu den Merkmalen der Krebsentstehung. Trotzdem ist die gezielte Bildung von DSB für bestimmte physiologische Prozesse wie die Meiose oder die Differenzierung von Zellen des Immunsystems essentiell. Deswegen ist eine präzise Kontrolle der DSB Signalisierung und damit der Reparatur notwendig um die Stabilität des Genoms zu garantieren. Zwei verschiedene Formen der DSB Reparatur können unterschieden werden: nichthomologes Endjoining (NHEJ) und homologe Rekombination (HR). Die DNS Reparatur durch NHEJ benötigt keine homologen Partnersequenzen und funktioniert deshalb während des gesamten Zellzyklus. HR wird durch 5'-3' DNS Endresektion initialisiert, das zur Formation von einzelsträngiger DNA (ssDNA) führt. Im Gegensatz zu NHEJ ist für die HR das Vorhandensein von homologen, doppelsträngigen DNA-Abschnitten, vorzugsweise des Schwesterchromatids, eine Voraussetzung. Deshalb ist HR auf die S-und G2 Zellzyklusphasen beschränkt. Um jedoch die Integrität des Genoms zu erhalten muss das Gleichgewicht zwischen HR und NHEJ während dieser Phasen fein reguliert werden. Die DNS Endresektion ist dabei ein kritischer Schritt, der die Wahl zwischen den miteinander kompetitierenden DSB Reparaturwegen beeinflusst.

Im ersten Teil meiner Dissertation haben wir in menschlichen Zellen den Prozess der DNS Endresektion auf molekularer Ebene untersucht. Wir zeigen, dass Exonuklease 1 (Exo1) in Abhängigkeit von CtIP (CtBP-interacting protein) zu DSB rekrutiert wird. Weiterhin beobachten wir, dass CtIP mit Exo1 interagiert und *in vitro* dessen Aktivität hemmt. Interessanterweise konnten wir auch feststellen, dass Zellen, in denen beide Faktoren fehlen, eine höhere Resistenz gegenüber Replikations-assozierten DSB aufweisen als solche, die lediglich CtIP-defizient sind. Dies ist jedoch mit einer erhöhten Anzahl von Chromosomentranslokation verbunden, die durch unerwünschtes NHEJ hervorgerufen wurden. Basierend auf unseren Daten schlagen wir ein Modell vor, in dem CtIP und Exo1

kollabierten Replikationsgabeln verhindern und somit eine fehlerfreie Reparatur durch HR garantieren. Auf diese Weise tragen beide Faktoren zur Stabilität des Genoms bei.

Der zweite Teil meiner Studie konzentrierte sich darauf, die Rolle der CtIP-Phosphorylierungen für die Regulation der DSB-Reparatur zu untersuchen. Dabei konnten wir zwei neue Phophorylierungsstellen innerhalb des CtIP-Proteins identifizieren und zeigen, dass diese für die Interaktion mit der Peptidil-prolyl cis/trans Isomerase PIN1 von entscheidender Bedeutung sind. Darüber hinaus zeigen wir, dass die Interaktion zwischen den beiden Faktoren nach DNS-Schäden verstärkt stattfindet. Dies bedeuted, dass eine spezifische Funktion der Isomerisierung von CtIP für die Reparatur von DSB notwendig ist. Dementsprechend finden wir, dass Zellen die eine Mutation der CtIP-Sequenz tragen, welche die PIN1-CtIP Interaktion verhindert, eine erhöhte Hyperphosphorylierung und Rekrutierung von RPA2 zu DSB aufweisen. Beides indiziert eine erhöhte DNS Endresektion. Weiterhin beobachten wir, dass die von PIN1 induzierte Isomerisierung von CtIP vor allem nach DNS Schäden zu einer niedrigeren CtIP-Proteinstabilität führt, was indirekt der Endresektion entgegenwirkt. Dementsprechend weisen PIN1-defiziente Zellen einen erhöhten Anteil an HR und damit verbunden ein niedrigeres Level von NHEJ auf. Auf der anderen Seite ist in PIN1-überexprimierenden Zellen die HR beeinträchtigt. Zusammengefasst schlagen wir eine Phosphorylierungs-abhängige Isomerisierung von Proteinen, die das Gleichgewicht der DSB Reparatur beeinflusst, als neuen Mechanismus der Entscheidung zwischen konkurrierenden DSB Reparaturmechanismen vor.

Die Studien der vorliegende Dissertation zeigen zusammengefasst, dass die Kontrolle der DNS Endresektion essentiell ist um die Stabilität des Genomes zu erhalten.

SUMMARY

DNA double-strand breaks (DSBs) are highly cytotoxic lesions, which can arise either during replicative stress or from exposure to DNA damaging agents. In addition to cell death, DSBs can cause chromosomal rearrangements, which can trigger the transformation of a normal cell into a cancerous cell and are therefore a hallmark of cancer. However, DSBs are required to generate diversity during physiological processes such as meiosis or the establishment of the immune repertoire. Thus, a precise regulation of DSB signaling and repair is necessary for the maintenance of genomic stability. Two major pathways have evolved for the repair of DSBs: non-homologous end joining (NHEJ) and homologous recombination (HR). NHEJ does not require a homologous partner DNA sequence and can therefore religate DSBs throughout the cell cycle. In contrast, HR is initiated by the resection of DSBs to create single-stranded DNA (ssDNA) and requires sequence homology with an intact partner, preferentially the sister chromatid, thus restricting repair to S and G2 phases of the cell cycle. During these stages, cells must regulate a fine balance between NHEJ and HR in order to maintain genome stability and DNA end resection is considered to be the critical event driving the choice between the two competing DSB repair pathways.

In the first part of my PhD study, we have investigated the process of DNA end resection at the molecular level in human cells. We find that Exonuclease 1 (Exo1) is recruited to DSBs in a CtIP (CtBP-interacting protein)-dependent manner. We also show that CtIP interacts with Exo1 and that CtIP restrains Exo1 activity *in vitro*. Interestingly, cells lacking both factors display increased resistance to replication-associated DSBs compared to CtIP-deficient cells. However, this is accompanied with an increase in chromosome rearrangements indicative of an aberrant increase in NHEJ. Based on our data we hypothesized that CtIP and Exo1 act in concert to block NHEJ at broken replication forks and to promote error-free repair by HR, thus maintaining genomic stability.

My second project aimed at defining the role of CtIP phosphorylation in the regulation of DSB repair. During the course of this study, we have identified two novel CtIP

phosphorylation sites and demonstrate that these sites prime the association with the peptidyl-prolyl *cis*/*trans* isomerase PIN1. We show that the interaction is increased after DNA damage implicating a specific function of CtIP isomerisation required for DSB repair. Accordingly, we find that cells expressing a CtIP mutant unable to interact with PIN1 display an increase in DSB-induced RPA2 hyperphosphorylation and RPA2 recruitment to DSBs, both events tightly linked to DNA end resection. We also provide evidence that PIN1-mediated isomerisation leads to a decrease in CtIP stability, particularly after DNA damage, thereby counteracting the initiation of DNA end resection. Consequently, cells depleted for PIN1 display increased HR but decreased NHEJ, while HR is significantly impaired in cells overexpressing PIN1. In summary, our data implicate phosphorylation-dependent isomerisation as a novel mechanism controlling DSB repair pathway choice and establish PIN1 as a novel key factor in the cellular response to genotoxic insults.
Collectively, work described in this thesis highlight the importance of controlling DNA end resection in the maintenance of genome stability.

TABLE OF CONTENTS

ABBREVIATIONS

53BP1	p53-binding protein 1
AD	Alzheimer's disease
APFL	apraxin and polynucleotide kinase-like factor
AT	ataxia telangiectasia
ATM	ataxia telangiectasia mutated
ATR	ataxia telangiectasia mutated and Rad3 related
BER	base excision repair
bp	base pair
BRCA 1/2	breast cancer susceptibility gene 1/2
CHK 1/2	checkpoint kinase 1/2
CDKs	cyclin-dependent kinases
Cdc	cell division cycle
CIN	chromosomal instability
CPT	camptothecin
CSR	class switch recombination
CtBP	carboxy-terminal binding protein
CtIP	CtBP-interacting protein
DDR	DNA damage response
DAPK	death associated protein kinase
DNA-PK	DNA-dependent protein kinase
DNA-PKcs	DNA-PK catalytic subunit
DSG	daughter strand gap
ssDNA	single-stranded DNA
dsDNA	double-stranded DNA
DSB	double-strand break
EMSA	electrophoretic-mobility shift assay
ERKs	extracellular signal-regulated kinases
Exo 1	exonuclease 1
FA	fanconi anaemia
GFP	green fluorescent protein
GSK 3	glycogen synthase kinase-3
HIPKs	homeodomain-interacting protein kinases
HJ	holliday junction
dHJ	double HJ
HR	homologous recombinaton
ICLs	interstrand crosslinks
IR	ionizing radiation
JNKs	c-Jun-N-terminal kinases
Lig IV	DNA ligase IV
MDC1	mediator of DNA damage checkpoint 1
MEFs	mouse embryonic fibroblasts

MMR	mismatch repair
MMEJ	microhomology-mediated end joining
Mre11	meiotic recombination 11 homolog 1
MRN	Mre11-Rad50-Nbs1
MS	mass spectrometry
MSI	microsatellite instability
Nbs	Nijmegen breakage syndrome
NER	nucleotide excision repair
NHEJ	nonhomologous end joining
alt-NHEJ	alternative NHEJ
c-NHEJ	classical NHEJ
NMR	nuclear magnetic resonance
PARP	Poly(ADP-ribose) polymerase
PFGE	pulsed field gel electrophoresis
PIKK	phosphatidylinositol 3-kinase-like protein kinase
PLA	proximity ligation assay
PNK	polynucleotide kinase
PPIase	peptidyl-prolyl cis/trans isomerase
PTMs	post-translational modifications
pRb	retinoblastoma protein
Sae2	sporulation in absence of spo eleven
SAPKs	stress-activated kinases
SDSA	synthesis dependent strand annealing
SMC	structural maintenance of chromosomes
Spo11	Sporulation-specific protein 11
SSA	single-strand annealing
SSBR	single-strand break repair
TLS	translesion synthesis
XLF	XRCC4-like factor
XRCC4	X-ray repair cross-complementing protein 4

1. INTRODUCTION

1.1 Genome stability, DNA damage response and cancer

All organisms transmit their genetic information encoded by the DNA to their offspring faithfully across generations. It is therefore crucial to maintain the genetic code free of errors that could potentially lead to mutations, cell death or cell transformation and cancer development in multicellular organisms. It is estimated that the DNA encounters up to 10^5 lesions per cell per day[1]. These lesions can arise either through environmental sources of damage or by damage generated spontaneously during DNA metabolism. For instance, toxic byproducts formed by various enzymes during cell metabolism (e.g. free radicals, such as reactive oxygen and nitrogen species) can have harmful effects on DNA molecules. Likewise, elements in the environment such as UV-light, X-rays and an immense number of chemical compounds including those used for cancer therapy continuously threaten the DNA integrity[2,3]. When bases in the DNA get chemically modified and mutations arise due to faulty repair or replication across the lesion, these changes get fixed into the genome and are thus propagated to descendant cells. A dangerous consequence of mutations is the improper activation of oncogenes and/or the inactivation of tumor-suppressor genes, which in turn can trigger cellular transformation to malignancy[4]. On the other hand, alterations in the DNA fuel evolution, the fundamental process of biological diversity. DNA repair reactions that restore the structure and functionality of the damaged DNA provide therefore a delicate balance between evolution and development of disease[5]. To promote repair of the damaged DNA, cells have evolved an elaborate apparatus consisting of a complex network of specialized repair pathways, each focusing on a specific type of lesion (Figure 1)[6]. For instance, mispaired DNA bases are corrected by the mismatch repair (MMR) system and small chemical modifications of DNA (e.g. oxidated bases) by base excision repair (BER)[7,8]. Similarly, single-strand breaks (SSBs) are repaired by single-strand break repair (SSBR) and double-strand breaks (DSBs) by either homologous recombination (HR) or non-

homologous end joining (NHEJ)[9,10]. Lesions such as pyrimidine dimers or intra-strand crosslinks are repaired via the nucleotide excision repair (NER) machinery and inter-strand crosslinks (ICLs) via a combination of pathways, using part of the HR machinery, translesion synthesis (TLS) and NER in conjunction with more than 13 Fanconi's anemia proteins[11,12].

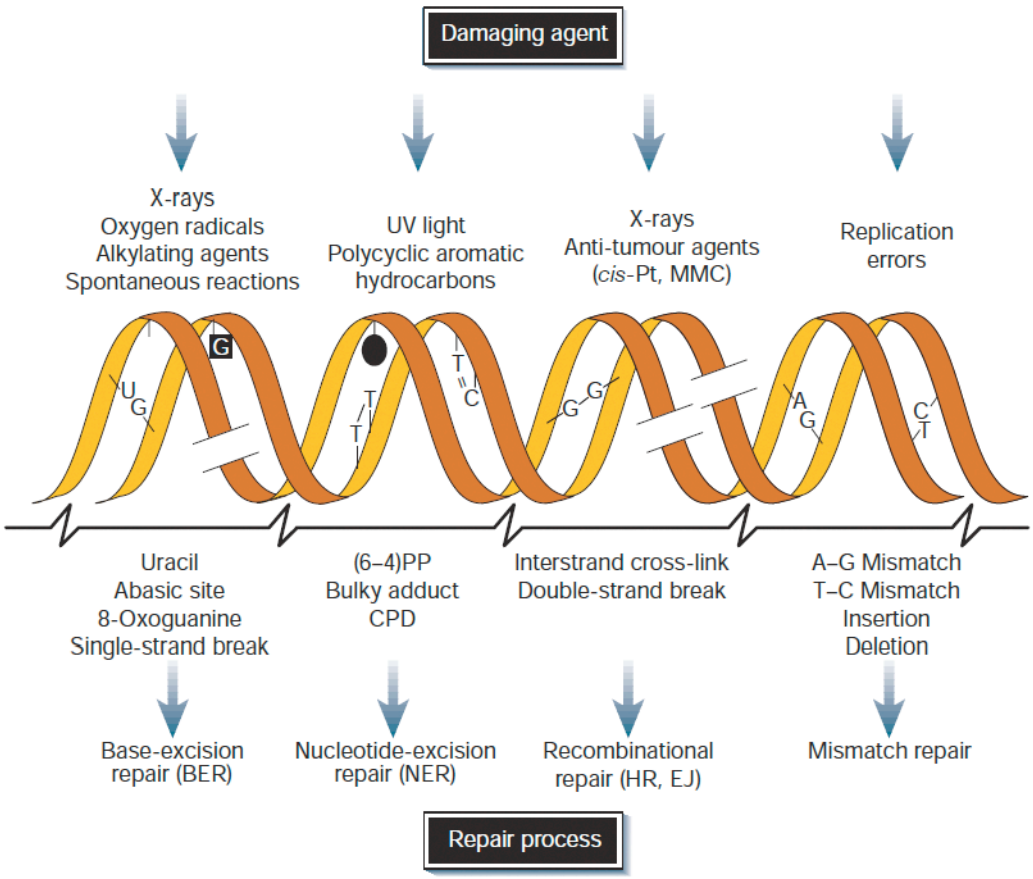

Figure 1: DNA damage and DNA repair mechanisms. Various DNA damaging agents (top) induce a broad variety of lesions (middle), which are removed by specialized DNA repair pathways (bottom). Abbreviations: *cis*-Pt and MMC, cisplatin and mitomycin C, respectively (both DNA-crosslinking agents); (6–4)PP and CPD, 6–4 photoproduct and cyclobutane pyrimidine dimer, respectively (both induced by UV light); BER and NER, base and nucleotide-excision repair, respectively; HR, homologous recombination; EJ, end joining. Adapted from [13].

To ensure proper activation and regulation of each repair pathway, eukaryotic cells possess an intricate system in which sensors of DNA damage, signal transmitters, and effectors are coupled to replication, transcription, and chromatin remodeling. This network consisting of processes recognizing DNA lesions, signaling their presence and promoting their repair is collectively known as the DNA damage response (DDR). The DDR can be described as a complex signal transduction pathway that is primarily mediated by proteins of the phosphatidylinositol 3-kinase-like protein kinase (PIKK) family - ATM, ATR and DNA-PK. Although different DNA lesions are addressed by specialized repair systems, their signaling occurs by a common general program (Figure 2).

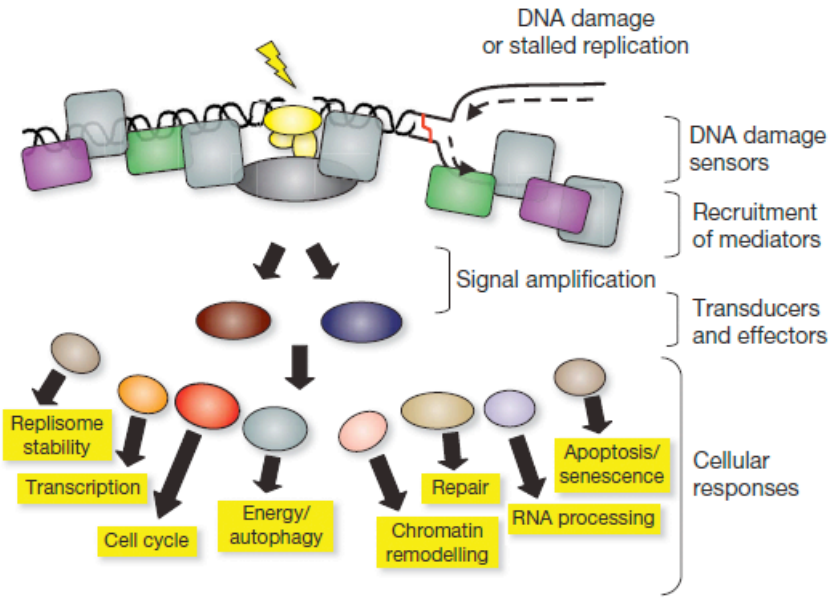

Figure 2. The DNA damage response (DDR). Specialized DNA damage sensors (e.g. MRN, RPA, PARP) recognize the presence of a lesion in the DNA. Through the recruitment of mediator proteins (e.g. BRCA1, 53BP1) the presence of the lesion is signaled and, with the help of accessory signal transducing factors (e.g. ATM, ATR), the response amplified. Effector proteins (e.g. Chk1, Chk2) evoke a cellular response, which include cell cycle arrest, activation of a broad transcriptional program, DNA repair and, in case the damage is too severe, apoptosis. Adapted from [14].

ATM and DNA-PK are activated by DSBs, while the activation of ATR is triggered by RPA-coated single-stranded DNA (ssDNA) arising from replicative stress or the resection of DSBs[6,15]. In contrast to ATM and ATR, which phosphorylate a multitude of targets, the action of DNA-PK is restricted to a small subset of proteins mostly involved in NHEJ. Besides the PIKKs, poly(ADP-ribose) polymerases (PARPs, mainly PARP1 and PARP2) also have a crucial role in mediating the cellular response to DNA damage[16]. Upon binding to DNA breaks, PARPs promote the formation of poly(ADP-ribose) chains on proteins (e.g. histones) to facilitate the recruitment of DDR factors to damaged chromatin.

Once DNA damage has been sensed by specialized factors (e.g. MRN or RPA) required for the full activation of ATM and ATR, effector proteins are activated (e.g. CHK1 and CHK2) with the help of additional mediator proteins (e.g. MDC1, 53BP1 BRCA1)[6]. Consequently, the DNA damage-induced signaling cascade triggers cell cycle checkpoint activation, in order to allow time for repair and, thus, avoiding genome replication and cell division in the presence of DNA lesions. In parallel, the DDR coordinates the action of DNA repair pathways by post-translational modifications (PTMs) such as phosphorylation, acetylation, sumoylation, and ubiquitylation[17]. Upon completion of repair, the DDR is inactivated and normal cell cycle progression is resumed. Alternatively, if the damage is too severe, chronic DNA damage signaling triggers apoptosis or cellular senescence[18]. These latter functions are absolutely critical in order to avoid propagation of mutations and aneuploidy to daughter cells. Thus, terminal cellular differentiation (i.e. senescence) and programmed cell death are considered to be anti-tumorigenic[19]. In summary, DNA damage can trigger a highly conserved, anti-cancer survival response that suppresses metabolism and growth and boosts defenses that maintain the integrity of the cell (Figure 2).

A major hallmark of all cancer cells is genomic instability, which mainly results from damaged DNA[20]. Thus, acquired or inherited defects in the DDR commonly predispose to cancer and favour tumor cell survival and proliferation at the expense of enhanced mutation rates and genomic instability. At least two different forms of genomic instability exist and all of them contribute to carcinogenesis. Chromosome instability (CIN) is

characterized by a high rate of changes in chromosome structure (e.g. translocations) and/or chromosome number. CIN was reported for individuals with germline mutations in DSB repair genes (e.g. BRCA1, BRCA2, PALB2, Nbs1, BLM) and in FA genes (e.g. FANCC and FANCD2). Consequently, mutations in these genes predispose to cancer, in particular to breast cancer and different types of hematopoietic malignancies[21-23].

Microsatellite instability (MSI), on the other hand, is characterized by the expansion or contraction of the number of nucleotide repeats present in microsatellite sequences and is observed in patients harbouring defects in MMR, predominantly in the MLH1 gene[7].

The identification of mutations in DNA repair genes in hereditary cancers provides strong support for the mutator hypothesis, which states that genomic instability is present in precancerous lesions and drives tumor development by increasing the spontaneous mutation rate[24]. The genomic instability observed in precancerous lesions of hereditary cancers are due to mutations in so called caretaker genes; that is, genes that primarily function in genome stability maintenance[25]. In fact, in hereditary cancers, germline mutations targeting DNA repair genes are present in every cell of the body and a single event represented by the loss of the remaining wild type allele can drive genomic instability and tumor development.

In sporadic (non-hereditary) cancers, however, mutations in caretaker genes are rare. In fact, analysis of DNA sequences of 100 cell cycle checkpoint and DNA repair genes in early passage human colon cancer cell lines identified very few mutations[26]. Thus, unlike in hereditary cancers, the molecular basis of genomic instability in sporadic cancers cannot be justified by the mutator hypothesis. Instead, the oncogene-induced DNA replication stress model provides a valid explanation for tumorigenesis in non-hereditary cancers. According to this model, constitutive activation of proto-oncogenes and/or inactivation of oncosuppressors elicit a growth- and, associated with this, a replication-rate increase, which ultimately leads to the activation of the DDR[19]. Indeed, the DDR is commonly activated in early neoplastic lesions and is thought to protect against malignancy[27,28]. For instance, both apoptotic and senescent cells can be found in precancerous lesions coinciding with elevated levels of activated DDR proteins[27]. Therefore, the DDR is

considered to act as an anti-cancer barrier in early neoplasia. However, constitutive activation of the DDR bears a certain danger, namely an increased chance of mutagenesis arising from faulty attempts to repair the damaged DNA. Indeed, there is evidence to suggest that mutations driven by the combination of oncogene-induced replication stress and activated DNA repair account for the transition from precancerous lesion to cancer[29]. Taken together, the concept of DDR as an anti-cancer barrier described above helps to explain the high frequency of DDR defects in human cancers (Figure 3).

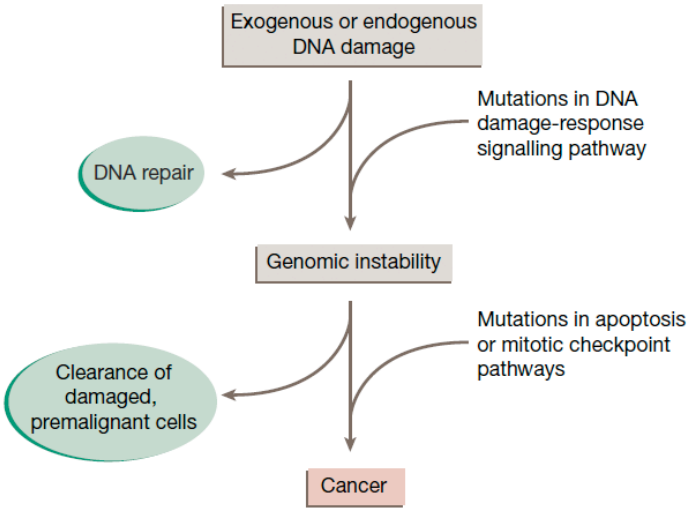

Figure 3. Contribution of proteins involved in the DDR to carcinogenesis. If DNA damage occurring due to activated oncogenes or exogenous sources is repaired efficiently, the likelihood of tumor formation is low. If cells harbour mutations in DNA repair genes, genomic instability occurs. Now, if the same cells possess an intact DNA damage-signaling network (i.e. DDR) and manage to arrest or apoptose they will be eliminated. However, mutations in apoptotic and checkpoint pathways can permit continuous growth of these cells enhancing the chance of malignant transformation. Adapted from [29].

As mentioned, germline mutations in DSB repair genes can predispose to CIN and a variety of cancers. In the next section, I will outline in detail how DSBs can arise and how cells deal with them, with a special focus on the two main DSB repair pathways, HR and NHEJ.

1.2 DNA double-strand break (DSB) repair

DSBs are generated when the two complementary strands of the DNA double helix are broken simultaneously. In metazoans, a single DSB can trigger cell death if left unrepaired and can also be a major source for genomic instability. DSBs represent the most dangerous DNA lesion and, thus, not surprisingly, four independent DSB repair pathways have been identified: homologous recombination (HR), two mechanistically completely different forms of end joining - classical and alternative non-homologous end joining (c-NHEJ and alt-NHEJ, sometimes referred to as microhomology-mediated end-joining (MMEJ)), and single-strand annealing (SSA). The most important determinant for DSB repair pathway choice is the extent of DNA end processing. Whereas c-NHEJ does not require resection of the break, alt-NHEJ as well as SSA and HR depend on the generation of ssDNA tracts as repair intermediate. DSB processing is limited for MMEJ (5-25 nt) and more extensive for HR and SSA[30].

1.2.1 Endogenous and exogenous sources of DSBs

DSBs can arise from both endogenous and exogenous sources. Exogenous sources include ionizing radiation (IR) such as X-rays or γ-rays as well as chemical agents such as DNA topoisomerase I and II poisons (e.g. camptothecin, etoposide and their derivatives) and radio-mimetic drugs (e.g. bleomycin and neocarzinostatin)[31,32]. DSBs can also be caused during DNA replication when a DNA polymerase encounters a DNA single-strand break. Furthermore, stalled replication forks can be converted into DSBs. Despite representing a threat to genomic integrity, DSBs are deliberately created in certain situations. The best characterized example of this in higher eukaryotes is the pathway of V(D)J-recombination, which occurs in developing B- and T-lymphocytes to provide the basis for the antigen-binding diversity of the immunoglobulin and T-cell receptor proteins[33,34]. In this tightly regulated process the site-specific nucleases RAG1 and RAG2 induce DSBs at defined loci and DSB repair proteins repair the lesion to complete the formation of a

mature antigen receptor gene. Other examples of controlled DSB formation are the processes of meiotic recombination and class switch recombination (CSR)[35,36].

1.2.2 Non-homologous end joining (NHEJ)

NHEJ represents the major pathway for the repair of DSBs in human cells[37]. This is mainly because NHEJ, in contrast to HR, can operate throughout the entire cell cycle[38]. In simple words, NHEJ can directly re-ligate DSBs without any major processing of the DNA ends. However, DSBs induced by IR and radio-mimetic compounds often contain non-ligatable, chemically modified nucleotides that have to be "cleaned-up" before ligation of two juxtaposed DSB ends can occur. This can lead to loss of nucleotides from either side of the break, making NHEJ potentially error-prone. Arising DSBs are bound within seconds and independently of accessory factors by the Ku70-Ku80 heterodimer (Ku), which recruits the catalytic subunit of DNA-PK (DNA-PKcs)[39,40]. Ku possesses a DNA-binding core that is able to associate with dsDNA ends with very high affinity *in vitro*[41]. Moreover, Ku assists in tethering broken DNA ends and is responsible for the recruitment of several downstream NHEJ factors to the DSB[42-47].

DNA-PKcs, as mentioned previously, is a huge protein kinase of the PIKK family consisting of more than 4000 residues. The Ku heterodimer in complex with DNA-PKcs and DNA is referred to as DNA-PK holoenzyme. *In vitro*, DNA-PKcs possesses a weak serine/threonine kinase activity which is greatly enhanced by the presence of Ku and dsDNA ends in the reaction[48]. DNA-PKcs contains two autophosphorylation clusters (known as ABCDE and PQR cluster) that play a critical role in stabilizing DNA ends and preventing DNA end resection through a series of autophosphorylation events[49]. Autophosphorylation on the ABCDE cluster results in destabilization of the interaction between DNA ends and DNA-PK facilitating the access of subsequent NHEJ factors such as Artemis to the DSB[49]. In contrast, phosphorylation of the PQR cluster seems to limit DNA end processing. Importantly, ATM can also phosphorylate the ABCDE cluster of DNA-PKcs and promotes in this way HR in case NHEJ fails[50]. Although DNA-PKcs was shown to phosphorylate multiple NHEJ factors *in vitro*, there is little evidence that these phosphorylation sites are

required for functional NHEJ *in vivo*[51-53]. Thus, it rather seems that the key substrate for DNA-PK-mediated phosphorylation is DNA-PKcs itself. Nevertheless, the importance of DNA-PK-mediated phosphorylation is underscored by the fact that cells either lacking DNA-PKcs or expressing an ABCDE cluster-mutant are highly radiosensitive and display defects in V(D)J-recombination[54,55].

Once the DNA ends have been detected and secured, the next step in NHEJ involves the processing of chemically modified DNA termini to remove non-ligatable end groups and other lesions. As mentioned previously, IR often generates highly complex DSBs and specialized enzymes are needed to remove modified nucleotides, fill in gaps and remove secondary structures[56,57]. A major factor involved in DNA overhang processing and hairpin opening during NHEJ (and VDJ recombination) is the structure-specific DNA endonuclease Artemis[58,59]. Artemis interacts with DNA-PKcs and is highly phosphorylated at the C-terminus but the function of these events still remains elusive[58,60-62]. Two other factors involved in the processing of DSB ends prior to the re-ligation step are the X-family DNA polymerases μ and λ required for gap-filling. However, cells lacking both DNA polymerases are only mildly sensitive to IR, indicating that they are needed for the repair of only a small subset of lesions[63]. PNK (polynucleotide kinase) and APLF (aprataxin and PNK-like factor) are other factors involved in the processing of dsDNA ends[64,65]. PNK has both 3'-DNA phosphatase and 5'-DNA kinase activities and is thus ideally suited to generate ligatable DNA ends. Notably, deficiency in PNK leads to elevated radiation sensitivity and defects in DSB repair[66].

The final step of the NHEJ repair pathway is the re-ligation of the DSB ends. This reaction is catalyzed by DNA ligase IV (Lig IV), which exists in a highly flexible complex together with XRCC4 and XLF (XRCC4-like factor). Lig IV has the unusual property of being able to ligate one DNA strand at the time, perhaps allowing processing enzymes to act simultaneously on end groups on the opposite strands[67]. Similar to Lig IV, cells lacking either XRCC4 or XLF are deficient in NHEJ and V(D)J recombination[68,69].

In conclusion, NHEJ is the major pathway responsible for the repair of IR-induced DSBs in mammalian cells and does not require extensive DNA end processing.

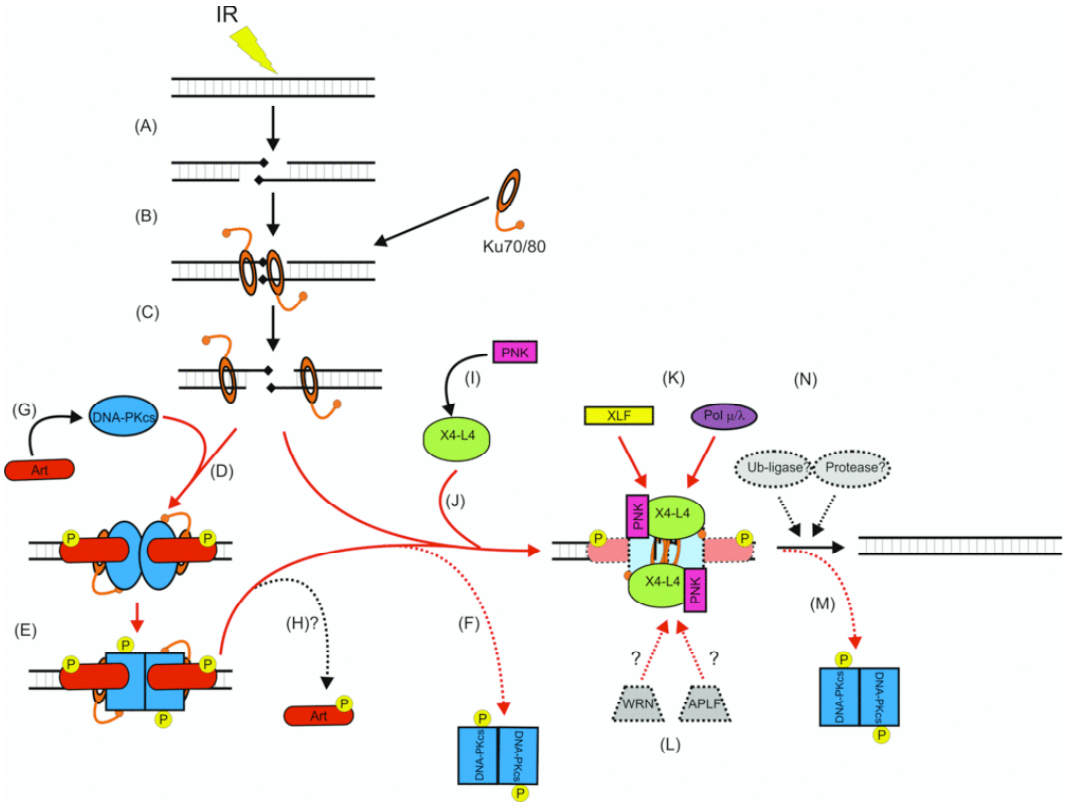

Figure 4. A model for NHEJ. Chemically modified DNA ends (**A**, indicated by ◆) arising from IR-induced lesions are recognized by the Ku70/Ku80 heterodimer (**B**), which by translocating inwards, recruits DNA-PKcs (**C-D**). The assembly of the holoenzyme consisting of DNA-PKcs and DNA bound Ku triggers DNA-PKcs autophosphorylation (**E**). Artemis is recruited by DNA-PKcs (**G**) but when or if Artemis is released from the DNA-PKcs complex is not clear (**H**). (**I**) PNK interacts with XRCC4-Lig IV (X4-L4) and is recruited to the break with it (**J**). Whether DNA-PKcs is released prior to X4-L4 recruitment (**F**) or stays till repair is completed (**M**) is not known. The polymerases μ and λ as well as XLF interact with both X4-L4 and Ku suggesting that they are recruited together with X4-L4 (**K**). Other enzymes such as WRN and APFL may also be recruited by interacting with X4-L4 (**L**). Once the ends are processed (if needed), the X4-L4 complex seals the break by ligation. It is not clear how the different factors are released from the break but it is possible that ubiquitylation and/or proteolysis are important for this step (**N**). Reactions requiring DNA-bound Ku are shown in red. Adapted from [70].

1.2.3 Alternative non-homologous end joining (alt-NHEJ)

The existence of a Ku- and Lig IV-independent end-joining mechanism involved in the repair of DSBs, has been recently elucidated and termed alt-NHEJ. The hallmarks of this highly mutagenic pathway are deletions at repair junctions and the frequent use of distal microhomologies. It is important to note that although microhomology-mediated end joining (MMEJ) is the major form of alt-NHEJ, other types of error free end joining also occur at low frequency in the absence of XRCC4 or Lig IV[71]. Alt-NHEJ was long thought to function only as backup to the classical NHEJ pathway (c-NHEJ), implicating that under normal physiological conditions this pathway would not be active. However, several lines of evidences demonstrated that MMEJ operates as a DSB repair pathway in normal cells, the most important example being represented by the process of class switch recombination CSR[36,72]. The foremost distinguishing property of MMEJ is the use of 5–25 base pair (bp) microhomologous sequences during the alignment of broken ends before joining, thereby resulting in deletions flanking the original break. In order to expose microhomologies in close proximity of a DSB, nucleolytic DNA end resection is required[73]. Studies in yeast implicated several factors in this processing step including the orthologues of human Mre11, Exo1 and CtIP[73,74]. Although DNA end resection activities normally require the action of CDK1/2 and are in principle restricted to S/G2 phases of the cell cycle, limited end resection needed for MMEJ can also occur in G1 cells[75,76]. In addition, DNA helicase activity might provide an alternative mechanism to expose microhomologous sequences located adjacent to the initial DSBs. The exposed microhomology resulting from DNA unwinding or resection is subsequently annealed and the remaining, non-complementary 3' flaps removed before ligation. The yeast structure-specific endonuclease Rad1-Rad10 complex and its mammalian counterpart XPF-ERCC1 have a key role in removing 3' overhangs during MMEJ[77]. Inserted nucleotides are often observed at the MMEJ junctions indicating that error-prone polymerases might act in the processing steps before repair is completed. Finally, in mammalian cells, alt-NHEJ is completed through the action of DNA ligase I or DNA ligase III, which act in concert with XRCC1[78,79]. Furthermore, there is increasing evidence indicating that c-NHEJ counteracts

MMEJ. In fact, MMEJ activity was shown to increase in Ku- or DNA-PKcs-deficient cells[80]. Nevertheless, MMEJ has certainly an important role in mammalian DSB repair since it can operate even in the context of intact c-NHEJ and HR repair.

1.2.4 Homology-directed repair (HDR)

Two distinct mechanisms of HDR have been identified in mammalian cells, HR and single-strand annealing (SSA). Whereas HR is considered to be error free, SSA is highly mutagenic.

HR can be defined as a DSB-repair reaction in which DNA strands between two homologous DNA molecules get exchanged. In somatic cells, the repair of DSBs through HR is restricted to the S/G2 phases of the cell cycle in which a template for HDR becomes available, the replicated sister chromatid. As mentioned earlier, DSBs can be deliberately induced in the genome by special enzymes (e.g. Spo11, a DNA topoisomerase) during the process of meiotic recombination. This controlled process, being part of the sexual reproduction cycle, is crucial to guarantee genomic diversity in eukaryotes by creating new allele combinations[81]. DSBs created in somatic cells through collapse of stalled replication forks are also repaired by HR[82]. Moreover, replication may be reinitiated downstream of a certain lesion, leaving a lesion-containing ssDNA stretch that cannot be filled-in due to the presence of the blocking lesion. These so-called daughter strand gaps (DSGs) can be repaired via HR[83].

Immediately after a DSB is created, cells must ensure that the broken ends, as well as the sister chromatids are held in close proximity. Members of the structural maintenance of chromosomes (SMC) family of proteins, Rad50 (part of the Mre11/Rad50/Nbs1-MRN complex) and the cohesion complex, account for this step in mammalian cells[84-86]. Next, 3' ssDNA-overhangs, crucial intermediates for the repair by HR, are created. This process, known as 5'-3' DNA end resection is aided by a variety of nucleases, helicases and accessory proteins and is conserved in all kingdoms of life. While in prokaryotes, such as *E. coli*, the nuclease and helicase functions are provided by the RecBCD complex, more proteins appear to influence this step in eukaryotes[87]. In yeast, the MRX

(Mre11/Rad50/Xrs2) complex, in cooperation with Sae2, is important for initiating DNA resection[88]. More extensive ssDNA is subsequently created through the action of the Sgs1 helicase in cooperation with the Dna2 and Exo1 endo- and exonucleases, respectively[89]. In higher eukaryotes, the MRN complex, assisted by the function of CtIP, orchestrates initial resection of DNA ends[90,91]. Subsequently, and in perfect analogy to the situation in yeast, the DNA helicase BLM together with Exo1 and Dna2 are responsible for the second, more processive step of DNA end resection[92,93]. Noteworthy, in contrast to the proposed unidirectional (5'-3') DNA end resection model, a recent study in yeast showed that Mre11 accounts for the resection of up to 300 nucleotides of a DSB in direction 3'-5'[94]. From the results obtained in this study, a new model of bidirectional resection was proposed in which Mre11 accounts for 3'-5' DNA processing activity from a distal region of the break whereas Exo1 in conjunction with Sgs1-Dna2 for DNA resection in the opposing 5'-3' direction.

The MRN complex has multiple functions during the initial processing of the DNA ends and is recruited to DSBs without the need of accessory factors. As outlined above, Rad50 holds the broken DNA ends nearby and Mre11 nuclease activity accounts for the initial DNA end processing action. The third unit of the complex, Nbs1, has been reported to physically recruit ATM to DSBs via a conserved region in the C-terminus[95]. Recruitment of ATM to the sites of break is required for the phosphorylation of the C-terminal tail of histone H2AX (γ-H2AX), which in turn serves a docking platform for MDC1[96]. MDC1 is able to bind both phosphorylated Nbs1 and H2AX and promotes in this way gradual spreading of γ-H2AX that provides the basis for a productive assembly of most (if not all) of the DNA damage-modified chromatin components[97-99].

DNA end resection ultimately leads to the formation of 3' ssDNA-overhangs of several kilobases (kb) in length and the recruitment of RPA to those ssDNA tracts. RPA is a heterotrimeric complex consisting of three subunits (RPA1, RPA2, RPA3) able to stabilize ssDNA formed during DNA replication and repair[100]. RPA coated ssDNA arising from 5'-3' end resection has an essential role in ATR-mediated checkpoint activation. It recruits the ATR/ATRIP complex through direct interaction with ATRIP and facilitates the loading of

the PCNA-related Rad9-Hus1-Rad1 (911) complex which in turn helps to recruit the ATR-kinase stimulating protein TopBP1[15,101,102]. At this point, ATR is fully proficient in phosphorylating downstream targets and to activate cell cycle checkpoints.

If the resected break contains highly repetitive DNA sequences such as mini- or microsatellites, SSA can act as an alternative to HR. For this purpose, the DNA repeats are aligned in a Rad52-dependent manner before the created 3' flaps are removed by XPF/ERCC1[103].

To complete the repair via HR, the ssDNA bound RPA is replaced by multimers of the recombinase Rad51 in order to form a recombinogenic nucleoprotein filament. In mammalian cells, a mediator complex composed of BRCA1/BARD1, BRCA2 (FANCD1) and PALB2 (FANCN) promotes this exchange reaction[104,105]. The Rad51 nucleoprotein filament then captures duplex DNA and searches for homology. Following synapsis, the invading strand sets up a D-loop intermediate, whereby the 3'-end primes DNA synthesis using the duplex DNA as template. It is not fully clear which polymerase(s) is/are responsible for D-loop extension *in vivo*, but Pol η can perform this function *in vitro*[106]. If the second DNA end of the break is captured by the D-loop a Holliday junction (HJ) is formed and depending on the symmetry of its resolution, yielding either crossover or non-crossover products. During somatic HR mostly non-crossover products are formed and this observation is explained by the synthesis-dependent strand annealing model (SDSA)[107,108]. In SDSA, the invading strand is first extended and pairs subsequently with the processed end of the second strand. In contrast, DSB repair by HR as it was originally proposed, involves capturing of the second end of the break leading to the formation of a double HJ (dHJ). Although SDSA is now considered to be the major mechanism during somatic HR, dHJs might be formed in special scenarios, for example during daughter strand gap (DSG) repair. Furthermore, dHJs can undergo branch migration generating increasing or decreasing length of heteroduplex DNA. The ATPase Rad54 can promote this branch migration in either 3'-5' or 5'-3' direction in human cells[109]. Also RecQ helicase family members (BLM, WRN and RecQ5) can promote branch migration although they show anti-recombinogenic characteristics *in vitro*[110]. HJs can be resolved in different ways. For

instance, BLM together with Topoisomerase IIIα promotes HJ dissolution to form non-crossover products[111]. In contrast, several endonucleases including Mus81-Eme1, Gen1 and SLX1/4 have been involved in the resolution of HJs to give rise to crossover and non-crossover products[112-114]. An overview of the different HDR pathways is illustrated in Figure 5.

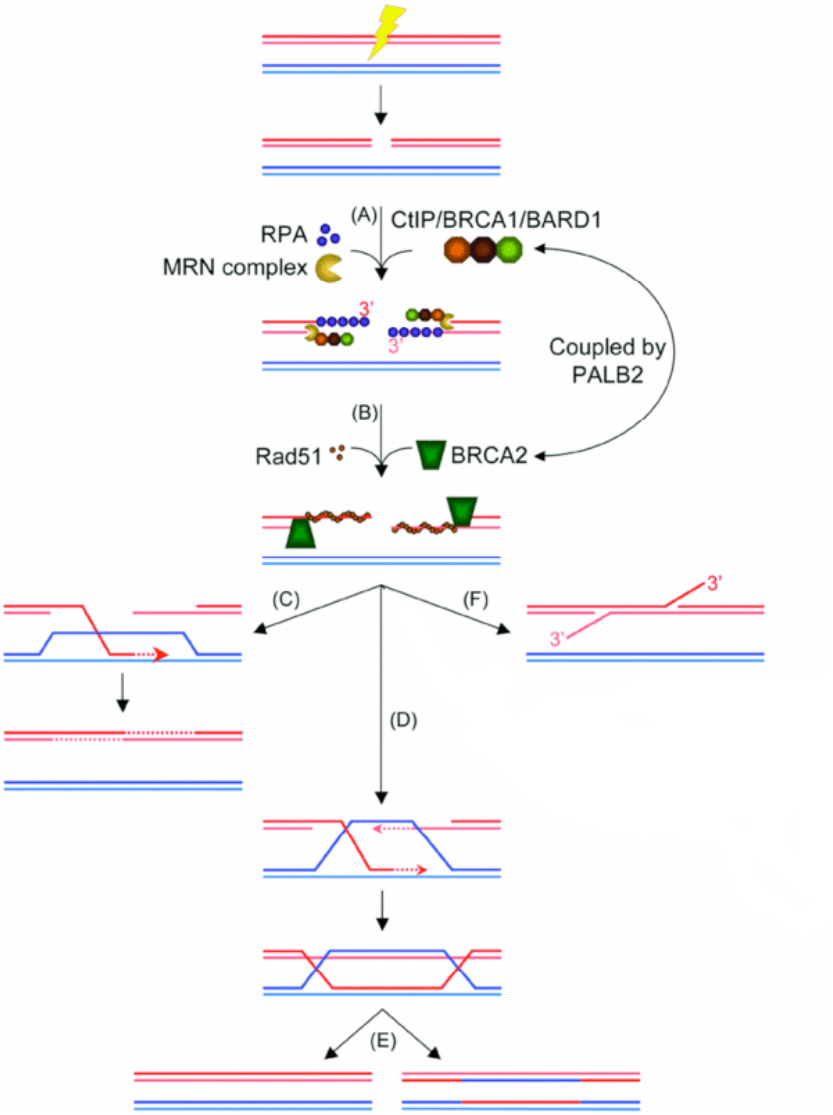

Figure 5. Homology-directed repair in eukaryotic cells. Upon induction of a DSB, the MRN complex binds to DNA ends and participates in end processing together with CtIP (A). RPA binds to ssDNA and is replaced by Rad51 with the help of BRCA1/BARD1 together with BRCA2 and PALB2 (B). Rad51 nucleoprotein filaments promote homology search and strand invasion. (C) The SDSA model predicts that a migrating D-loop fails to capture the second end and, following extension, the invading strand is displaced and anneals with the resected second end. (D) The DSB repair model predicts that the second DNA end is captured by annealing to the extended D-loop, forming a dHJ. (E) This intermediate can be resolved to form either non-crossover or crossover products. (F) SSA repair pathway: the annealing of two complementary sequences next to a DSB leads to deletion of the intervening sequences. Adapted and modified from [30].

1.2.5 Regulation of DSB repair

The repair of DSBs is a highly regulated process influenced by a broad variety of factors. In this section I will give an overview of the multiple layers of regulation of DSB repair.

The first layer of regulation is given by the extent of resected DNA, which depends on the structure of the DNA ends and the phase of the cell cycle in which the DSB occurs. For instance, the two protein complexes MRN and Ku can recognize DNA ends and both of them initiate a different mode of repair. Importantly, cells lacking NHEJ genes reveal a DSB repair bias in favour of HR, suggesting that the two repair pathways compete between each other[115]. Moreover, MRN has the ability to displace Ku from DNA ends in order to facilitate HDR[116,117]. However, if the MRN complex was constantly available to bind DSBs and displace Ku from DNA ends, NHEJ would never get a chance to repair DSBs. The MRN complex is assembled and abundant throughout the cell cycle suggesting that the binding of MRN to DNA ends is insufficient to promote HR at the expense of NHEJ. Thus, the decision-making process of DNA end resection initiation has further requirements. For example, protein levels of the MRN-interacting protein CtIP are regulated in a cell cycle specific manner, with low levels during G1 and much higher amounts during S and G2 phases[118]. It is thus tempting to speculate that expression levels and/or stability of proteins involved in DNA resection are determining factors controlling the switch between NHEJ and HR. Reversible PTMs, mainly protein phosphorylation, are another prominent way to activate/deactivate the function of a protein, thereby providing an elegant on/off switch. CDKs are obvious candidates to mediate this, as the increase in CDK activity that triggers G1-S transition coincides with the switch between NHEJ and HR. In fact, analysis in yeast showed that G1-arrested cells fail to efficiently resect broken DNA ends, to load RPA and Rad51 and to activate Mec1/ATR[76]. Moreover, the inefficient resection activity correlated with low Cdc28/CDK1 activity and inhibition of CDK1 activity in G2 prevented extensive resection and checkpoint activation. Important targets phosphorylated by CDKs and regulating the balance between NHEJ and HR are Mre11 and CtIP. Indeed, CDK-mediated phosphorylation of these factors regulates the balance between HR and NHEJ in yeast[76,119]. The fact that CtIP, the human orthologue of

Sae2, is phosphorylated by CDKs at several sites and that these sites are important for DNA end resection suggests that similar CDK-mediated control mechanisms of resection operate in higher eukaryotes[120,121]. RPA2 and Dna2 are two additional factors of the resection machinery phosphorylated by CDKs[122]. Whereas CDK-mediated phosphorylation of Dna2 regulates nuclear entry of the protein in S phase, the role of RPA2 phosphorylation has yet to be determined[123]. The yeast protein Rad9 and its human orthologue 53BP1 promote NHEJ and undergo multiple CDK-mediated phosphorylations, but it is unknown whether these negatively affect resection[124,125]. The fact that depletion of Rad9 can partially bypass the CDK requirement for resection, suggests that the identified CDK phosphorylation sites could indeed be important for allowing DNA end processing[126].

Although phosphorylation has long been known to play a major role in regulating proteins at sites of DNA damage, other important PTMs, particularly sumoylation and ubiquitylation are also critically engaged in such responses. Several E3 ubiquitin ligases and ubiquitin binding proteins are involved, directly or indirectly, in the repair of DSBs[127]. An intriguing factor of this group of enzymes postulated to play an important role in the competition between HR and NHEJ is BRCA1. Whereas mice expressing an alternatively spliced variant of BRCA1 lacking exon 11 (i.e. inactive protein) harbour increased chromosomal instability and tumorigenesis, the ubiquitin ligase activity does not seem to be essential for these functions[128]. Intriguingly, the chromosomal abnormalities and defects in HR associated with loss of BRCA1 are rescued by 53BP1 depletion[129,130]. It is therefore evident that 53BP1 and BRCA1 are key factors in driving DSB repair pathway choice - BRCA1 favouring HR, 53BP1 favouring NHEJ. A critical function of BRCA1 might be the ubiquitylation and subsequent removal of 53BP1 and other factors from DNA breaks allowing resection to proceed. Interestingly, in certain situations (e.g. in G1) the retention of Ku and 53BP1 at DNA breaks is dependent on DSB-induced ubiquitilations[131,132].

Besides BRCA1, several other ubiquitin and SUMO E3 ligases including RNF8, RNF168, RNF4, HERC2, PIAS1 and PIAS4 have been involved in the repair of DSBs with a major role

in modifying the chromatin structure and creating a platform for recruitment of repair proteins[133-137].

In summary, the commitment to DSB end resection is influenced by several factors including cell cycle stage, availability of repair proteins and PTMs. Once repair has been channeled into HR, several modifications on proteins are needed in order to stepwise control successful repair and optimize genome stability.

1.2.6 DSB repair and cancer

As outlined earlier, inherited mutations in BRCA1 and BRCA2 predispose these individuals to breast and ovarian cancer. Similarly, inactivating mutations in genes of the FA pathway are linked to the development of several forms of cancer, predominantly leukemia. Moreover, mutations in the ATM gene cause the syndrome Ataxia-telangiectasia (AT) developmental defects, immunodeficiency and radiosensitivity[138]. Approximately one third of AT patients develop malignancies, predominantly lymphomas and leukemias of T cell origin[139]. Similarly, Nijmegen breakage syndrome (Nbs) is caused by hypomorphic mutations in the NBN gene and the phenotype of Nbs patients greatly overlaps with that of AT patients[140,141]. Furthermore, the steady state levels of NHEJ proteins are frequently altered in cancer cell lines and repaired DSBs in these cells lines are characterized by large deletions around the break-point junction and joining of DNA ends at regions of DNA sequence microhomology[142,143]. These observations indicate that alt-NHEJ is frequently upregulated in cancer cells to compensate for the loss of c-NHEJ. For this purpose, alt-NHEJ factors might be a potential therapeutic target to inhibit repair of DSBs in these cancers.

Cancer therapy has until recently been focused on creating cytotoxicity through DNA damaging agents, such as IR, camptothecins, mitomycin C, cisplatin and temozolomide[144]. Although differences in the DDR between normal and cancer cells presumably precondition the ability of these agents to preferentially kill cancer cells, their use is often limited by normal tissue toxicity. Since abnormalities in the DDR of cancer cells are becoming more clearly defined, there is growing interest in the development of small

molecules that will selectively target the abnormal DNA repair in cancer cells with the prospect that these compounds either alone or in combination with DNA damaging agents will effectively kill cancer cells, while minimizing damage to normal cells. Since ATM is one of the apical kinases initiating the DDR and is responsible for the repair of DSBs, the use of ATM inhibitor in combination with DSB-inducing agents should very effectively kill cancer cells. In fact, the ATM inhibitor KU-55933 greatly sensitizes tumor cells to IR as well as to the chemotherapeutic agents camptothecin and etoposide[145]. A potential problem with using ATM inhibitors in the clinics is that they may also sensitize normal tissues to DNA damage. Furthermore, it would be of advantage to know the genetic background of a given patient. Treatment with ATM inhibitor might be of particular interest for the treatment of hereditary cancers harbouring a specific mutation in a DNA repair gene. For example it was shown that KU-55933 selectively kills cancer cells harbouring mutations in FA genes[146].

The recombinase Rad51 is frequently overexpressed in human cancers and is associated with poor prognosis[147]. The overexpression frequently correlates with resistance to chemotherapeutic agents indicating that Rad51 is a potential target for antitumor drugs.

PARP1 is another prominent target for cancer therapy. PARP binds to SSBs and DSBs and synthesizes poly(ADP-ribose) chains that are attached on PARP itself and on other DNA repair factors[148,149]. By inhibiting PARP activity, SSBs cannot be successfully repaired and are converted into DSBs during DNA replication. It is estimated that in normal human cells approximately 1% of SSBs are converted to approximately 50 DSBs per cell per cell cycle[150]. Since HR would normally repair these replication-associated DSBs, cells that are defective in HR are hypersensitive to PARP inhibitors. Based on this rationale, potent and specific inhibitors of PARP were developed as therapeutic agents for inherited forms of breast and ovarian cancer as the PARP inhibitor should be cytotoxic for BRCA1- or BRCA2-deficient tumors but not affect normal tissues with a functional BRCA1 or BRCA2 allele, respectively[151,152]. As predicted, PARP inhibition sensitizes BRCA1 and BRCA2 defective tumors, both in tumor models *in vivo* and in the clinic[153,154]. The genetic interaction between BRCA1 (or BRCA2) and PARP can be described as synthetic lethal. Synthetic

lethality between two genes occurs where individual loss of either gene is compatible with life, but simultaneous loss of both genes results in cell death. Thus, the BRCA-PARP interaction provides the first successful example of a synthetic lethal approach that has entered the clinic[155].

Another valid approach for targeting a DNA repair enzyme is to inhibit DNA-PK. It is upregulated in some human cancers indicating that it might contribute to tumor survival. Moreover, specific inhibition of DNA-PK enhanced cytotoxicity of both IR and chemotherapeutic agents in cultured tumor cells as well as in mouse xenograft models[156].

A broad variety of DNA damage inducing drugs is used in clinics to treat tumors but often the genetic background of the patient is neglected. An understanding of the DDR in these patients would help to design novel therapeutic strategies involving the use of inhibitors of the DNA damage response alone or in combination with DNA damaging agents that selectively target the altered DNA damage response in cancer cells.

In the next section I will describe in detail the function of an important player in the repair of DSBs, namely CtIP. Since recent evidences indicate that this molecule possesses enzymatic activity, it might represent a potential future drug target to suppress DNA repair in fast replicating cells.

1.3 CtIP

1.3.1 Role in tumorigenesis and DSB repair

CtIP (also known as RBBP8) is a nuclear phosphoprotein of 897 amino acids and was first characterized in 1998 as a cofactor for the transcriptional repressor CtBP and acquired thereby its name, CtBP-interacting protein[157]. The interaction is mediated through a PLDLS motif on the N-terminus of CtIP, a sequence motif highly conserved among viral and cellular CtBP binding proteins[158]. In a yeast two-hybrid screen, CtIP was found to interact with pRb/p105 and the Rb family members p107 and p130 through a characteristic Rb binding motif (LECEE)[159]. It was proposed that CtIP might exert its activity in transcriptional repression by interaction with Rb and recruiting CtBP. CtIP was also identified in search for proteins interacting with the C-terminal BRCT domain of the tumor suppressor BRCA1. Importantly, tumor specific mutation in the BRCT-domain of BRCA1 abrogated its interaction with CtIP, highlighting the functional relevance of CtIP interaction for the tumor suppressive functions of BRCA1[160]. In addition, CtIP was also found to interact with Ikaros family members, Krüppel-like zinc finger transcription factors that regulate early hemo-lymphopoiesis and differentiation[161]. Ikaros proteins act as tumor suppressors in lymphoid tissues and deregulation of gene expression is observed in human leukemias[162]. The fact that CtIP associates with at least three established tumor suppressor proteins together with the observation that haploid deficiency of CtIP contributes to lymphomagenesis in $CtIP^{-/+}$ heterozygotic mice suggests that CtIP is a tumor suppressor[163]. $CtIP^{-/-}$ mice die during early embryogenesis (E4.0), the blastocysts fail to enter S-phase, accumulate in G1 and exhibit increased cell death. Notably, the CtIP-dependent arrest at the G1/S transition is lost in pRb-deficient mouse fibroblasts and human cancer cell lines lacking pRb, demonstrating an essential role in promoting S-phase entry of CtIP and suggesting a genetic interaction between the two factors.

The fact that CtIP on one hand represses transcription through pRb and CtBP and on the other hand counteracts the pRb-mediated G1 arrest of cells seems to be contradictory. Since pRb plays diverse, but concerted roles in G1/S transition, CtIP may serve as an adaptor to recruit different factors, which counter pRb action in this context. Moreover, the precise mode of transcriptional activation or repression mediated by CtIP relies probably on the specific context of a given promoter, and it is probably influenced by cell cycle stage, microenviromental condition or the developmental status. In support of the idea of transcriptional activation, CtIP activates a subset of E2F-responsive promoters in the G1 phase of the cell cycle, amongst them its own and the one of cyclin D1. This releases pRb-mediated transcriptional repression and promotes G1/S progression[164].

CtIP is ubiquitously expressed at low levels in different cell types with the highest amount in testis and thymus[159,165]. Apart from the specific sequences important for pRb and CtBP binding, CtIP contains two coiled domains. One such domain on the N-terminus is responsible for homodimerization and crucial for proper function during the repair of DNA DSBs[166,167]. CtIP only shares sequence similarity with homologous proteins in higher eukaryotes (including mouse, chicken and frog) apart from a short region in the C-terminus, which seems to be conserved in different yeast species and to be crucial for CtIP protein turnover and DNA repair functions[90,168]. Moreover, CtIP was reported to contain a PCNA binding box and a DNA binding motif (Figure 6)[169,170].

The pattern of CtIP expression is equivalent to the one of BRCA1 and Rad51, two proteins involved in HR. Similar to CtIP, BRCA1 and Rad51 are highly expressed in testis and thymus, tissues in which DSB formation occurs frequently[171,172]. These evidences indicate that CtIP might play a crucial role in the repair of DSBs. In fact, several reports have now established CtIP as a central player in the resection of DSBs, with increasing evidence suggesting that CtIP controls DSB repair pathway choice[90,121,170,173,174]. The protein levels of CtIP are kept low during G1, increase steadily during S and peak in G2[118]. During S and G2 phases, CtIP undergoes CDK-mediated phosphorylation on serine 327 (S327), a priming event needed for BRCA1 interaction and originally reported to be crucial for G2/M checkpoint activation[174]. Subsequent studies on BRCA1-CtIP association revealed

that this event also influences DSB repair pathway choice or, alternatively, is specifically required for the efficient processing of DNA ends that are covalently trapped by DNA topoisomerases[121,175]. Upon DSB induction, at least three different serines in the C-terminus are targeted by ATM. Although these events were initially thought to be required for BRCA1-CtIP dissociation in order to activate BRCA1-mediated transcription of checkpoint sustaining factors, the actual function remains still elusive[170,176,177].

For its resection function, CtIP directly interacts with the MRN complex and the concomitant action of these proteins is crucial for the initiation of DSB repair by HR (Figure 6)[90,178,179]. CtIP promotes 5'-3' DNA end resection of DSBs and helps to form 3'-single-stranded overhangs necessary for homology sequence search. The ssDNA overhangs are then coated by RPA, which in turn triggers ATR/Chk1-mediated checkpoint signaling and subsequent cell cycle arrest[90,170]. Interestingly, since alt-NHEJ also requires ssDNA intermediates, CtIP can participate in this error-prone subtype of DSB repair[121,180].

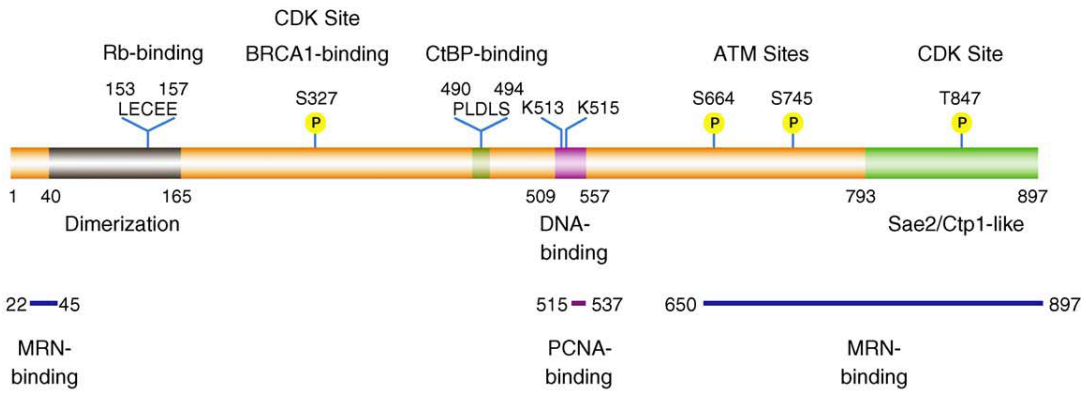

Figure 6. Schematic representation of the CtIP protein, its domains and interaction partners. See text for details. Adapted from [181].

1.3.2 Regulation of CtIP

The function of CtIP in DSB repair is highly regulated to ensure that DNA end resection and HR can only occur in appropriate stages of the cell cycle. The first layer of regulation is given by CtIP protein levels, which are low in G1 and high during S/G2 phases when a template for HDR becomes available[118,121]. Since transcript levels of CtIP do not change throughout the cell cycle, posttranscriptional and/or posttranslational ways of CtIP protein level regulation must exist[118]. A possible candidate responsible for CtIP polyubiquitylation and subsequent proteasomal degradation during G1 is the E3-ubiquitin ligase SIAH1[182]. In addition, CtIP is a CDK target and is phosphorylated on at least two different sites, namely serine 327 (pS327) and threonine 847 (pT847). While pS327 mediates the interaction with BRCA1, pT847 is required for DSB resection and subsequent HR in S and G2 phases[174,183,120].

Conclusively, CtIP is a multivalent adaptor protein at the intersection of cell cycle control, checkpoint signaling and DNA repair. Before and after DNA damage, CtIP receives signals from both CDKs and ATM that regulate its function in DNA damage signaling and repair. Importantly, the engagement of CtIP-dependent DSB resection commits cells irreversibly to repair via HR. For this reason CtIP is considered to be one of the major determinants influencing DSB repair pathway choice.

1.4 PIN1

1.4.1 Structure and function of PIN1

Biological processes are extremely dynamic and complex and need to be choreographed both spatially and temporally. Phosphorylation is a key cellular signaling mechanism to regulate most of the biological processes in a cell including the response to DNA damage[184]. For example, the phosphorylation of many tyrosine residues and some serine/threonine residues acts as a signal to recruit proteins to signaling networks or to place enzymes close to their substrates. Moreover protein phosphorylation can activate or block the catalytic site of enzymes and can promote or inhibit protein degradation. Especially the reversible phosphorylation on certain serine or threonine residues preceding a proline (pS/T-P), a major regulatory phosphorylation motif in cells, represents a key switch for controlling the function of many signaling molecules in various cellular processes. Enzymes responsible for such phosphorylation belong to a large superfamily of proline-directed kinases, which include CDKs, extracellular signal-regulated kinases (ERKs), stress-activated kinases/c-Jun-N-terminal kinases (SAPKs/JNKs), p38 kinases, glycogen synthase kinase-3 (GSK3) and homeodomain-interacting protein kinases (HIPKs). These kinases play a crucial role in diverse cellular processes such as cell growth and stress response as well as human diseases such as cancer and Alzheimer's disease (AD)[185,186]. The unique stereochemistry of proline means that it can adopt two completely different conformational states, namely the *cis* and the *trans* isomers. Prolines in the *cis* conformation occur with a frequency of 5-6% in protein structures[187]. Moreover, a large majority of the observed *cis* peptide bonds occur in surface-accessible bend, coil or turn conformations[188]. Thus, proline residues can typically adopt two distinct conformations in proteins and are usually exposed on the surface of proteins. Due to the relatively large energy barrier, uncatalyzed cis/*trans*-isomerisation of prolines is a very slow process but can be greatly accelerated by peptidyl-prolyl *cis/trans* isomerases (PPIases). Family members of these enzymes include cyclophilins (Cyps) and FK506-binding proteins

(FKBPs). Although they seem to play a crucial role in protein folding, all eight genes encoding PPIases are dispensable for cell growth in budding yeast[189]. Therefore, it was initially thought that all PPIases perform non-essential cellular roles until the discovery of the phosphorylation-specific PPIase PIN1 (protein interacting with NIMA (never in mitosis A)-1)[190]. It is the only PPIase that specifically recognizes and isomerises phosphorylated pS/T-P peptide motifs. PIN1 is a relatively small protein composed of 163 amino acids with a molecular weight of approximately 18 kDa. It contains an N-terminal WW domain that acts as a phosphoprotein-binding module and a C-terminal catalytic isomerase domain that is distinct from other conventional PPIases (Figure 6)[191-193]. The discovery of PIN1 led to the hypothesis of a new signaling mechanism in which *cis/trans* isomerisation acts in a post-phosphorylation-dependent manner to control the fate of the target protein[191,194]. Isomerisation of pS/T-P motifs is especially important because kinases and phosphatases specifically recognize the *cis* or *trans* conformation of the prolyl peptide bond of their substrates and phosphorylation further slows down the spontaneous isomerisation rate of prolines[195,196]. By inducing a *cis/trans* conformational change, PIN1 controls the function of an increasing number of proteins involved in cell cycle regulation and cell growth, response to genotoxic stress, immune response, neuronal differentiation and survival[197]. Moreover, PIN1 itself is tightly regulated and its deregulation can contribute to human diseases including cancer, neurological disorders, and autoimmune and inflammatory diseases[197-201].

PIN1-mediated post-phosphorylation regulation can have profound effects on phosphorylation-dependent signaling by regulating a spectrum of target activities, including protein-protein interaction, enzymatic activity, protein localization, and the most common consequence, protein stability[197]. Notably, phosphorylation on S/T-P motifs constitutes a major regulatory mechanism in controlling ubiquitin-mediated proteolysis and recent evidence indicates that PIN1 is involved in this process[202-204]. PIN1 was in fact shown to regulate the turnover of a number of proteins amongst them cyclin D1, β-catenin, p53 and p27[205-208].

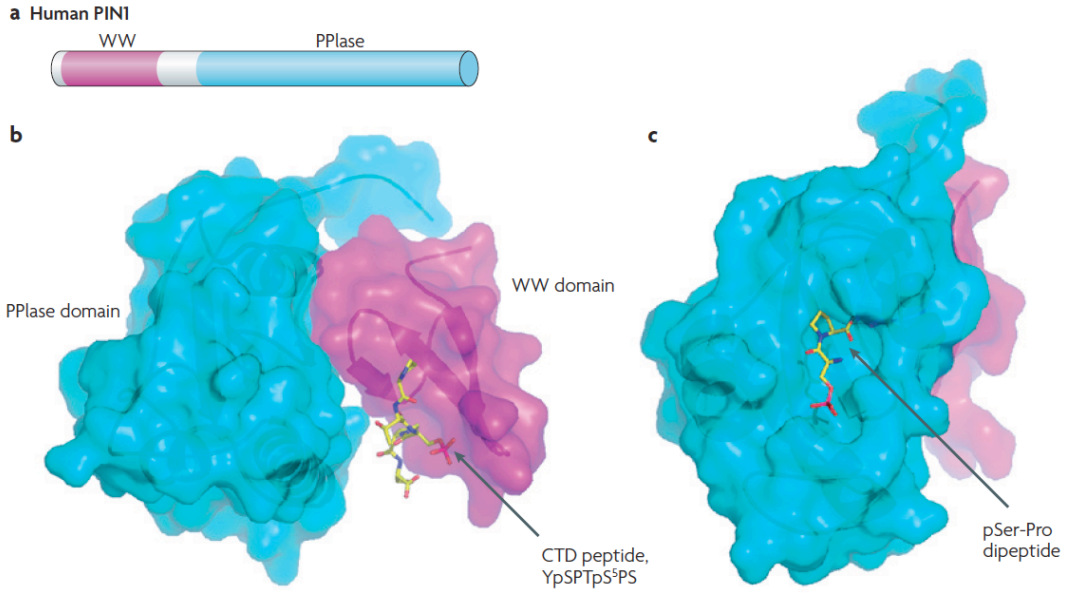

Figure 6: Structure of human PIN1. (a) The domain architecture of PIN1. PIN1 contains an N-terminal WW domain responsible for specific pThr/Ser binding and a C-terminal peptidyl-prolyl cis/trans isomerase (PPIase) domain that catalyses isomerisation of pThr/Ser motifs in the substrate. (b) X-ray structures of PIN1 in complex with a C-terminal domain (CTD) peptide (YpSPTpSPS) in the WW domain. Ser16, Arg17 and Tyr23 in the WW domain are responsible for binding the phosphate of pSer5 (the fifth residue in the peptide) and the aromatic rings of Tyr23 and Trp34 form an aromatic clamp, which accommodates the ring atom of Pro6 (the sixth residue). (c) X−ray structure of PIN1 in complex with a pSer-Pro dipeptide modeled in the PPIase domain. A set of conserved catalytic residues in all PIN1-type PPIases project outward from the barrel structure and define the binding pocket for the proline and the peptide bond that undergoes cis/trans isomerisation. The side chains of Lys63, Arg68 and Arg69 form a basic cluster that sequesters pSer in the substrate. Lys63 is conserved in PIN1- and parvulin-type PPIases and is involved in basic catalysis. In contrast, Arg68 and Arg69 are conserved only in PIN1-type PPIases and are responsible for the unique phosphorylation specificity of PIN1-type PPIases. Adapted from [209].

1.4.2 PIN1 in oncogenic signaling and tumorigenesis

Studies in cells, mice and humans highlight the fact that understanding the role of PIN1 in tumorigenesis is still at an early stage, and remains enigmatic and controversial. Several PIN1-binding proteins have been identified that have roles in oncogenesis, but the actions of PIN1 can either inactivate and/or degrade or activate and/or stabilize these molecules (Figure 7). Several studies support the concept that absence or inhibition of PIN1 would lead to decreased susceptibility to tumor formation. On the other hand, other reports

argue that decreased PIN1 levels would render cells more sensitive to oncogenesis. Results obtained from studies with genetically altered mice suggest that, depending on the genetic modifiers present in a particular genetic background, PIN1 might have a positive or negative role in tumor formation, perhaps in a cell-type-selective manner.

More consistently, a number of studies show that PIN1 is overexpressed in human malignancies including breast, prostate, lung, ovary, cervical and brain tumors and is associated with poor diagnosis, indicating that PIN1 levels might have prognostic value[210-214]. Furthermore, increased PIN1 levels are positively correlated with a higher risk of, and a shorter period to, tumor recurrence following radical prostatectomy in a set of primary prostate cancers[215]. Consistent with its pro-oncogenic role, PIN1 regulates a number of oncogenes and tumor suppressors including Cyclin D1, β-catenin, Akt, NF-κB, p53 and Bcl2[205-207,216-219]. Interestingly, overexpression of PIN1 and its substrates Cyclin D1 and β-catenin is often positively correlated in human cancers[220-223]. Since it is known that PIN1 can regulate the protein levels of both β-catenin and cyclin D1, it appears that PIN1 deregulation results in tumor formation as a consequence of its ability to regulate the levels of these proteins. In fact, protein levels of cyclin D1 are decreased in cells derived from $PIN1^{-/-}$ mice maintained in a mixed genetic background (129/SvJae/C57BL/6)[205]. Moreover, PIN1 can regulate cyclin D1 levels transcriptionally by controlling Jun activity as well as post-translationally by controlling directly its protein stability[201]. Collectively, these results suggest that decreased levels or inhibition of PIN1 might result in decreased cancer susceptibility while overexpression promotes oncogene-mediated tumorigenesis.

In support of this hypothesis, PIN1 is overexpressed in human mammary tumors, and $PIN1^{-/-}$ mice of mixed genetic background fail to undergo pregnancy-induced mammary epithelial expansion[205,224]. HER-2/Neu and Ras oncogenes control the expression of cyclin D1 so it appears logical that PIN1 might contribute to tumor growth induced by these factors[224]. In fact, crossing mice overexpressing Ras or HER-2/Neu with $PIN1^{-/-}$ mice from a mixed genetic background prevents Ras (or HER-2/Neu)-mediated cyclin D1 expression and development of breast cancer. On the other hand, it has been reported that decreased cellular levels of PIN1 lead to a selective growth disadvantage owing to an

owing to an increase in time required for G1/S transition[225,226]. Several studies show that PIN1 negatively regulates c-myc and cyclin E protein levels through a common mechanism, leading to the timely degradation of these proteins by the SCF (Skp-Cullin1-F-box) ubiquitin ligase complex[227,228]. Importantly, the deregulation of cyclin E in cancer correlates with increased genomic instability[229,230]. Accordingly, PIN1$^{-/-}$ mouse embryonic fibroblasts (MEFs) harbour increased levels of both cyclin E and c-myc and show enhanced time-dependent genomic instability compared to wild-type cells[231]. Moreover, since Ras collaborates with both cyclin E as well as c-myc in cell transformation, the absence of PIN1 in MEFs can facilitate Ras-induced tumorigenesis. In contrast to the above-mentioned role of PIN1 in promoting tumorigenesis, these results are in clear favour of a possible protective role of PIN1 in oncogenesis, at least in MEFs derived from an isogenic (C57BL/6) genetic background.

Possible explanations for these apparently discrepant observations are that the conflicting studies were conducted with mice of different genetic backgrounds and in different cell types. Whereas studies suggesting PIN1 might facilitate tumorigenesis were carried out in a mixed genetic background in organ epithelial cells, studies supporting a tumor-suppressor role for PIN1 were carried out in an isogenic B6 background in fibroblasts. The resolution of these remarkable differences will require animals from the two lines of genetically altered mice to be subjected to identical experimental protocols using relevant *in vivo* models of mouse tumorigenesis. Until such data are available, and in spite of the remarkable number of important cell-cycle proteins that PIN1 has been proposed to regulate, the role of PIN1 in cancer will remain enigmatic. Since PIN1 recognizes phosphorylated S/T-P motifs in proteins and these phosphorylation events depend on the activity of proline-directed kinases, there may be hundreds of potential PIN1 targets within any given cell (Figure 7). Therefore, the action of PIN1 may be influenced considerably by the activation or inactivation of various signaling pathways that influence the phosphorylation of proteins on S/T-P motifs.

Besides being an important regulator of many proteins, PIN1 is subjected to post-translational modification itself and is found to by hypophosphorylated in cancer

tissues[201,232]. The protein kinase death-associated protein kinase 1 (DAPK1), a known tumor suppressor, is indeed able to phosphorylate PIN1 in the catalytic domain thereby inhibiting its activity. Thus, PIN1 is an important catalyst for tumorigenesis that acts by switching on or off numerous oncogenes or tumor suppressors, respectively, at several steps at the same time.

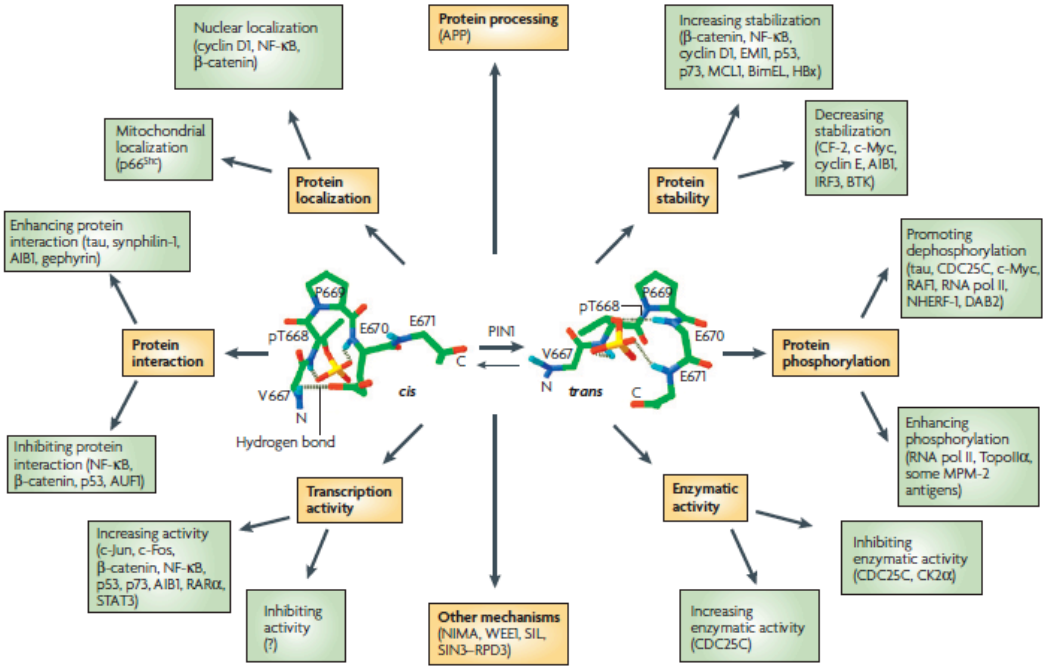

Figure 7. Functional targets of PIN1. PIN1 can regulate phosphorylation dependent protein cis/trans isomerisation of a number of substrates. Such a conformational change has profound effects on the activity of the target protein. PIN1 can enhance or decrease protein stability, alter the phosphorylation status or affect the transcription activity of proteins. Moreover, PIN1 can interfere with protein-protein interactions and with protein localization. Importantly, many of the factors controlled by PIN1 such as cyclin D1, cyclin E or β-catenin play an important role in tumorigenesis. Adapted from [209].

2. AIMS

DSBs are among the most deleterious lesions a cell can encounter. Thus, a thorough understanding of the mechanisms involved in the repair of DSBs is of major interest, particularly in the field of cancer biology. Moreover, many drugs used in the clinics for the treatment of malignant tumors induce the formation of DSBs. Further expanding our knowledge of the regulation of DSB repair pathways and their individual players is therefore the major goal of my PhD thesis.

My first aim was to determine the relative contribution of CtIP and Exo1, two factors involved in DNA end resection, for the repair of DSBs by HR. The second aim of my work was to study the consequences of CtIP phosphorylation on DSB repair.

2.1 Elucidating the collaborative function of CtIP and Exo1 during DNA end resection

Given the rather unclear data on DNA end processing for repair via HR in mammalian cells, we set out to address the collaborative role of CtIP and Exo1 during this step. While data in yeast suggest that the MRX complex together with Sae2 initiate resection and Dna2 and/or Exo1/Sgs1 are responsible for long-range resection, such data were not available for mammalian cells (outlined in section 1.2.4). Although both the helicase BLM as well as the exonuclease Exo1 were described to control long-patch resection in mammalian cells, the interplay between these factors and the initiators of resection (MRN complex and CtIP) were not known.

We therefore used RNA interference strategies to deplete Mre11, CtIP and Exo1 in mammalian cells and assessed the ability to form RPA-coated ssDNA, a hallmark of DNA end resection, on laser induced DSBs. Furthermore, we tested the possibility whether the recruitment of Exo1 to DSBs is dependent on the initial DNA end-trimming activity of either Mre11 and/or CtIP. To address this point, we used laser micro-irradiation of mammalian cells to induce local DSB formation and test the ability of GFP-tagged Exo1 for

recruitment to these sites of damage. These experiments were performed both with fixed cells and in live cell mode.

Since both Exo1 and CtIP play a fundamental role in DNA resection, we also wanted to establish whether the two factors physically interact by co-immunoprecipitation experiments. Moreover, we addressed the possible regulation of Exo1 by CtIP in DNA end resection *in vitro*. We also tested the DNA binding capacity of both Exo1 and CtIP to a defined DNA-substrate by an electrophoretic-mobility shift assay (EMSA). Finally, we investigated the role of both Exo1 and CtIP during HR repair *in vivo* via colony formation assays and metaphase chromosomal analysis.

The results obtained from these experiments were submitted and published in the scientific journal of EMBO reports. The published research paper is illustrated in section 3.1.

2.2 Addressing the role of PIN1 during DSB repair

CtIP is a nuclear protein and becomes hyperphosphorlyated upon induction of DSBs. Moreover, CtIP is phosphorylated at least at two S/T-P sites by proline-directed kinases, most probably CDKs. While pS327 mediates BRCA1 interaction, pT847 is required for DNA end resection. Besides these two well-described phosphorylation sites, CtIP contains another 10 S/T-P motifs, some of them highly conserved among different CtIP homologs. However, given that many of these sites could simultaneously be targeted by several proline-directed kinases, it remains largely unknown how these phosphorylation events are coordinated to regulate CtIP. On top of that, phosphorylation of certain sites may trigger PIN1-catalyzed isomerisation, an important regulatory mechanism for many phosphoproteins involved in cell cycle progression, but so far never been linked to DNA repair.

We therefore aimed at identifying novel CtIP phosphorylation sites and testing whether some of the phosphorylation events are required for PIN1-mediated *cis/trans* isomerisation. To answer these questions we performed two separate mass

spectrometry-based screens. At first we immunoprecipitated endogenous CtIP from human cells and analysed the peptides for the presence of phosphorylated residues. In addition, we performed a GST-PIN1 pull-down assay using human cells and identified many, potentially novel PIN1 substrates involved in the repair on DSBs (e.g. BRCA1, 53BP1 and CtIP).

We next investigated the interaction between CtIP and PIN1 in more details using various complementary approaches including pull-down assays, co-immunoprecipitation, *in situ* proximity ligation assay (PLA) and far-western blot analysis. We also aimed at defining the pS/T-P motifs in CtIP crucial for PIN1 interaction. Moreover, we raised phospho-specific antibodies against two, novel CtIP phosphorylation sites. To test whether PIN1 can indeed isomerise CtIP, we performed nuclear magnetic resonance (NMR) spectroscopy experiments on CtIP phospho-peptides. We further tested whether CtIP mutants deficient in PIN1 interaction are still recruited to sites of DNA damage and able to perform DNA end resection. We also examined the DSB repair kinetics in cells expressing CtIP mutants by PFGE. To study the role of PIN1 itself in the regulation of DSB repair pathway, we used established GFP-based reporter cell lines in which the successful repair of an endonuclease-induced DSB can be monitored by flow cytometry.

The results of these experiments are presented in the form of a scientific manuscript in section 3.2.

3. RESULTS

3.1 DNA end resection by CtIP and exonuclease 1 prevents genomic instability

article published in EMBO Reports, 2010

authors: Wassim Eid*, Martin Steger*, Mahmoud El-Shemerly*, Lorenza P. Ferretti, Javier Peña Diaz, Christiane König, Emanuele Valtorta, Alessandro A. Sartori and Stefano Ferrari (*equal contribution)

contributions: I contributed the figures 1, 3D, S1B and F, S3B-C, S3E-F and S4B. WE, MES, LPF, JPD, CK and EV contributed the other data. AAS and SF wrote the manuscript.

EMBO reports

scientific report

DNA end resection by CtIP and exonuclease 1 prevents genomic instability

Wassim Eid, Martin Steger*, Mahmoud El-Shemerly*†, Lorenza P. Ferretti, Javier Peña-Diaz, Christiane König, Emanuele Valtorta, Alessandro A. Sartori+ & Stefano Ferrari++*

Institute of Molecular Cancer Research, University of Zurich, Zurich, Switzerland

End resection of DNA—which is essential for the repair of DNA double-strand breaks (DSBs) by homologous recombination—relies first on the partnership between MRE11–RAD50–NBS1 (MRN) and CtIP, followed by a processive step involving helicases and exonucleases such as exonuclease 1 (EXO1). In this study, we show that the localization of EXO1 to DSBs depends on both CtIP and MRN. We also establish that CtIP interacts with EXO1 and restrains its exonucleolytic activity *in vitro*. Finally, we show that on exposure to camptothecin, depletion of EXO1 in CtIP-deficient cells increases the frequency of DNA–PK-dependent radial chromosome formation. Thus, our study identifies new functions of CtIP and EXO1 in DNA end resection and provides new information on the regulation of DSB repair pathways, which is a key factor in the maintenance of genome integrity.

Keywords: DNA double-strand break repair; CtIP; exonuclease 1; camptothecin

EMBO *reports* (2010) **11**, 962–968. doi:10.1038/embor.2010.157

INTRODUCTION

DNA double-strand breaks (DSBs) are the most cytotoxic lesions that can be generated by ionizing radiation, certain chemotherapeutic drugs, collapse of stalled DNA replication forks or during physiological processes such as meiotic recombination (Bassing *et al*, 2002; Whitby, 2005). DSBs that are not properly repaired can cause gross chromosomal aberrations that trigger carcinogenesis through activation of oncogenes or inactivation of tumour suppressor genes. Cells use two main mechanisms to repair DSBs: non-homologous end-joining (NHEJ) and homologous recombination (HR; Wyman & Kanaar, 2006; Misteli & Soutoglou, 2009). NHEJ repair takes place throughout the cell cycle, whereas HR is restricted to S- and G2-phases. HR is initiated by 5′–3′ resection of DSBs to produce single-strand DNA (ssDNA) tails that function as a signal for ATR-mediated DNA damage checkpoint activation before the recruitment of recombination proteins (Pardo *et al*, 2009).

Several studies have investigated the molecular mechanisms of DNA end resection in genetically amenable organisms. These have implicated the MRE11–RAD50–NBS1/Xrs2 (MRN/MRX) complex and CtIP/Sae2 in the early stages of DSB processing, followed by the redundant action of BLM/Sgs1 helicase and exonuclease 1 (EXO1) in the generation of long stretches of ssDNA (Mimitou & Symington, 2009). Accordingly, only the simultaneous depletion of BLM and EXO1 resulted in accumulation of partly resected intermediates and hypersensitivity to DSB-inducing agents (Gravel *et al*, 2008; Mimitou & Symington, 2008; Zhu *et al*, 2008). These studies led to a two-step model according to which in human cells the initial 'end-trimming' is carried out by MRN and CtIP, followed by resection by two mechanisms depending on either EXO1 or BLM (Niu *et al*, 2009).

In this study, we show that EXO1 is recruited to laser-induced DSBs in a CtIP-dependent manner and that CtIP interacts with EXO1, thereby retarding processive degradation of DNA by EXO1 *in vitro*. Furthermore, we provide evidence that concomitant depletion of CtIP and EXO1 in camptothecin-treated cells leads to chromosomal rearrangements, probably as a result of illegitimate NHEJ-dependent repair of DSBs.

RESULTS AND DISCUSSION

EXO1 localization to sites of DNA damage

On the basis of the two-step model of DNA end resection, we hypothesized that the recruitment of EXO1 to DSBs was dependent on the initial processing by MRN and CtIP. As endogenous levels of EXO1 are undetectable by direct immunostaining (El-Shemerly *et al*, 2005), we examined EXO1 localization to laser microirradiation-induced DSBs (Bekker-Jensen *et al*, 2006) by using U2OS cells stably expressing green fluorescent protein (GFP)-tagged EXO1 (Gravel *et al*, 2008). Similarly to previous reports, we observed accumulation of EXO1 at sites of DSBs (Bolderson *et al*, 2010; Fig 1A; supplementary Fig S1A,B online). We therefore asked whether depletion of CtIP or the MRN complex (Fig 1B) would affect EXO1 recruitment to DSBs. Both fixed and live-cell imaging showed that depletion of either CtIP or

Institute of Molecular Cancer Research, University of Zurich, Winterthurerstrasse 190, Irchel Campus, Zurich CH-8057, Switzerland
*These authors contributed equally to this work
†Present address: Institute for Clinical and Biomedical Research, Lauchefeld 31, CH-9548 Matzingen, Switzerland
+Corresponding author. Tel: +41 44 635 3473; Fax: +41 44 635 3484; E-mail: sartori@imcr.uzh.ch
++Corresponding author. Tel: +41 44 635 3471; Fax: +41 44 635 3484; E-mail: sferrari@imcr.uzh.ch

Received 26 May 2010; revised 2 September 2010; accepted 13 September 2010; published online 5 November 2010

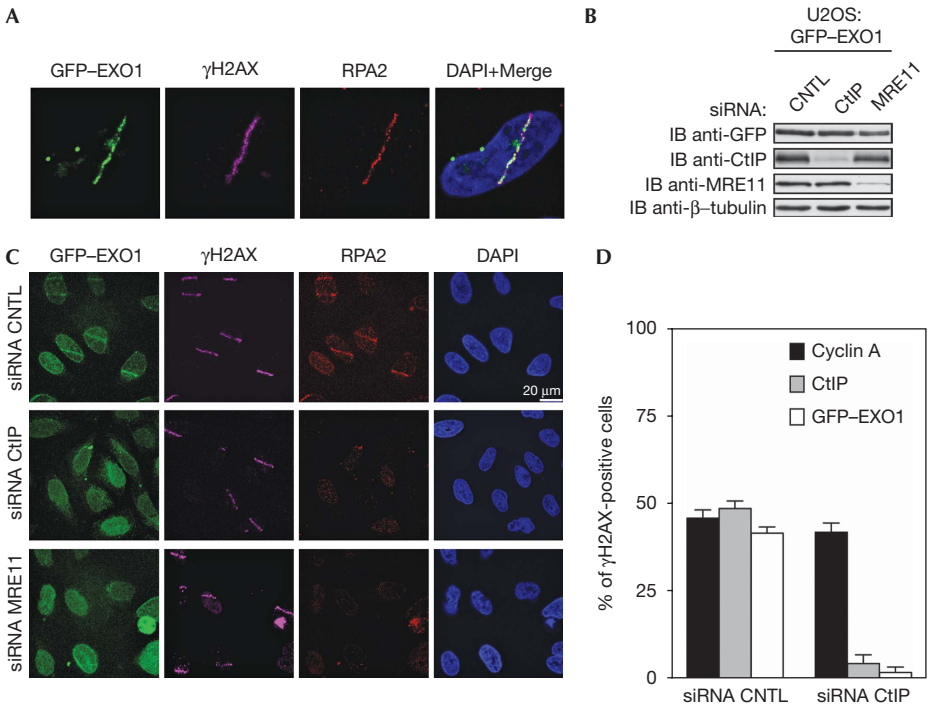

Fig 1 | Exonuclease 1 localization to sites of DNA damage requires both CtIP and MRE11. (**A**) U2OS cells stably expressing GFP–EXO1 were microirradiated and 30 min later fixed, immunostained with γH2AX and RPA2 antibodies, and analysed by fluorescence microscopy. Nuclei were visualized with DAPI. (**B**) GFP–EXO1 cells were transfected with Luciferase- (CNTL), CtIP- or MRE11-specific siRNA oligonucleotides and grown for 72 h. Protein expression was examined by immunoblot (IB) using the indicated antibodies. (**C**) siRNA-transfected GFP–EXO1 cells from (**B**) were microirradiated, fixed and analysed as in (**A**). (**D**) GFP–EXO1 cells treated as in (**A**) were co-immunostained with γH2AX, Cyclin A and CtIP antibodies. γH2AX-positive cells were quantified for EXO1, Cyclin A and CtIP staining. A total of 50 cells per sample were counted in two independent experiments. EXO1, exonuclease 1, GFP, green fluorescent protein; RPA2, replication protein A; siRNA, small interfering RNA.

MRE11 impaired the recruitment of EXO1 and replication protein A (RPA) 2 to DSBs (Fig 1C; supplementary Fig S1B online). Furthermore, in CtIP-depleted cells we did not observe any localization of EXO1 to sites of DSBs, even at late time points (supplementary Fig S1A,B online). In addition, downregulation of BLM did not impair EXO1 recruitment to DSBs (data not shown). Consistent with the S/G2-specific recruitment of CtIP to DSBs (Sartori *et al*, 2007), accumulation of GFP–EXO1 at DSBs was only observed in cyclin A-positive cells and was strictly CtIP-dependent (Fig 1D). Finally, EXO1, but not CtIP, did not localize to sites of laser-induced DSBs in ataxia telangiectasia-like disorder 1 (ATLD1) cells, which are deficient in DSB resection due to a hypomorphic mutation of the *MRE11* gene (Stewart *et al*, 1999; Carson *et al*, 2003; supplementary Fig S1C–E online). This defect was rescued on re-expression of wild-type MRE11 (supplementary Fig S1F online). From these observations, we concluded that the recruitment of EXO1 to DSBs depends on the initial DSB-end trimming carried out by MRN together with CtIP.

CtIP interacts with EXO1 and restrains its activity

Although they are independently recruited to sites of DSB (supplementary Fig S1E online; Lisby *et al*, 2004; Chen *et al*, 2008), CtIP was shown to interact with MRN and stimulate its endonuclease activity *in vitro* (Sartori *et al*, 2007), indicating a functional relationship between these factors during DNA end resection. This prompted us to examine whether EXO1 physically associates with the MRN–CtIP complex. To test this, CtIP or EXO1 was immunoprecipitated from HEK293T whole-cell extracts and the recovered complexes were analysed by immunoblotting. Interestingly, CtIP but not MRE11 was present in anti-EXO1-immunocomplexes both in non-stressed cells and in cells treated with camptothecin (Fig 2A)—a chemotherapeutic agent known to induce DSBs exclusively during DNA replication by trapping DNA topoisomerase 1 cleavage complexes (Pommier, 2006). Although we noticed that EXO1 preferentially interacts with the hyperphosphorylated form of CtIP in damaged cells (Fig 2A, lane 8), we did not observe differences in CtIP–EXO1 interaction on phosphatase treatment of the CtIP–EXO1 immunocomplex (supplementary Fig S2A online). We confirmed the previously reported CtIP–MRE11 interaction, but did not detect EXO1 in anti-CtIP immunocomplexes, probably due to low cellular levels of EXO1 (El-Shemerly *et al*, 2005). Therefore, we immunoprecipitated CtIP from HEK293T cells transiently expressing OMNI-tagged EXO1. Under these conditions, we detected EXO1 in anti-CtIP immunocomplexes, both in the presence and absence of hydroxyurea (supplementary Fig S2B online).

To investigate whether the interaction between CtIP and EXO1 is direct or reliant on bridging factors, we examined CtIP–EXO1 complex formation by using purified, recombinant proteins in an anti-EXO1 immunoprecipitation experiment (Fig 2B). Although a

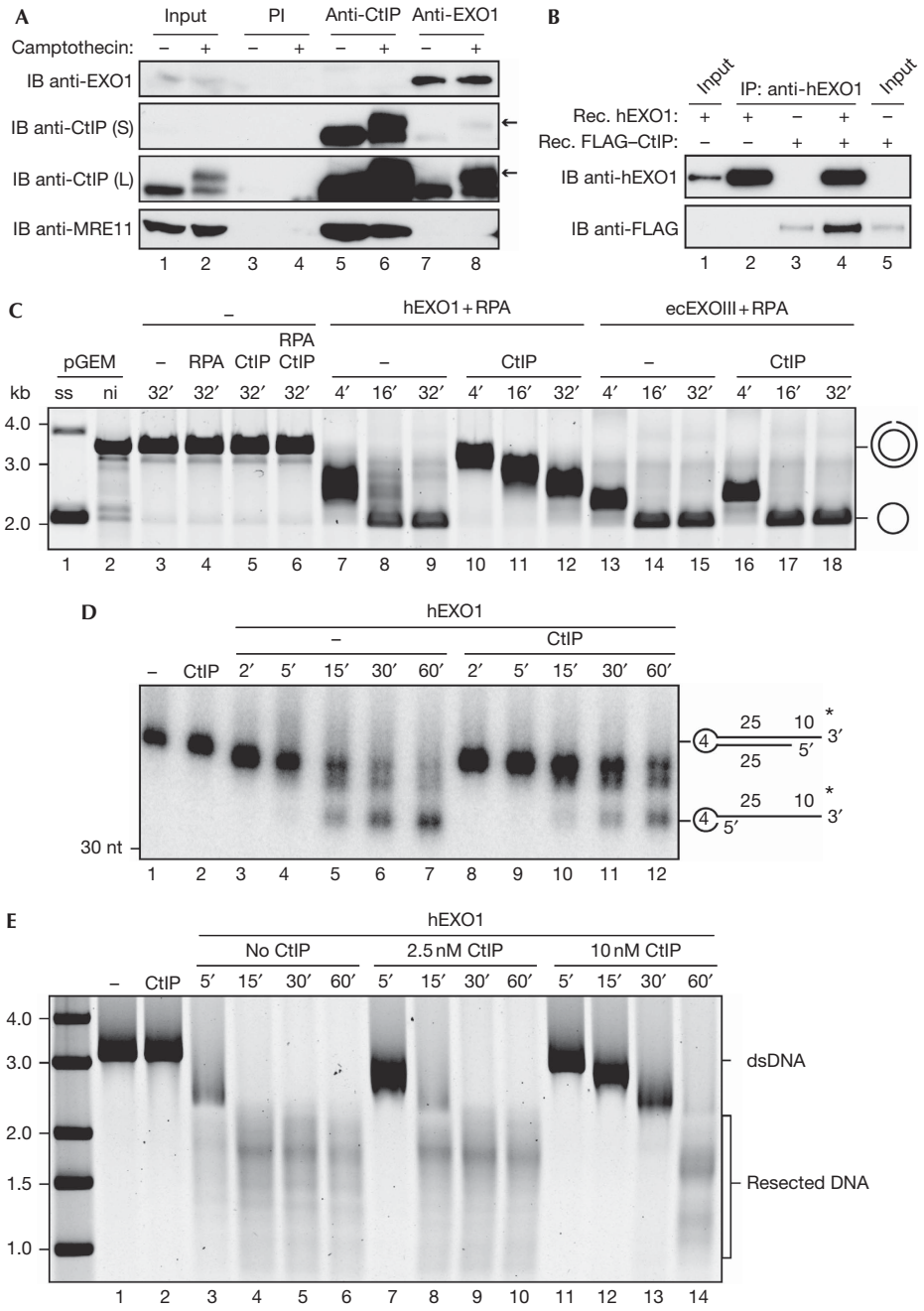

Fig 2 | CtIP interacts with exonuclease 1 and restrains its exonucleolytic activity. (**A**) WCEs (5 mg) from mock or camptothecin-treated (1 μM, 1 h) HEK293T cells were immunoprecipitated with preimmune serum, CtIP or EXO1 polyclonal antibodies. Proteins were detected by immunoblot (IB) with the indicated antibodies. For CtIP, short (S) and long (L) exposure times are shown. Arrows indicate the hyperphosphorylated form of CtIP. The membrane was stripped and re-probed using a monoclonal EXO1 antibody. Input = 1% of the WCEs used for immunoprecipitation. (**B**) Purified, recombinant (Rec.) EXO1 (200 ng) and FLAG-tagged CtIP (200 ng) were incubated either alone or together before immunoprecipitation with an hEXO1 antibody. Proteins were visualized with the indicated antibodies. Recombinant hEXO1 (50 ng, lane 1) and FLAG–CtIP (20 ng, lane 5) were loaded as inputs. (**C**) Nicked plasmid (3.75 nM) was incubated with hEXO1 (15 nM) or ecEXOIII (10 U) in the presence or absence of CtIP (15 nM). RPA (300 nM) was present where indicated. Products were resolved as described in the Methods section. The migration patterns of the double-stranded, nicked plasmid and of the single-stranded product are indicated. (**D**) Radiolabelled oligonucleotide (1 nM, lane 1) was incubated with CtIP alone (1 nM, lane 2), hEXO1 alone (1 nM, lanes 3–7) or both together at equimolar concentrations (lanes 8–12). Reactions were terminated at the indicated time points and the products were analysed as described in the Methods section. (**E**) Linearized plasmid with 3′-overhangs (2.5, 5 nM DNA ends) was incubated at 37 °C with hEXO1 (15 nM), RPA (300 nM) and the indicated amounts of CtIP. Reactions were terminated at the indicated time points and the products were analysed as described in the Methods section. ecEXOIII, *Escherichia coli* exonuclease III; hEXO1, human exonuclease 1; PI, preimmune; RPA, replication protein A; WCE, whole-cell extract.

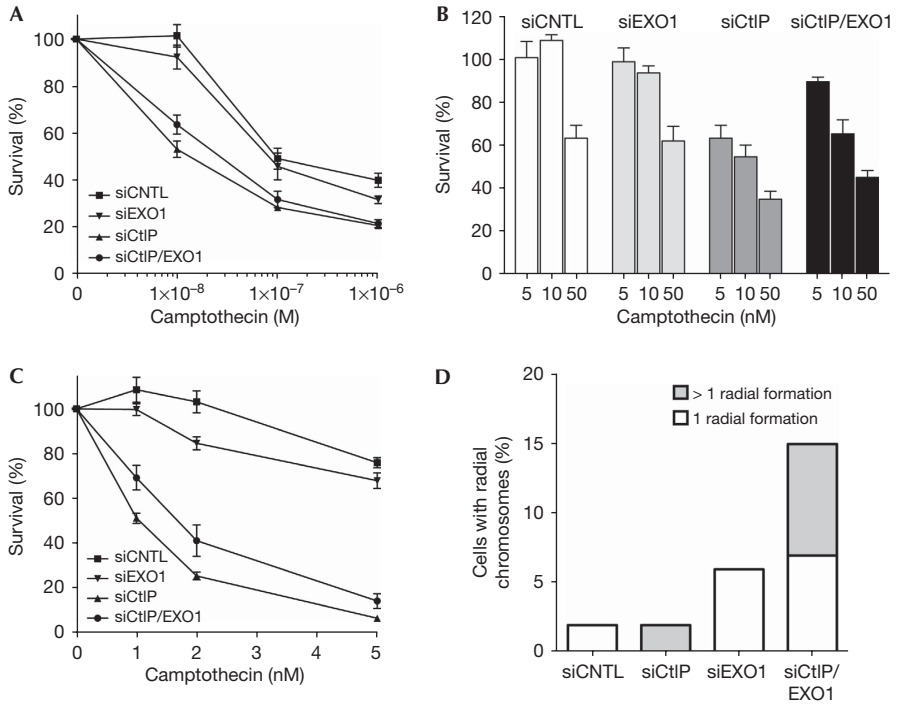

Fig 3 | CtIP and exonuclease 1 protect cells from chromosomal damage. (**A**) At 72 h after transfection with the indicated siRNA oligonucleotides, U2OS cells were treated with either DMSO or camptothecin (1 h, 1 μM; acute treatment) and survival was determined by colony formation. Data represent the mean ± s.e.m. of five independent experiments. (**B**) Cell survival at low doses of camptothecin from the data shown in (**A**). Data represent the mean ± s.e.m. of five independent experiments. (**C**) Cells transfected as in (**A**) were treated with either DMSO or camptothecin for 24 h (chronic treatment) and survival was determined by colony formation. Data represent the mean ± s.e.m. of three independent experiments. (**D**) Metaphase spreads from cells transfected and treated as described in (**A**) were analysed for chromosomal aberrations. A total of 50 metaphase spreads was analysed for each sample. The percentages of metaphase spreads displaying the indicated numbers of radial chromosomes are shown. CNTL, control; DMSO, dimethyl sulphoxide; EXO1, exonuclease 1; siRNA, small interfering RNA.

small fraction of CtIP was unspecifically bound to beads, CtIP was enriched when equimolar amounts of EXO1 were present (Fig 2B, lane 4), demonstrating that the two proteins are able to bind directly to each other *in vitro*.

Saccharomyces cerevisiae Sae2 shows endonuclease activity on defined substrates (Lengsfeld *et al*, 2007). Although similar activity has not yet been reported for human CtIP, CtIP was shown to enhance the endonucleolytic activity of the MRE11–RAD50 complex (Sartori *et al*, 2007). On the basis of these observations, we asked whether CtIP might also affect the 5′–3′ exonuclease activity of EXO1 *in vitro*. First, we examined the activity of purified recombinant EXO1 (supplementary Fig S2C online) using a singly nicked plasmid DNA substrate. Only wild-type EXO1, not a catalytically dead mutant, was able to completely degrade the nicked strand within 30 min of incubation, indicating that there was no contaminant exonuclease activity in our preparation (supplementary Fig S2D online). The addition of equimolar amounts of CtIP decreased exonucleolytic processing, whereas it did not inhibit the activity of *Escherichia coli* exonuclease III (Fig 2C). Under similar assay conditions, MRE11–RAD50 did not substantially affect EXO1 activity (supplementary Fig S2E online). We observed a similar inhibitory effect of CtIP on EXO1 activity using either a radiolabelled DNA oligonucleotide substrate (Fig 2D) or a linearized plasmid (Fig 2E) both containing 3′-overhangs, which are the preferred substrate for EXO1 *in vitro* (supplementary Fig S2G online; Lee & Wilson, 1999). Electrophoretic mobility shift assays showed that, in contrast to EXO1, CtIP did not efficiently bind to the oligonucleotide substrate (supplementary Fig S2F online), excluding the possibility of a nonspecific inhibition of EXO1 by CtIP through steric hindrance. As observed with the nicked plasmid, CtIP did not inhibit the activity of *E. coli* exonuclease III on the linear substrate (data not shown). Furthermore, neither MRE11–RAD50 nor BLM affected EXO1 activity on the plasmid with 3′-overhangs (supplementary Fig S2H online). Interestingly, pre-incubation of CtIP with either blunt-ended or 5′-overhang substrates facilitated processing by EXO1, which did not occur when the proteins were added in the reverse order (supplementary Fig S2I online).

These biochemical data might suggest that CtIP is able to restrain long-range resection by EXO1, thereby generating appropriate recombinogenic ssDNA structures (Mimitou & Symington, 2009; Niu *et al*, 2009). Inhibition of EXO1 activity was also reported during repair of DNA mismatches. However, whereas in mismatch repair RPA (Genschel & Modrich, 2009) or possibly MutLα (Zhang *et al*, 2005) are required for terminating EXO1 activity on removal of the mismatch, our data suggest that CtIP might act to fine tune the nucleolytic activity of EXO1.

CtIP and EXO1 promote error-free repair of DSBs

Our observations indicate that the initial end-trimming activity of MRN–CtIP is required for the recruitment of EXO1 to sites of

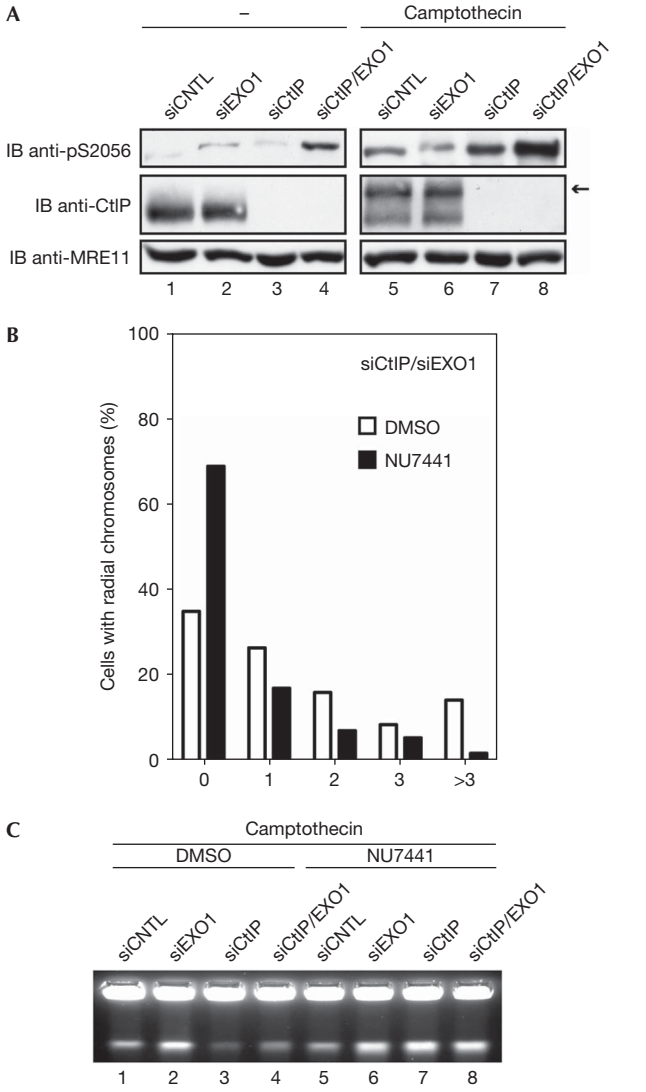

Fig 4 | Inhibition of DNA-PKcs rescues radial chromosomes formation. (**A**) U2OS cells transfected with siRNA oligonucleotides were treated with DMSO or camptothecin (1 μM, 1 h) and DNA-PKcs autophosphorylation at S2056 was monitored. Arrow indicates the hyperphosphorylated form of CtIP. (**B**) Metaphase spreads were generated from cells transfected as in (**A**) and treated with camptothecin (1 μM, 1 h) in the presence or absence of NU7441 (10 μM). In total, more than 100 spreads were analysed for both conditions in two independent experiments. The average number of radial chromsomes per spread was 1.65 (DMSO) and 0.59 (NU7441), equivalent to a 2.8-fold reduction in radial formation. (**C**) Cells transfected as in (**A**) were treated with DMSO or camptothecin (2.5 μM, 4 h) in the presence or the absence of NU7441 (10 μM). The amount of broken DNA was assessed by pulsed-field gel electrophoresis. CNTL, control; DMSO, dimethyl sulphoxide; EXO1, exonuclease 1; IB, immunoblot; siRNA, small interfering RNA.

DNA damage and that CtIP might subsequently control EXO1 exonucleolytic activity to facilitate HR. This prompted us to examine whether some of the phenotypes reported for CtIP-deficient cells in response to camptothecin require EXO1 (Sartori *et al*, 2007). By using siRNA-mediated downregulation of CtIP and EXO1, we monitored various DNA damage phenotypes in response to camptothecin. Single or combined depletion of CtIP and EXO1 did not significantly affect transition through S-phase, as shown by flow cytometry and incorporation of 5-ethynyl-2′-deoxyuridine in DNA (supplementary Fig S3A,B online). As previously shown, CtIP knockdown led to a decrease in CHK1 and RPA2 phosphorylation (supplementary Fig S3C online), indicative of inefficient resection and impaired ATR activation (Sartori *et al*, 2007). However, EXO1 depletion had no impact on ATR signalling, apart from a modest increase in RPA2 hyperphosphorylation (supplementary Fig S3C online). Furthermore, the pattern of camptothecin-triggered DNA-damage-signalling events in cells simultaneously depleted for CtIP and EXO1 did not vary from that of CtIP singly depleted cells (supplementary Fig S3C online). Taken together, these data support the view that EXO1 acts downstream from CtIP and MRN in DNA end resection and are consistent with studies reporting an alternative, EXO1-independent mode of processive resection (Gravel *et al*, 2008; Mimitou & Symington, 2008).

Next, we analysed the sensitivity of these cells to an acute treatment with camptothecin by colony formation assays. Consistent with previous reports, we observed that CtIP downregulation caused hypersensitivity to camptothecin, whereas EXO1 depletion conferred only minor cytotoxicity (Fig 3A; Sartori *et al*, 2007; Gravel *et al*, 2008). Interestingly, we observed a partial, but statistically significant rescue of sensitivity at low camptothecin concentrations by simultaneous downregulation of CtIP and EXO1 (Fig 3A,B). Consistent with this, we found a similar increase in survival on chronic treatment with camptothecin (Fig 3C). We then treated cells with Olaparib, an inhibitor of poly(ADP-ribose) polymerase (PARP; Helleday *et al*, 2008). As PARP is involved in the repair of DNA single-strand breaks (Hoeijmakers, 2001), it was proposed that PARP inhibition results in the accumulation of replication-associated DSBs (Bryant *et al*, 2005; Farmer *et al*, 2005), creating lesions similar to those caused by camptothecin (Pommier, 2006). Treating singly or doubly depleted cells with Olaparib resulted in a pattern of hypersensitivity similar to that caused by camptothecin (supplementary Fig S3D online).

The above data indicate that CtIP and EXO1 act in the same pathway, but they also point to a potentially new genetic interdependency between these factors during the repair of replication-associated DSBs. To gain further, structure-based insight into the repair of camptothecin-induced lesions, we analysed metaphase spreads from cells lacking CtIP and EXO1. Compared with control cells, EXO1-deficient cells had a slight increase in broken chromatids, whereas depletion of CtIP led to a reduction of this type of chromosomal aberration (supplementary Fig S3E online). However, we noticed a significant increase in the number of radial chromosomes specifically in doubly depleted cells, indicative of illegitimate repair by end joining (Fig 3D; supplementary Fig S3F online).

CtIP and EXO1 cooperate to prevent NHEJ

It has been shown that DNA-replication-associated DSBs, such as those induced by camptothecin, activate DNA-PKcs, indicated by autophosphorylation on S2056 (Chen *et al*, 2005; Sakasai *et al*, 2010; supplementary Fig S4A online). By analysing S2056

autophosphorylation, we observed increased DNA-PKcs activation particularly in doubly depleted cells, and the signal was further amplified in response to camptothecin (Fig 4A). This prompted us to reexamine camptothecin-induced chromosomal aberrations on inhibition of DNA-PKcs (supplementary Fig S4A online). Under these conditions, we observed an almost threefold reduction in the number of radial structures in EXO1/CtIP-deficient cells, whereas DNA-PKcs inhibition had no major effect in singly depleted cells (Fig 4B; supplementary Fig S4B online; data not shown). Consistent with this and in agreement with an upregulation of NHEJ in the absence of CtIP and EXO1, DNA-PKcs inhibition markedly increased the number of camptothecin-induced breaks measured by PFGE (Fig 4C; supplementary Fig S4C online).

CONCLUSIONS

Our data imply that two factors involved in DNA end resection, CtIP and EXO1, probably act together to maintain genomic stability by protecting cells from the deleterious consequences of end-joining-mediated repair of camptothecin-induced DNA lesions. A similar scenario was reported for the repair defects in Fanconi anaemia cells (Adamo *et al*, 2010; Pace *et al*, 2010). Therefore, we speculate that hypersensitivity to replication-associated DSBs in resection-compromised cells is probably the result of inappropriate NHEJ rather than HR deficiency alone.

METHODS

Live-cell imaging and laser microirradiation. Double-strand breaks were generated in the nuclei of living cells on 18-mm glass cover slips by microirradiation of arbitrarily shaped regions of interest (ROIs) at 355 nm with 15-mW output power of the laser (Genesis 355-80, Coherent; Walter *et al*, 2003). The ROIs were irradiated 10 times consecutively and identical ROIs were used in all experiments. Subsequently, fluorescence time-lapse imaging was performed for GFP (488 nm excitation, 525–560 nm emission; SP5, Leica, Mannheim, Germany) using an HCX Plan-Apo $\times 63$/NA 1.40 oil immersion objective. Pre-sensitization with 10 μM bromodeoxyuridine was used to avoid artefacts by high local density of DSBs. Non-pre-sensitized control cells showed a lack of EXO1 and CtIP recruitment under the same conditions. Cells were kept in complete growth medium under 5% CO_2 at 37 °C during the experiments.

For fixed-cell imaging, DSBs in defined nuclear volumes were generated by microirradiation (MMI CellCut) with a 355-nm UV-A laser adjusted at 50% of the power. Before irradiation, cells were grown for 24 h in the presence of 10 μM bromodeoxyuridine.

See supplementary information online for additional Methods. **Supplementary information** is available at EMBO *reports* online (http://www.emboreports.org).

ACKNOWLEDGEMENTS

We thank S. Jackson for providing GFP–HA–EXO1 U2OS cells, R. Baer for CtIP antibodies and purified CtIP protein, M. Weitzman for ATLD1-Tert cells, F. Marini for the GFP–EXO1 construct and P. Janscak for purified RPA, BLM and MRE11–RAD50 complex. We also thank M. Stucki and P. Janscak for critical reading of the paper, and U. Ziegler (University of Zurich, Center for Microscopy and Image Analysis) for guidance in the optimization of live-cell imaging. This work was supported by grants of the Swiss National Science Foundation (SNF), the UBS Foundation, the Novartis Foundation for Medical and Biological Research, the University of Zurich Research Priority Program (URPP) and the Désirée and Niels Yde Foundation (to S.F.), the Vontobel-Foundation (to A.A.S.), by an Ambizione fellowship from the Swiss National Science Foundation (SNSF; to A.A.S.) and by the Forschungskredit from the University of Zurich (to M.S.).

CONFLICT OF INTEREST

The authors declare that they have no conflict of interest.

REFERENCES

Adamo A, Collis SJ, Adelman CA, Silva N, Horejsi Z, Ward JD, Martinez-Perez E, Boulton SJ, La Volpe A (2010) Preventing nonhomologous end joining suppresses DNA repair defects of Fanconi anemia. *Mol Cell* **39:** 25–35

Bassing CH, Swat W, Alt FW (2002) The mechanism and regulation of chromosomal V(D)J recombination. *Cell* **109:** S45–S55

Bekker-Jensen S, Lukas C, Kitagawa R, Melander F, Kastan MB, Bartek J, Lukas J (2006) Spatial organization of the mammalian genome surveillance machinery in response to DNA strand breaks. *J Cell Biol* **173:** 195–206

Bolderson E, Tomimatsu N, Richard DJ, Boucher D, Kumar R, Pandita TK, Burma S, Khanna KK (2010) Phosphorylation of Exo1 modulates homologous recombination repair of DNA double-strand breaks. *Nucleic Acids Res* **38:** 1821–1831

Bryant HE, Schultz N, Thomas HD, Parker KM, Flower D, Lopez E, Kyle S, Meuth M, Curtin NJ, Helleday T (2005) Specific killing of BRCA2-deficient tumours with inhibitors of poly(ADP-ribose) polymerase. *Nature* **434:** 913–917

Carson CT, Schwartz RA, Stracker TH, Lilley CE, Lee DV, Weitzman MD (2003) The Mre11 complex is required for ATM activation and the G2/M checkpoint. *EMBO J* **22:** 6610–6620

Chen BP, Chan DW, Kobayashi J, Burma S, Asaithamby A, Morotomi-Yano K, Botvinick E, Qin J, Chen DJ (2005) Cell cycle dependence of DNA-dependent protein kinase phosphorylation in response to DNA double strand breaks. *J Biol Chem* **280:** 14709–14715

Chen L, Nievera CJ, Lee AY, Wu X (2008) Cell cycle-dependent complex formation of BRCA1–CtIP–MRN is important for DNA double-strand break repair. *J Biol Chem* **283:** 7713–7720

El-Shemerly M, Janscak P, Hess D, Jiricny J, Ferrari S (2005) Degradation of human exonuclease 1b upon DNA synthesis inhibition. *Cancer Res* **65:** 3604–3609

Farmer H *et al* (2005) Targeting the DNA repair defect in BRCA mutant cells as a therapeutic strategy. *Nature* **434:** 917–921

Genschel J, Modrich P (2009) Functions of MutLα, replication protein A (RPA), and HMGB1 in 5′-directed mismatch repair. *J Biol Chem* **284:** 21536–21544

Gravel S, Chapman JR, Magill C, Jackson SP (2008) DNA helicases Sgs1 and BLM promote DNA double-strand break resection. *Genes Dev* **22:** 2767–2772

Helleday T, Petermann E, Lundin C, Hodgson B, Sharma RA (2008) DNA repair pathways as targets for cancer therapy. *Nat Rev Cancer* **8:** 193–204

Hoeijmakers JH (2001) Genome maintenance mechanisms for preventing cancer. *Nature* **411:** 366–374

Lee BI, Wilson DM III (1999) The RAD2 domain of human exonuclease 1 exhibits 5′ to 3′ exonuclease and flap structure-specific endonuclease activities. *J Biol Chem* **274:** 37763–37769

Lengsfeld BM, Rattray AJ, Bhaskara V, Ghirlando R, Paull TT (2007) Sae2 is an endonuclease that processes hairpin DNA cooperatively with the Mre11–Rad50–Xrs2 complex. *Mol Cell* **28:** 638–651

Lisby M, Barlow JH, Burgess RC, Rothstein R (2004) Choreography of the DNA damage response: spatiotemporal relationships among checkpoint and repair proteins. *Cell* **118:** 699–713

Mimitou EP, Symington LS (2008) Sae2, Exo1 and Sgs1 collaborate in DNA double-strand break processing. *Nature* **455:** 770–774

Mimitou EP, Symington LS (2009) DNA end resection: many nucleases make light work. *DNA Repair (Amst)* **8:** 983–995

Misteli T, Soutoglou E (2009) The emerging role of nuclear architecture in DNA repair and genome maintenance. *Nat Rev Mol Cell Biol* **10:** 243–254

Niu H, Raynard S, Sung P (2009) Multiplicity of DNA end resection machineries in chromosome break repair. *Genes Dev* **23:** 1481–1486

Pace P, Mosedale G, Hodskinson MR, Rosado IV, Sivasubramaniam M, Patel KJ (2010) Ku70 corrupts DNA repair in the absence of the Fanconi anemia pathway. *Science* **329:** 219–223

Pardo B, Gomez-Gonzalez B, Aguilera A (2009) DNA repair in mammalian cells: DNA double-strand break repair: how to fix a broken relationship. *Cell Mol Life Sci* **66:** 1039–1056

Pommier Y (2006) Topoisomerase I inhibitors: camptothecins and beyond. *Nat Rev Cancer* **6:** 789–802

Sakasai R, Teraoka H, Tibbetts RS (2010) Proteasome inhibition suppresses DNA-dependent protein kinase activation caused by camptothecin. *DNA Repair (Amst)* **9:** 76–82

Sartori AA, Lukas C, Coates J, Mistrik M, Fu S, Bartek J, Baer R, Lukas J, Jackson SP (2007) Human CtIP promotes DNA end resection. *Nature* **450:** 509–514

Stewart GS, Maser RS, Stankovic T, Bressan DA, Kaplan MI, Jaspers NG, Raams A, Byrd PJ, Petrini JH, Taylor AM (1999) The DNA double-strand break repair gene hMRE11 is mutated in individuals with an ataxia-telangiectasia-like disorder. *Cell* **99:** 577–587

Walter J, Cremer T, Miyagawa K, Tashiro S (2003) A new system for laser-UVA-microirradiation of living cells. *J Microsc* **209:** 71–75

Whitby MC (2005) Making crossovers during meiosis. *Biochem Soc Trans* **33:** 1451–1455

Wyman C, Kanaar R (2006) DNA double-strand break repair: all's well that ends well. *Annu Rev Genet* **40:** 363–383

Zhang Y, Yuan F, Presnell SR, Tian K, Gao Y, Tomkinson AE, Gu L, Li GM (2005) Reconstitution of 5′-directed human mismatch repair in a purified system. *Cell* **122:** 693–705

Zhu Z, Chung WH, Shim EY, Lee SE, Ira G (2008) Sgs1 helicase and two nucleases Dna2 and Exo1 resect DNA double-strand break ends. *Cell* **134:** 981–994

Supplementary Information for " DNA end resection by CtIP and Exonuclease 1 prevents genomic instability"

Wassim Eid[1,2], Martin Steger[1,2], Mahmoud El-Shemerly[2,3], Lorenza P. Ferretti[1], Javier Peña-Diaz[1], Christiane König[1], Emanuele Valtorta[1], Alessandro A. Sartori[1,4] and Stefano Ferrari[1,4]

[1]Institute of Molecular Cancer Research, University of Zurich, Winterthurerstrasse 190, CH-8057 Zurich, Switzerland

[2] These authors contributed equally to the study

[3] Present address: Biomedical Research Foundation, Lauchefeld 31, CH-9548 Matzingen, Switzerland

[4] Corresponding Authors: sferrari@imr.uzh.ch and sartori@imcr.uzh.ch

This pdf file includes:

- Supplementary Methods
- Supplementary References
- Supplementary Figure Legends
- Supplementary Figures S1 to S4

Supplementary Methods

Cell culture and transfections - HEK293T cells were maintained as described (El-Shemerly et al, 2005). Human U2OS osteosarcoma cells and U2OS cells stably expressing GFP-HA-EXO1 (kindly provided by S. P. Jackson, University of Cambridge, UK) were cultured in DMEM supplemented with 10% fetal calf serum, standard antibiotics and G-418 (0.5 mg/ml). Immortalized ATLD1 cells transduced with retrovirus expressing the wild-type MRE11 cDNA (ATLD1/MRE11) or retrovirus harboring the empty vector (ATLD1/vector) (a kind gift of M. Weitzman, Salk Institute, S. Diego, CA) were grown in DMEM supplemented with 20% FCS, streptomycin/penicillin (100 U/ml) and 1 µg/ml puromycin (Sigma). GFP-EXO1

(kindly provided by F. Marini, University of Milano, Italy) was transiently transfected in ATLD1 cells using Fugene HD (Roche).

All siRNA duplexes were purchased from Microsynth (Switzerland) with the exception of MRE11 siRNA, which was purchased from Dharmacon (USA). siRNA sequences are as follow: Luciferase (siCNTL) (CGUACGCGGAAUACUUCGATT) (Sartori et al, 2007), CtIP (GCUAAAACAGGAACGAAUCTT) (Sartori et al, 2007), EXO1 (CAAGCCUAUUCUCGUAUUUTT) (Gravel et al, 2008), and MRE11 (GAGCAUAACUCCAUAAGUATT) (Adams et al, 2006). siRNA duplexes were transfected into cells using Lipofectamine RNAiMAX (Invitrogen) in two consecutive rounds to a final concentration of 80 nM as follows: control (80 nM luciferase siRNA), EXO1 (40 nM EXO1 siRNA + 40 nM control siRNA), CtIP (40 nM CtIP siRNA + 40 nM control siRNA), or combined EXO1 and CtIP (40 nM EXO1 siRNA + 40 nM CtIP siRNA). Experiments were typically performed 72h.

Antibodies and chemicals - Antibodies were purchased from S. Cruz Biotech. (goat polyclonal anti-CtIP and anti-OMNI, mouse monoclonal anti-CHK1 and anti-GFP, rabbit polyclonal anti-Cyclin A); Sigma (mouse monoclonal anti-beta-tubulin and anti-FLAG); Cell Signaling Tech. (rabbit monoclonal anti-γH2AX and anti-CHK1-pS345); Upstate Biotech. Inc. (mouse monoclonal anti-γH2AX); Novus Biologicals (rabbit polyclonal anti-MRE11); GeneTex (mouse monoclonal anti-MRE11); Calbiochem (mouse monoclonal anti-RPA2); NeoMarkers (mouse monoclonal anti-EXO1); Abcam (rabbit polyclonal anti-pS2056-DNA-PKcs); or described previously (rabbit polyclonal anti-EXO1, F-15) (El-Shemerly et al, 2005)

Polyclonal and mouse monoclonal anti-CtIP antibodies (Sartori et al, 2007) were provided by R. Baer (Columbia University, New York, NY). Secondary HRP-conjugated anti-mouse and anti-rabbit antibodies were form GE-Healthcare and the HRP-conjugated anti-goat was from S. Cruz Biotech. Alexa Fluor-488, -594, and -647-conjugated secondary antibodies were from Invitrogen.

Camptothecin (Sigma) and AZD2281 (Olaparib, Selleck Chemicals) were dissolved in DMSO at 1 mM and 10 mM stock concentrations, respectively. Hydroxyurea (Sigma) was dissolved in water at 1 M stock concentration. EdU (5-ethynyl-2'-deoxyuridine) was from Invitrogen. The DNA-PKcs inhibitor NU7441 (Tocris Bioscience) (Leahy et al, 2004) was dissolved in DMSO at 5 mM stock concentration. The *E. coli* exonuclease EXOIII was from New England Biolabs.

Immunofluorescence staining and analyses - Cells grown on cover slips were either fixed directly in ice-cold methanol for 15 min or pre-extracted for 5 min on ice using 25 mM HEPES pH 7.4, 50 mM NaCl, 1 mM EDTA, 3 mM $MgCl_2$, 300 mM sucrose and 0.5% Triton X-100 before fixation in 4% formaldehyde (w/v) in PBS for 15 min at room temperature (RT). Cover slips were incubated overnight at 4 °C with primary antibodies and Alexa–conjugated secondary antibodies for 1h at RT. The cover slips were mounted with Vectrashield® (Vector Laboratories) containing DAPI. Images were acquired either using a Leica confocal SP2 or an Olympus IX81 fluorescence microscope.

Western blotting and Immunoprecipitation – Cells lysis, immunoprecipitation and immunoblot analysis were performed as described previously (El-Shemerly et al, 2008). To ensure that the observed interactions were not DNA-mediated, ethidium bromide was included in all samples.

In vitro **protein interaction -** 200 ng of purified, recombinant CtIP (Sartori et al, 2007) and EXO1 (El-Shemerly et al, 2005) were incubated either alone or together for 30 min at 4 ^{o}C in 1 ml TNE buffer containing 50 mM Tris-HCl, pH 7.5, 140 mM NaCl, 1 mM EDTA and 10 μg/ml BSA. Proteins were immunoprecipitated with the antibody F-15 for 2h at 4 ^{o}C. Protein-A sepharose (GE Healthcare) immunocomplexes were analyzed as described (El-Shemerly et al, 2005).

Exonuclease assays - The nicked substrate was generated by incubating the pGEM-13Zf(+) plasmid derivative with *N.Bst*NBI (Fischer et al, 2007) and purified by gel extraction (Qiagen). Exonuclease activities were assayed in a buffer containing 50 mM Tris-HCl pH 7.5, 50 mM NaCl, 2 mM $MgCl_2$, 1 mM DTT and 0.1 mg/ml BSA. Where indicated, final concentrations of purified recombinant proteins were as follows: 15 nM EXO1, 15 nM CtIP and 300 nM RPA. Notably, the presence of purified RPA in the reaction resulted in a defined pattern of nucleolytic processing (Fig 2B) as compared to reactions without RPA (supplementary Fig 2E). Reactions were stopped by incubation in 10 mM EDTA, 0.25 % SDS and 100 μg/ml Proteinase K for 10 min at 37° C. DNA products separated on 0.8% agarose were stained with

either ethidium bromide or SYBR Gold and analyzed with a Typhoon PhosphorImager (GE Healthcare).

Hairpin exonuclease assays were performed in 20 µl with 1 nM DNA substrate (annealed 3' labeled HL1: 5'-TCATTGCCTATCCTGACAGTCCGACACATCGGACTGTCAGGATAGGCAAT GATCTTTTTTTTT -3'), 50 mM Tris-HCl pH 7.5, 50 mM NaCl, 5 mM $MgCl_2$, 1 mM DTT and 50 ng/µl BSA at 37ºC with the indicated protein concentrations and time-points. Reactions were terminated by addition of an equal volume of 99% (v/v) formamide 0.1% (w/v) bromophenol blue and heating at 95°C for 5 min. Products were resolved by electrophoresis in 15% (w/v) polyacrylamide gel containing 8 M urea (acrylamide/bis-acrylamide 19:1) run in 1xTBE buffer at 25 mA. Gels were dried and analyzed with a Typhoon PhosphorImager (GE Healthcare).

Linearized plasmids were generated by incubating the pGEM-13Zf(+) plasmid derivative with either Ban*II* (5' overhangs), Hind*III* (3' overhangs) or Sca*I* (blunt ends) followed by column purification (Qiagen). Proteins used in the assay were mixed and incubated on ice prior to addition into reaction tubes containing 50 mM Tris-HCl pH 7.5, 50 mM NaCl, 2 mM $MgCl_2$, 1 mM DTT and 0.1 mg/ml BSA. DNA products were separated as described above.

DNA-Binding assays - Gel mobility shift assays were performed in a volume of 20 µl containing 5 nM of annealed 5' radiolabeled DNA oligonucleotide substrates, 50 mM Tris-HCl pH 7.5, 50 mM NaCl, 1 mM EDTA, 1 mM DTT, 50 ng/µl BSA. The reactions were pre-incubated with the corresponding proteins, 10 nM EXO1, 50 nM CtIP for 15 min at RT before addition of the substrate and further incubated for 60 min. After addition of glycerol to a final 10% concentration, separation was performed in a 6% (w/v) native polyacrylamide gel run in 1xTBE buffer at 25 mAmp. Gels were analyzed as described above.

Pulse-field gel electrophoresis - Subconfluent cultures of U2OS were mock-treated (DMSO) or camptothecin-treated for 4h. Cells were harvested by trypsinization, and agarose plugs of 10^6 cells were prepared in a disposable plug mold (BioRad). Plugs were then incubated in lysis buffer (100 mM EDTA, 1% (w/v) sodium lauryl sarcosyl, 0.2% (w/v) sodium deoxycholate, 1mg/ml proteinase K) at 37 ^oC for 72h. Plugs were then washed four times in 20 mM Tris-HCl pH 8.0, 50 mM EDTA before loading

onto an agarose gel. Electrophoresis was performed for 23h at 14 ^{o}C in 0.9% (w/v) Pulse Field Certified Agarose (BioRad) containing Tris-borate/EDTA buffer according to the conditions described in (Hanada et al, 2007) and adapted to a BioRad CHEF DR III apparatus. The gel was then stained with ethidium bromide and analyzed using an Alpha Innotech Imaging system.

Colony formation assay - Cells were either mock-treated (DMSO) or treated with the indicated doses of camptothecin 72h after the first siRNA transfection. The drug was removed 1h upon treatment and cells were cultured for 10–14 days at 37°C. For the PARP-inhibitor AZD2281, continuous exposure to the compound was ensured by a first addition 72h after the siRNA transfection, and a second addition 72 h after the first. Colonies were stained with a crystal violet/ethanol (0.5%/20%) solution and counted.

Chromosome analysis - After treatment with camptothecin, cells were allowed to recover for 8h in complete medium before chromosome preparation. Caffeine (2 mM) was added for the last 5h to override the G2/M checkpoint, and colcemid (0.1 μg/ml) was added for the last 3h to arrest cells in metaphase. Metaphase chromosomes were stained with DAPI.

Supplementary References

Adams KE, Medhurst AL, Dart DA, Lakin ND (2006) Recruitment of ATR to sites of ionising radiation-induced DNA damage requires ATM and components of the MRN protein complex. *Oncogene* **25**(28)**:** 3894-3904

El-Shemerly M, Hess D, Pyakurel AK, Moselhy S, Ferrari S (2008) ATR-dependent pathways control hEXO1 stability in response to stalled forks. *Nucleic Acids Res* **36**(2)**:** 511-519

El-Shemerly M, Janscak P, Hess D, Jiricny J, Ferrari S (2005) Degradation of human exonuclease 1b upon DNA synthesis inhibition. *Cancer Res* **65**(9)**:** 3604-3609

Fischer F, Baerenfaller K, Jiricny J (2007) 5-Fluorouracil is efficiently removed from DNA by the base excision and mismatch repair systems. *Gastroenterology* **133**(6)**:** 1858-1868

Gravel S, Chapman JR, Magill C, Jackson SP (2008) DNA helicases Sgs1 and BLM promote DNA double-strand break resection. *Genes Dev* **22**(20)**:** 2767-2772

Hanada K, Budzowska M, Davies SL, van Drunen E, Onizawa H, Beverloo HB, Maas A, Essers J, Hickson ID, Kanaar R (2007) The structure-specific endonuclease Mus81 contributes to replication restart by generating double-strand DNA breaks. *Nat Struct Mol Biol* **14**(11)**:** 1096-1104

Leahy JJ, Golding BT, Griffin RJ, Hardcastle IR, Richardson C, Rigoreau L, Smith GC (2004) Identification of a highly potent and selective DNA-dependent protein kinase (DNA-PK) inhibitor (NU7441) by screening of chromenone libraries. *Bioorg Med Chem Lett* **14**(24)**:** 6083-6087

Sartori AA, Lukas C, Coates J, Mistrik M, Fu S, Bartek J, Baer R, Lukas J, Jackson SP (2007) Human CtIP promotes DNA end resection. *Nature* **450**(7169)**:** 509-514

Supplementary Figure Legends

Supplementary Figure S1 - CtIP- and MRN-dependent recruitment of EXO1 to DSBs

(A) Recruitment of GFP-EXO1 to laser lines visualized by fluorescence microscopy at early (5 min) and late (240 min) time points.

(B) Live cell imaging of microirradiated GFP-EXO1 cells transfected with control (CNTL), CtIP or MRE11 siRNA. Scale bar = 10 μm.

(C-E) CtIP recruitment to DSBs in ATLD1 cells is insufficient for DNA end resection. MRE11-deficient ATLD1 fibroblasts, stably transfected with an empty vector or with a vector directing the expression of full-length MRE11, were treated with camptothecin (1 μM, 1 h) and analyzed by immunoblotting with the indicated antibodies *(C)*. The same pair of cells was microirradiated, fixed after 30 min and co-stained with either γH2AX and RPA2 *(D)* or γH2AX and CtIP *(E)* antibodies. Nuclei were visualized with DAPI.

(F) Live cell imaging of vector- or wild-type MRE11-complemented ATLD1 fibroblasts, transiently transfected with GFP-EXO1 and microirradiated.

Supplementary Figure S2 - Biochemical characterization of the EXO1-CtIP interaction

(A) WCEs (5 mg) from DMSO or camptothecin-treated (2h, 2.5 μM) HEK293T cells were immunoprecipitated using an anti-EXO1 antibody. Immunocomplexes bound to

sepharose beads were incubated with 10 units of calf intestinal phosphatase (CIP) for 10 min at 37 ^{o}C, washed with 3x 1ml TNET buffer (El-Shemerly et al, 2005), resolved by SDS-PAGE and analyzed by immunoblotting.

(B) WCEs (5 mg) from HEK293T cells overexpressing OMNI-tagged EXO1, treated or not with hydroxyurea (2 mM, 16h) were immunoprecipitated with PI serum or an anti-CtIP antibody. Proteins were detected by immunoblotting with the indicated antibodies.

(C) Human recombinant $EXO1_{wt}$ and the catalytically-dead mutant $EXO1_{D173A}$ were expressed and purified as described (El-Shemerly et al, 2005). Peak fractions from the chitin affinity column were pooled, loaded on a Hi-Trap SP-FF (1 ml) cartridge and proteins eluted with a linear salt gradient (0.0 - 0.5 M NaCl). Aliquots of the load (L, 5 μl), flow-through (FT, 5 μl), wash (W, 5 μl) fractions and of the OD_{280} peak (20 μl) were resolved by 8% SDS-PAGE and stained with Coomassie brilliant blue.

(D) Purified wild-type EXO1 (15 nM; lanes 1-7) or catalytically-dead EXO1 (D173A, 15 nM; lanes 9-15) were incubated with 5 nM *N.BstNBI*-digested pGEM-13Zf(+) plasmid for the indicated time points and the products resolved on a 0.8% agarose gel before ethidium bromide staining.

(E) Gel-purified pGEM-13Zf(+)-nicked plasmid substrate (3.75 nM) was incubated at 37°C for the indicated time periods with purified EXO1 (15 nM) in the presence or absence of purified CtIP (15 nM) or MRE11-RAD50 (15 nM). The products were resolved as described in Supplementary Methods.

(F) Radiolabelled oligonucleotide (5 nM) was incubated for 60 min at room temperature with purified EXO1 (10 nM), CtIP (50 nM) or both together in a buffer containing 1 mM EDTA. The products were analyzed as described in Supplementary Methods. The migration patterns of free and EXO1-bound oligonucleotide are indicated.

(G) Purified linearized pGEM-13Zf(+) plasmid (2.5 nM, 5 nM DNA ends) containing either 3' overhangs, 5' overhangs or blunt ends was incubated for 30 min at 37°C with EXO1 (15 nM) in the presence or absence of RPA (300 nM) as indicated. The products were resolved as described in Supplementary Methods.

(H) Purified linearized pGEM-13Zf(+) plasmid containing 3' overhangs (2.5 nM, 5 nM DNA ends) was incubated at 37°C with EXO1 (15 nM) in the presence of RPA

(300 nM) and either CtIP (15 nM), MRE11-RAD50 (15 nM) or BLM (15 nM). The products were resolved as described in Supplementary Methods.

(I) Purified linearized pGEM-13Zf(+) plasmid (2.5 nM, 5 nM DNA ends) containing either blunt ends or 5' overhangs was incubated at 37°C with EXO1 (15 nM) in the presence of RPA (300 nM) or pre-incubated with either EXO1 (15 nM) or CtIP (15 nM) for 5 min at RT, followed by addition of CtIP or EXO1, respectively. The products were resolved as described in Supplementary Methods.

Supplementary Figure S3 - Effect of CtIP, EXO1 or CtIP/EXO1 downregulation on genome stability

(A) 72h after the transfection with the indicated siRNA oligonucleotides U2OS cells were subjected to propidium iodide (PI) staining for cell cycle analysis.

(B) U2OS cells grown on glass cover slips and transfected as described in *(A)* were incubated for 20 min with 10 μM EdU (5-ethynyl-2'-deoxyuridine). Immediately after fixation with 4% formaldehyde cover slips were processed following manufacturers instructions (Invitrogen). At least 150 cells were counted for each condition. Percentages indicate the number of EdU-positive cells.

(C) 72h after the transfection with the indicated siRNA oligonucleotides U2OS cells were treated with either DMSO or camptothecin (1h, 1 μM). WCEs were analyzed by immunoblot (*left panel*) or immunoprecipitation (*right panel*) with the indicated antibodies.

(D) Cells transfected as described in *(A)* were treated with the indicated doses of AZD2281 (Olaparib) and survival was determined by colony formation. Data represent the mean ± SEM of three independent experiments.

(E) Cells transfected as in (A) were treated with camptothecin (1 μM, 1h) and allowed to recover for 8h in complete medium before chromosome preparation. Caffeine (2 mM) was added for the last 5h to override the G2/M checkpoint, and colcemid (0.1 μg/ml) was added for the last 3h to arrest cells in metaphase. 50 metaphase spreads were analyzed for each sample. The percentages of metaphase spreads displaying the indicated numbers of broken chromosomes are shown.

(F) Representative images of chromosomal abnormalities detected in metaphase spreads of camptothecin treated cells: broken chromatids (arrowheads); radial chromosomes (ellipses). Scale bar, 10 μm.

Supplementary Figure S4 - Inhibition of DNA-PKcs rescues camptothecin-induced radials formation in CtIP/EXO1 depleted cells

(A) WCEs obtained from U2OS that were treated with camptothecin (1h, 1 μM) in the presence or the absence of NU7441 (10 μM), were analyzed by immunoblot with the indicated antibodies. Autophosphorylation at S2056 was use as read-out for inhibition of DNA-PKcs activity by NU7441.

(B) 72h after the transfection with the indicated siRNA oligonucleotides, U2OS cells were treated with DMSO or camptothecin (2.5 μM, 4h) in the presence or the absence of the DNA-PKcs inhibitor NU7441 (10 μM). Representative images of chromosomal abnormalities detected in metaphase spreads are shown. Radial chromosomes (ellipses) and broken chromatids (arrowheads) are indicated.

(C) Cells transfected as in *(B)* were treated with DMSO or camptothecin (1h, 1 μM). The amount of broken DNA was assessed by PFGE as described in supplementary Methods.

Eid *et al.*, Supplemental Figure 1

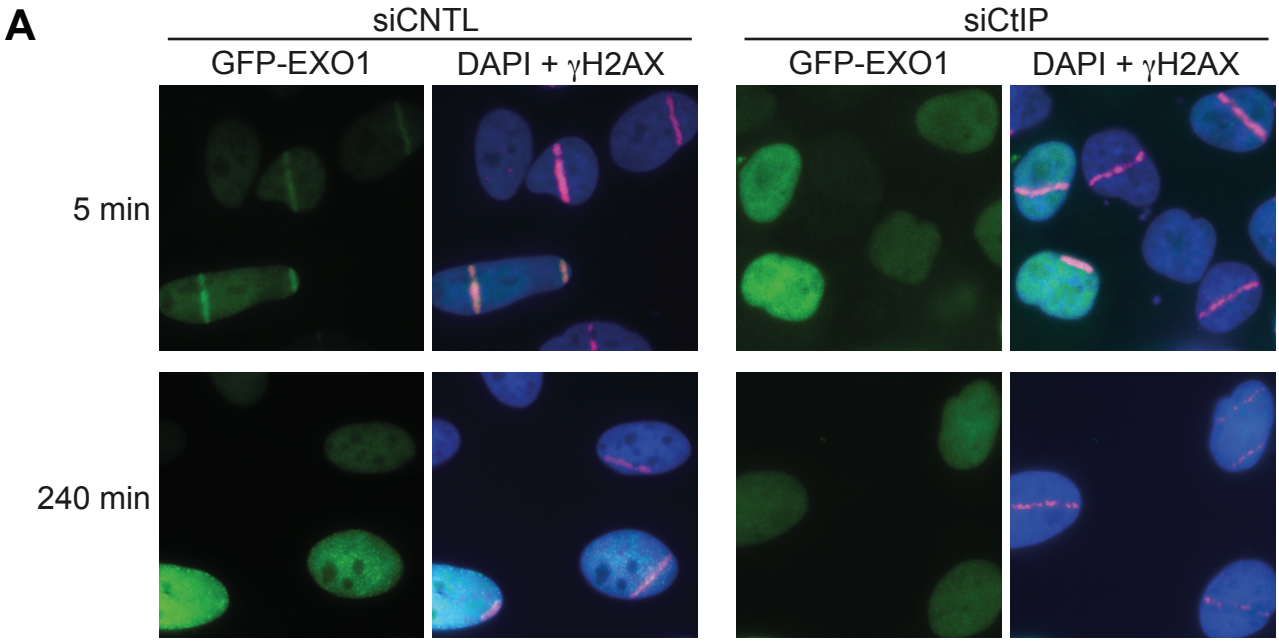

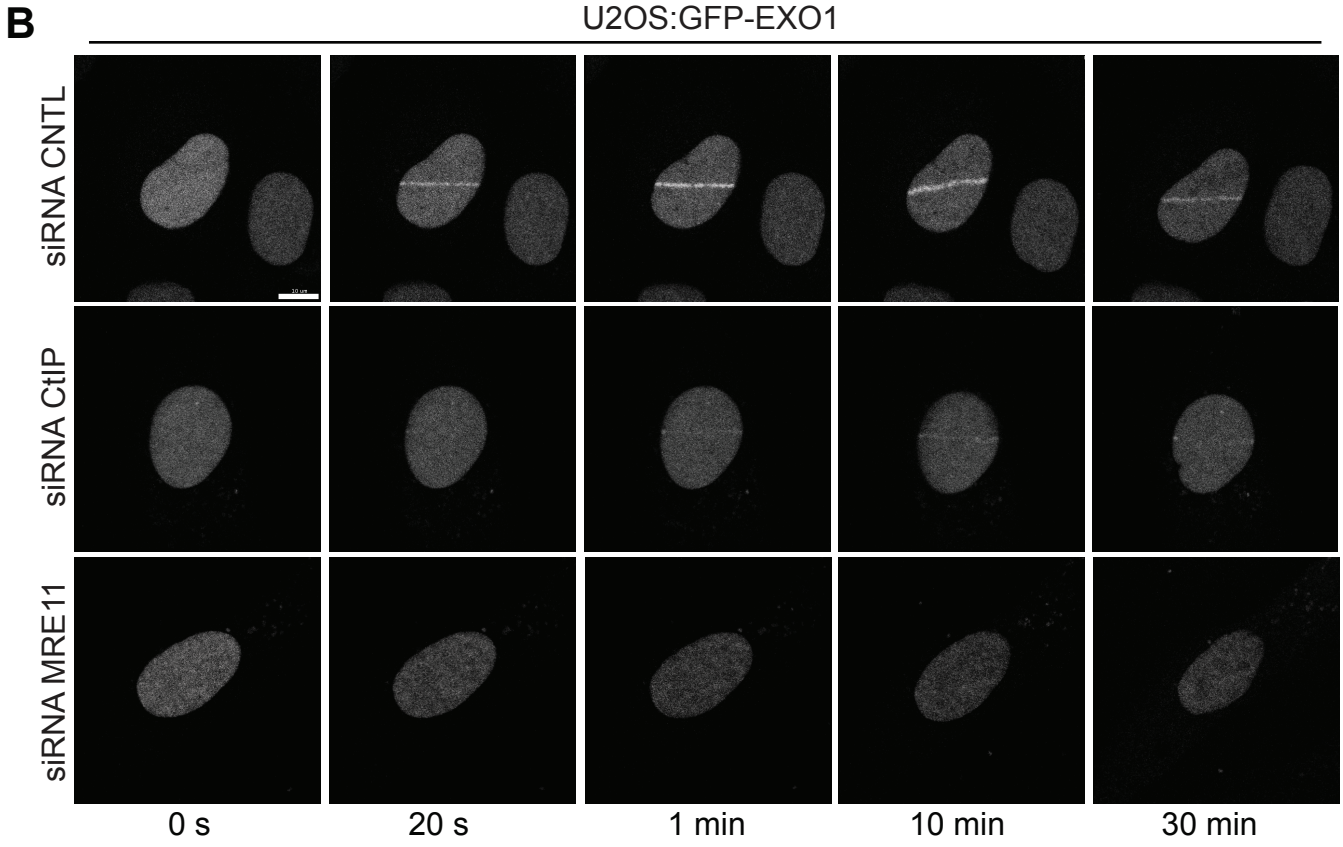

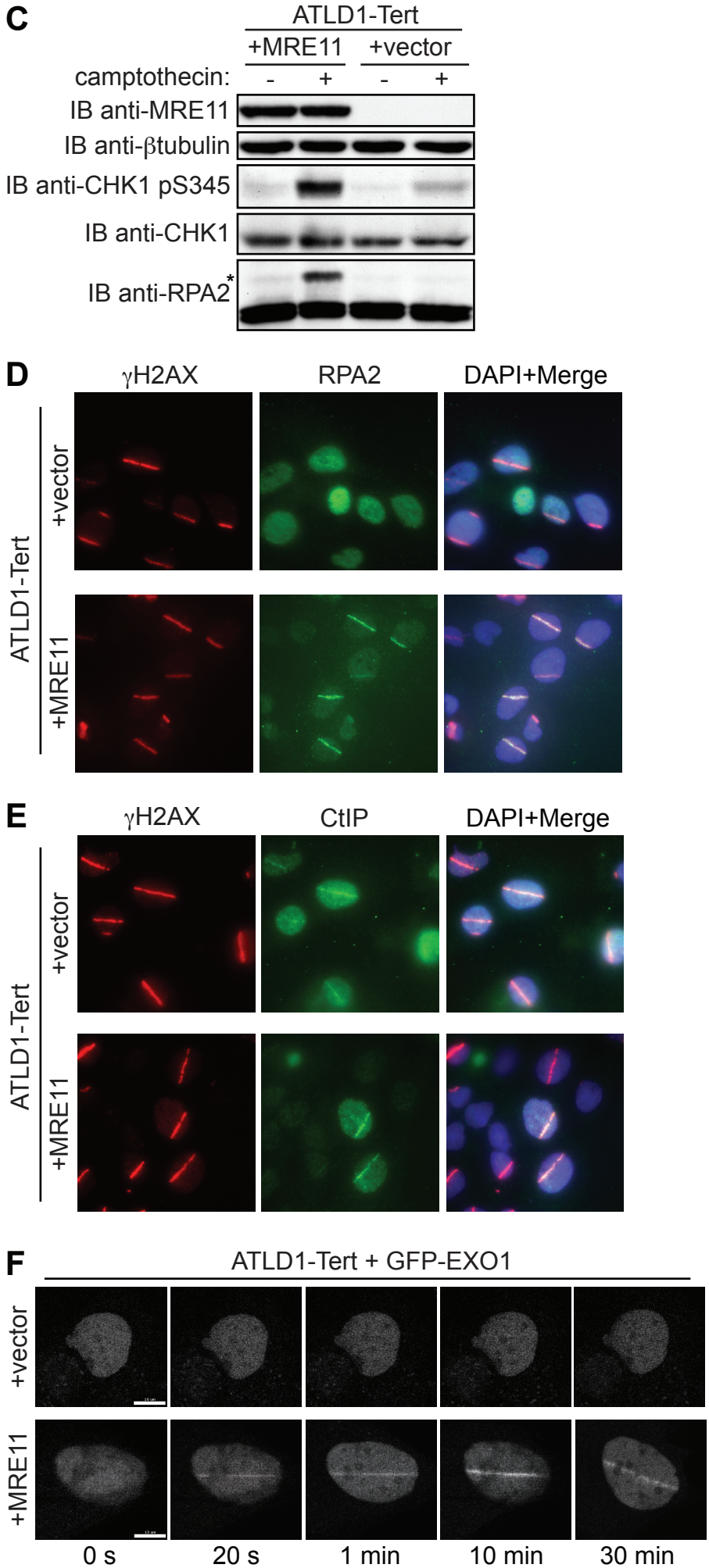
C
ATLD1-Tert
+MRE11
+vector
camptothecin:
-
+
-
+
IB anti-MRE11
IB anti-βtubulin
IB anti-CHK1 pS345
IB anti-CHK1
IB anti-RPA2*
D
γH2AX
RPA2
DAPI+Merge
ATLD1-Tert
+vector
+MRE11
E
γH2AX
CtIP
DAPI+Merge
ATLD1-Tert
+vector
+MRE11
F
ATLD1-Tert + GFP-EXO1
+vector
+MRE11
0 s
20 s
1 min
10 min
30 min

Eid *et al.*, Supplemental Figure 2

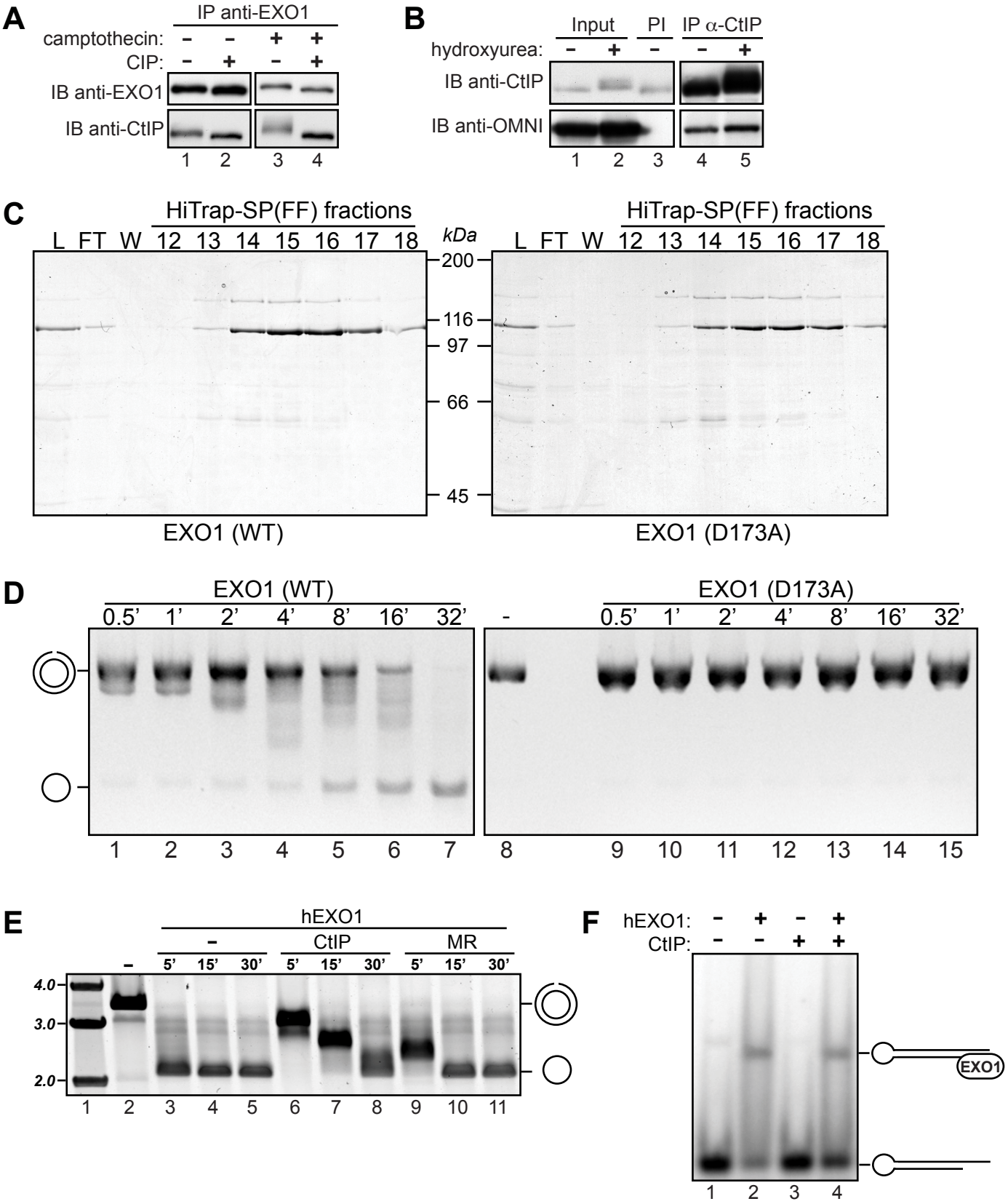

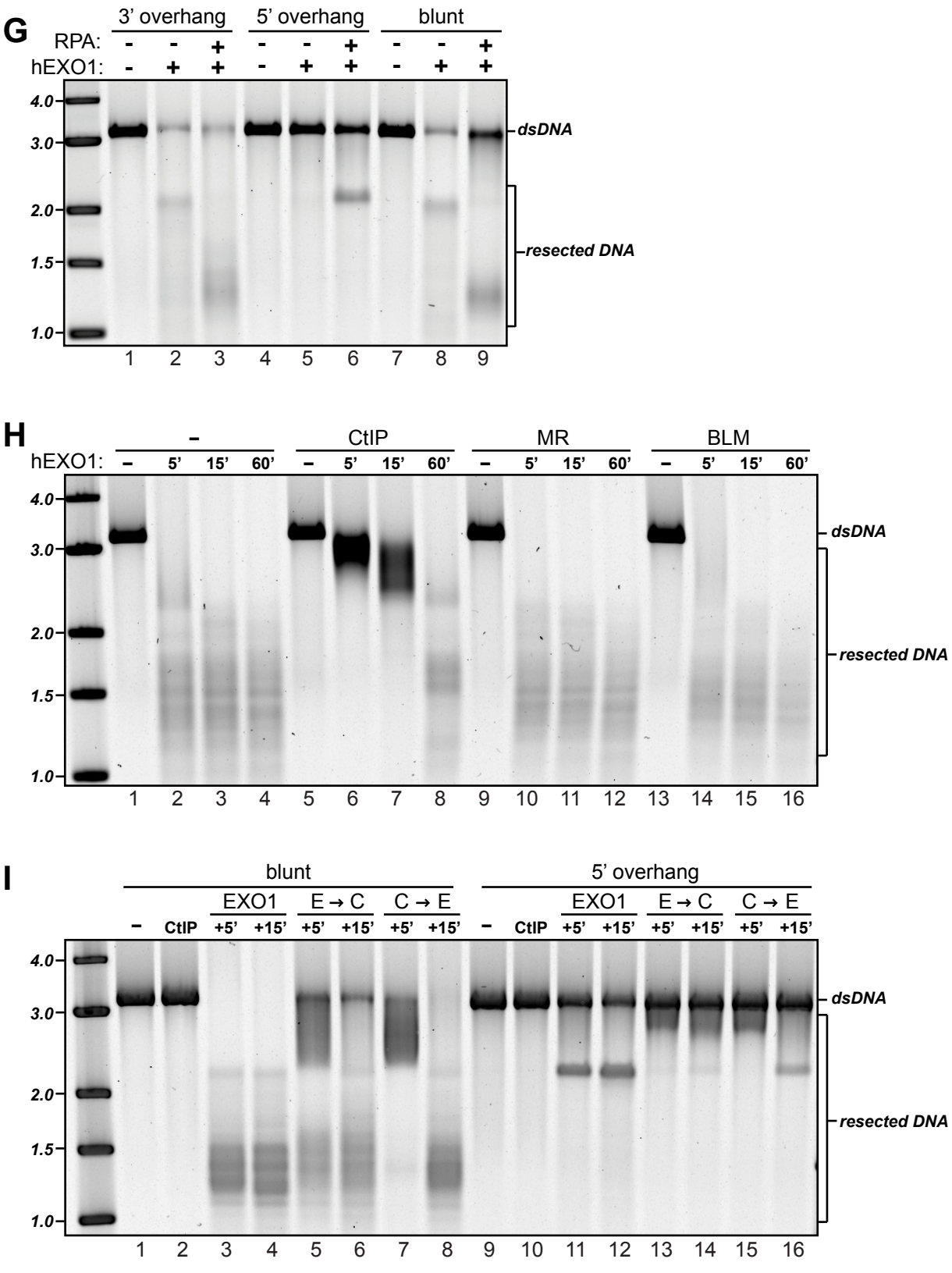
G
3' overhang
5' overhang
blunt
RPA: - - + - - + - - +
hEXO1: - + + - + + - + +
4.0
3.0
2.0
1.5
1.0
dsDNA
resected DNA
1 2 3 4 5 6 7 8 9
H
–
CtIP
MR
BLM
hEXO1: – 5' 15' 60' – 5' 15' 60' – 5' 15' 60' – 5' 15' 60'
4.0
3.0
2.0
1.5
1.0
dsDNA
resected DNA
1 2 3 4 5 6 7 8 9 10 11 12 13 14 15 16
I
blunt
5' overhang
EXO1
E → C
C → E
– CtIP +5' +15' +5' +15' +5' +15' – CtIP +5' +15' +5' +15' +5' +15'
4.0
3.0
2.0
1.5
1.0
dsDNA
resected DNA
1 2 3 4 5 6 7 8 9 10 11 12 13 14 15 16

Eid *et al*., Supplemental Figure 3

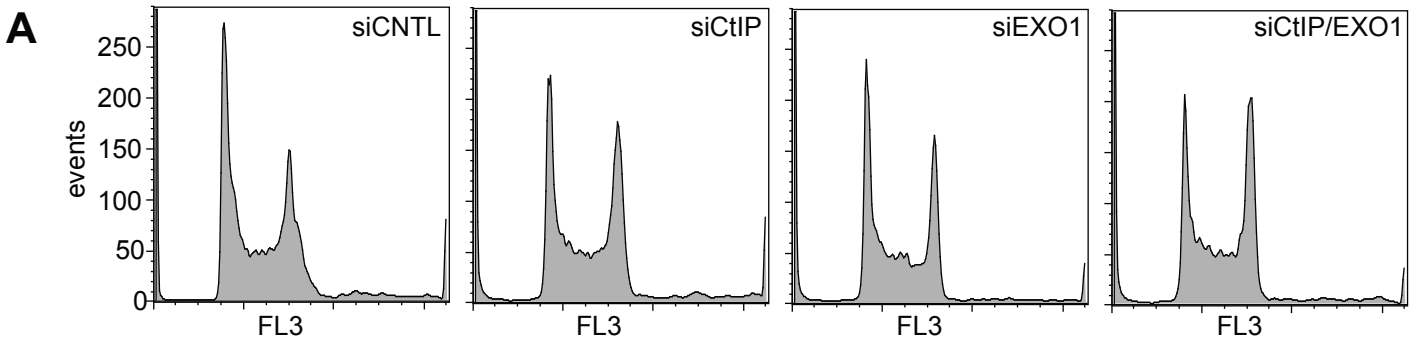

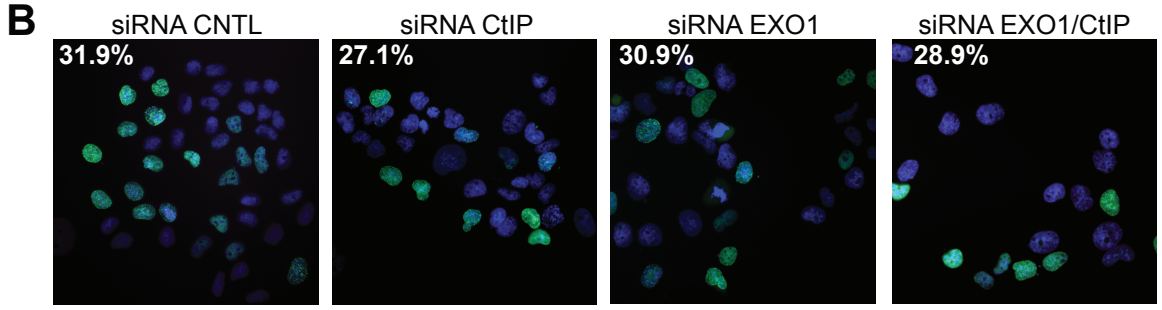

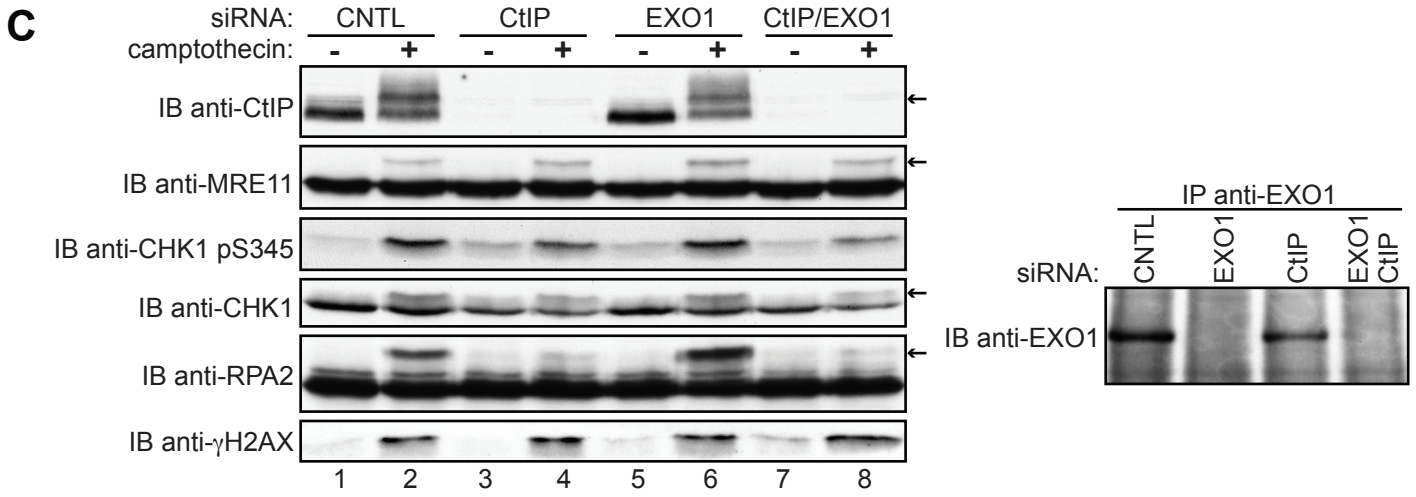

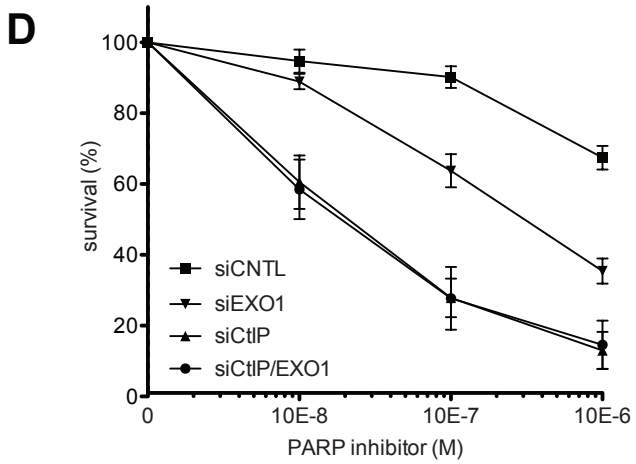

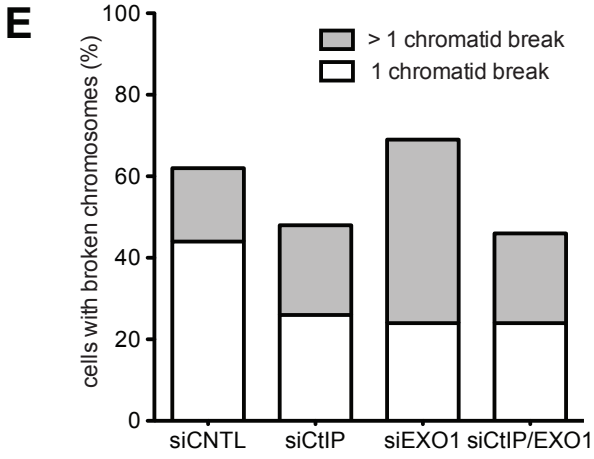

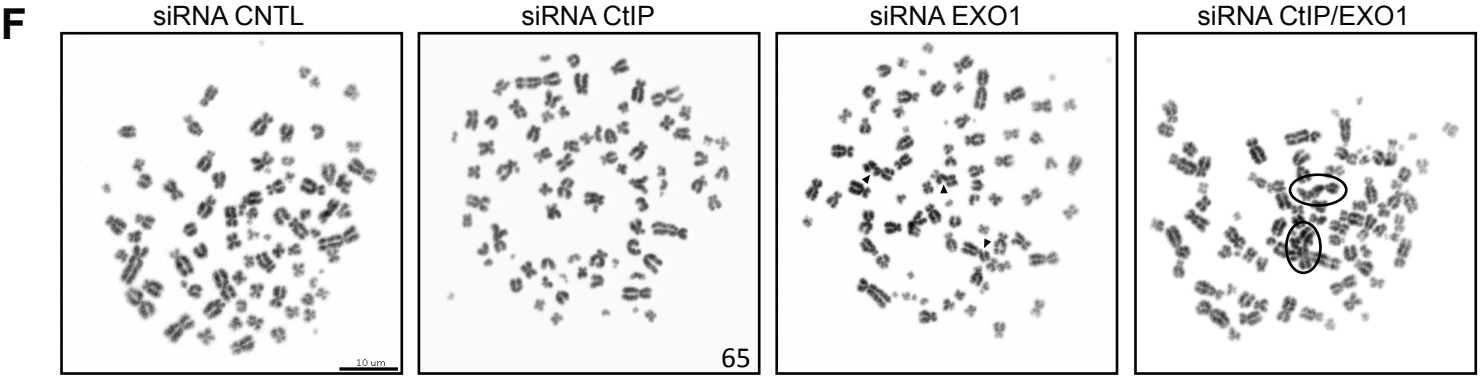

Eid *et al.*, Supplemental Figure 4

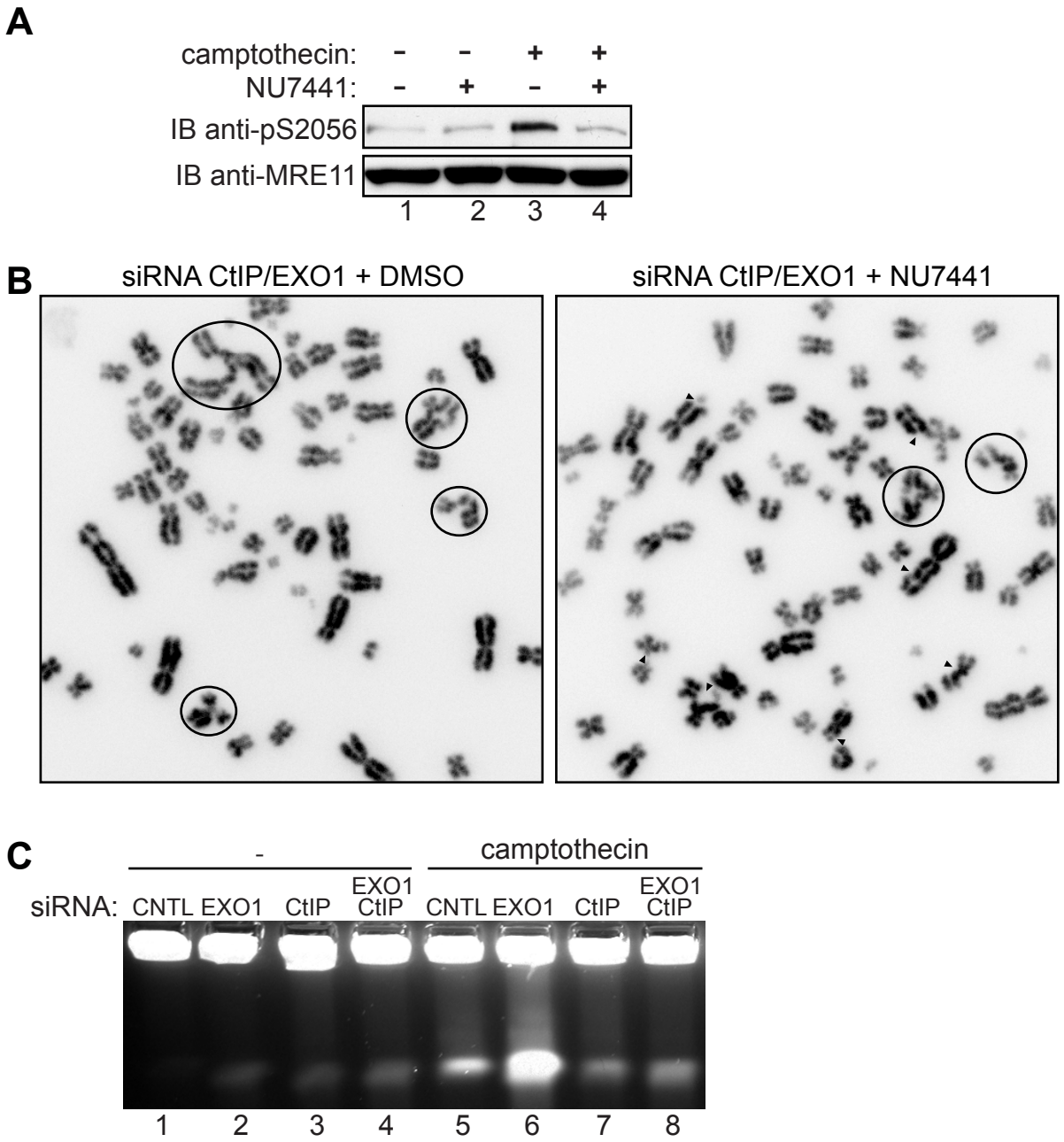

3.2 PIN1-mediated isomerization of CtIP determines DSB repair pathway choice

manuscript in preparation

authors: Martin Steger, Olga Murina, Daniela Hühn, Reto Walser, Shreya Paliwal, Kay Hänggi, Lorenzo Lafranchi, Christine Neugebauer, Bertran Gerrits, Pavel Janscak, Oliver Zerbe and Alessandro A. Sartori

contributions: I contributed most of the figures and wrote the manuscript together with AAS, RW and OZ. OM and SP performed GFP-based HR assays, DH performed PFGE experiments, RW performed NMR spectroscopy, KH and LL performed some IPs and GST-pulldown assays, BG performed MS analysis, CN performed all survival assays, PLA experiments and helped in optimizing many other experiments. PJ and OZ provided tools.

PIN1-mediated isomerisation of CtIP determines double-strand break repair pathway choice

Martin Steger[1], Olga Murina[1], Daniela Hühn[1], Reto Walser[2], Shreya Paliwal[1], Kay Hänggi[1], Lorenzo Lafranchi[1], Christine Neugebauer[1], Bertran Gerrits[3], Pavel Janscak[1], Oliver Zerbe[2] and Alessandro A. Sartori[1,*]

[1] Institute of Molecular Cancer Research, University of Zurich, Winterthurerstrasse 190, CH-8057 Zurich, Switzerland

[2] Institute of Organic Chemistry, University of Zurich, Winterthurerstrasse 190, CH-8057 Zurich, Switzerland

[3] Functional Genomic Center, University of Zurich, Winterthurerstrasse 190, CH-8057 Zurich, Switzerland

Running title: PIN1 limits DNA end resection by regulating CtIP

Keywords: DNA damage, peptidyl-prolyl cis/trans isomerisation, double-strand break repair pathway choice, non-homologous end joining, homologous recombination, human CtIP, human PIN1, etoposide

* Corresponding Author:

sartori@imcr.uzh.ch
phone (+41) 44 635 3473
fax (+41) 44 635 3484

Abstract

Protein phosphorylation plays a crucial role in regulating DNA double-strand break (DSB) repair. Here, we show that human PIN1, a phosphorylation-specific peptidyl-prolyl *cis/trans* isomerase (PPIase), is able to interact with several prominent DSB repair factors and controls the balance between homologous recombination (HR) and non-homologous end joining (NHEJ). We find that PIN1-deficient cells display reduced NHEJ due to increased DNA end resection, while HR is compromised in PIN1-overexpressing cells. In addition, we identify CtIP, a key DNA end resection factor, as a novel PIN1 substrate. Phosphorylation of CtIP at two previously uncharacterized Ser/Thr-Pro motifs (S276 and T315) is responsible for PIN1 binding and isomerisation. We also provide evidence that PIN1-dependent isomerisation decreases CtIP protein stability, particularly after DNA damage. Finally, we report that cells expressing a CtIP mutant refractory to PIN1 recognition exhibit hyperresection of DSBs and reduced NHEJ. Thus, our results reveal phosphorylation-dependent proline isomerisation as an important mechanism to fine-tune the balance between DSB repair pathways.

Introduction

DNA double-strand breaks (DSBs) are cytotoxic lesions, but can also cause genomic instability. Chromosomal aberrations caused by faulty DSB repair can in turn trigger cellular transformation and carcinogenesis[1]. To counteract these lesions, cells activate a complex network of repair and signaling pathways, collectively known as the DNA damage response (DDR)[2]. The DDR coordinates diverse processes including cell cycle checkpoints, DNA repair and cellular senescence or apoptosis. Two major pathways address DSBs: non-homologous end-joining (NHEJ) and homologous recombination (HR). Because of the need for an intact sister chromatid, HR has a limited role in G1 and is the predominant DSB repair pathway during S and G2 phases of the cell cycle. HR is initiated by DNA end resection, which generates 3'-single-stranded DNA (ssDNA) overhangs required for RAD51-dependent strand invastion[3]. In mammalian cells this process is dependent upon the MRN complex and CtIP[4,5]. CtIP is therefore a central factor coordinating DSB repair by homologous recombination (HR) and cell cycle checkpoints[7]. Indeed, impairment of CtIP function has been linked to various DSB repair defects and to carcinogenesis[4,8].

Proline-directed phosphorylation of Ser/Thr-Pro motifs is a central signaling mechanism in diverse cellular processes including DNA repair[9,10]. Such phosphorylation events, especially those catalyzed by cyclin-dependent kinases (CDKs), play a fundamental role in the process of DSB repair[9]. Indeed, CtIP has been shown to undergo CDK-mediated phosphorylation during S/G2 phases of the cell cycle, thus, ensuring proper DNA repair and checkpoint function[11-13]. Recent studies have indicated that many phosphorylated Ser/Thr-Pro motifs are prone to undergo conformational changes[14,15], because prolyl peptide bonds can exist in two different conformation, *cis* or in *trans*. The interconversion of the two isomers is catalyzed by the unique prolyl-isomerase PIN1[14,15]. Through its WW-domain PIN1 interacts with several substrates at pSer/Thr-Pro motifs and, through its carboxy-terminal peptidyl-prolyl isomerase (PPIase) domain, catalyzes *cis/trans* isomerisation of the intervening peptide bond. PIN1 isomerisation functions as a molecular timer, regulating a variety of proteins including β-catenin, p53, cyclin D1 and

cyclin E[16-20]. Moreover, deregulation of PIN1 has been associated with several human pathologies, including Alzheimer's diesase and cancer[21,22].

In this study, we report the identification of two novel proline-directed phosphorylation sites in CtIP which promote PIN1 binding and subsequent CtIP isomerisation. Moreover, we show that PIN1 fine-tunes the balance between NHEJ and HR. Accordingly, we find that CtIP phospho-mutants unable to associate with PIN1 display increased DNA end resection, correlating with decreased NHEJ. Thus, our data highlight PIN1-mediated *cis/trans* isomerisation of proteins as an important determinant of DSB repair pathway choice.

Results and Discussion

PIN1 affects the choice of DSB repair by counteracting homology-directed repair

PIN1 functions as a molecular timer to regulate a growing number of cellular processes including cell signaling and gene expression but its possible direct involvement in the process of DSB repair has not been specifically addressed[23]. While PIN1 has been clearly implicated in controlling the function of various tumor suppressors such as p53 or pRb and been reported to undergo ATM-mediated phosphorylation upon genotoxic stress, no direct participation in the repair of DNA damage has been investigated[24-26]. Therefore, we aimed at identifying novel phosphorylation-dependent PIN1 targets important for DNA repair. To this end, we performed a mass spectrometry (MS) screen using GST-PIN1 as bait protein. Strikingly, beside a number of known PIN1-interacting proteins, we found a large amount of novel PIN1 interaction partners, amongst them factors previously implicated in various aspects of DNA damage repair (Suppl. Fig. 1 and suppl. table 1). Notably, several known DSB-repair factors including CtIP, BRCA1, MDC1 and 53BP1 were found, which are important determinants previously shown to be able to modulate the balance between homology-directed repair (HDR) and non-homologous end joining (NHEJ)[4,27,28]. Thus, we speculated that PIN1 might affect the choice of DSB repair pathways by binding and isomerising one or several DSB repair factors. To test this hypothesis we performed GFP-reporter assays for both HR and NHEJ in cells depleted for PIN1. DSBs were generated by overexpression of the endonuclease I-*Sce*I and analysed using DR-GFP (for HR) or EJ5-GFP (for NHEJ) reporters in stable HEK293 cells[29]. Depletion of CtIP which is known to decrease HR or 53BP1 and XRCC4, important components of the NHEJ pathway, respectively, served as positive controls[4,27]. Interestingly, the knock-down of PIN1 using different siRNA-oligonucleotides indeed led to a strong reduction in NHEJ efficiency (Fig. 1a). Conversely, while CtIP-depleted cells showed a marked decrease in HR-reporter signal, we observed a slight, but statistically significant, increase in HR-frequency upon knockdown of PIN1 (Fig. 1b). Interestingly, an increased HR rate was previously reported for NHEJ-deficient mouse embryonic stem cells (Ku, XRCC4, and DNA-PKcs), demonstrating that proteins of the NHEJ pathway can have suppressive effects on

HR[30]. Therefore, we postulated that overexpression of PIN1 would interfere negatively with HR-mediated repair of I-*Sce*I induced DSBs. Indeed, we found that overexpression of HA-PIN1-wt dramatically reduced the HR-reporter signal (Fig. 1c). Importantly, the observed decrease in HR frequency was partially dependent on both the WW-domain (W34A) and the PPIase-domain (C113A) of PIN1, pointing out a crucial role of substrate recognition and enzymatic activity, respectively. In fact, PIN1 harboring mutations in the WW-domain such as W34A are unable to bind pSer/Thr-Pro motifs whereas PPIase-domain mutants (C113A) show decreased catalytic cis/trans-isomerisation activity[31,32]. The differences in the efficiency of I-*Sce*I induced DSB repair by HDR were not due to alterations in cell-cycle distribution, as the percentage of cycling cells was similar in all genotypes tested (Suppl. Fig. 2a).

Since CtIP was identified as a specific interaction partner of PIN1 in the MS-screen (Suppl. Fig. 1) and is a fundamental component of the DNA end resection machinery, we next tested whether the defect in NHEJ of PIN1-depleted cells was dependent on the DNA-end resection activity promoted by CtIP[6]. To this end, we depleted both CtIP and PIN1 from HEK293 cells stably expressing the EJ5-GFP reporter and measured repair by NHEJ following expression of I-*Sce*I. Whereas depletion of CtIP led to slight, but not statistically significant, increase in NHEJ efficiency, the co-depletion of CtIP and PIN1 partially rescued the observed NHEJ-defect in PIN1-depleted cells (Figure 1d). Collectively, these strongly indicate that PIN1 negatively affects HDR as measured by GFP-based reporter assays and suggest a functional interaction between CtIP and PIN1.

Since the NHEJ-defects in PIN1-depleted cells were dependent on CtIP, we next examined the underlying molecular mechanism by which this control is exerted. During the process of DNA end resection, replication protein A (RPA) is loaded onto single stranded DNA (ssDNA), where it is then phosphorylated[33]. To determine whether loss of PIN1 affects resection, we first depleted PIN1 transiently from U2OS cells by RNA interference and analysed the ability to resect DNA breaks in response to etoposide. We found that the proportion of hyper-phosphorylated RPA2 was markedly elevated in PIN1-deficient cells compared to luciferase (CNTL)-depleted cells (Fig. 1e), indicative of increased rates of

DNA end resection, while the cell cycle distribution was not altered (Suppl. Fig. 2b). We observed the same phenomenon when we used a pool of 3 different siRNA oligonucleotides to deplete PIN1 from U2OS cells, thus ruling out an siRNA off-target effect (Suppl. Fig. 2d). It is known that the absence of NHEJ factors including Ku and DNA ligase IV leads to a resistance to replication associated DSB, such as those created by camptothecin (CPT), due to the fact that toxic end-joining events triggered by these factors are repressed[34]. Our NHEJ reporter assays revealed that PIN1 might be important for efficient NHEJ similar to the classical end-joining factor XRCC4 or the end-joining promoting factor 53BP1 (Fig 1a)[27]. Thus, we speculated that knockdown of PIN1 would have a similar impact on cell survival upon CPT treatment. Indeed, we found that depletion of PIN1 using two different siRNA oligonucleotides resulted in CPT-resistance identical to XRCC4, unlike knockdown of CtIP, which resulted in marked cellular hypersensitivity (Suppl. Fig. 2c). These results further confirm an important function of PIN1 during the repair of DSBs and show that PIN1 shares some functional features with classic NHEJ factors such as XRCC4.

The marked decrease of PIN1 overexpressing cells in DR-GFP repair (Fig. 1d) prompted us to test whether this defect resulted from diminished DNA resection capacity. Indeed, cells overexpressing PIN1 and treated with ionizing radiation (IR) showed a clear reduction in RPA2 hyperphosphorylation compared to parental cells or to cells expressing a PIN1-binding mutant (W34A) (Fig. 1f and suppl. Fig. 2e). These results further suggest that PIN1 might controls the choice of DSB repair by regulating DNA resection. Finally, to test whether the PIN1-associated increase in DNA resection was dependent on CtIP, we performed siRNA-mediated knockdown of CtIP and PIN1 alone or in combination and assessed the number of cells forming RPA2 foci after etoposide treatment (Suppl. Fig. 2f). As expected and shown previously, depletion of CtIP diminished the number of RPA foci-displaying cells drastically[4]. In contrast, transient knockdown of PIN1 led to a marked increase of RPA foci-forming cells, which was entirely dependent on CtIP, as concomitant depletion of CtIP in these cells decreased the number of RPA2 foci-positive cells to that of CtIP-deficient cells. To further determine whether the absence of PIN1 in cells would

indeed cause a DSB-repair balance shift from NHEJ to HR, we monitored the integrity of DNA during recovery following exposure to etoposide by using pulsed-field gel electrophoresis (PFGE), a technique that allows the separation of intact chromosomes from DSB-induced DNA fragments[35]. To this end, we exposed mouse embryonic fibroblasts (MEFs), derived from PIN1$^{-/-}$ animals and infected with retroviruses expressing either an empty vector (pLPC) or PIN1, to etoposide. As expected, we observed an increase in hyperphosphorylated RPA2 and a concomitant increase in DSB accumulation in PIN1-deficient MEFs compared to PIN1-complemented cells demonstrating that these cells indeed repair DSBs preferentially via HR and therefore with slower repair kinetics (Figure 1g). Collectively, these results indicate that PIN1 promotes repair via NHEJ by actively counteracting CtIP-mediated DNA end resection essential for HR.

PIN1 interacts with CtIP in a phosphorylation-dependent manner

To determine whether PIN1 and CtIP physically interact, thus confirming the results obtained by our mass spectrometry analysis (Suppl. Fig. 1 and suppl. table 1), we subjected whole cell extracts obtained from U2OS cells or U2OS cells stably expressing GFP-CtIP to GST-PIN1 pull-down assays. We found that endogenous as well as a GFP-tagged version of CtIP interact with GST-PIN1-wt but not with the binding mutant GST-PIN1-W34A (Fig. 2a). The importance of the WW-domain of PIN1 for CtIP interaction suggested that phosphorylation of CtIP might be involved in this interaction. Indeed, we found that λ-phosphatase treatment of U2OS cell lysates dramatically reduced the association of CtIP with PIN1 *in vitro* (Suppl. Fig. 3a-b). Next, we assessed CtIP-PIN1 complex formation in HEK293T cells expressing epitope-tagged CtIP and PIN1 after genotoxic stress. Strikingly, compared to untreated cells, we observed an increase in GFP-CtIP-HA-PIN1 interaction in etoposide-treated cells, pointing to a damage-specific regulation of CtIP by PIN1 (Figure 2b). To confirm the interaction between endogenous PIN1 and CtIP, we performed *in situ* proximity ligation assay, an elegant method to detect protein-protein interactions *in situ* with single molecule resolution[36]. By using this method, we were able to readily detect *in situ* CtIP-PIN1 interaction in fixed U2OS cells (Fig. 2c). S-phase cells, labeled by a short pulse with the thymidine analog 5'-Ethynyl-2'-

Ethynyl-2'-deoxyuridine (EdU), overall showed more distinct dots corresponding to single protein-protein interactions compared to EdU-negative cells. Moreover, single fluorescent signals were present only when both primary antibodies against CtIP and PIN1 were used or in non-transfected cells but not in PIN1 down-regulated cells, confirming the specificity of the approach (Suppl. Fig. 3c). These results establish a physical interaction between CtIP and PIN1 *in vivo.* CtIP contains a total of 12 Ser/Thr-Pro motifs that represent potential proline-directed kinase consensus sites and therefore PIN1 binding sites (Suppl. Fig. 3d). Consequently, we evaluated the importance of several Ser/Thr-Pro motifs in PIN1 binding. To this end, we introduced several Ser/Thr→Ala point mutations into CtIP and tested the binding capacity to PIN1 in a GST pull-down experiment (Fig. 2d and Suppl. Fig. 3e-g). Importantly, we found that two well-studied CDK-phosphorylation sites, namely S327 and T847, didn't influence the capacity of PIN1 binding *in vitro* (Suppl. Fig. 3e-f)[12,13,37,38]. Instead, we found that CtIP-S276A substitution mildly affected the PIN1-binding capacity whereas the effect of a second point mutation (T315A) was much stronger (Suppl. Fig. 3g). We next generated a double mutant (CtIP-S276A/T315A= CtIP-2A) and found that the interaction with PIN1 was nearly abolished (Fig. 2d). Consistent with this result, co-immunoprecipitation experiments showed that the interaction between CtIP-2A and PIN1 was greatly reduced in HEK293T cells (Fig. 2e and suppl. Fig. 3h). Finally, by Far Western blotting, we demonstrated that the interaction between PIN1 and CtIP is direct with T315 being the stronger binding site (Fig. 2f and suppl. Fig. 3i). Thus, taken together these results highlight that CtIP and PIN1 interact directly in a phosphorylation-dependent manner both *in vitro* and *in vivo* and indicate a DNA damage-specific regulation of CtIP by PIN1.

PIN1 catalyzes the conformational change of Ser/Thr-Pro motifs in CtIP

We noticed that the two identified PIN1 binding sites of CtIP (S276 and T315) are highly conserved amongst mammals (Suppl. Fig. 4a). To assess whether these sites are indeed phosphorylated *in vivo*, we raised two phospho-specific antibodies. As shown in Fig. 3a, both the antibodies were able to detect FLAG-CtIP-wt expressed in HEK293T cells but not the Ser/Thr→Ala mutants, confirming the specificity of the antibodies. Additionally, we

could determine that endogenous CtIP is phosphorylated at T315 (Fig. 3b). To further confirm the novel identified phosphorylation sites, we performed mass spectrometry analysis using cell endogenous CtIP precipitated from HEK293T cells. Notably, with this approach we were able to confirm pT315-CtIP as an *in vivo* phosphorylation site (Suppl. Fig. 4b). To determine which of the phosphorylation sites had a bigger impact on PIN1 binding we carried out *in vitro* binding-competition experiments (Fig. 3c and suppl. Fig. 4c). To this end, we synthesized the phosphorylated and non-phosphorylated peptides, -ETQGPM(p)SPLGDELY-NH_2 and -FSDSTSK(p)TPPQEEY-NH_2, which were derived from S276-CtIP and T315-CtIP, respectively, and used them to specifically compete for GST-PIN1 binding with CtIP. The T315 phospho-peptide partially competed GST-PIN1 binding with CtIP whereas the phosphorylated S276 peptide as well as both the non-phosphorylated forms failed to do so. Collectively, these results suggest that although both residues are phosphorylated, pT315 is the preferred PIN1 binding site while pS276 might serve as a secondary docking residue and/or isomerisation site.

To determine whether PIN1 was able to catalyze the cis-trans isomerisation at positions S276 and T315 in CtIP we made use of exchange nuclear magnetic resonance (NMR) spectroscopy. To this end, we expressed and purified GST-PIN1-wt and the catalytically inactive mutant GST-PIN1-C113A (Suppl. Fig. 5a). Next, we made use of the above-mentioned S276-CtIP and T315-CtIP peptides and assigned their proton resonances with the help of a set of TOCSY, DQF-COSY and ROESY experiments using standard procedures[39]. For many residues in the proximity of Pro residues two sets of peaks were observed due to the cis and trans isomers about the Ser/Thr-Pro peptide bond, that in absence of PIN1 do not interconvert on the NMR timescale. While signal overlap in the ^{1}H-spectra precludes a reliable estimate of the cis to trans ratio, well-separated signals are observed in the ^{31}P spectra allowing us to calculate the trans:cis ratio as 12-20 and 4 for pT315-CtIP and pS276-CtIP, respectively (Suppl. Fig. 5b). Exchange spectroscopy, in particular rotating-frame nuclear Overhauser spectroscopy (ROESY) was used to monitor the exchange process[40,41]. In the absence of PIN1, ROESY spectra recorded with mixing times of 110 ms were devoid of any cross peak relating signals from the cis with those

from the trans form. After addition of PIN1-wt but not the catalytic dead mutant PIN1-C113A, however, we detected exchange cross peaks in the ROESY spectrum of the phosphorylated S276-CtIP peptide but not in the non-phosphorylated form (Fig. 3d and suppl. Fig. 5c). Surprisingly, we were not able to detect any exchange for the pT315-CtIP peptide in the presence of PIN1-wt (Suppl. Fig. 5d). We noted that this peptide comprises of a TPP sequence motif and hypothesised that the presence of the two consecutive Pro residues in this substrate might hinder PIN1 mediated cis-trans isomerisation, similar to previously published data[42,43]. To confirm this assumption, we synthesized a modified T315-CtIP peptide harboring a Pro→Leu substitution (-FSDSTSK(p)TPLQEEY-NH_2) and observed that the phosphorylated form of this modified pT315-CtIP peptide was isomerised by PIN1 (Suppl. Fig. 5e). These experiments indicate that PIN1 may act as a peptidyl-prolyl isomerase on the pS276-P277 peptide bond and pT315-P316 is not a substrate for PIN1-mediated isomerisation due to the presence of the second Pro residue flanking the pThr-Pro motif. Thus, the phospho-peptide competition experiments together with the NMR spectroscopy studies support a model in which pT315-CtIP is the PIN1 docking site whereas pS276-P277 might represent the proline isomerisation site.

CDK2 mediates CtIP-PIN1-binding

Next, we examined which kinase(s) is/are responsible for S276 and T315 phosphorylation in CtIP. Since CtIP protein levels are regulated in a cell cycle specific manner and several residues are reported to be CDK phosphorylation sites, we tested whether CDK inhibition would interfere with CtIP-PIN1 interaction[12,44,45]. Indeed, we found that treatment of U2OS cells with R-Roscovitine (general CDK inhibitor) but not with RO-3306 (specific CDK1 inhibitor), reduced CtIP binding to PIN1 dramatically *in vitro*, suggesting that a CDK different from CDK1 might be the responsible mediator for the interaction (Fig. 4a and suppl. Fig. 6a). Moreover, treatment of U2OS cells with R-Roscovitine dramatically reduced the phosphorylation of T315-CtIP (Fig. 4b and suppl. Fig. 6b). To further substantiate our findings, we expressed dominant negative (dn) variants of CDK1, 2 and 4 in HEK293T cells and subjected whole cell extracts to GST-PIN1 pull-down assays. Strikingly, we found that expression of CDK1-dn and CDK2-dn affected the interaction *in*

vitro while CDK4-dn had no significant effect (Fig. 4c). However, it is very likely that the reduced CtIP-PIN1 interaction resulting from CDK1-dn expression is due to the abnormal cell cycle distribution of this cell population, as seen from a marked increase in the G2/M population (Suppl. Fig. 6c). In addition, we found that the expression of CDK2-wt in HEK293T cells resulted in a modest increase in CtIP-PIN1 interaction (Suppl. Fig. 6d) and recombinant CDK2 was able to phosphorylate both S276 and T315 residues *in vitro* (Fig. 4d). To further confirm these results, we synchronised U2OS cells by a double thymidine block and analysed phosphorylation of CtIP on T315. As reported previously, we observed a steady increase in CtIP protein levels during S-phase that peak in G2[44]. Interestingly, T315 phosphorylation levels mirrored this pattern with the levels peaking towards late S/G2 (Suppl. Fig. 6e). Thus, we conclude that CDK2 plays an important role in mediating the interaction between CtIP and PIN1 and show supportive evidence for CDK2 being responsible for direct phosphorylation of T315-CtIP.

CtIP–S276A/T315A loss of function mutations cause DNA break hyper-resection and delayed DSB repair kinetics

To assess the potential function of the CtIP-2A mutations (S276A/T315A) and the importance of PIN1-mediated cis/trans isomerisation during the process of DSB repair by HR, we depleted endogenous CtIP from U2OS cell clones stably expressing either GFP-CtIP-wt or GFP-CtIP-2A and assessed their cell cycle distribution (Suppl. Fig. 7a and b). Since PIN1 has been shown to affect protein-protein interactions, we also tested whether CtIP-2A was able to interact with BRCA1 and Mre11, two known CtIP-associating proteins, and found that the interaction with both these factors was not abrogated (Suppl. Fig. 7c)[4,14,45]. In addition, we examined whether the recruitment of the CtIP-2A mutant to laser-induced DSBs was affected (Suppl. Fig. 7d). In agreement with previous published work, we observed that GFP-CtIP-wt was recruited to sites of laser-induced DNA damage exclusively in S/G2 phases of the cell cycle (i.e. in cyclin A-positive cells) and the abrogation of PIN1 interaction did not affect the recruitment of the GFP-CtIP-2A mutant to laser-induced DSBs[4]. We further measured long-term survival of the newly established

CtIP-2A cells upon exposure to CPT by colony formation assays and found that unlike cells expressing CtIP-T847A, unable to resect DNA breaks, or cells depleted for CtIP which are hypersensitive to CPT, CtIP-2A cells were slightly more resistant compared to CtIP-wt expressing cells (Suppl. Fig. 7e). These results indicate that the PIN1-interaction is required neither for the recruitment of CtIP to DSBs nor for the interaction with other HR proteins as well as for long-term survival upon genotoxic stress induced by CPT.

However, as our results suggest that PIN1 regulates DNA end resection and CtIP-PIN1 interaction is increased after genotoxic stress (Fig. 2b and Suppl. Fig. 7f), we analysed the DDR in the GFP-CtIP variant expressing cell lines. To this end, we examined the recovery of wt and CtIP-2A mutant cell lines from DNA damage created by an acute dose of etoposide (Fig. 5a). Interestingly, while the wild-type CtIP-expressing cells showed RPA2 hyper-phosphorylation only 2 hours after etoposide treatment, GFP-CtIP-2A cells displayed marked RPA2 hyper-phosphorylation immediately after the treatment that further increased after 2 hours of release. Furthermore, a substantial increase in CHK1-pS345 and H2AX-pS139 phosphorylation was observed in the CtIP-2A mutant, indicative of defective/altered DSB repair. Similar results were obtained when GFP-CtIP-wt or 2A cells were treated with etoposide and RPA2 foci-positive cells were enumerated by immunofluorescence analysis (Suppl. Fig. 8a). Since RPA2 coating of single-stranded DNA is a mark for DSB processing in the course of HR-mediated DNA repair, the increase in RPA2-positive GFP-CtIP-2A cells together with the marked increase in RPA2 hyperphosphorylation in these cells might indicate increased rates of DNA break resection and thus slower repair kinetics, reminiscent of PIN1 depleted cells[33]. To determine whether the expression of GFP-CtIP-2A in cells indeed affects the repair of DSBs, we monitored the integrity of DNA during recovery following exposure to etoposide by PFGE. Etoposide-induced DSBs are generally rapidly repaired in a NHEJ-dependent manner as evidenced by the absence of any broken DNA 6 hours after acute treatment with Etoposide as well as the persistence of DNA breaks in the presence of DNA-PKcs inhibitor NU-7441 (Suppl. Fig. 8b). Strikingly, exposure to the drug resulted in increased accumulation of DSBs and a slight repair-delay in GFP-CtIP-2A cells compared to wild-type

(Fig. 5b, compare lanes 2-3 to lanes 8-9). Moreover, the increase in DSB accumulation in CtIP-2A-expressing cells correlated with increased DNA end resection (hyperphosphorylated RPA2) indicating that NHEJ-dependent repair is partially blocked in these cells. This notion is supported by the fact that co-treatment with the DNA-PKcs inhibitor NU-7441 resulted in a massive increase in DSB-formation in CtIP-2A cells compared to wt (Fig. 5b, compare lanes 5-6 to lanes 11-12). Collectively, these data demonstrate that PIN1-mediated regulation of CtIP is responsible for limiting DSB resection and hence promoting repair by NHEJ.

PIN1 plays an important role in regulating the turnover of multiple proteins[23]. We observed that CtIP levels fluctuate in I-*Sce*I expressing HEK293 GFP-reporter cells (Fig. 1b-d, lower panels) and speculated therefore that PIN1 might regulate CtIP protein turnover specifically after genotoxic stress thereby facilitating DSB repair via NHEJ. In fact, CtIP protein levels seemed to correlate with the efficiency of HR repair. This observation might indicate that PIN1 regulate CtIP protein levels or turnover upon genotoxic stress as it was shown previously for other PIN1 targets[17,46]. To solidify this assumption, we exposed our established GFP-CtIP cell lines expressing either wild type CtIP or the PIN1-interaction mutant CtIP-2A to etoposide and analysed CtIP protein turnover via cycloheximide-mediated block of *de novo* protein synthesis. Strikingly, GFP-CtIP-wt protein levels rapidly dropped after etoposide treatment and release in cycloheximide-containing media whereas the CtIP-2A protein persisted even 4 hours after the release indicating that PIN1 indeed controls CtIP protein turnover after genotoxic insults (Fig. 5c). Moreover, treatment of cells expressing wild type CtIP with the proteasome inhibitor MG-132 resulted in rapid CtIP accumulation demonstrating a proteasome-mediated protein turnover. Strikingly, the impact of MG-132 treatment on CtIP-2A protein levels was much lower further demonstrating a crucial role for PIN1 in promoting CtIP degradation via the ubiquitin-proteasome pathway (Suppl. Fig. 8c).

Collectively, these data point to a model in which PIN1 controls the repair of DSBs via CtIP-mediated isomerisation. The enhanced PIN1-CtIP interaction upon genotoxic insults indicates that PIN1 triggers CtIP protein degradation thus promoting repair via NHEJ. We

therefore propose that PIN1 is an important determinant influencing the DSB repair pathway choice by regulating CtIP.

Here we show that human PIN1 interacts with multiple factors crucial for the successful repair of DNA-DSBs. We demonstrate that PIN1 can influence the DSB-repair pathway choice by facilitating NHEJ-mediated repair. In fact, absence of PIN1 results in increased HR frequency accompanied with overall higher rates of DNA end resection as a result of more stable CtIP protein (Fig 5d, left part). Consequently, in cells overexpressing PIN1 repair via NHEJ predominates due to lower CtIP levels (Fig. 5d, right part). Moreover, we provide strong evidence that PIN1 and CtIP interact both *in vitro* and *in vivo* in a phosphorylation-dependent manner and show that the NHEJ-defect of PIN1-depleted cells is partially CtIP-dependent. Whether PIN1 controls one or more targets other than CtIP to determine which DSB-repair pathway is chosen to accomplish repair has to be addressed in future studies. Since both BRCA1 and 53BP1 have been previously shown to influence DSB-repair pathway choice and both proteins contain multiple putative PIN1 binding sites (Ser/Thr-Pro motifs) it is tempting to speculate that PIN1 might additionally control the function of these factors by protein isomerisation[27].

We further demonstrate that the two residues S276 and T315 on CtIP are crucial for PIN1-interaction. We identify CDK2 as the candidate kinase responsible for the phosphorylation of T315 *in vivo* and S276 *in vitro.* Whether CDK2 or another kinase is responsible for the phosphorylation of S276 *in vivo* remains unclear. Since the interaction between PIN1 and CtIP is enhanced upon genotoxic stress (Figure 2b and suppl. Fig. 7f), it is very likely that a stress-induced kinase (e.g. SAPK, p38MAPK, JNK) might be the mediator. In addition, it remains possible that the interaction depends on DNA damage-induced posttranslational modifications on PIN1[26]. Future studies are needed to address these unsolved issues.

Finally, our data demonstrate that cells deficient for PIN1 and cells overexpressing mutant CtIP (CtIP-2A) unable to interact with PIN1 display delayed repair kinetics of DSBs as a consequence of enhanced rates of DNA end resection. These data implicate that PIN1-mediated isomerisation of CtIP is required to determine the choice between NHEJ-

mediated repair and HR. Since the recruitment of CtIP to DSBs is not PIN1 dependent (Suppl. Fig. 7d), yet the interaction between the two proteins is DNA damage-dependent, two possible scenarios can be envisaged. First, CtIP is recruited to DSBs and consequently PIN1 facilitates the removal from damaged chromatin by directly triggering protein degradation via the ubiquitin-proteasome pathway. Alternatively, one or more accessory factors of modifications on CtIP are needed to release the protein from chromatin and PIN1-mediated protein isomerisation subsequently results in rapid CtIP degradation. Future investigations are needed to solve these open questions.

Collectively, our data identify PIN1 as a novel, crucial determinant involved in the repair of DSBs and demonstrate for the first time that PIN1-mediated isomerisation could be a general mechanism used to govern the spatio-temporal regulation of protein phosphorylation/dephosphorylation events during DNA repair. The findings of our study are summarised in a simplified model in Fig. 5d.

Materials and Methods

Cell culture, compounds and treatments

U2OS, HEK293T, PIN1$^{-/-}$ MEFs and HEK293T retroviral packaging cells (PNX-Eco, gifts from Giannino del Sal, LNCIB, Trieste) were maintained at 37°C in Dulbecco's modified Eagle's medium (DMEM, Gibco) supplemented with 10 % fetal calf serum (Gibco), 100 U/ml penicillin and 100 µg/ml streptomycin (Sigma). Human U2OS cells stably expressing GFP-CtIP were cultured in DMEM supplemented with 10% fetal calf serum, standard antibiotics and 0.5mg/ml G-418 (Gibco).

RO-3306, R-Roscovitine (Calbiochem), Etoposide and Camptothecin (SIGMA) were solubilised in DMSO at 10 mM stock concentration and used as specified. EdU (5-ethynyl-2'-deoxyuridine) was from Invitrogen. The DNA-PKcs inhibitor NU7441 (Tocris Bioscience) was dissolved in DMSO at 5 mM stock concentration[47].

Retroviral infection

Phoenix packaging cells were transfected with the indicated vectors by a standard calcium phosphate method. After 48 h incubation at 32 °C, the supernatants containing viral particles were collected, filtered, supplemented with 8 µg/ml polybrene, and used to infect PIN1$^{-/-}$ MEFs. After infection, cells were selected for 2-4 days in puromycin (2 µg/ml), the polyclonal populations of infected cells were analysed for PIN1 expression, expanded and further processed.

Plasmids

The pEGFP-C1 and the pcDNA3.1 plasmids encoding siRNA-resistant FLAG- or GFP-tagged CtIP wt and ΔC mutant were described previously.[4,48] The construct for bacterial expression of recombinant GST-tagged PIN1 (pGEX4T3) was a kind gift from Christopher Nelson (University of Victoria, Canada). pBABE, pLPC as well as pcDNA3.1 plasmids containing PIN1 (wt, C113A, S67E, W34A) were a gift from Dr. Giannino del Sal (LNCIB, Italy). pUHD10-3 vectors containing dominant negative HA-CDK1, HA-CDK4, HA-CDK5 or HA-CDK2 (wt and D146N) were purchased from Addgene. The pCBASce vector containing

I-*Sce*I was a gift from Dr. J.M. Stark (Beckman Research Institute of City of Hope, Duarte, CA). The pGEX4T1 construct for bacterial expression of recombinant GST-tagged CtIP (45-371) was described previously.[4] All other single amino acid substitution mutants of CtIP and PIN1 were obtained by site-directed mutagenesis PCR following manufacturer's instructions (Expand Long Template, Roche). All of the constructs were confirmed by DNA sequencing.

For generation of cell lines stably expressing siRNA-resistant GFP-tagged wild-type and mutant CtIP, U2OS cells were transfected with the appropriate constructs and, following antibiotic selection, resistant clones were tested for expression and nuclear localization of the transgene-product by immunofluorescence microscopy.

Plasmid and siRNA transfections

See table S2 for used siRNA oligonucleotides. Cells were transfected with siRNA (final concentration 40nM), using Lipofectamine RNAiMAX according to manufacturer's instructions (Invitrogen). Experiments were performed either 48 h or 72 h after transfection. Plasmids were transfected either by using the standard calcium phosphate method or FuGene 6 (Roche) according to manufacturer's instructions.

RNA interference sequences

The following RNA interference were purchased from Microsynth: luciferase (5'-CGUACGCGGAAUACUUCGA-3'), CtIP (5'-GCUAAAACAGGAACGAAUC-3'; Ref [4]), PIN1-3'UTR (5'-CCGUCACACAGUAUUUAUU-3'), PIN1_2 (5'-GCUACAUCCAGAAGAUCAA-3', Ref [49]) and XRCC4 (5'-AUAUGUUGGUGAACUGAGA-3'). TP53BP1 (5'-CAGGACAGTCTTTCCACGAAT-3') was purchased from Qiagen and PIN1-smartpool from Dharmacon (L-003291-00-0005).

Antibodies

The primary antibodies used in this study are listed in supporting table 1 (supplemental information). Secondary HRP-conjugated anti-mouse and anti-rabbit antibodies were form GE-Healthcare and the HRP-conjugated anti-goat was from Santa Cruz Biotech. Alexa Fluor-488, -594, and -647-conjugated secondary antibodies were from Invitrogen.

CtIP phospho-antibodies (pS276- ETQGPMpSPLGDEL and pT315- SDSTSKpTPPQEE) were obtained from eurogentec.

Phosphatase treatment, *in vitro* binding, immunoprecipitation, western blot and far western

For *in vitro* GST pulldown assays and Immunoprecipitation assays cells were lysed in NP-40 extraction buffer (Tris-HCl pH 7.5, 50 mM; NaCl, 120 mM; NaF, 20 mM; EDTA, 1 mM; EGTA, 6 mM; sodium pyrophosphate, 15 mM; NP-40, 1%; supplemented with 1 mM benzamidine, 0.1 mM PMSF and 1 mM sodium orthovanadate) or in RIPA buffer (Tris-HCl pH 7.4, 50 mM; NP-40, 1%; Sodium deoxycholate, 0.25 %; NaCl, 150 mM; EDTA, 1 mM; supplemented with 0.1% SDS, 1 mM benzamidine, 0.1 mM PMSF, and 1 mM sodium orthovanadate) and clarified by centrifugation at 14000 rpm. For PIN1 immunoprecipitations cells were lysed in modified NP-40 buffer (HEPES pH 7.5, 10 mM; NaCl, 250 mM; NP-40, 0.1%; EDTA, 5mM; supplemented with 0.5 mM DTT, 0.05 % SDS, 1mM benzamidine, 0.1mM PMSF and 1mM sodium orthovanadate). In the case of phosphatase treatment, phosphatase inhibitors were omitted in the RIPA buffer, λ-phosphatase (400 U ml^{-1}) was added to cell extracts and the reaction was continued for 1 h at 30°C, according to the manufacturer's instructions (New England Biolabs) before GST pulldown.

GST pull-down experiments were performed by incubating cell lysates for 2 h at 4°C with 20 µl Glutathione-Sepharose 4B beads (GE Healthcare) loaded with GST–Pin1 and bound proteins were loaded and separated in SDS-PAGE followed by western blotting on nitro-cellulose membranes (Amersham).

For immunoprecipitation assays, the indicated antibody was added to the cell lysate and incubated over night at 4°C with gentle shaking. The following day, antibodies were trapped by incubating the lysates with sepharose A/G beads (GE Healthcare) for 2 h at 4°C. Subsequently the beads were washed 4 times with NP-40 or RIPA extraction buffer and bound proteins were eluted with SDS-PAGE sample buffer, separated by SDS-PAGE followed by western blotting. Proteins were visualised using the ECL detection system (Amersham).

Far-western blot analysis was performed as described previously[50]. Briefly, proteins were immunoprecipitated with the indicated antibody, resolved by SDS-PAGE and blotted onto a nitrocellulose membrane. After re-naturation of the proteins, the membrane was incubated with purified GST-PIN1 protein and bound proteins visualised by standard western blotting. Densitometric values of protein levels in western blot analyses were obtained by Image J software.

Immunocytochemistry, laser microirradiation and flow cytometry

For immunocytochemistry, cells grown on cover slips were either fixed directly in 4% Formaldehyde for 10-15 minutes and permeabilised in PBS/0.5% Triton or underwent pre-extraction for 10 min on ice (25 mM HEPES pH 7.4, 50 mM NaCl, 1 mM EDTA, 3 mM $MgCl_2$, 300 mM sucrose and 0.5% Triton) prior to fixation in 4% Formaldehyde. After washing 3 times in PBS and blocking in PBS/3% non-fat dry milk (blocking solution), cover slips were incubated for 2h at room temperature with the appropriate primary antibodies diluted in blocking solution. Upon thorough washing with blocking solution, cells were incubated with Alexa–conjugated secondary antibodies (Invitrogen) for 1 h at room temperature. The cover slips were then mounted with DAPI containing Vectashield® (Vector Labs) and sealed. Images were taken on a Leica confocal SP2 microscope. *In situ* proximity ligation assay (PLA®, Olink Bioscience) was performed according to manufacturer's instructions. Laser microirradiation was performed as described previously[51].

For flow cytometry, cells were harvested by trypsinization and after washing in PBS fixed in 70% Ethanol for at least 30 minutes on ice. After an additional wash in PBS, cells were treated with 100 µg/ml RNase A and stained with propidium iodide (20 µg/ml) for 30 minutes at room temperature. Subsequently cells were analysed on a CyAn ADP 9 flow cytometer (Dako).

Homologous recombination and non-homologous end joining reporter assays

To measure homology-directed repair and non-homologous end joining in DR-GFP and EJ5 GFP-reporter HEK293 cells, 0.55×10^6 cells were plated in a 6-well dish (poly-L-lysine

coated). After 24 h, siRNA knockdown was carried out against negative control (CNTL, luciferase), CtIP, 53BP1, XRCC4, PIN1-3'UTR (PIN1), PIN1-smartpool (PIN1-SP), PIN1_2 or a combination of PIN1-3'UTR and CtIP (all 40 nM). The next day, 0.2×10^6 cells were plated per 12-well plate (poly-L-lysine coated) and 24 h later transfection with 0.6 µg of an I-*Sce*I expression plasmid (pCBASce) or mock transfection (pcDNA3.1) was carried out using 1.2 µl of JetPrime (Polyplus). 4 h after the plasmid transfection the media was replaced with fresh one followed by a second siRNA transfection against the indicated transcript (15nM). 48 h later cells were analysed by flow cytometry on a CyAn ADP 9 (Dako). Maintenance of the DR–GFP and EJ5-GFP HEK293 cell line, culture conditions and FACS analysis were carried out as described previously[29].

Expression and purification of GST-PIN1

GST-PIN1 (wt, W34A, C113A) were produced in E. coli (BL21) after induction of protein expression by IPTG for 20 h at 16°C. After centrifugation, the bacterial pellet was re-suspended in cold PBS supplemented 0.2 % Triton X-100 and with protease inhibitors (1 mM PMSF, 1 mM benzamidine and Roche protease inhibitor cocktail). After sonication and solubilization, the insoluble fraction was removed by centrifugation. GST-PIN1 was then purified loading the surnatant on a FPLC packed with Glutathione-Sepharose 4B beads (GE Healthcare) according to manufacturer's instructions.

***In vitro* kinase assay**

Bacterially expressed GST-CtIP (residues 45-371) loaded onto GST-sepharose beads was incubated in kinase reaction buffer (100 mM NaCl, 50 mM Tris-HCl, 10 mM $MgCl_2$, 1 mM DTT, 0.5 mM sodium orthovanadate, 5 mM *para*-nitrophenylphosphate, 150 µM ATP, 200 ng CDK2/CyclinE (purchased from proteinkinase.de)) for 1 h at 37°C. The products of the kinase reaction were separated by SDS-PAGE and visualised by western blotting using phospho-specific antibodies against CtIP.

Pulsed field gel electrophoresis

At indicated time points after exposure to Etoposide, cells were collected by

trypsinization, and agarose plugs containing 10^7 cells were prepared using CHEF disposable plug moulds (BioRad). Plugs with cells were processed as described previously before agarose gel electrophoresis[35]. The electrophoresis was carried out for 21 h at 14 °C, with 0.9 % agarose containing 0.5x TBE, using a CHEF-DR III apparatus (BioRad) with the following parameters: first block, 9 h; included angle 120°, 5.5 V cm^{-1}, intervals (switch) 30 s to 5 s; second block, 6 h; included angle 117°, 4.5 V cm^{-1}, intervals (switch) 18 s to 9 s; third block, 6 h; included angle 112°, 4.5 V cm^{-1}, intervals (switch) 9 s to 5 s. The gels were stained with ethidium bromide and analysed using a CCD camera (BioRad) and quantified by Image J software.

NMR sample preparation, measurements and data interpretations

Phosphorylated and non-phosphorylated CtIP peptides ((p)S276- ETQGPM(p)SPLGDELY-NH_2, (p)T315 -FSDSTSK(p)TPPQEEY-NH_2 and (p)-T315-P317L (-FSDSTSK(p)TPLQEEY-NH_2) were purchased from Bachem. Unless stated otherwise all NMR samples contained 2.4 mM solutions of the respective CtIP peptide (phosphorylated or non-phosphorylated) in 20 mM sodium phosphate buffer at pH 6.5. To these solutions PIN1-wt or the mutant or PIN1-C113A were added at a concentration of 30 µM.

All ^{1}H-detected spectra were acquired on Bruker AV-600 or AV-700 spectrometer equipped with triple-resonance cryoprobes. The ^{31}P spectra were recorded on a Bruker AV2-500 spectrometer equipped with a QNP cryoprobe. All NMR experiments were conducted at 298K, except when stated otherwise, and water suppression was achieved by presaturation. Experimental data were processed under Topspin 2.1 and analysed further in XEASY[52].

Resonance assignment was achieved based on 75 ms TOCSY, DQF-COSY and 110 ms ROESY spectra[40,53,54]. All spectra were acquired with 2048 x 256 complex points, using a spectral width of 5400 Hz in both dimensions, 16 to 32 scans per increment and a 2 s interscan delay. ^{31}P-spectra were acquired with ^{1}H-decoupling, 512 scans per experiment and an interscan delay of 3 s. Two-dimensional [^{31}P, ^{31}P]-EXSY spectra were typically acquired with 1024 x 32 complex points, using a spectral width of 500 Hz in both dimensions, 256 scans per increment, a 2 s interscan delay, and a mixing time of 110 ms.

Mass Spectrometry analysis, database searching and criteria for protein identification

Following separation of the proteins of interest by SDS-PAGE, the gel was stained either by colloidal commassie blue or by silver staining. Gel parts of interest were sliced out and washed 3 times with 50 % acetonitrile (ACN) followed by drying of the material using a Speed-Vac centrifuge (Eppendorf). For reduction of disulphide bridges, the gel pieces were incubated for 45 minutes at 56 °C in 25 mM ammonium-bicarbonate (NH_4HCO_3) buffer containing 10 mM DTT. Cysteines were alkylated by iodoacetamide (50 mM) treatment for 1 hour in the dark. After additional washing in 50 % ACN gel pieces were dried and in-gel tryptic digestion carried out over night at 37 °C in 25 mM NH_4HCO_3-buffer containing 1 ng/µl of trypsin (Trypsin Gold, Promega). The next day, the peptides resulting form tryptic digestion were dried, resuspended in 5 % ACN containing 0.1 % formaldehyde and further purified using C18-resin containing ZipTips according to manufacturer's instructions (millipore).

Tandem mass spectra were extracted, charge state deconvoluted and deisotoped by Mascot Distiller version 1.1. All MS/MS samples were analysed using Mascot (Matrix Science, London, UK; version Mascot). Mascot was set up to search the fgcz_9606_20080923 database (September 2009, 53323 entries) assuming the digestion enzyme non-specific. Mascot was searched with a fragment ion mass tolerance of 0.80 Da and a parent ion tolerance of 10.0 ppm. Iodoacetamide derivative of cysteine was specified in Mascot as a fixed modification. Oxidation of methionine and phosphorylation of serine, threonine and tyrosine were specified in Mascot as variable modifications.

Scaffold (version Scaffold 3.3.1, Proteome Software Inc., Portland, OR) was used to validate MS/MS based peptide and protein identifications. Peptide identifications were accepted if they could be established at greater than 95.0% probability as specified by the Peptide Prophet algorithm[55]. Protein identifications were accepted if they could be established at greater than 99.0% probability and contained at least 1 identified peptide. Protein probabilities were assigned using the Protein Prophet algorithm[56]. Proteins that contained similar peptides and could not be differentiated based on MS/MS analysis alone were grouped to satisfy the principles of parsimony.

Statistics

Statistical analyses were carried out using unpaired, two-tailed t-tests. P values expressed as * ($P<0.05$), ** ($P<0.001$) and *** ($P<0.0001$) were considered significant.

References

1. Jackson, S.P. & Bartek, J. The DNA-damage response in human biology and disease. *Nature* 461, 1071-8 (2009).
2. Ciccia, A. & Elledge, S.J. The DNA damage response: making it safe to play with knives. *Molecular cell* 40, 179-204 (2010).
3. Mimitou, E.P. & Symington, L.S. DNA end resection--unraveling the tail. *DNA repair* 10, 344-8 (2011).
4. Sartori, A.A. et al. Human CtIP promotes DNA end resection. *Nature* 450, 509-14 (2007).
5. Takeda, S., Nakamura, K., Taniguchi, Y. & Paull, T.T. Ctp1/CtIP and the MRN complex collaborate in the initial steps of homologous recombination. *Molecular cell* 28, 351-2 (2007).
6. You, Z. et al. CtIP links DNA double-strand break sensing to resection. *Molecular cell* 36, 954-69 (2009).
7. You, Z. & Bailis, J.M. DNA damage and decisions: CtIP coordinates DNA repair and cell cycle checkpoints. *Trends in cell biology* 20, 402-9 (2010).
8. Chen, P.L. et al. Inactivation of CtIP leads to early embryonic lethality mediated by G1 restraint and to tumorigenesis by haploid insufficiency. *Molecular and cellular biology* 25, 3535-42 (2005).
9. Aylon, Y. & Kupiec, M. Cell cycle-dependent regulation of double-strand break repair: a role for the CDK. *Cell cycle* 4, 259-61 (2005).
10. Blume-Jensen, P. & Hunter, T. Oncogenic kinase signalling. *Nature* 411, 355-65 (2001).
11. Buis, J., Stoneham, T., Spehalski, E. & Ferguson, D.O. Mre11 regulates CtIP-dependent double-strand break repair by interaction with CDK2. *Nature structural & molecular biology* 19, 246-52 (2012).
12. Huertas, P. & Jackson, S.P. Human CtIP mediates cell cycle control of DNA end resection and double strand break repair. *The Journal of biological chemistry* 284, 9558-65 (2009).
13. Yun, M.H. & Hiom, K. CtIP-BRCA1 modulates the choice of DNA double-strand-break repair pathway throughout the cell cycle. *Nature* 459, 460-3 (2009).
14. Lu, K.P. & Zhou, X.Z. The prolyl isomerase PIN1: a pivotal new twist in phosphorylation signalling and disease. *Nature reviews. Molecular cell biology* 8, 904-16 (2007).
15. Yeh, E.S. & Means, A.R. PIN1, the cell cycle and cancer. *Nature reviews. Cancer* 7, 381-8 (2007).
16. Zacchi, P. et al. The prolyl isomerase Pin1 reveals a mechanism to control p53 functions after genotoxic insults. *Nature* 419, 853-7 (2002).
17. Mantovani, F. et al. Pin1 links the activities of c-Abl and p300 in regulating p73 function. *Molecular cell* 14, 625-36 (2004).
18. Liou, Y.C. et al. Loss of Pin1 function in the mouse causes phenotypes resembling cyclin D1-null phenotypes. *Proceedings of the National Academy of Sciences of the United States of America* 99, 1335-40 (2002).
19. Ryo, A., Nakamura, M., Wulf, G., Liou, Y.C. & Lu, K.P. Pin1 regulates turnover and subcellular localization of beta-catenin by inhibiting its interaction with APC. *Nature cell biology* 3, 793-801 (2001).
20. Yeh, E.S., Lew, B.O. & Means, A.R. The loss of PIN1 deregulates cyclin E and sensitizes mouse embryo fibroblasts to genomic instability. *The Journal of biological chemistry* 281, 241-51 (2006).

21. Bao, L. et al. Prevalent overexpression of prolyl isomerase Pin1 in human cancers. *The American journal of pathology* 164, 1727-37 (2004).
22. Pastorino, L. et al. The prolyl isomerase Pin1 regulates amyloid precursor protein processing and amyloid-beta production. *Nature* 440, 528-34 (2006).
23. Liou, Y.C., Zhou, X.Z. & Lu, K.P. Prolyl isomerase Pin1 as a molecular switch to determine the fate of phosphoproteins. *Trends in biochemical sciences* 36, 501-14 (2011).
24. Girardini, J.E. et al. A Pin1/mutant p53 axis promotes aggressiveness in breast cancer. *Cancer cell* 20, 79-91 (2011).
25. Rizzolio, F. et al. Retinoblastoma tumor-suppressor protein phosphorylation and inactivation depend on direct interaction with Pin1. *Cell death and differentiation* 19, 1152-61 (2012).
26. Matsuoka, S. et al. ATM and ATR substrate analysis reveals extensive protein networks responsive to DNA damage. *Science* 316, 1160-6 (2007).
27. Bunting, S.F. et al. 53BP1 inhibits homologous recombination in Brca1-deficient cells by blocking resection of DNA breaks. *Cell* 141, 243-54 (2010).
28. Stucki, M. et al. MDC1 directly binds phosphorylated histone H2AX to regulate cellular responses to DNA double-strand breaks. *Cell* 123, 1213-26 (2005).
29. Bennardo, N., Cheng, A., Huang, N. & Stark, J.M. Alternative-NHEJ is a mechanistically distinct pathway of mammalian chromosome break repair. *PLoS genetics* 4, e1000110 (2008).
30. Pierce, A.J., Hu, P., Han, M., Ellis, N. & Jasin, M. Ku DNA end-binding protein modulates homologous repair of double-strand breaks in mammalian cells. *Genes & development* 15, 3237-42 (2001).
31. Shen, M., Stukenberg, P.T., Kirschner, M.W. & Lu, K.P. The essential mitotic peptidyl-prolyl isomerase Pin1 binds and regulates mitosis-specific phosphoproteins. *Genes & development* 12, 706-20 (1998).
32. Lu, P.J., Zhou, X.Z., Shen, M. & Lu, K.P. Function of WW domains as phosphoserine- or phosphothreonine-binding modules. *Science* 283, 1325-8 (1999).
33. Jazayeri, A. et al. ATM- and cell cycle-dependent regulation of ATR in response to DNA double-strand breaks. *Nature cell biology* 8, 37-45 (2006).
34. Adachi, N., So, S. & Koyama, H. Loss of nonhomologous end joining confers camptothecin resistance in DT40 cells. Implications for the repair of topoisomerase I-mediated DNA damage. *The Journal of biological chemistry* 279, 37343-8 (2004).
35. Hanada, K. et al. The structure-specific endonuclease Mus81 contributes to replication restart by generating double-strand DNA breaks. *Nature structural & molecular biology* 14, 1096-104 (2007).
36. Soderberg, O. et al. Direct observation of individual endogenous protein complexes in situ by proximity ligation. *Nature methods* 3, 995-1000 (2006).
37. Huertas, P., Cortes-Ledesma, F., Sartori, A.A., Aguilera, A. & Jackson, S.P. CDK targets Sae2 to control DNA-end resection and homologous recombination. *Nature* 455, 689-92 (2008).
38. Nakamura, K. et al. Collaborative action of Brca1 and CtIP in elimination of covalent modifications from double-strand breaks to facilitate subsequent break repair. *PLoS genetics* 6, e1000828 (2010).
39. Wüthrich, A. *NMR of Proteins and Nucleic Acids*, (Wiley-Interscience, New York, 1986).
40. Bothner-By, A.A., Stephens, R.L., Lee, J., Warren, C.D. & Jeanloz, R.W. Structure determination of a tetrasaccharide: transient nuclear Overhauser effects in the rotating frame. *J. Am. Chem. Soc.* 106, 811-813 (1984).

41. **Bax, A., Davis, D.G. Practical aspects of two-dimensional transverse NOE spectroscopy. *J. Magn. Reson.* 63, 207-213 (1985).**
42. **Smet, C., Wieruszeski, J.M., Buee, L., Landrieu, I. & Lippens, G. Regulation of Pin1 peptidyl-prolyl cis/trans isomerase activity by its WW binding module on a multi-phosphorylated peptide of Tau protein. *FEBS letters* 579, 4159-64 (2005).**
43. **Lippens, G., Landrieu, I. & Smet, C. Molecular mechanisms of the phospho-dependent prolyl cis/trans isomerase Pin1. *The FEBS journal* 274, 5211-22 (2007).**
44. **Yu, X. & Baer, R. Nuclear localization and cell cycle-specific expression of CtIP, a protein that associates with the BRCA1 tumor suppressor. *The Journal of biological chemistry* 275, 18541-9 (2000).**
45. **Yu, X. & Chen, J. DNA damage-induced cell cycle checkpoint control requires CtIP, a phosphorylation-dependent binding partner of BRCA1 C-terminal domains. *Molecular and cellular biology* 24, 9478-86 (2004).**
46. **Mantovani, F. et al. The prolyl isomerase Pin1 orchestrates p53 acetylation and dissociation from the apoptosis inhibitor iASPP. *Nature structural & molecular biology* 14, 912-20 (2007).**
47. **Leahy, J.J. et al. Identification of a highly potent and selective DNA-dependent protein kinase (DNA-PK) inhibitor (NU7441) by screening of chromenone libraries. *Bioorg Med Chem Lett* 14, 6083-7 (2004).**
48. **Yu, X., Fu, S., Lai, M., Baer, R. & Chen, J. BRCA1 ubiquitinates its phosphorylation-dependent binding partner CtIP. *Genes & development* 20, 1721-6 (2006).**
49. **Phan, R.T., Saito, M., Kitagawa, Y., Means, A.R. & Dalla-Favera, R. Genotoxic stress regulates expression of the proto-oncogene Bcl6 in germinal center B cells. *Nature immunology* 8, 1132-9 (2007).**
50. **Wu, Y., Li, Q. & Chen, X.Z. Detecting protein-protein interactions by Far western blotting. *Nature protocols* 2, 3278-84 (2007).**
51. **Eid, W. et al. DNA end resection by CtIP and exonuclease 1 prevents genomic instability. *EMBO reports* 11, 962-8 (2010).**
52. **Bartels, C., Xia, T.-H., Billeter, M., Güntert, P. and Wüthrich, K. . The program XEASY for computer-supported NMR spectral analysis of biological macromolecules. *J. Biomolecular NMR* 5, 1-10 (1995).**
53. **Bax, A.D., Davis, D.G. MLEV-17-based two-dimensional homonuclear magnetization transfer spectroscopy. *Journal of Magnetic Resonance* 65, 355-360 (1985).**
54. **Rance, M., Sorensen, O. W., Bodenhausen, G., Wagner G., Ernst R. R., Wüthrich, K. *Biochem. Biophys. Res. Commun.* 117, 479-485 (1983).**
55. **Keller, A., Nesvizhskii, A.I., Kolker, E. & Aebersold, R. Empirical statistical model to estimate the accuracy of peptide identifications made by MS/MS and database search. *Analytical chemistry* 74, 5383-92 (2002).**
56. **Nesvizhskii, A.I., Keller, A., Kolker, E. & Aebersold, R. A statistical model for identifying proteins by tandem mass spectrometry. *Analytical chemistry* 75, 4646-58 (2003).**

Figure legends

Figure 1. PIN1 regulates the choice of DSB repair pathways

(a, b and d) Readout of homologous recombination (HR) and non-homologous end-joining (NHEJ) GFP-reporter assays after treatment with indicated siRNAs; CtIP, XRCC4 and 53BP1 served as positive controls. Western blot analyses of I-*Sce*I treated cells are represented. (c) HR assay and immunoblot analysis as in (b) but with overexpression of HA-PIN1 variants (wt, W34A or C113A). (e) Luciferase (CNTL)- or PIN1-depleted U2OS cells (48 h) were treated with etoposide (ETOP) and cell extracts analysed by western blotting. Asterisks indicate hyperphosphorylated forms of CtIP and RPA2. (f) HEK293T cells were transfected with an empty vector (EV= pcDNA3.1) or HA-PIN1, 72 h later treated with ionizing radiation (IR) and released for 1 h or 3 h. Whole cell extracts were analysed by immunoblotting. Asterisk indicates hyperphosphorylated form of RPA2. (g) MEFs derived from $PIN1^{-/-}$ animals were complemented by retroviral infection with pLPC empty vector (EV) or PIN1. After selection in puromycin (2 µg/ml) the polyclonal population was treated with etoposide (ETOP) and lysed or released in fresh media for 30 minutes and 120 minutes. The amount of broken DNA was assessed by PFGE (lower part) and whole cell extracts for the same time-points were used for immunoblotting using the indicated antibodies (upper part). Asterisk indicates unspecific band recognized by the CtIP antibody. Abbreviations: HR: homologous recombination, NHEJ: Non-homologous end-joining, PIN1-SP: PIN1-smartpool. Error bars, s.e.m. * $P<0.05$, ** $P<0.001$, *** $P<0.0001$.

Figure 2. CtIP interacts with PIN1 through phosphorylated Ser/Thr-Pro motifs.

(a) Immobilised GST-PIN1 was incubated with whole cell extracts (WCEs) of U2OS cells (lanes 2-3) or U2OS cells stably expressing GFP-CtIP (lanes 5-6) and bead fractions were subjected to immunoblotting with α-CtIP antibodies. GST-PIN1-W34A was used as negative control. Ponceau staining is shown to illustrate that equal amounts of GST-PIN1 were used (b) HEK293T cells transfected with GFP-CtIP and HA-PIN1 (wt or W34A) for 48 h were mock treated or with 10 µM etoposide (ETOP) for 2 h and whole cell lysates were used for co-immunoprecipitations using α-GFP antibodies. Immunocomplexes were

separated on SDS-PAGE and indicated proteins visualised by western blotting. Asterisk indicates immunoglobulin light chain recognized by the HA antibody. (c) *Left,* detection of endogenous PIN1 and CtIP complexes by *in situ* polymerase-linked assay (PLA). U2OS cells were pulse-labeled for 15 minutes with 5'-Ethynyl-2'-deoxyuridine (EdU, 10μM), fixed and incubated with antibodies against PIN1 and CtIP and protein-protein interactions were detected using fluorescence labeled probes (PLA-613). Nuclei were visualised by DAPI-staining. EdU detection was carried out according to manufacturer's instructions. *Right,* quantification of the PLA signals/cell. For each condition (EdU- and EdU+) the PLA signals from at least 50 cells were enumerated. The experiment was repeated trice and the indicated results represent the quantification of one representative experiment (d) *Left*, GST-PIN1 pull-down using WCEs of HEK293T cells expressing FLAG-tagged CtIP-wt, CtIP-S276A, CtIP-T315A and CtIP-2A (S276A/T315A). The signal intensities were quantified using Image J and represented as ratio Input/pull-down (I/P). *Right*, Mean values of densitometry quantification from 3 independent experiments with error bars ± sem. (e) HEK293T cells were transfected with HA-PIN1 and FLAG-CtIP (wt, S276A, T315A and 2A). WCEs were used for co-immunoprecipitations using α-HA antibodies followed by immunoblotting with the indicated antibodies. (f) Anti-FLAG immunoprecipitates from control pcDNA3 (-) or FLAG-CtIP (wt or 2A) transfected HEK293T cells were subjected to far-western blotting using purified GST-PIN1 as a probe, followed by anti-GST immunoblotting. Anti-FLAG western blot analysis of the upper panel after stripping is shown. Error bars, s.e.m. Scale bars= 5 μm. * P<0.05, ** P<0.001, *** P<0.0001. ns indicates that the difference between two groups is not significant.

Figure 3. PIN1 catalyzes cis-trans isomerisation of pS276-Pro in CtIP

(a) FLAG-tagged CtIP variants expressed for 48 h in HEK293T cells were blotted with pS276/pT315-CtIP or with FLAG antibodies. (b) CtIP was immunoprecipitated from HEK293T cells and analysed by immunoblotting with pT315 antibody as above. No signal was detected after λ-phosphatase (λ-PPase) treatment, showing the phospho-specificity of the antibody. (c) GST-PIN1 pull-down was performed using U2OS cell lysates in

presence of phosphorylated or non-phosphorylated T315-CtIP or S276-CtIP peptides (all 80 µg). Ponceau staining is shown to illustrate that equal amounts of GST-PIN1 were used (d) Selected region of two-dimensional ROESY spectra of the phosphorylated S276-CtIP peptide in the presence of GST-PIN1-wt (upper part) or GST-PIN1-C113A (lower part).

Figure 4. CDK2 mediates CtIP-PIN1 interaction

(a) GST-PIN1 pulldown assay using whole cell extracts from U2OS cells treated with R-Roscovitine or RO-3306 for 2 h (25µM). (b) HEK293T cells were mock (DMSO) treated or with the indicated dose of R-Roscovitine (ROSC) for 2 h and phosphorylation of T315-CtIP analysed by anti-pT315-CtIP immunoprecipitation. Ponceau staining is shown to illustrate that equal amounts of antibodies were used for immunoprecipitations. (c) Dominant negative (dn) versions of CDK1, 2, and 4 were expressed in HEK293T cells and GST-PIN1 pull-down performed as above. Ponceau staining is shown to illustrate that equal amounts of GST-PIN1 or antibodies were used. (d) The recombinant GST-CtIP fragment ranging from amino acid 45 to 371 was phosphorylated *in vitro* with CDK2/CyclinE and detected with phospho-specific antibodies raised against pS276- and pT315-CtIP. Total protein was visualized by Ponceau S staining. The ratios Input/pulldown (I/P) and Input/IP (I/IP) were obtained by densitometry quantification using Image J. Abbreviations: IgG: Immunoglobulin heavy chain.

Figure 5. Hyper-resection and delay in DSB repair in CtIP-2A cells

(a) At 72 h after transfection with CtIP-specific siRNA oligonucleotides, U2OS cells expressing GFP-CtIP (wt and 2A) were left untreated, treated with etoposide (5 µM) for 1 h and lysed directly or released for 2 h and 6 h prior to cell lysis. Whole cell lysates were analysed by immunoblotting using the indicated antibodies. The asterisk indicates the hyperphosphorylated form of RPA2. (b) Same cells as in (a) were either left untreated or treated with 10 µM etoposide in presence or in absence of DNA-PKcs inhibitor (NU7441, 10 µM) for 2 h and directly processed or released in fresh media for 30 minutes. The amount of broken DNA was assessed by pulsed-field gel electrophoresis (lower part) and

whole cell extracts for the same time-points were used for immunoblotting with the indicated antibodies (upper part). (c) GFP-CtIP cells (wt and 2A) were treated with 200 µg/ml cycloheximide (CHX) for 4 h (lane 2) or with etoposide (ETOP, lane 3) and then released in the absence (lane 4) or presence of cycloheximide (lanes 5-8) for the indicated time. Whole cell extracts were analysed by western blotting using the indicated antibodies. (d) Model summarizing our findings.

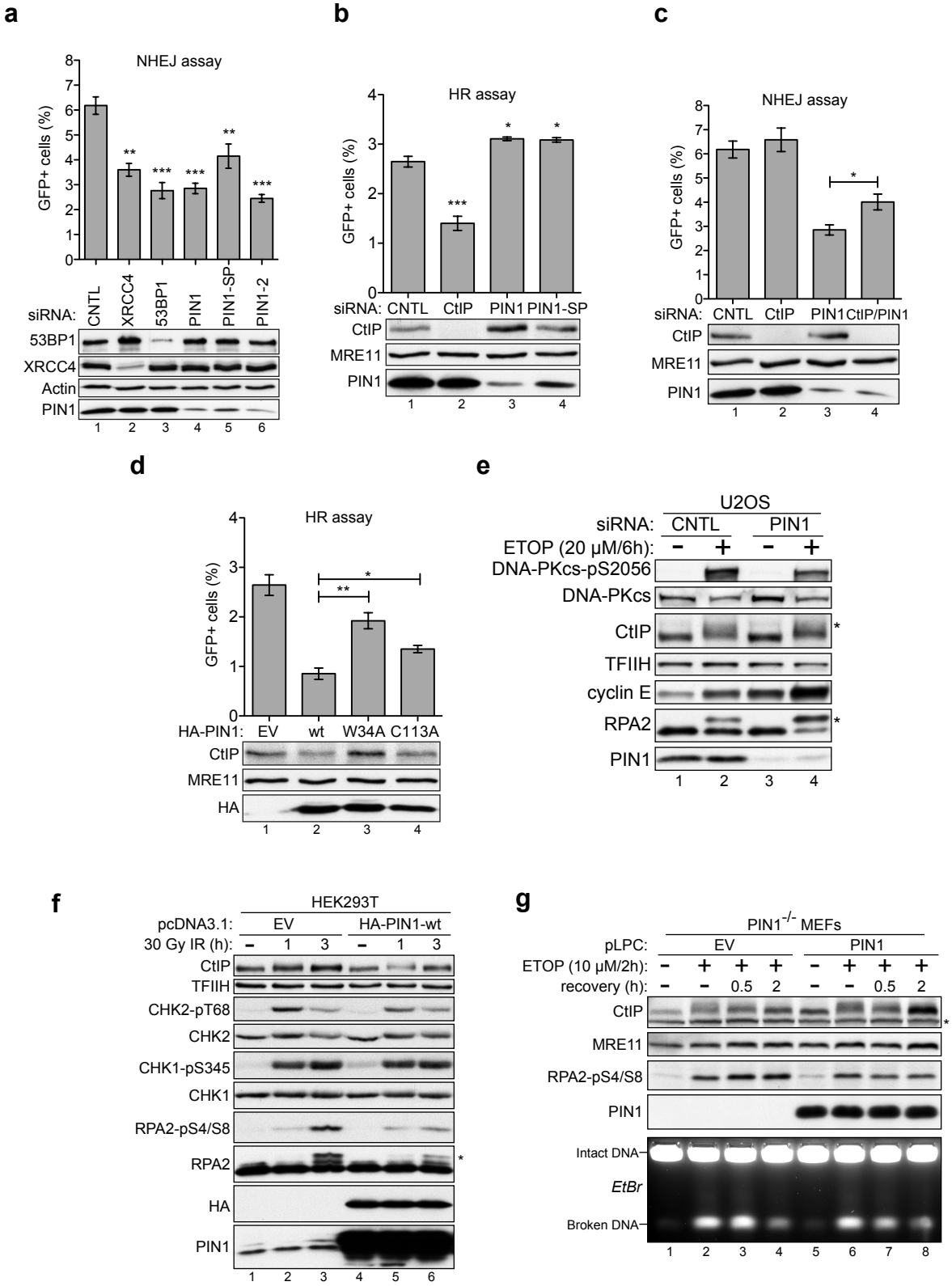
a
NHEJ assay
GFP+ cells (%)
siRNA: CNTL XRCC4 53BP1 PIN1 PIN1-SP PIN1-2
53BP1
XRCC4
Actin
PIN1
b
HR assay
GFP+ cells (%)
siRNA: CNTL CtIP PIN1 PIN1-SP
CtIP
MRE11
PIN1
c
NHEJ assay
GFP+ cells (%)
siRNA: CNTL CtIP PIN1 CtIP/PIN1
CtIP
MRE11
PIN1
d
HR assay
GFP+ cells (%)
HA-PIN1: EV wt W34A C113A
CtIP
MRE11
HA
e
U2OS
siRNA: CNTL PIN1
ETOP (20 μM/6h): - + - +
DNA-PKcs-pS2056
DNA-PKcs
CtIP
TFIIH
cyclin E
RPA2
PIN1
f
HEK293T
pcDNA3.1: EV HA-PIN1-wt
30 Gy IR (h): - 1 3 - 1 3
CtIP
TFIIH
CHK2-pT68
CHK2
CHK1-pS345
CHK1
RPA2-pS4/S8
RPA2
HA
PIN1
g
PIN1-/- MEFs
pLPC: EV PIN1
ETOP (10 μM/2h): - + + + - + + +
recovery (h): - - 0.5 2 - - 0.5 2
CtIP
MRE11
RPA2-pS4/S8
PIN1
Intact DNA
EtBr
Broken DNA

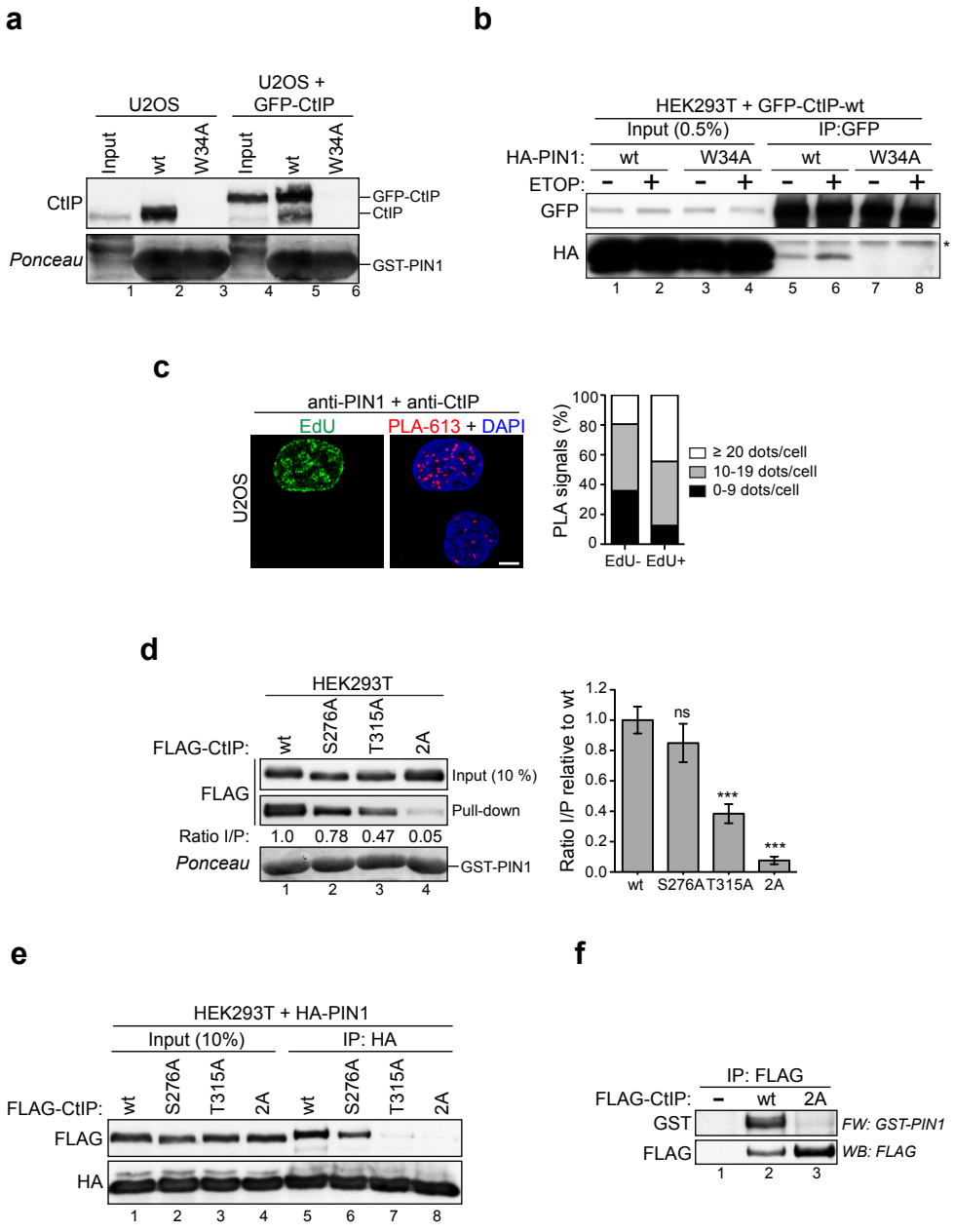
a
U2OS
U2OS + GFP-CtIP
Input
wt
W34A
Input
wt
W34A
CtIP
GFP-CtIP
CtIP
Ponceau
GST-PIN1
1 2 3 4 5 6
b
HEK293T + GFP-CtIP-wt
Input (0.5%)
IP:GFP
HA-PIN1:
wt
W34A
wt
W34A
ETOP:
- + - + - + - +
GFP
HA
*
1 2 3 4 5 6 7 8
c
anti-PIN1 + anti-CtIP
EdU
PLA-613 + DAPI
U2OS
PLA signals (%)
100
80
60
40
20
0
≥ 20 dots/cell
10-19 dots/cell
0-9 dots/cell
EdU- EdU+
d
HEK293T
FLAG-CtIP:
wt
S276A
T315A
2A
FLAG
Input (10 %)
Pull-down
Ratio I/P:
1.0 0.78 0.47 0.05
Ponceau
GST-PIN1
1 2 3 4
Ratio I/P relative to wt
1.2
1.0
0.8
0.6
0.4
0.2
0.0
ns
***
***
wt S276A T315A 2A
e
HEK293T + HA-PIN1
Input (10%)
IP: HA
FLAG-CtIP:
wt
S276A
T315A
2A
wt
S276A
T315A
2A
FLAG
HA
1 2 3 4 5 6 7 8
f
IP: FLAG
FLAG-CtIP:
-
wt
2A
GST
FLAG
FW: GST-PIN1
WB: FLAG
1 2 3

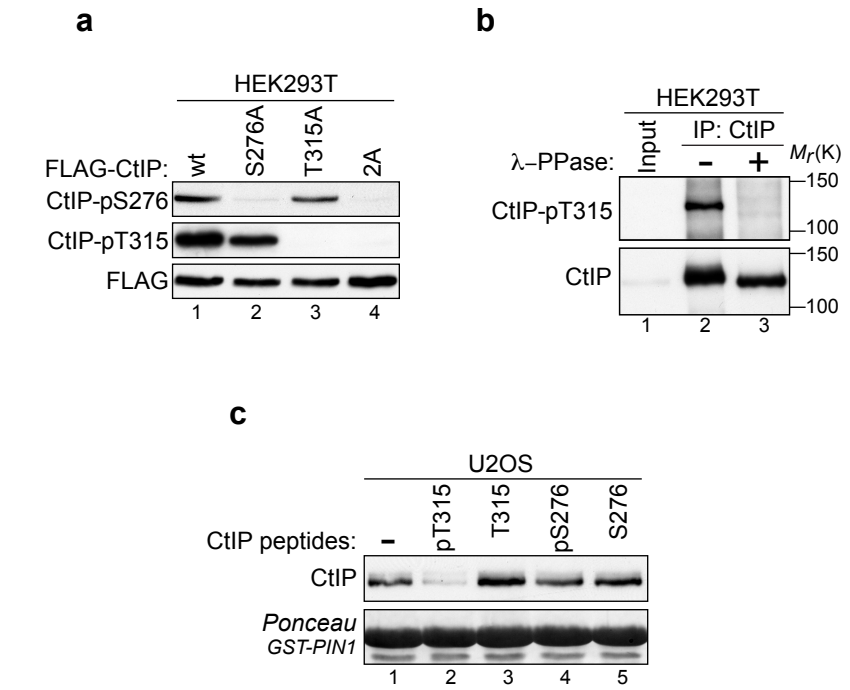
a
HEK293T
FLAG-CtIP:
wt
S276A
T315A
2A
CtIP-pS276
CtIP-pT315
FLAG
1 2 3 4
b
HEK293T
Input
IP: CtIP
λ–PPase:
-
+
M_r(K)
CtIP-pT315
CtIP
150
100
150
100
1 2 3
c
U2OS
CtIP peptides:
-
pT315
T315
pS276
S276
CtIP
Ponceau
GST-PIN1
1 2 3 4 5
d
PIN1-wt + pS276
s7->S7
s7
I9->L9
L9
S7
s7->S7
I9->L9
I9
ETQGPMpSPLGDELY
8.7 8.6 8.5 8.4 8.3 8.2 8.1 8.0 ppm
PIN1-C113A + pS276
s7
L9
S7
ETQGPMpSPLGDELY
8.7 8.6 8.5 8.4 8.3 8.2 8.1 8.0 ppm

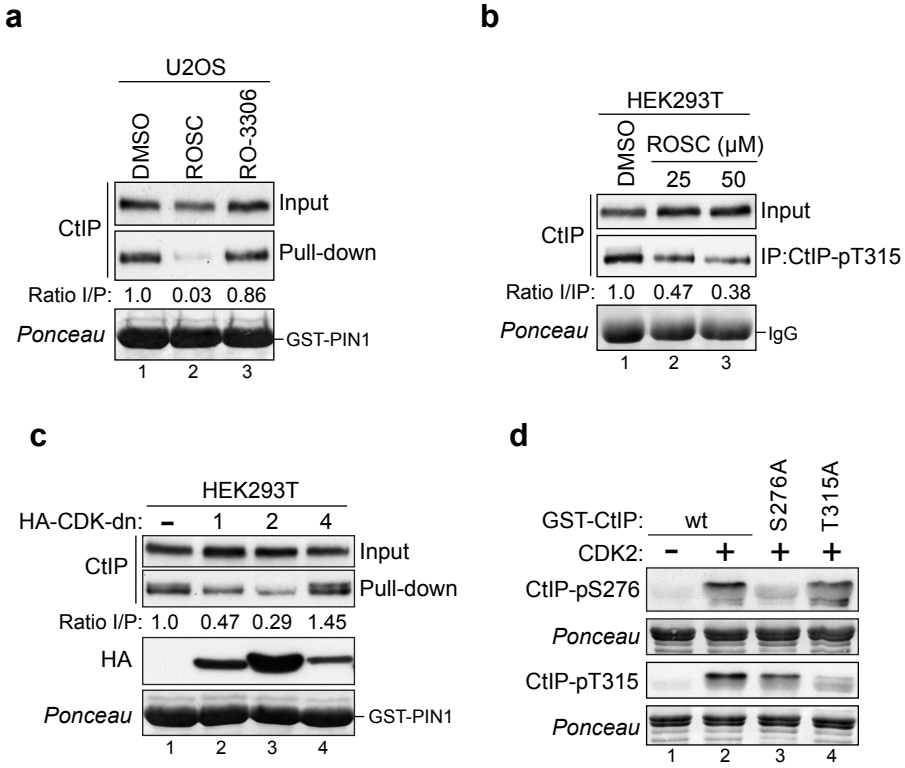
a
U2OS
DMSO
ROSC
RO-3306
CtIP
Input
Pull-down
Ratio I/P: 1.0 0.03 0.86
Ponceau
GST-PIN1
1 2 3
b
HEK293T
DMSO
ROSC (μM)
25 50
CtIP
Input
IP:CtIP-pT315
Ratio I/IP: 1.0 0.47 0.38
Ponceau
IgG
1 2 3
c
HEK293T
HA-CDK-dn: – 1 2 4
CtIP
Input
Pull-down
Ratio I/P: 1.0 0.47 0.29 1.45
HA
Ponceau
GST-PIN1
1 2 3 4
d
GST-CtIP: wt S276A T315A
CDK2: – + + +
CtIP-pS276
Ponceau
CtIP-pT315
Ponceau
1 2 3 4

a

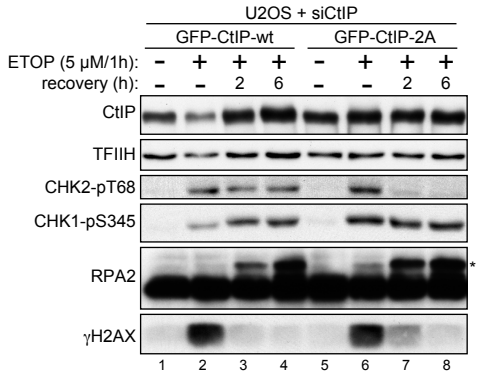
U2OS + siCtIP
GFP-CtIP-wt
GFP-CtIP-2A
ETOP (5 μM/1h):
recovery (h):
CtIP
TFIIH
CHK2-pT68
CHK1-pS345
RPA2
γH2AX
1 2 3 4 5 6 7 8

b

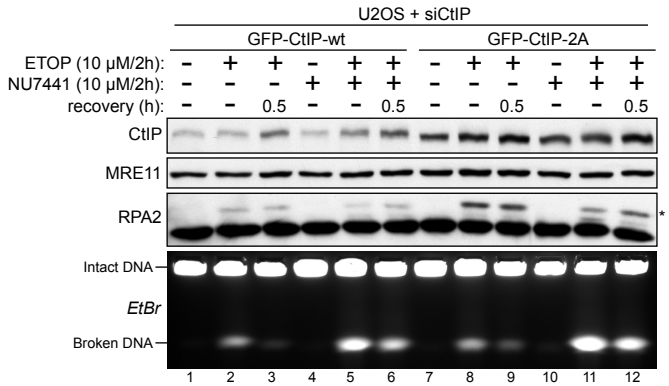
U2OS + siCtIP
GFP-CtIP-wt
GFP-CtIP-2A
ETOP (10 μM/2h):
NU7441 (10 μM/2h):
recovery (h):
CtIP
MRE11
RPA2
Intact DNA
EtBr
Broken DNA
1 2 3 4 5 6 7 8 9 10 11 12

c

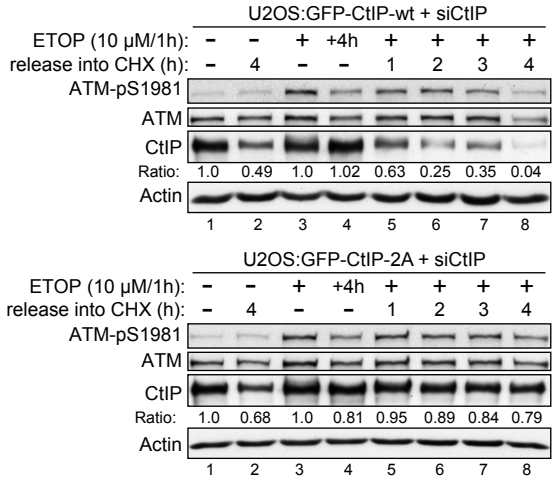
U2OS:GFP-CtIP-wt + siCtIP
ETOP (10 μM/1h):
release into CHX (h):
ATM-pS1981
ATM
CtIP
Ratio: 1.0 0.49 1.0 1.02 0.63 0.25 0.35 0.04
Actin
1 2 3 4 5 6 7 8
U2OS:GFP-CtIP-2A + siCtIP
ETOP (10 μM/1h):
release into CHX (h):
ATM-pS1981
ATM
CtIP
Ratio: 1.0 0.68 1.0 0.81 0.95 0.89 0.84 0.79
Actin
1 2 3 4 5 6 7 8

d

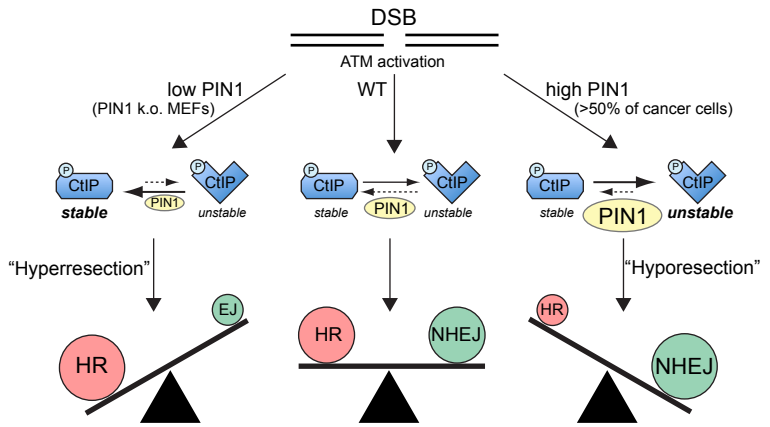
DSB
ATM activation
low PIN1
(PIN1 k.o. MEFs)
WT
high PIN1
(>50% of cancer cells)
CtIP
stable
PIN1
unstable
"Hyperresection"
"Hyporesection"
EJ
HR
NHEJ

Supplemental Information

PIN1-mediated isomerisation of CtIP determines double-strand break repair pathway choice

Martin Steger[1], Olga Murina[1], Daniela Hühn[1], Reto Walser[2], Shreya Paliwal[1], Kay Hänggi[1], Lorenzo Lafranchi[1], Christine Neugebauer[1], Bertran Gerrits[3], Pavel Janscak[1], Oliver Zerbe[2] and Alessandro A. Sartori[1,*]

[1] Institute of Molecular Cancer Research, University of Zurich, Winterthurerstrasse 190, CH-8057 Zurich, Switzerland

[2] Institute of Organic Chemistry, University of Zurich, Winterthurerstrasse 190, CH-8057 Zurich, Switzerland

[3] Functional Genomic Center, University of Zurich, Winterthurerstrasse 190, CH-8057 Zurich, Switzerland

* Corresponding Author:

sartori@imcr.uzh.ch
phone (+41) 44 635 3473
fax (+41) 44 635 3484

This pdf file includes:

Supporting Table 1: Primary antibodies

Antibody target	Species	Supplier/Reference	Application
ATM (2C1)	mouse	GTX70103 (GeneTex)	IB
pATM S1981	rabbit	2152-1 (Epitomics)	IB
α-Actin (I-19)	rabbit	sc-1616 (Santa Cruz)	IB
53BP1 (H-300)	rabbit	sc-22760 (Santa Cruz)	IB
CtIP (14-1)	mouse	gift from Richard Baer	IB
CtIP	rabbit	A300-488A (Bethyl)	IP
CtIP (D-4)	mouse	sc-271339 (Santa Cruz)	IB
CtIP (T-16)	goat	sc-5970 (Santa Cruz)	IP and IB
CHK1 (G4)	mouse	sc-8408 (Santa Cruz)	IB
pCHK1 S345	rabbit	2341(Cell Signaling)	IB
CHK2	rabbit	gift from Grant Stewart	IB
pCHK2 T68 (C13C1)	rabbit	2197P (Cell Signaling)	IB
Cyclin A (C-19)	rabbit	sc-596 (Santa Cruz)	IF
Cyclin D1	rabbit	RB-010 (NeoMarkers)	IB
pDNA-PKcs S2056	rabbit	ab18192 (Abcam)	IB
FLAG	mouse	F3165 (Sigma)	IP and IB
GAPDH	mouse	MAB374 (Millipore)	IB
GFP	rabbit	ab290 (Abcam)	IP and IB
GFP	mouse	sc-9996 (Santa Cruz)	IB
GST	mouse	A00865 (GenScript)	IB
HA	mouse	sc-7392 (Santa Cruz)	IP and IB
γH2AX (JBW301)	mouse	05-636 (Millipore)	IF
γH2AX (20E3)	rabbit	9718 (Cell Signaling)	IB and IF
MRE11	mouse	GTX70212 (GeneTex)	IB
MRE11	rabbit	NB100-142 (Novus)	IB
PIN1	rabbit	2136-1 (Epitomics)	IB and IF
PIN1	rabbit	600-401-A20 (Rockland)	IP
p53 (DO-1)	mouse	sc-126 (Santa Cruz)	IB

Supporting table 1 (continued)

RAD51 (H-92)	rabbit	sc-8349 (Santa Cruz)	IB
RPA2 (Ab-3)	mouse	NA19L (Calbiochem)	IF and IB
RPA2 (9H8)	mouse	ab2175 (Abcam)	IB
pRPA S4/S8 (BL647)	rabbit	A300-245A (Bethyl)	IB
β-Tubulin (D-10)	mouse	sc-5274 (Santa Cruz)	IB
TFIIH p89 (S-19)	rabbit	sc-293 (Santa Cruz)	IB
XRCC4	rabbit	ab145 (Abcam)	IB

IB: Immunoblot, IF: Immunofluorescence, IP: Immunoprecipitation

Supplemental figure legends

Supplemental Figure 1. Multiple DNA repair factors interact specifically with PIN1

(a) *Left,* 5 mg of HEK293T whole cell lysates were subjected to GST-PIN1 pulldown assay and bound proteins separated on SDS-PAGE. After silver stain the indicated parts of the gel were excised and processed for mass spectrometry (MS) analysis (see Materials and Methods). *Right,* Table illustrating examples of known and novel identified PIN1-interacting factors from the MS screen (b) Chart summarizing the results obtained from the MS analysis.

Supplemental Figure 2. Effects of PIN1 overexpression or depletion in mammalian cells

(a) HA-PIN1 (wt, W34A or C113A) was expressed in HEK293 (DR-GFP) cells for 96 h. Cells were ethanol-fixed and after propidium iodide staining analysed by flow cytometry. (b) U2OS cells were transfected with luciferase (Ctrl) or PIN1-specific siRNAs for 48 h, ethanol-fixed and stained with propidium iodide. Flow cytometry profiles are represented. (c) 48 h after transfection with CtIP-, XRCC4-, or PIN1-specific siRNA oligonucleotides, U2OS cells were treated with either DMSO or camptothecin (CPT) for 1 h at the indicated dose and survival was determined by colony formation. Data represent the mean±s.e.m. of three independent experiments (d) Same cells as in (b) were treated with etoposide (ETOP) for the indicated time and whole cell extract subjected to SDS-PAGE followed by western blotting using the indicated antibodies. Asterisks mark hyperphosphorylated forms of RPA2 and CtIP. (e) HEK293T cells were transfected with empty vector (EV= pcDNA3.1), HA-PIN1-wt or W34A plasmid constructs, 72 h later left untreated or treated with ionizing radiation (IR) and released for 3 h. Whole cell extracts were analysed by immunoblotting. (f) U2OS cells were transfected with siRNAs against luciferase (CNTL), PIN1, CtIP or a combination of CtIP and PIN1 for 48 h and treated with etoposide (ETOP) for 1 h. Cells were stained with antibodies against γ-H2AX and RPA2 and analysed by fluorescence microscopy. Nuclei were stained with DAPI. (*Right panels*). RPA foci-positive cells (cells harboring more than 10 foci were scored as positive) were enumerated. Data represent the mean ± s.e.m. of three independent experiments (*Lower*

left chart). A western blot analysis of the same cells is shown above. Abbreviations: PIN1-SP: PIN1-smartpool. Scale bar= 10 µm. Error bars, s.e.m. * $P<0.05$.

Supplemental Figure 3. Phosphorylation-dependent CtIP-PIN1 interaction.

(a) HEK293T cells were transfected with FLAG-CtIP expression constructs and whole cell lysates were prepared at 48 h post-transfection. Lysates were either left untreated, pre-treated with λ-phosphatase (λ-PPase) or a combination of λ-phosphatase and phosphatase inhibitors (50 mM EDTA and 1 mM sodium-orthovanadate) and subjected to GST-PIN1 pulldown. (b) U2OS WCEs were treated with increasing concentrations of λ-phosphatase (λ-PPase, lanes 2-3 and 5-6) prior to GST-PIN1 pulldown. (c) Detection of endogenous PIN1 and CtIP complexes by *in situ* PLA. U2OS cells were either transfected with siRNA against PIN1 for 48 h or not transfected and pulse-labeled with 5'-Ethynyl-2'-deoxyuridine (EdU, 10µM) for 15 minutes prior to fixation. After incubated with antibodies against CtIP alone (upper panel) or both CtIP and PIN1 together (middle and lower panels), protein-protein interactions were detected using fluorescence labeled probes (PLA-613). EdU detection was carried out according to manufacturer's instructions and nuclei were stained with DAPI. (d) Schematic illustration of human CtIP. The 12 S/TP motifs spanning over the whole amino acid sequence are represented. S327 and T847, two known phosphorylation sites, are illustrated in bold. Coiled-coil domain and conserved C-terminal domain (CTD) are shown. (e-g) GST-PIN1 pulldowns using WCEs of HEK293T cells expressing either wild type or several point-mutant FLAG-tagged versions of CtIP. Ponceau staining is shown to illustrate that equal amounts of GST-PIN1 were used. ΔC refers to a mutant of CtIP lacking the C-terminal portion including T847 and S889. (h) HEK293T cells were transfected with either FLAG-CtIP (-) alone or with both FLAG-CtIP and HA-PIN1 (wt, W34A or C113A). WCEs were subjected to co-immunoprecipitations using α-HA antibodies followed by SDS-PAGE and immunoblotting with the indicated antibodies. (i) Anti-FLAG immunoprecipitates from control pcDNA3 (-) or FLAG-CtIP (wt, S276A and T315A) transfected HEK293T cells were subjected to far-western blotting using purified GST-PIN1 as a probe, followed by anti-GST

immunoblotting. Anti-FLAG western blot analysis of the upper panel after stripping is shown. Scale bar= 10 μm.

Supplemental Figure 4. T315-CtIP is phosphorylated in vivo and is the primary PIN1 binding site

(a) Amino acid sequence alignment of CtIP surrounding the residues S276 and T315. (b) *Upper part,* Cell endogenous CtIP precipitated from HEK293T cells was subjected to MS analysis. The obtained sequence coverage was 23% with the identified peptides highlighted. Note that a peptide containing T315 was extracted whereas S276 was not covered by the analysis. Both residues are marked in red. *Lower part,* Collision induced dissociation tandem mass spectrum of parent ion [M+3H]3+ = 667.3056. After peak extraction, the resulting data was searched against the human portion (taxonomy ID: 9606) of the UniProt database including common contaminants. The phosphopeptide FSDSTSKTPPQEELPTR was unambiguously identified with a Mascot Ion score of 64. Ions score is -10*Log (P), where P is the probability that the observed match is a random event. Individual ions scores > 28 indicate identity ($p<0.05$). The phosphosite identification statistically yields two possible candidates, namely T8 and S6.[1] The other possible phosphorylation sites have an extremely diminished chance. (c) GST-PIN1 pull-down was performed using HEK293T whole cell extracts (WCE) in presence of phosphorylated (lanes 3-6) or non-phosphorylated (lane 7) T315-CtIP peptides. Ponceau staining is shown to illustrate that equal amounts of GST-PIN1 were used.

Supplemental Figure 5. NMR spectra of CtIP-peptides

(a) GST-PIN1 (wt and C113A) were expressed in *E. coli* (BL21) and after solubilization subjected to purification via FPLC. Several fractions were collected, loaded and separated on SDS-PAGE and stained with commassie blue (b) $^{31}P(^{1}H)$ spectra obtained from pS276 and pT315 peptides (both 2.4 mM) in 20 mM sodium phosphate (pH 6.8) at 25 °C. The ratios of trans to cis are 4 and approximately 16 for pS276 and pT315, respectively, as judged by the integrals under the peaks. Note the presence of two weak cis peaks in

pT315 peptide due to the TPP motif. The strong, capped peak at 0.55 ppm results from the phosphate buffer. (c-e) Selected region of the two-dimensional ROESY spectra of non-phosphorylated S276-peptide (c), pT315 peptide (d) or modified pT315-CtIP peptide (pT315-P317L, (e)) in presence of GST-PIN1-wt at a mixing time of 110 ms.

Supplemental Figure 6. CDK2 is crucial for CtIP-PIN1 interaction

(a) U2OS cells were treated with DMSO or R-Roscovitine at the indicated dose for 2 h and cell extracts were used for GST-PIN1 pull-down. The ratio Input/pull-down (I/P) was obtained by densitometry quantification using Image J. (b) 4 μg of pT315-CtIP antibodies were used to immunoprecipitate GFP-CtIP (wt and T315) from U2OS cells. (c) HEK293T cells were transfected with 4μg of HA-CDK1-dn or with HA-CDK2-dn for 48h, ethanol-fixed and stained with propidium iodide prior to flow cytometry analysis. (d) HA-CDK2 (wt and dn) were transfected into HEK293T cells and whole cell lysates were used for GST-PIN1 pulldown assays 48h later. (e) U2OS cells were synchronized by thymidine (2 mM) treatment (18 h) followed by a 12 h release and a second thymidine block of 17 h (dT). After release cells were harvested at the indicated time points. For each time point, cells were analyzed by flow cytometry. WCE (2 mg) were used to immunoprecipitate CtIP at each time point. Ponceau staining is shown to illustrate that equal amounts of antibodies were used. Abbreviations: IgG= Immunoglobulin heavy chain, dT= double thymidine.

Supplemental Figure 7. Phenotypical analysis of GFP-CtIP-expressing cells

(a) U2OS cells stably expressing siRNA resistant GFP-CtIP variants were transfected with CtIP-specific siRNA for 72 h and whole cell extracts were subjected to immunoblot analysis using the indicated antibodies. (b) Same cells as in (a) were fixed, stained with propidium iodide and analyzed by flow cytometry. (c) HEK293T cells were transfected with GFP-CtIP (wt and 2A) for 48 h and whole cell extracts used for co-immunoprecipitations using α-GFP antibodies. Immunocomplexes were separated on SDS-PAGE and indicated proteins visualized by western blotting. Ponceau staining is shown to visualize that equal amounts of antibodies were used for immunoprecipitations

(d) HEK293T cells co-transfected with GFP-CtIP (wt and 2A) and HA-PIN1 for 48 h were mock treated or with etoposide (ETOP) and whole cell lysates were used for co-immunoprecipitations using α-GFP antibodies. Immunocomplexes were separated on SDS-PAGE and indicated proteins visualised by western blotting. (e) U2OS cells stably expressing GFP-CtIP (wt and 2A) were transfected with siRNA against CtIP. 72 h later cells were laser-microirradiated and fixed after 30 minutes, stained with γ-H2AX and Cyclin A antibodies, and analysed by fluorescence microscopy. Nuclei were visualized with DAPI. (f) 72 h after transfection with luciferase (CNTL)- or CtIP-specific siRNA oligonucleotides, U2OS cells stably expressing GFP alone or GFP-CtIP (wt, T847A or 2A) were treated with either DMSO or camptothecin (CPT) for 1 h at the indicated dose and survival was determined by colony formation. Data represent the mean±s.e.m. of three independent experiments. Scale bar= 10 μm. Abbreviations: IgG: Immunoglobulin heavy chain.

Supplemental Figure 8. GFP-CtIP-2A cells display increased number of RPA-foci upon etoposide treatment

(a) U2OS cells stably expressing GFP-CtIP (wt and 2A) were transfected with siRNA against CtIP. 72 h later cells were treated with of etoposide (ETOP) and fixed (*upper left part*) or released for 2 h (*lower left part*) and immunostained with γ-H2AX and RPA antibodies followed by fluorescence microscopy analysis. Nuclei were stained with DAPI. (*Right charts*) Quantification of RPA foci-positive cells (cells harboring more than 10 foci were scored as positive). Data represent the mean ± s.e.m of two independent experiments. (b) U2OS cells were treated with DMSO or etoposide (ETOP) (lanes 1-2) and then released in fresh medium for 6 h (lane 4) or co-treated with a combination of etoposide and DNA-PKcs inhibitor (NU-7441) and then released for 6 h (lane 3). Pulsed-field gel electrophoresis (*lower part*) was used to determine DSB-repair kinetics and whole cell extracts of the corresponding time-points were used for western blotting (*upper part*). Asterisks indicate hyperphosphorylated forms of RPA2 and CtIP. (c) HEK293T cells were transfected with FLAG-CtIP (wt or 2A), 8 h later splitted and another 16 h later treated with DMSO (-) or with the proteasome inhibitor MG-132. Whole cell extracted proteins

were separated on SDS-PAGE and visualized by western blotting using the indicated antibodies. The signal intensities were quantified using Image J and normalized to actin. Represented values correspond to relative CtIP levels compared to untreated (-). Scale bars= 20 µm. Error bars, s.e.m. * $P<0.05$, ** $P<0.001$.

a

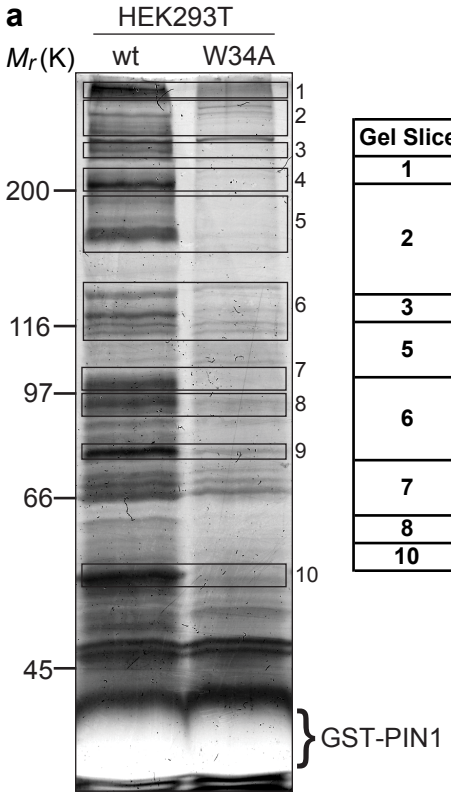

Gel Slice	Identified Protein	Acc No.	wt/W34A*	Pathways	References
1	MAP1A	P78559	53/0	Mitotic regulation	Endoh et al. 2011
2	SMRT	Q9Y618	41/0	Signal transduction	Stanya et al. 2008
	MDC1	Q14676	84/2	DSB repair	*this study*
	53BP1	Q12888	3/0	DSB repair	*this study*
	BRCA1	P38398	14/2	DSB repair	*this study*
3	SLX4	Q8IY92	45/5	DSB repair	*this study*
5	TOP2A	P11388	7/0	Mitotic regulation	Xu and Manley, 2007
	BLM	P54132	14/10	DSB repair	*this study*
6	PTIP	Q6ZW49	14/0	DSB repair	*this study*
	RB	P06400	13/0	Cell proliferation	Rizzolio et al. 2012
	CtIP	Q99708	2/0	DSB repair	*this study*
7	BARD1	Q99728	20/2	DSB repair	*this study*
	BCL6	P41182	1/0	Apoptosis	Phan et al. 2007
8	β-catenin	P35222	13/0	Cell proliferation	Ryo et al. 2001
10	p54nrb	Q15233	90/43	Mitotic regulation	Proteau et al. 2005

b

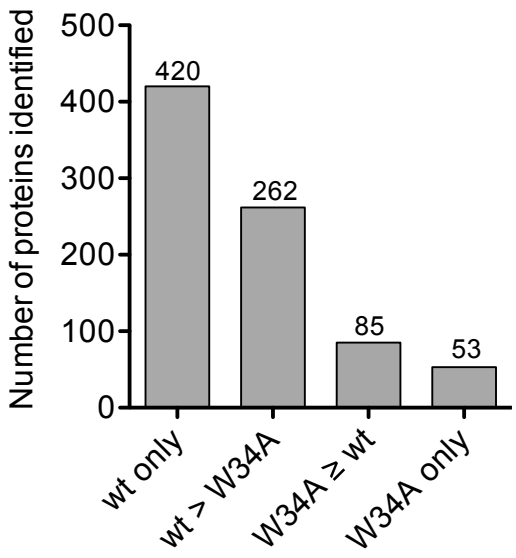

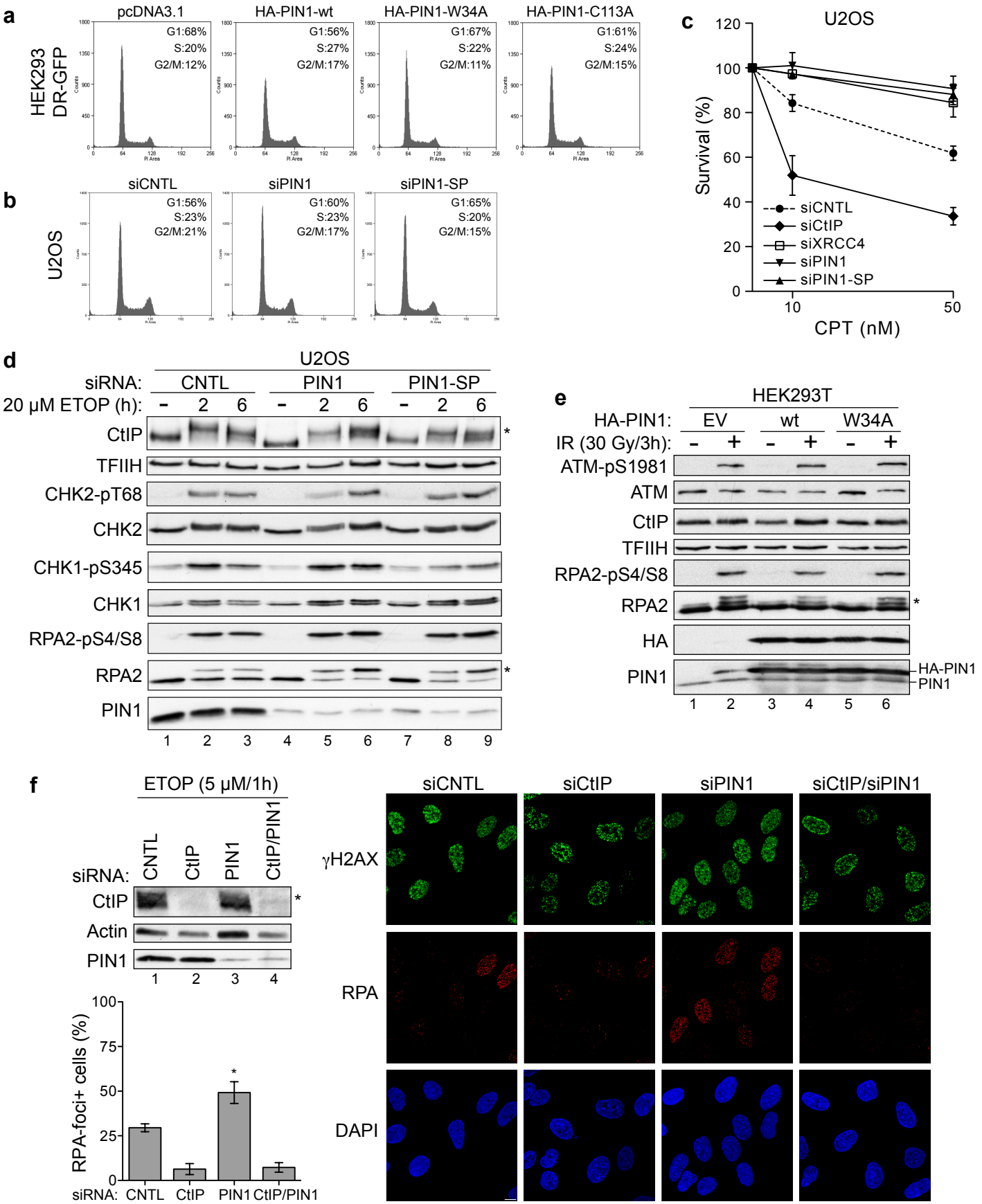
a
HEK293 DR-GFP
pcDNA3.1
G1:68%
S:20%
G2/M:12%
HA-PIN1-wt
G1:56%
S:27%
G2/M:17%
HA-PIN1-W34A
G1:67%
S:22%
G2/M:11%
HA-PIN1-C113A
G1:61%
S:24%
G2/M:15%
b
U2OS
siCNTL
G1:56%
S:23%
G2/M:21%
siPIN1
G1:60%
S:23%
G2/M:17%
siPIN1-SP
G1:65%
S:20%
G2/M:15%
c
U2OS
Survival (%)
siCNTL
siCtIP
siXRCC4
siPIN1
siPIN1-SP
CPT (nM)
d
U2OS
siRNA: CNTL PIN1 PIN1-SP
20 μM ETOP (h): - 2 6 - 2 6 - 2 6
CtIP
TFIIH
CHK2-pT68
CHK2
CHK1-pS345
CHK1
RPA2-pS4/S8
RPA2
PIN1
e
HEK293T
HA-PIN1: EV wt W34A
IR (30 Gy/3h): - + - + - +
ATM-pS1981
ATM
CtIP
TFIIH
RPA2-pS4/S8
RPA2
HA
PIN1
HA-PIN1
PIN1
f
ETOP (5 μM/1h)
siRNA: CNTL CtIP PIN1 CtIP/PIN1
CtIP
Actin
PIN1
RPA-foci+ cells (%)
siRNA: CNTL CtIP PIN1 CtIP/PIN1
siCNTL
siCtIP
siPIN1
siCtIP/siPIN1
γH2AX
RPA
DAPI

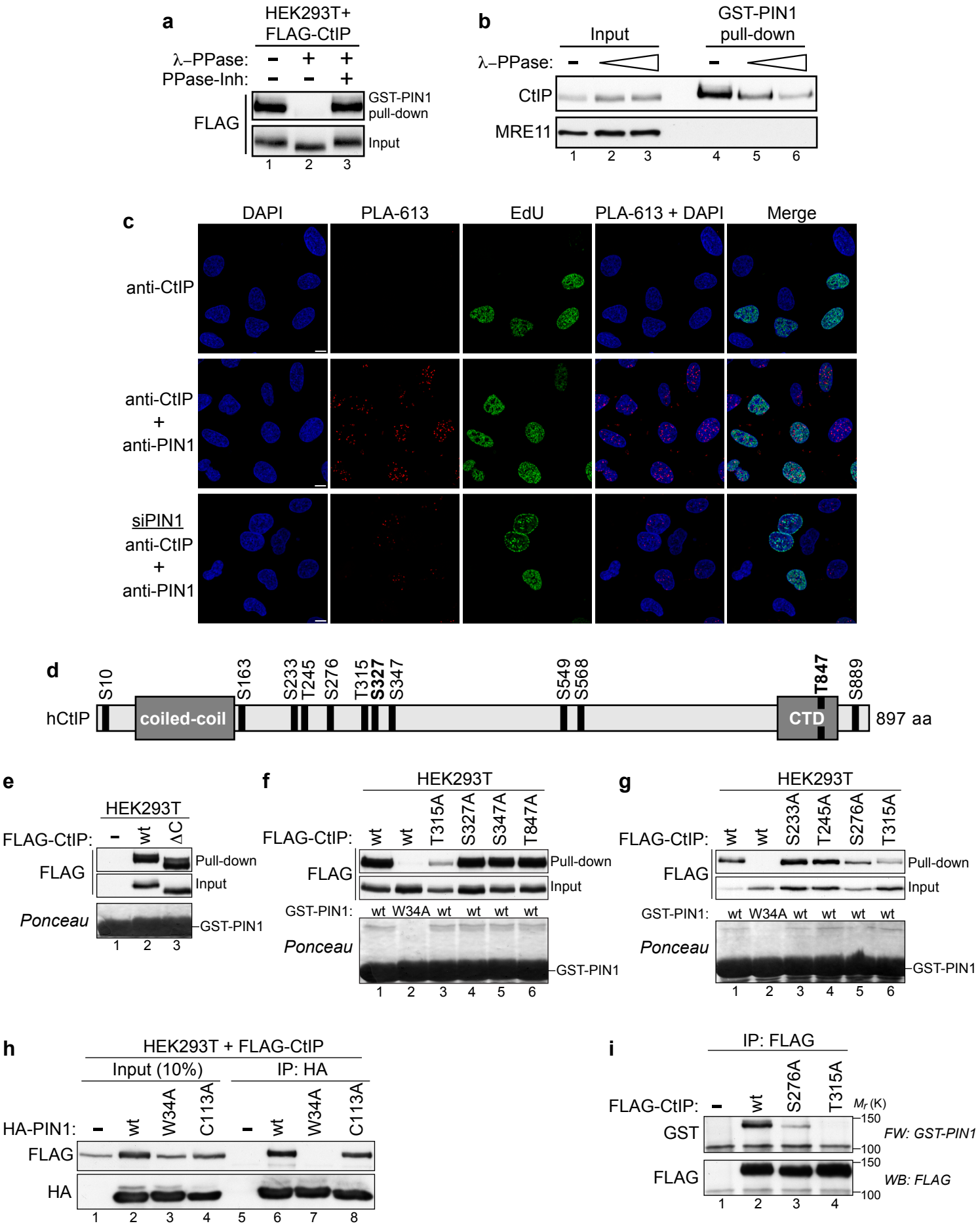
a
HEK293T+
FLAG-CtIP
λ–PPase:
PPase-Inh:
FLAG
GST-PIN1
pull-down
Input
1 2 3
b
Input
GST-PIN1
pull-down
λ–PPase:
CtIP
MRE11
1 2 3 4 5 6
c
DAPI
PLA-613
EdU
PLA-613 + DAPI
Merge
anti-CtIP
anti-CtIP
+
anti-PIN1
siPIN1
anti-CtIP
+
anti-PIN1
d
hCtIP
coiled-coil
CTD
897 aa
S10
S163
S233
T245
S276
T315
S327
S347
S549
S568
T847
S889
e
HEK293T
FLAG-CtIP:
wt
ΔC
FLAG
Pull-down
Input
Ponceau
GST-PIN1
1 2 3
f
HEK293T
FLAG-CtIP:
wt
wt
T315A
S327A
S347A
T847A
FLAG
Pull-down
Input
GST-PIN1:
wt W34A wt wt wt wt
Ponceau
GST-PIN1
1 2 3 4 5 6
g
HEK293T
FLAG-CtIP:
wt
wt
S233A
T245A
S276A
T315A
FLAG
Pull-down
Input
GST-PIN1:
wt W34A wt wt wt wt
Ponceau
GST-PIN1
1 2 3 4 5 6
h
HEK293T + FLAG-CtIP
Input (10%)
IP: HA
HA-PIN1:
wt
W34A
C113A
FLAG
HA
1 2 3 4 5 6 7 8
i
IP: FLAG
FLAG-CtIP:
wt
S276A
T315A
M_r (K)
GST
FLAG
150
100
FW: GST-PIN1
WB: FLAG
1 2 3 4

a

```
human 270 ETQGPMSPLGDELY -x25- FSDSTSKTPPQEEL 321
  dog 270 ESQGPVSPLGDELY -x24- FSDSKSRTPPQEEL 320
  pig 266 ESRGPRSPLGDELY -x25- FSDSISKTPPQEEL 317
horse 270 EPQGPVSPLDDELY -x25- FPDCNSKTPPQEEL 321
mouse 270 EPQGPMSPLGSELY -x25- FSDSASKTPPQEFT 321
```

b

>sp|Q99708|RBBP8_HUMAN
22 unique peptides, 202/897 amino acids (23% coverage)

MNISGSSCGSPNSADTSSDFKDLWTKLKECHDREVQGLQVKVTKLKQERILDAQRLEEFFTKNQQLREQQ
KVLHETIKVLEDRLRAGLCDRCAVTEEHMRKKQQEFENIRQQNLKLITELMNERNTLQEENKKLSEQLQQ
KIENDQQHQAAELECEEDVIPDSPITAFSFSGVNRLRRKENPHVRYIEQTHTKLEHSVCANEMRKVSKSS
THPQHNPNENEILVADTYDQSQSPMAKAHGTSSYTPDKSSFNLATVVAETLGLGVQEESETQGPMSPLGD
ELYHCLEGNHKKQPFEESTRNTEDSLRFSDSTSKTPPQEELPTRVSSPVFGATSSIKSGLDLNTSLSPSL
LQPGKKKHLKTLPFSNTCISRLEKTRSKSEDSALFTHHSLGSEVNKIIIQSSNKQILINKNISESLGEQN
RTEYGKDSNTDKHLEPLKSLGGRTSKRKKTEEESEHEVSCPQASFDKENAFPFPMDNQFSMNGDCVMDKP
LDLSDRFSAIQRQEKSQGSETSKNKFRQVTLYEALKTIPKGFSSSRKASDGNCTLPKDSPGEPCSQECII
LQPLNKCSPDNKPSLQIKEENAVFKIPLRPRESLETENVLDDIKSAGSHEPIKIQTRSDHGGCELASVLQ
LNPCRTGKIKSLQNNQDVSFENIQWSIDPGADLSQYKMDVTVIDTKDGSQSKLGGETVDMDCTLVSETVL
LKMKKQEQKGEKSSNEERKMNDSLEDMFDRTTHEEYESCLADSFSQAADEEEELSTATKKLHTHGDKQDK
VKQKAFVEPYFKGDERETSLQNFPHIEVVRKKEERRKLLGHTCKECEIYYADMPAEEREKKLASCSRHRF
RYIPPNTPENFWEVGFPSTQTCMERGYIKEDLDPCPRPKRRQPYNAIFSPKGKEQKT

FSDSTSKTPPQEELPTR

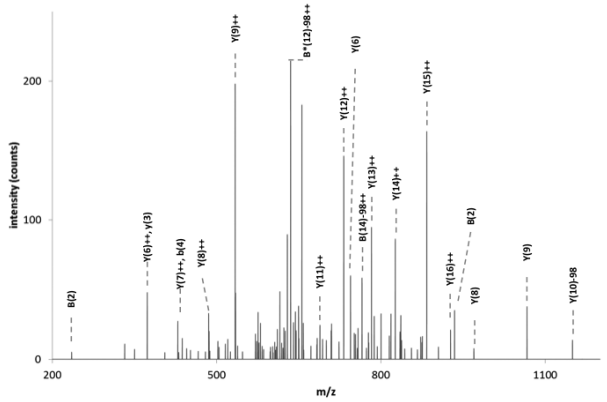

c

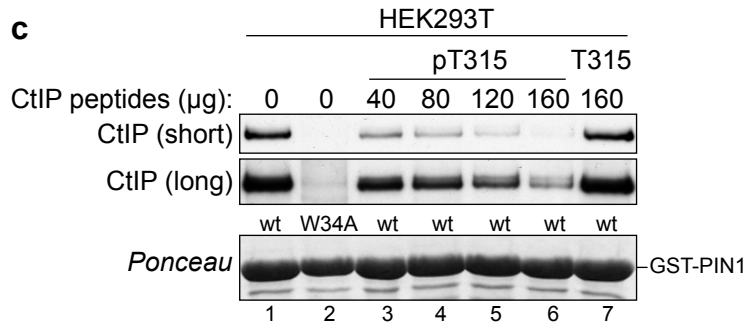

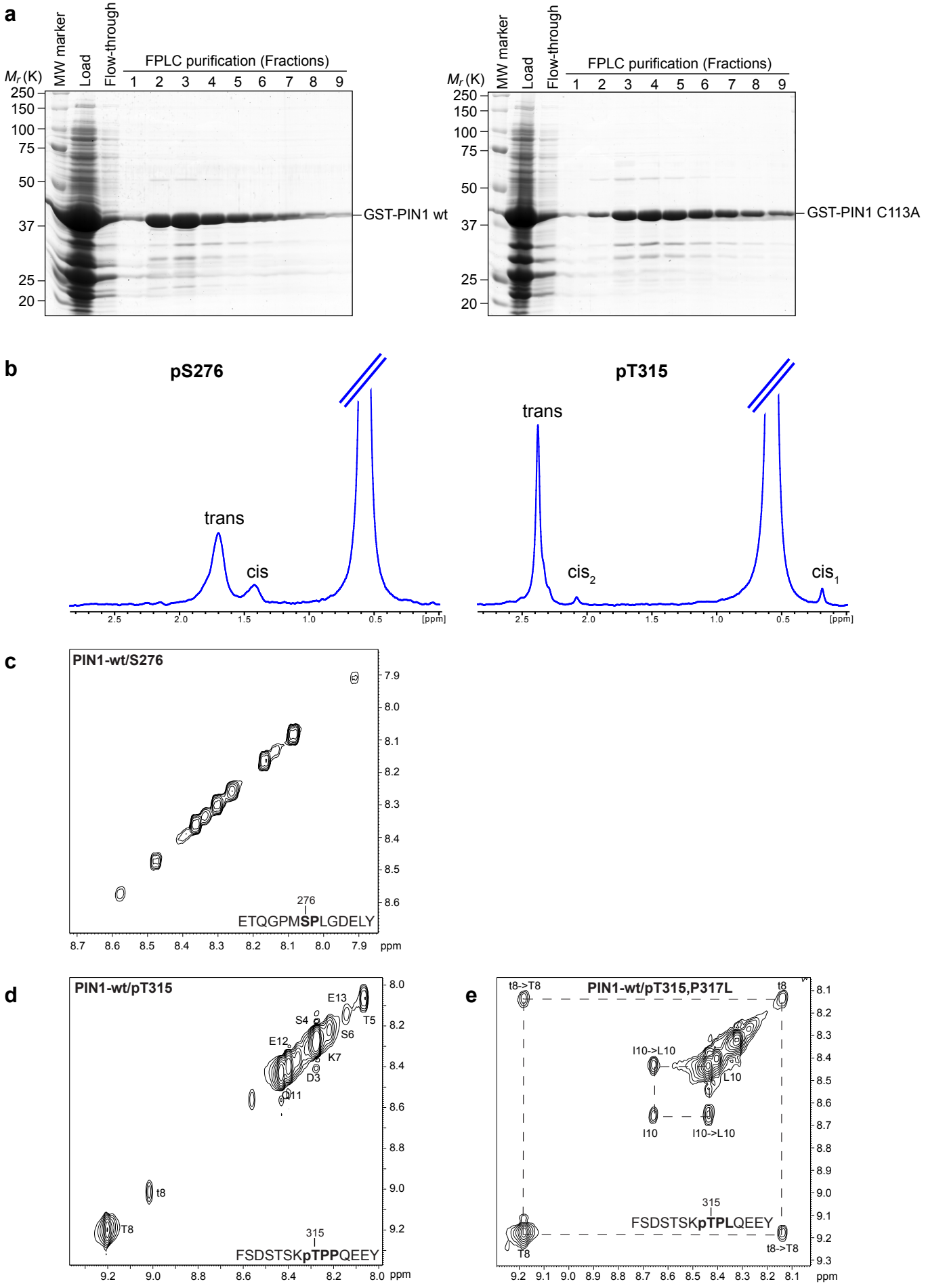
a
MW marker
Load
Flow-through
FPLC purification (Fractions)
1 2 3 4 5 6 7 8 9
M_r (K)
250
150
100
75
50
37
25
20
GST-PIN1 wt
GST-PIN1 C113A
b
pS276
trans
cis
pT315
trans
cis$_2$
cis$_1$
2.5 2.0 1.5 1.0 0.5 [ppm]
c
PIN1-wt/S276
276
ETQGPM**SP**LGDELY
8.7 8.6 8.5 8.4 8.3 8.2 8.1 8.0 7.9 ppm
d
PIN1-wt/pT315
E13
T5
S4
S6
E12
K7
D3
D11
t8
T8
315
FSDSTSK**pTPP**QEEY
9.2 9.0 8.8 8.6 8.4 8.2 8.0 ppm
e
PIN1-wt/pT315,P317L
t8->T8
t8
I10->L10
L10
I10
I10->L10
315
FSDSTSK**pTPL**QEEY
T8
t8->T8
9.2 9.1 9.0 8.9 8.8 8.7 8.6 8.5 8.4 8.3 8.2 8.1 ppm

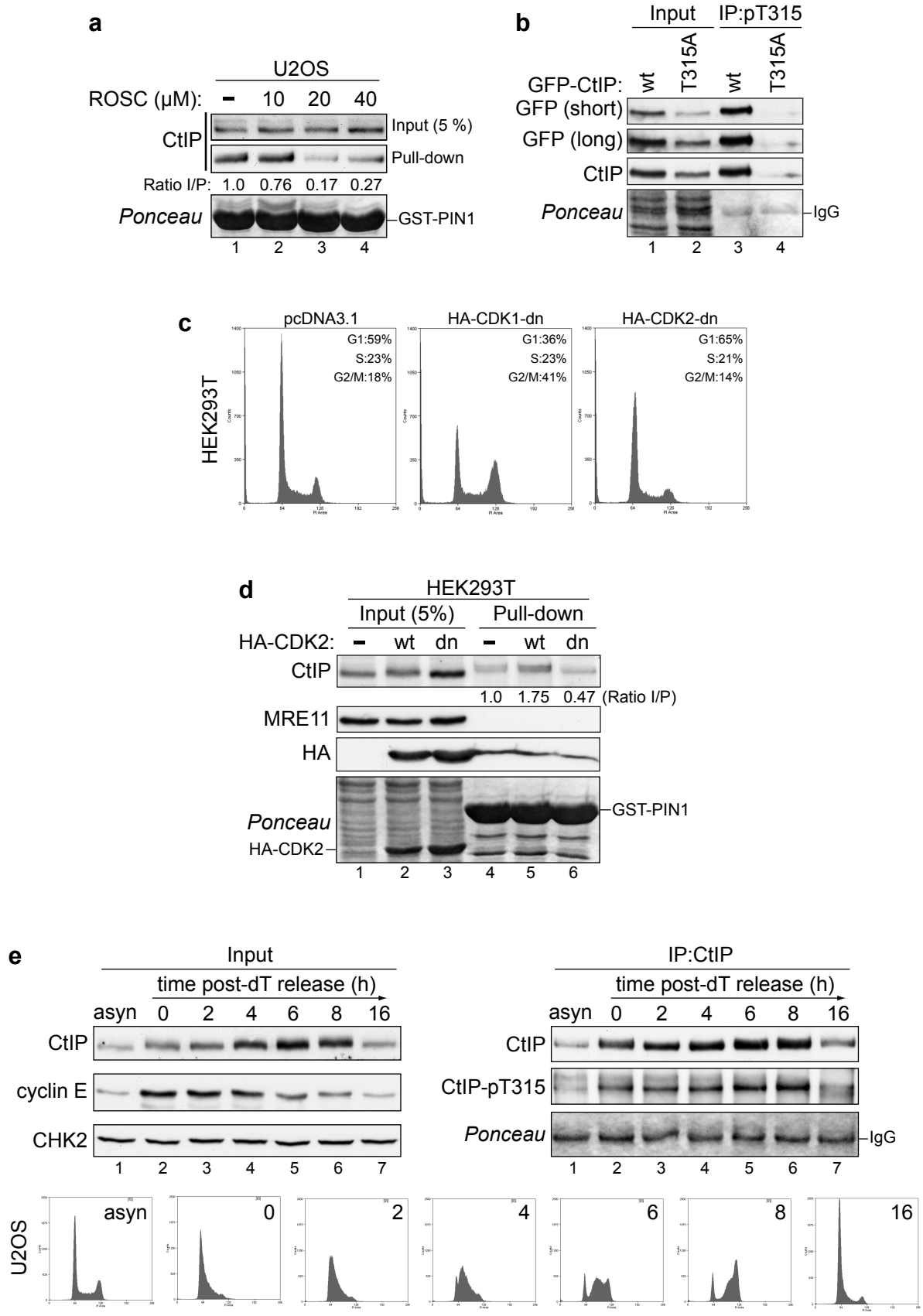
a
U2OS
ROSC (μM): - 10 20 40
CtIP
Input (5 %)
Pull-down
Ratio I/P: 1.0 0.76 0.17 0.27
Ponceau
GST-PIN1
1 2 3 4
b
Input
IP:pT315
GFP-CtIP: wt T315A wt T315A
GFP (short)
GFP (long)
CtIP
Ponceau
IgG
1 2 3 4
c
pcDNA3.1
HA-CDK1-dn
HA-CDK2-dn
HEK293T
G1:59%
S:23%
G2/M:18%
G1:36%
S:23%
G2/M:41%
G1:65%
S:21%
G2/M:14%
d
HEK293T
Input (5%)
Pull-down
HA-CDK2: - wt dn - wt dn
CtIP
1.0 1.75 0.47 (Ratio I/P)
MRE11
HA
Ponceau
HA-CDK2
GST-PIN1
1 2 3 4 5 6
e
Input
IP:CtIP
time post-dT release (h)
asyn 0 2 4 6 8 16
CtIP
cyclin E
CHK2
CtIP-pT315
Ponceau
IgG
1 2 3 4 5 6 7
U2OS
asyn
0
2
4
6
8
16

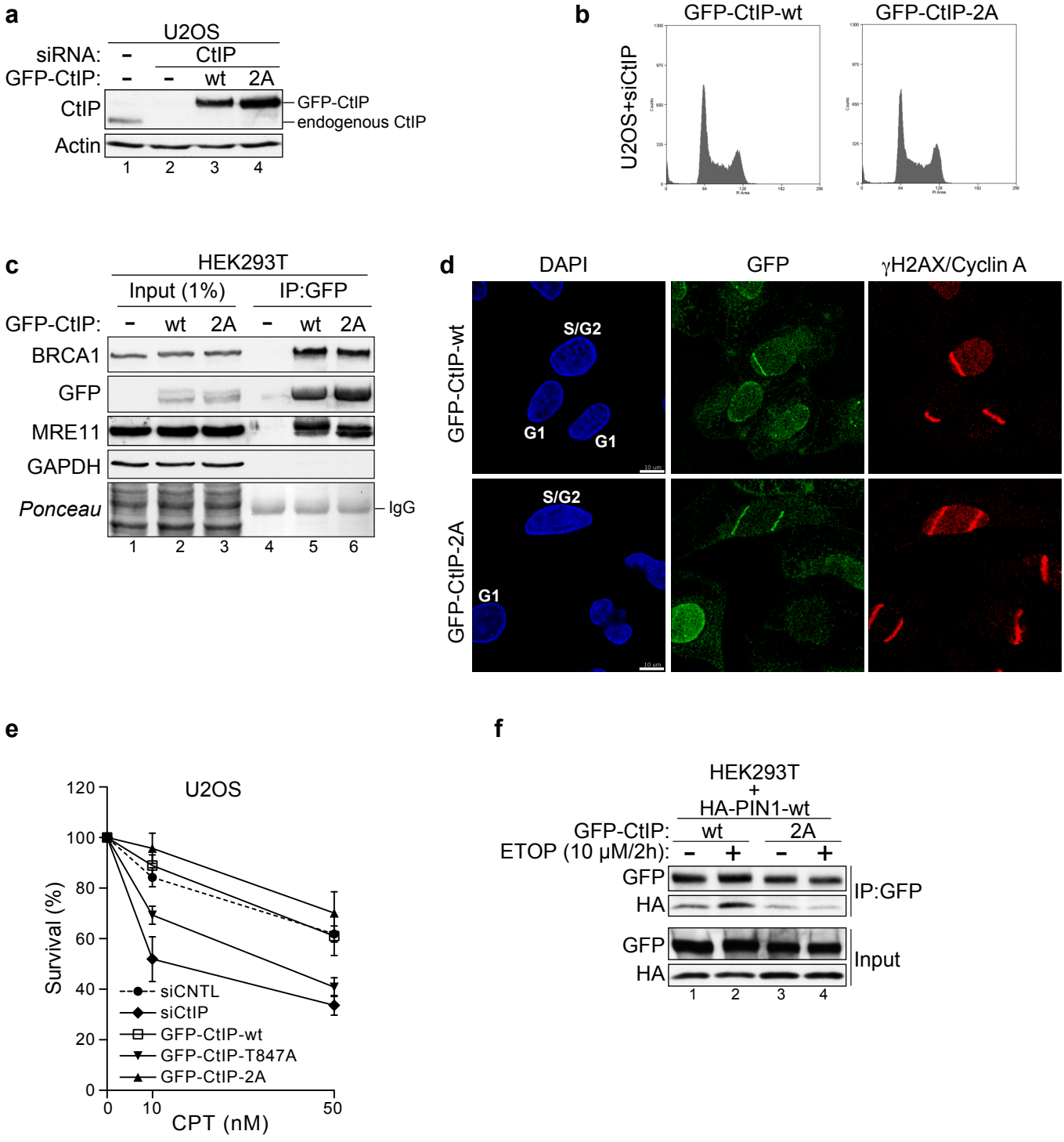
a
U2OS
siRNA: - CtIP
GFP-CtIP: - - wt 2A
CtIP
Actin
GFP-CtIP
endogenous CtIP
1 2 3 4
b
GFP-CtIP-wt
GFP-CtIP-2A
U2OS+siCtIP
c
HEK293T
Input (1%)
IP:GFP
GFP-CtIP: - wt 2A - wt 2A
BRCA1
GFP
MRE11
GAPDH
Ponceau
IgG
1 2 3 4 5 6
d
DAPI
GFP
γH2AX/Cyclin A
GFP-CtIP-wt
GFP-CtIP-2A
S/G2
G1
G1
S/G2
G1
e
U2OS
Survival (%)
120
100
80
60
40
20
0
0 10 50
CPT (nM)
siCNTL
siCtIP
GFP-CtIP-wt
GFP-CtIP-T847A
GFP-CtIP-2A
f
HEK293T
+
HA-PIN1-wt
GFP-CtIP: wt 2A
ETOP (10 μM/2h): - + - +
GFP
HA
IP:GFP
GFP
HA
Input
1 2 3 4

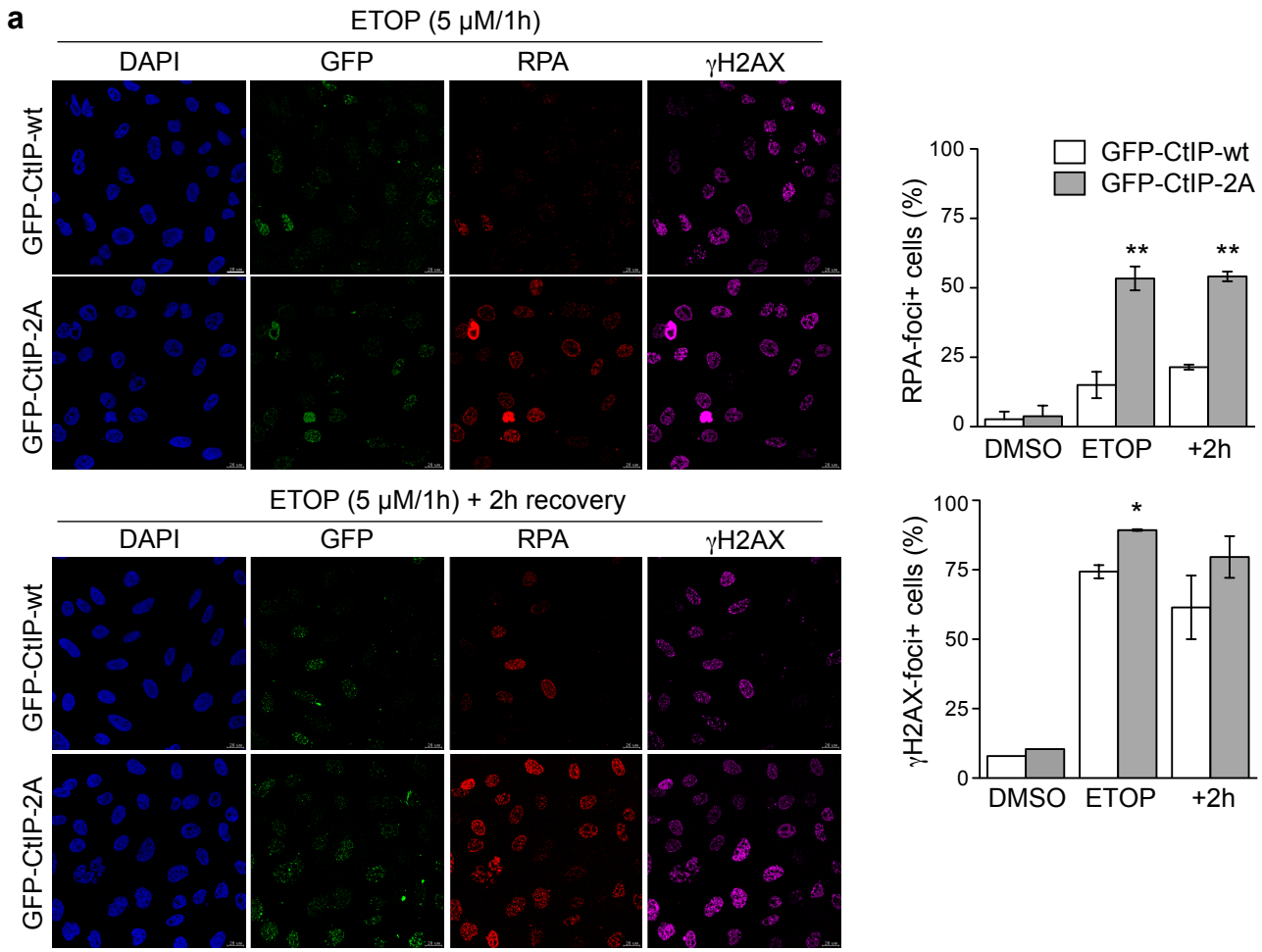
a
ETOP (5 μM/1h)
DAPI
GFP
RPA
γH2AX
GFP-CtIP-wt
GFP-CtIP-2A
ETOP (5 μM/1h) + 2h recovery
GFP-CtIP-wt
GFP-CtIP-2A
RPA-foci+ cells (%)
GFP-CtIP-wt
GFP-CtIP-2A
DMSO
ETOP
+2h
γH2AX-foci+ cells (%)
DMSO
ETOP
+2h

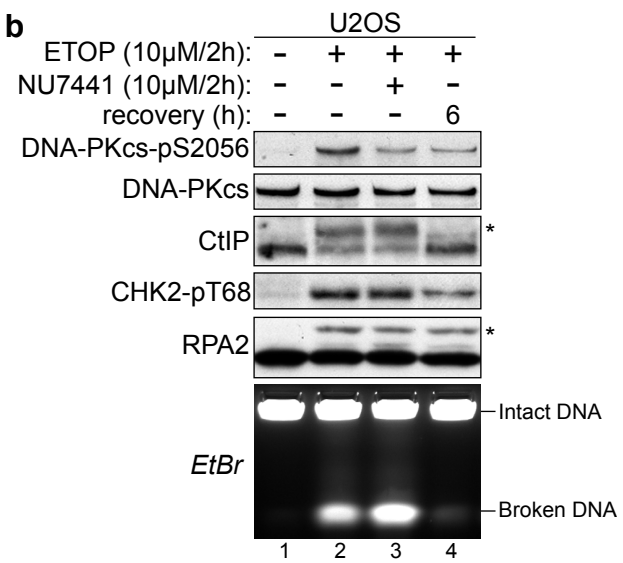
b
U2OS
ETOP (10μM/2h):
NU7441 (10μM/2h):
recovery (h):
DNA-PKcs-pS2056
DNA-PKcs
CtIP
CHK2-pT68
RPA2
EtBr
Intact DNA
Broken DNA
1 2 3 4

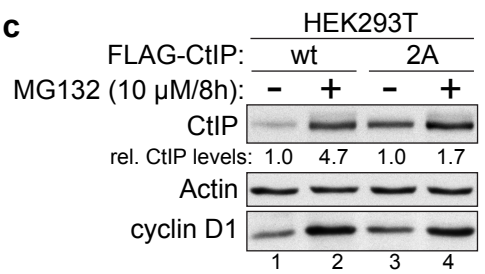
c
HEK293T
FLAG-CtIP:
wt
2A
MG132 (10 μM/8h):
CtIP
rel. CtIP levels: 1.0 4.7 1.0 1.7
Actin
cyclin D1
1 2 3 4

4. DISCUSSION

4.1 DNA end resection by CtIP and exonuclease 1 prevents genomic instability

In the first part of my thesis (section 3.1) we have investigated the interplay between Mre11, CtIP and Exo1 in the repair of DSBs by HR. Our goal was to determine whether the recruitment of Exo1 to sites of DNA damage was dependent on Mre11 and/or CtIP. Moreover, we wanted to establish whether the two factors physically interact and whether CtIP could regulate Exo1 activity. Finally, we examined the role of both Exo1 and CtIP in the maintenance of genomic stability.

By siRNA-mediated knockdown of either CtIP or Mre11 followed by micro-laser irradiation in cells expressing GFP-Exo1, we found that the recruitment of Exo1 to the sites of DNA damage was impaired. This observation strongly supports the hypothesis that initial DNA end resection carried out by MRN and CtIP are needed for Exo1 loading at sites of DNA damage. In support of this hypothesis is the fact that cells depleted for either CtIP or Mre11 are resection-deficient, illustrated by impaired ssDNA formation and, consequently, impaired RPA recruitment.

The molecular basis of DNA end resection facilitated by MRN and CtIP seems to vary among different eukaryotes. For instance, in fission yeast, Nbs1 recruits Ctp1 (ortholog of human CtIP) through direct interaction in a phosphorylation-dependent manner to sites of damage[233]. In contrast, in mammalian cells the recruitment of CtIP to DSBs is independent of MRN and rather occurs via direct DNA binding[170]. In budding yeast, initiation of resection is carried out by the MRX complex with the help of Sae2. Interestingly, an intrinsic endonuclease activity was reported for Sae2 whereas no such activity has been reported for any of its orthologues[234]. However, Sae2 does not physically interact with the MRX complex, while human CtIP directly associates with MRN and stimulates its endonucleolytic activity[90,234]. Besides these differences, it seems clear that the collaborative action of both the MRN complex and CtIP is required to facilitate loading of Exo1 at the sites of damage.

The requirement for MRX and Sae2 in DNA end resection is highly dependent on the nature of the DNA ends. For instance, resection of clean DSBs, such as those induced by rare-cutting endonucleases (e.g. HO nucleases) can occur without MRX and Sae2. In budding yeast, such DSBs are for instance processed in the absence of Mre11, Rad50 and Sae2 but resection of modified ends (i.e. IR-induced DSBs or covalently-trapped DNA topoisomerase adducts) depends on these factors[235-237]. In fact, DNA ends bound by Spo11 during meiotic recombination are processed in a Sae2- and MRX-dependent manner[234,238,239]. The observation that both MRN and CtIP are needed to initiate resection prior to Exo1 recruitment is therefore not surprising.

The function of MRN and CtIP in DNA end resection is perhaps best understood in the context of how well the long-range resection machinery is able to access and further process DSB ends. In other words, the severe defects in DNA resection and DSB repair caused by the depletion of CtIP is most likely due to impaired recruitment of Exo1 and probably other accessory factors rather than a specific requirement to initiate resection at clean ends.

We found that the recruitment of Exo1 is independent of the BLM helicase. This result is not surprising since both factors have been associated with the second, more excessive phase of resection operating in two parallel, partially redundant pathways[237]. However, the involvement of BLM in the resection process remains somewhat controversial. For instance, it was reported that BLM can stimulate the exonuclease activity of Exo1 *in vitro* or the affinity of Exo1 towards DNA ends, suggesting their cooperation during resection[93,240]. The latter of the two studies further demonstrated the involvement of two independent resection machineries, involving either Exo1 or Dna2[93]. Moreover, yeast Mre11 was reported to directly interact with Sgs1 thereby recruiting it to DNA ends[241,242]. Further experiments in both yeast and human cells are clearly needed to resolve the question which of described scenarios is more likely to reflect the situation within a living cell. For example, in our studies, it remains to be tested whether the initial DNA end-trimming step performed by CtIP and Mre11 is required for BLM recruitment to DSBs. Besides these different observations, it should be noted that an active role of BLM in the

generation of ssDNA at DSBs is inconsistent with the phenotype of cells derived from patients with Bloom syndrome which display hyper-recombination phenotypes rather than a deficiency in HR. Therefore, it is possible that, at least in higher eukaryotes, another RecQ helicase family member (i.e. RecQ1, WRN, RecQ4 or RecQ5) is part of the resection machinery. Moreover, it is possible that multiple DNA end resection pathways can act in parallel as demonstrated by the fact that the absence of BLM or Exo1 alone does not impair resection in mammalian cells[92].

We found that CtIP physically interacts with Exo1 and is able to restrain Exo1 exonucleolytic activity *in vitro* both on circular as well as linear substrates. The most straightforward explanation for this observation is that the association between CtIP and Exo1 at sites of damage is needed to fine-tune the nucleolytic activity of Exo1. According to our data, CtIP and Mre11 activities would be needed to perform the initial end-trimming step during DSB repair, which in turn allows Exo1 to be loaded onto damaged chromatin. CtIP then further regulates the processing activity of Exo1 in order to limit extensive resection. In line with our observations, *S. cerevisiae* MRX-Sae2 was reported to perform the initial end-trimming step on a linear DNA substrate in order to facilitate Exo1-mediated resection[243]. Nevertheless, no restraining activity of Sae2 on Exo1 was observed in this report. Another study analyzed the effect of MRN on Exo1 activity *in vitro*[93]. In this report, MRN stimulated the activity of Exo1 to degrade a linear substrate but the effect of CtIP on the resection capability of Exo1 was not tested. Further investigations are needed to clarify these issues.

We also found that Exo1 does not interact with Mre11 whereas it physically associates with CtIP. In contrast, no protein-protein interactions could be detected between yeast MRX, Sae2 and Exo1[243]. However, MRX, Sae2 and Exo1 formed complexes in the context of DNA, as evidenced by cooperative binding to oligonucleotide substrates when all proteins were present[243]. Altogether, different factors involved in DNA end processing might play slightly diverse roles in different eukaryotes. For example, whereas budding yeast Sae2 plays a minor role in resection initiation, the defects of fission yeast cells lacking Ctp1 are similar to Mre11 null cells[173]. Since Ctp1 is more similar to CtIP than Sae2,

both in terms of function as well as protein sequence, it would be interesting to study the cooperative function of Ctp1 with MRN and Exo1 during DNA resection in *S. pombe*.

Our observations indicate that the initial end-trimming activity of MRN–CtIP is required for the recruitment of EXO1 to sites of DNA damage and that CtIP might subsequently control EXO1 exonucleolytic activity to facilitate HR. To examine the interplay between Exo1 and CtIP *in vivo*, we analyzed DNA damage signaling in cells lacking CtIP, Exo1 or both proteins. As reported previously, depletion of CtIP strongly abrogated the formation of ssDNA, as measured by RPA2 hyperphosphorylation after treatment with camptothecin (CPT)[90]. In contrast, we did not observe any difference in RPA2 hyperphosphorylation in Exo1-deficient cells compared to control cells. This indicates that the absence of Exo1 does not impair efficient formation of long tracts of ssDNA needed for HR. Our observations are in line with data obtained by others showing no overt resection defects of cells lacking Exo1, giving further evidence for the presence of an alternative, compensating long-range resection pathway involving BLM and Dna2[92,93]. On the other hand, data in budding yeast suggest that in absence of both Exo1 and Sgs1 long-patch resection may be delayed but the processive, exonucleolytic degradation of Exo1 can be partially compensated by the action of Mre11-Sae2[236]. In contrast, *S. pombe* Exo1 accounts for the majority of extensive resection and Exo1Δ cells exhibit a 70% reduction in resection activity[173]. Moreover, *S. pombe* Rqh1 (orthologue of human BLM) is relatively inefficient in compensating Exo1 function. Thus, based on our data indicating that in human cells the role of Exo1 is not essential for DNA end resection, checkpoint signaling and HR of replication-associated DSBs, we conclude that initial DSB processing differ between yeast and human cells.

To assess the importance of CtIP and Exo1 in promoting successful DSB repair and cellular survival we carried out colony formation assays. To this end, we analyzed the capability of cells depleted for Exo1, CtIP or both together in tolerating replication-associated DSBs, such as those induced by CPT and the PARP inhibitor Olaparib (AZD-2281). We found that cells lacking CtIP were hypersensitive to acute or chronic treatment with both drugs. These observations were not that surprising since the CPT hypersensitivity of CtIP-

deficient cells was shown previously and Olaparib induces lesions similar to the ones created by CPT[3,90]. The fact that cells depleted for CtIP are efficiently killed by agents inducing replication-associated DSBs suggests that the cells either completely fail to repair the breaks, or carry out erroneous rejoining of the DSBs which results in the formation of toxic radial chromosomes. Strikingly, depletion of Ku in a Ctp1-deficient background partially rescues the hypersensitivity of *S. pombe* cells to CPT indicating that faulty repair by NHEJ can account for the decreased viability of CtIP-deficient cells[244,245]. Moreover, in favour of this hypothesis, we could show by PFGE analysis that cells lacking CtIP accumulate only slightly more DSBs compared to control cells after treatment with CPT. As expected, depletion of Exo1 did not result in any significant decrease in cell survival. Thus, our results are in agreement with findings that an alternative, backup resection pathway can compensate for the loss of Exo1. For instance, it was demonstrated that the simultaneous knockdown of both Exo1 and BLM is needed in order to sensitize mammalian cells to DSB-inducing agents[92].

However, we found that concomitant knockdown of both Exo1 and CtIP leads to a small, but statistically significant increase in cell survival compared to CtIP depletion alone. At the same time, when analyzing metaphase chromosome spreads of CPT treated cells, we found an increase in radial chromosome formation in double-depleted versus single-depleted cells. Taken together, these results might indicate that even in the absence of CtIP, the exonuclease Exo1 is still able to somehow process DSBs that may limit Ku binding and subsequent deleterious end-joining events. The fact that the formation of radial chromosomes in cells lacking CtIP and Exo1 is reversed upon chemical inhibition of DNA-PKcs strongly supports this hypothesis. The observed inhibitory effect of CtIP on Exo1 activity *in vitro* might indicate that CtIP has a dual role in controlling Exo1 function. First, to initially process DSBs in conjunction with MRN thereby preparing suitable DNA substrates for Exo1 recruitment and, second, to limit its activity in order to create suitably-sized ssDNA tracts needed for subsequent strand invasion and repair by HR.

In the first part of the paper, we clearly show that Exo1 recruitment is impaired when CtIP is absent suggesting that Exo1 acts downstream of CtIP. However, in the second part,

we find that depletion of Exo1, at least partially, rescues CPT hypersensitivity of CtIP-depleted cells and results in a dramatic increase in NHEJ-dependent radial chromosome formation. These data suggest that Exo1 is able to process DSBs in absence of CtIP and points to a CtIP-independent function of Exo1 in limiting Ku binding and suppressing unwanted end-joining events. This apparent paradox that Exo1 is recruited to DSBs without CtIP needs to be further resolved in the future. For example, it is possible that MRN alone is sufficient to recruit some Exo1 to breaks. Moreover, in our live cell imaging approach we measure retention of DDR proteins to laser-induced DSBs rather than their recruitment. Thus, it is possible that Exo1 is initially recruited to DSBs in a CtIP- (and MRN-)independent manner but its stable and visible association requires the action of CtIP (and/or MRN). Therefore, more sensitive methods or alternative approaches and model systems are needed to answer this important question. Along the same line, it needs to be determined which domain of Exo1 is responsible for CtIP binding in order to create specific loss-of-function mutants of Exo1 unable to interact with CtIP. The availability of such interaction mutants would allow us to directly study the relationship between CtIP on Exo1 in DNA end resection.

4.2 PIN1-mediated isomerisation of CtIP determines DSB repair pathway choice

In the second part of the results (section 3.2) we aimed at identifying novel CtIP phosphorylation sites, their potential role in the regulation of DSB repair and to study the putative role(s) of the phosphorylation-specific peptidyl-prolyl *cis/trans* isomerase PIN1 in the DDR. At first, an unbiased mass spectrometry (MS)-based approach revealed several hundreds of putative, phospho-specific PIN1-interaction proteins. Most of the identified proteins were found to specifically interact with wild-type (wt) PIN1 but not with a binding mutant of PIN1 in which a tryptophan in the WW domain, crucial for substrate recognition, is substituted by alanine (W34A). The fact that so many proteins seem to be controlled by PIN1 is perhaps not surprising taking into consideration that phosphorylation at S/T-P motifs is a central signaling mechanism in diverse cellular

processes (refer to section 1.4 for details). PIN1-mediated *cis/trans* isomerisation of proteins was shown to coordinate several phosphorylation events in a spatio-temporal manner or to facilitate the crosstalk with other PTMs such as ubiquitylation[246]. Strikingly, in our MS-analysis a number of proteins previously implicated in the regulation of DSB repair pathway choice of DSBs, such as BRCA1, MDC1 and 53BP1, were identified[129,130]. Moreover, we could identify several proteins involved in the repair of DSBs and ICLs such as CtIP, SLX4 and BRIP1/FANCJ. These results prompted us to investigate whether lack or overexpression of PIN1 mutants may affect the efficiency of NHEJ and HR. By using two GFP-based reporter cell lines, we measured repair efficiency after induction of DSBs by the rare-cutting endonuclease I-*Sce*I. Interestingly, we found that siRNA-mediated downregulation of PIN1 using three different oligos led to a significant decrease in NHEJ, while HR was slightly elevated, suggesting that PIN1 might control one or more factors involved in DSB repair. Importantly, flow cytometry analysis revealed no alterations of the cell cycle profile upon PIN1 gene silencing. Moreover, the ectopic overexpression of PIN1 resulted in a dramatic decrease in HR that was partially dependent on both the binding capacity (W34A) and the catalytic activity (C113A). The fact that we did not observe a more substantial rescue of HR in PIN1 mutants could indicate that they are either still partially active (W34A) or that binding of PIN1-C113A to phospho-substrate essential for HR has a strong dominant-negative effect. Accordingly, we observed that the PIN1-W34A recombinant protein retains its capability in isomerising a phosphorylated peptide substrate as determined by NMR spectroscopy (data not shown). Similarly, catalytically inactive mutants of PIN1 such as C113A lose most of their activity but are not completely inactive while retaining their capability to bind phosphorylated substrates[193]. It is therefore possible that high amounts of PIN1, although not fully active or compromised in phospho-binding, can still induce protein isomerisation of cellular substrates, albeit at much lower efficiency. It would be thus interesting to test the effect of overexpressing a PIN1 double mutant (W34A/C113A) in our GFP-based HR reporter assay. In summary, our results points for the first time to a role of PIN1 in DSB repair and indicate that PIN1 might control the balance between HR and NHEJ. We hypothesized that PIN1 might target one

or more of the identified factor(s) in our mass spectrometry screen to shift the balance between HR and NHEJ. To investigate the mechanism(s) by which PIN1 controls the DSB repair pathway choice we treated cells with etoposide, a DNA topoisomerase II inhibitor inducing DSBs in a cell cycle-independent manner[31]. Interestingly, we found that knockdown of PIN1 results in increased RPA focus formation. Concomitantly, we observed an increase in hyperphosphorylated RPA2 when analyzing the same cells by immunoblotting. Both of these results indicate that in absence of PIN1 DSBs become hyperresected, thereby potentially suppressing NHEJ and channeling repair into HR. Moreover, we found that the increase in RPA focus formation observed in PIN1-deficient cells upon etoposide treatment is CtIP-dependent indicating that PIN1 might directly target CtIP in order to inhibit DNA end resection. Accordingly, we found that the decrease in NHEJ of PIN1-depleted cells is partially CtIP-dependent. These results support a model in which PIN1 controls DSB repair pathway choice by targeting a key component of the DNA end resection machinery, namely CtIP. However, co-depletion of CtIP and PIN1 did not result in a complete rescue of NHEJ as measured by GFP-based reporter assays. This could be explained by two possible scenarios: First, additional factors involved in DSB repair pathway choice such as 53BP1 or BRCA1 might be controlled by PIN1-mediated proline isomerisation. This notion is supported by the fact that both these factors were identified as PIN1 binding partners in our MS analysis. Nevertheless, further experiments are needed to determine the effect of PIN1-mediated isomerisation on 53BP1 and BRCA1. Second, since the our NHEJ reporter system (EJ5) is measuring total EJ events (c-NHEJ and alt-NHEJ), CtIP depletion may reduce repair efficiency due to its role in alt-NHEJ[247]. In fact, we did not observe an increase in NHEJ after CtIP depletion. In agreement with our observation that PIN1-deficient cells exhibit increased levels of DSB resection, we found that cells overexpressing PIN1 are partially deficient in DNA end resection. Taken together, our data clearly implicate PIN1 as a novel factor regulating the balance between NHEJ and HR by influencing the extent of DNA resection.

To further assess physical interaction between PIN1 and CtIP, we performed several experiments such as co-immunoprecipitation, pulldowns and PLA assays and found that

PIN1 indeed interacts with CtIP both *in vitro* and *in vivo*. Moreover, using far-western blot analysis we were able to demonstrate a direct association between the two proteins. PIN1 specifically targets phosphorylated S/T-P motifs to induce a *cis/trans* conformational change in the substrate[197]. We therefore aimed at identifying the pS/T-P motifs in CtIP responsible for PIN1 binding. CtIP contains in total 12 such motifs of which only two are known to be phosphorylated (S327 and T847)[120,174]. However, by substituting several serine or threonine residues with alanine, we found that S276 and T315 were critical for PIN1 interaction. Notably, we found that T315A much more strongly abrogates the binding to PIN1, while S276A only caused a minor reduction. However, only the CtIP S276A/T315A double mutant almost completely abolished the binding, favouring a model in which pT315 serves as the major binding site with pS276 potentially serving as a backup binding site when T315 is not available. By raising phospho-specific antibodies for either site, we could show that both residues are phosphorylated *in vivo.* Further*,* by using small-molecule inhibitors and dominant-negative version of CDKs we could show that the interaction between CtIP and PIN1 is mostly CDK2-dependent, indicating that T315 may be phosphorylated in a cell cycle-dependent manner. Accordingly, we showed that recombinant CDK2-cyclin complexes are able to phosphorylate both sites *in vitro.* Moreover, we observed that pT315 is increased during S phase progression, in line with high CDK2 activity. It thus appears that CDK2 primes CtIP at the entry of S-phase in order to promote PIN1 isomerisation whenever needed. Whether S276 is phosphorylated by a CDK or another proline-directed kinase *in vivo* remains to be determined. The primary amino acid sequence surrounding S276 suggests that MAPKs might phosphorylate this site *in vivo.*

To determine whether PIN1 was able to induce a *cis/trans* conformational change on the peptide bond between pS276-P277 and pT315-P316 we made use of NMR spectroscopy. It has been previously shown that this method is highly informative to determine the *cis* or *trans* state of a proline residue within a peptide[248]. Therefore, we synthesized pS276 and pT315 peptides as well as their corresponding, non-phosphorylated counterparts and found that PIN1 is able to isomerise the phosphorylated S276 peptide. Isomerisation of

pS276 was dependent on the catalytic activity, since PIN1-C113A did not trigger a conformational change. Moreover, a non-phosphorylated version of the same peptide was not isomerised by wild-type PIN1. Interestingly, as mentioned previously, we found that PIN1-W34A mutant was fully proficient in phospho-peptide isomerisation, indicating that the catalytic domain is sufficient to isomerise phosphorylated pS/T-P motifs under these conditions[209]. To our great surprise, no *cis/trans* proline isomerisation was detected with the pT315 peptide. This led us to hypothesize that the presence of a second, adjacent proline (P317) in the sequence may hinder PIN1-mediated isomerisation. In fact, we found that a peptide in which P317 was replaced with a leucine was efficiently isomerised by PIN1. In favour of this hypothesis are previous reports showing that the catalytic activity of PIN1 on a peptide containing a phosphorylated threonine followed by two consecutive prolines is very low[249,250]. Importantly, a recent study reported the production of conformation-specific antibodies able to recognize either the *cis* or the *trans* state of the tau protein involved in Alzheimer's disease[251].

In the last part of this study, we produced human cell lines (U2OS) stably expressing an siRNA-resistant, GFP-tagged S276A/T315A double mutant of CtIP (CtIP-2A). CtIP-2A was still able to interact with MRN, but not with PIN1, and was still efficiently recruited to laser-induced DSBs. Moreover, CtIP-2A localized to DSBs foci induced by IR and etoposide treatment. Taken together, we conclude that PIN1-mediated isomerisation is not required for CtIP redistribution to damaged chromatin. However, when we treated cells with etoposide and analyzed the capability of CtIP in resecting DNA ends, we found that cells expressing CtIP-2A displayed an increase in both RPA2 focus formation and RPA2 hyperphosphorylation, similar to what we observed in PIN1 downregulated cells. These results prompted us to investigate the interaction between PIN1 and CtIP in presence of DNA damage. Interestingly, we noted a small, but reproducible increase in PIN1-CtIP interaction upon etoposide. Furthermore, the increase was dependent on ATM activity as the binding was reversed to levels of untreated cells after co-treated with an ATM inhibitor (data not shown). This result can be interpreted in two different ways. First, DSB-induced ATM activation could lead to an increase in T315 and/or S276

phosphorylation, most likely by activating downstream kinases. Second, the accumulation of CtIP at damaged chromatin may enhance its chances for being recognised by PIN1. Although ATM was reported to induce Erk1/2 and p38 kinases in response to DNA damage, we did not observe any increase in S276 or T315 phosphorylation upon treatment with IR or etoposide (data not shown)[252,253]. However, it is also true that the recruitment of CtIP to DSBs depends on the ATM kinase[170]. Thus, the interaction is more likely to take place in the vicinity of DSBs than under non-stressed conditions, implicating that PIN1 may get recruited itself to sites of DSBs. To test this hypothesis we micro-irradiated cells but did not observe PIN1 localizing to laser-induced DSBs (data not shown). On the other hand it is quite likely that the DNA damage-induced CtIP-PIN1 interaction is very transient and is therefore not visibly detectable by standard IF techniques. This, of course raises the question on how DNA damage triggers CtIP-PIN1 interaction. A third, very exciting alternative could be that ATM directly phosphorylates PIN1 in response to DSBs, thereby stimulating the recognition and subsequent isomerisation of DDR proteins. Interestingly, it was reported previously that PIN1 is phosphorylated at S108 upon IR[177].

In order to determine the outcome of CtIP isomerisation by PIN1 on the molecular level, we examined whether PIN1 could either facilitate CtIP protein degradation or enhance its stability. Noteworthy, many substrates targeted and isomerised by PIN1 get degraded by the ubiquitin-proteasome pathway[246]. Interestingly, we found that the half-life of CtIP-2A protein was markedly enhanced after etoposide treatment when compared to CtIP-wt protein. In addition, treatment of cells with the proteasome inhibitor MG-132 stabilized the CtIP-wt protein by about 5-fold, while the levels of the CtIP-2A mutant increased by only about 2-fold in the over the same period of treatment. Moreover, we repeatedly noticed an increase in CtIP levels in cells depleted for PIN1, while we observed the opposite after PIN1 overexpression, in particular under DNA damaging conditions. We thus speculate that in response to DSBs, PIN1 induces a *cis/trans*-conformational change of CtIP thereby targeting CtIP for proteasome-mediated degradation. This is in line with our data showing increased DNA end resection in cells lacking PIN1 or in cells expressing

CtIP-2A defective in PIN1 binding. It is worth noting that the conserved sequence motif surrounding CtIP-T315 (TPP) is identical to sequences in c-Myc and cyclin E, both proteins known to be degraded upon phosphorylation and in a PIN1-dependent manner by the so-called SCF (Skp, Cullin1, F-box) ubiquitin-ligase complex[227,254]. It is therefore tempting to speculate that a similar regulatory mechanism exists for CtIP in situations where DSB resection, and, as a consequence of this, maintenance of checkpoint signaling and HR repair, is not favourable for a cell[255]. For example, we could envision such a scenario in situation where damage is too severe and cells prefer to undergo apoptosis. But if it could also be another way to regulate DSB repair pathway choice, particularly in G2 phase, where both NHEJ and HR are competing with each other. Future studies are needed to elucidate the exact mechanism by which CtIP is degraded in a PIN1-dependent manner and which ubiquitin-ligase complex is involved in this process.

In summary the results in this thesis shed further light into the complex pathways that deal with DSBs with special emphasis on protein-protein interactions and PTMs of human CtIP, both of which can alter the equilibrium between HR and NHEJ.

5. CONCLUSIONS AND PERSPECTIVES

DSB repair is crucial for the maintenance of genome integrity. In this context, the regulation of DNA end resection, an otherwise irreversible reaction, is of major importance and the wrong decision may lead to dramatic consequences.

Many years of research have culminated in a good understanding of the processes of DSB repair. Many proteins involved in the process of HR have been described and we also have good knowledge on the process of DNA end resection. Moreover, much is understood about how checkpoints are activated upon DNA damage and how they affect the cell cycle, and conversely, how the cell cycle stage influences the mode of DSB repair. A next challenge is to further broaden our understanding on how the different DSB repair pathways collaborate and whether crosstalks between them exist. Furthermore, an important issue that needs to be clarified in the future is whether the numerous studies on the mechanism of DSB processing conducted *in vitro* also hold true *in vivo.* Another important question is how PTMs influence the repair of DSBs. We have just started to appreciate the amount and variety of protein modifications involved in the DDR. For example, many protein phosphorylations are triggered by DNA damage but it needs to be established how these events control DSB repair. Moreover, we need a more detailed understanding on the functional consequences of protein-protein interactions during DSB repair. In the underlying studies, we aimed at answering some of these open questions with particular focus on PTMs and protein-protein interactions during DSB repair.

In the first part of my thesis the role of CtIP and Exo1 in the initiation of DNA end resection was studied in mammalian cells and we could confirm that CtIP is a fundamental factor involved in this process. CtIP interacts with both MRN and Exo1 to initiate DSB repair by HR and our studies indicate that inhibition of MRN and/or CtIP activities could represent an attractive way of blocking DNA end resection and hence repair by HR. Since many chemotherapeutic agents introduce DSBs in the genome and the repair of some of these breaks is dependent on HR, it could be of major use to develop specific small molecule inhibitors against CtIP or the MRN complex. However,

while Mre11 has nuclease activity that could be targeted, no enzymatic function of human CtIP has been reported to date. In addition, there is no structural data available that may allow designing other strategies of "inhibiting" the function of CtIP in DNA end resection. For example, an attractive way to interfere with DSB resection would be to specifically block protein-protein interactions of CtIP. The problem of therapies based on the inhibition of DNA repair proteins is that these factors often play an essential role in in any dividing cell in our body. Therefore it is of major importance to gain knowledge on the individual, genetic background of a given tumor and on the connection between the different DNA repair pathways often acting in parallel. For instance, based on the concept of synthetic lethality, if a particular DNA repair pathway is altered or dysfunctional in cancer cells and a backup repair mechanism exists, specific inhibitors targeting the backup pathways could efficiently trigger cell death in these cells without affecting normal cells. In this regard, it could be of major use to identify CtIP-deficient tumors rendering them hypersensitive to agents inducing DSBs in replicating cells.

In the second part of my thesis we investigated the ability of PIN1 in controlling CtIP. We found that PIN1 can bind CtIP and in this way affect the choice of DSB repair. Importantly, cells lacking PIN1 show decreased levels of NHEJ efficiency. Moreover, cells overexpressing PIN1 exhibit strong HR defects partly due to defects in CtIP-mediated DNA end resection. With this study we not only contribute in answering the long-standing question whether PIN1 presents an attractive target for drug development, but also show, for the first time, a role for PIN1 in DNA repair. Thus, our results suggest that inhibition of PIN1 may radiosensitize cancer cells. Unfortunately, juglone, the only small molecule inhibitors available to date, also inhibits RNA polymerase II, while a panel of structurally distinct compounds showing strong inhibition of PIN1, display unspecific cytotoxicity[256]. Second, in *S. cerevisae* and *A. nidulans*, the cellular levels of PIN1 can be reduced up to 50-fold with little or no effects on the cell cycle of these fungal organism[257,258]. Therefore, even if specific drugs could be developed they would need to also be highly efficacious to halt the division of tumor cells. Moreover, given that PIN1 is

overexpressed in most cancers, it might be extremely difficult to efficiently inhibit PIN1. However, it could be worth screening for tumors with high expression levels of PIN1, which, according to our results, co-incides with reduced rates of HR. Based on the concept of synthetic lethality, these types of cancers should be particularly sensitive to drugs causing replication-associated DSBs (e.g. PARP inhibitors and CPT) that can only be repaired in an error-free manner by HR. In this way PIN1 levels would serve as a diagnostic marker for cancer therapy rather than a direct drug target. But clearly, in future a lot of pre-clinical research has to be carried out in order to determine whether the results presented in this thesis can be applied for cancer treatment.

6. REFERENCES

1. Lindahl, T. Instability and decay of the primary structure of DNA. *Nature* **362**, 709-15 (1993).
2. Hoeijmakers, J.H. DNA damage, aging, and cancer. *The New England journal of medicine* **361**, 1475-85 (2009).
3. Pommier, Y. Topoisomerase I inhibitors: camptothecins and beyond. *Nature reviews. Cancer* **6**, 789-802 (2006).
4. Bartek, J., Lukas, J. & Bartkova, J. DNA damage response as an anti-cancer barrier: damage threshold and the concept of 'conditional haploinsufficiency'. *Cell cycle* **6**, 2344-7 (2007).
5. Hakem, R. DNA-damage repair; the good, the bad, and the ugly. *The EMBO journal* **27**, 589-605 (2008).
6. Harper, J.W. & Elledge, S.J. The DNA damage response: ten years after. *Molecular cell* **28**, 739-45 (2007).
7. Jiricny, J. The multifaceted mismatch-repair system. *Nature reviews. Molecular cell biology* **7**, 335-46 (2006).
8. Lindahl, T. & Barnes, D.E. Repair of endogenous DNA damage. *Cold Spring Harbor symposia on quantitative biology* **65**, 127-33 (2000).
9. Caldecott, K.W. Single-strand break repair and genetic disease. *Nature reviews. Genetics* **9**, 619-31 (2008).
10. West, S.C. Molecular views of recombination proteins and their control. *Nature reviews. Molecular cell biology* **4**, 435-45 (2003).
11. de Boer, J. & Hoeijmakers, J.H. Nucleotide excision repair and human syndromes. *Carcinogenesis* **21**, 453-60 (2000).
12. Moldovan, G.L. & D'Andrea, A.D. How the fanconi anemia pathway guards the genome. *Annual review of genetics* **43**, 223-49 (2009).
13. Hoeijmakers, J.H. Genome maintenance mechanisms for preventing cancer. *Nature* **411**, 366-74 (2001).
14. Jackson, S.P. & Bartek, J. The DNA-damage response in human biology and disease. *Nature* **461**, 1071-8 (2009).
15. Cimprich, K.A. & Cortez, D. ATR: an essential regulator of genome integrity. *Nature reviews. Molecular cell biology* **9**, 616-27 (2008).
16. Schreiber, V., Dantzer, F., Ame, J.C. & de Murcia, G. Poly(ADP-ribose): novel functions for an old molecule. *Nature reviews. Molecular cell biology* **7**, 517-28 (2006).
17. Huen, M.S. & Chen, J. The DNA damage response pathways: at the crossroad of protein modifications. *Cell research* **18**, 8-16 (2008).
18. Campisi, J. & d'Adda di Fagagna, F. Cellular senescence: when bad things happen to good cells. *Nature reviews. Molecular cell biology* **8**, 729-40 (2007).
19. Halazonetis, T.D., Gorgoulis, V.G. & Bartek, J. An oncogene-induced DNA damage model for cancer development. *Science* **319**, 1352-5 (2008).

20. Stratton, M.R., Campbell, P.J. & Futreal, P.A. The cancer genome. *Nature* **458**, 719-24 (2009).
21. Ripperger, T., Gadzicki, D., Meindl, A. & Schlegelberger, B. Breast cancer susceptibility: current knowledge and implications for genetic counselling. *European journal of human genetics : EJHG* **17**, 722-31 (2009).
22. Bachrati, C.Z. & Hickson, I.D. RecQ helicases: suppressors of tumorigenesis and premature aging. *The Biochemical journal* **374**, 577-606 (2003).
23. Kennedy, R.D. & D'Andrea, A.D. DNA repair pathways in clinical practice: lessons from pediatric cancer susceptibility syndromes. *Journal of clinical oncology : official journal of the American Society of Clinical Oncology* **24**, 3799-808 (2006).
24. Loeb, L.A. Mutator phenotype may be required for multistage carcinogenesis. *Cancer research* **51**, 3075-9 (1991).
25. Kinzler, K.W. & Vogelstein, B. Cancer-susceptibility genes. Gatekeepers and caretakers. *Nature* **386**, 761, 763 (1997).
26. Wang, Z. et al. Three classes of genes mutated in colorectal cancers with chromosomal instability. *Cancer research* **64**, 2998-3001 (2004).
27. Bartkova, J. et al. DNA damage response as a candidate anti-cancer barrier in early human tumorigenesis. *Nature* **434**, 864-70 (2005).
28. Gorgoulis, V.G. et al. Activation of the DNA damage checkpoint and genomic instability in human precancerous lesions. *Nature* **434**, 907-13 (2005).
29. Kastan, M.B. & Bartek, J. Cell-cycle checkpoints and cancer. *Nature* **432**, 316-23 (2004).
30. Hartlerode, A.J. & Scully, R. Mechanisms of double-strand break repair in somatic mammalian cells. *The Biochemical journal* **423**, 157-68 (2009).
31. Pommier, Y., Leo, E., Zhang, H. & Marchand, C. DNA topoisomerases and their poisoning by anticancer and antibacterial drugs. *Chemistry & biology* **17**, 421-33 (2010).
32. Lobrich, M. & Jeggo, P.A. The impact of a negligent G2/M checkpoint on genomic instability and cancer induction. *Nature reviews. Cancer* **7**, 861-9 (2007).
33. Jung, D., Giallourakis, C., Mostoslavsky, R. & Alt, F.W. Mechanism and control of V(D)J recombination at the immunoglobulin heavy chain locus. *Annual review of immunology* **24**, 541-70 (2006).
34. Fugmann, S.D., Lee, A.I., Shockett, P.E., Villey, I.J. & Schatz, D.G. The RAG proteins and V(D)J recombination: complexes, ends, and transposition. *Annual review of immunology* **18**, 495-527 (2000).
35. Keeney, S. & Neale, M.J. Initiation of meiotic recombination by formation of DNA double-strand breaks: mechanism and regulation. *Biochemical Society transactions* **34**, 523-5 (2006).
36. Yan, C.T. et al. IgH class switching and translocations use a robust non-classical end-joining pathway. *Nature* **449**, 478-82 (2007).
37. Branzei, D. & Foiani, M. Regulation of DNA repair throughout the cell cycle. *Nature reviews. Molecular cell biology* **9**, 297-308 (2008).

38. Rothkamm, K., Kruger, I., Thompson, L.H. & Lobrich, M. Pathways of DNA double-strand break repair during the mammalian cell cycle. *Molecular and cellular biology* **23**, 5706-15 (2003).
39. Kim, J.S. et al. Independent and sequential recruitment of NHEJ and HR factors to DNA damage sites in mammalian cells. *The Journal of cell biology* **170**, 341-7 (2005).
40. Roberts, S.A. et al. Ku is a 5'-dRP/AP lyase that excises nucleotide damage near broken ends. *Nature* **464**, 1214-7 (2010).
41. Downs, J.A. & Jackson, S.P. A means to a DNA end: the many roles of Ku. *Nature reviews. Molecular cell biology* **5**, 367-78 (2004).
42. Nick McElhinny, S.A., Snowden, C.M., McCarville, J. & Ramsden, D.A. Ku recruits the XRCC4-ligase IV complex to DNA ends. *Molecular and cellular biology* **20**, 2996-3003 (2000).
43. Cary, R.B. et al. DNA looping by Ku and the DNA-dependent protein kinase. *Proceedings of the National Academy of Sciences of the United States of America* **94**, 4267-72 (1997).
44. Yano, K. et al. Ku recruits XLF to DNA double-strand breaks. *EMBO reports* **9**, 91-6 (2008).
45. Mahajan, K.N., Nick McElhinny, S.A., Mitchell, B.S. & Ramsden, D.A. Association of DNA polymerase mu (pol mu) with Ku and ligase IV: role for pol mu in end-joining double-strand break repair. *Molecular and cellular biology* **22**, 5194-202 (2002).
46. Ma, Y. et al. A biochemically defined system for mammalian nonhomologous DNA end joining. *Molecular cell* **16**, 701-13 (2004).
47. Mari, P.O. et al. Dynamic assembly of end-joining complexes requires interaction between Ku70/80 and XRCC4. *Proceedings of the National Academy of Sciences of the United States of America* **103**, 18597-602 (2006).
48. Gottlieb, T.M. & Jackson, S.P. The DNA-dependent protein kinase: requirement for DNA ends and association with Ku antigen. *Cell* **72**, 131-42 (1993).
49. Meek, K., Dang, V. & Lees-Miller, S.P. DNA-PK: the means to justify the ends? *Advances in immunology* **99**, 33-58 (2008).
50. Shrivastav, M., De Haro, L.P. & Nickoloff, J.A. Regulation of DNA double-strand break repair pathway choice. *Cell research* **18**, 134-47 (2008).
51. Yu, Y. et al. DNA-PK phosphorylation sites in XRCC4 are not required for survival after radiation or for V(D)J recombination. *DNA repair* **2**, 1239-52 (2003).
52. Yu, Y. et al. DNA-PK and ATM phosphorylation sites in XLF/Cernunnos are not required for repair of DNA double strand breaks. *DNA repair* **7**, 1680-92 (2008).
53. Douglas, P., Gupta, S., Morrice, N., Meek, K. & Lees-Miller, S.P. DNA-PK-dependent phosphorylation of Ku70/80 is not required for non-homologous end joining. *DNA repair* **4**, 1006-18 (2005).
54. Meek, K., Gupta, S., Ramsden, D.A. & Lees-Miller, S.P. The DNA-dependent protein kinase: the director at the end. *Immunological reviews* **200**, 132-41 (2004).

55. Ding, Q. et al. Autophosphorylation of the catalytic subunit of the DNA-dependent protein kinase is required for efficient end processing during DNA double-strand break repair. *Molecular and cellular biology* **23**, 5836-48 (2003).
56. Budman, J. & Chu, G. Processing of DNA for nonhomologous end-joining by cell-free extract. *The EMBO journal* **24**, 849-60 (2005).
57. Cui, X. et al. Autophosphorylation of DNA-dependent protein kinase regulates DNA end processing and may also alter double-strand break repair pathway choice. *Molecular and cellular biology* **25**, 10842-52 (2005).
58. Ma, Y., Pannicke, U., Schwarz, K. & Lieber, M.R. Hairpin opening and overhang processing by an Artemis/DNA-dependent protein kinase complex in nonhomologous end joining and V(D)J recombination. *Cell* **108**, 781-94 (2002).
59. Ma, Y., Schwarz, K. & Lieber, M.R. The Artemis:DNA-PKcs endonuclease cleaves DNA loops, flaps, and gaps. *DNA repair* **4**, 845-51 (2005).
60. Poinsignon, C. et al. Phosphorylation of Artemis following irradiation-induced DNA damage. *European journal of immunology* **34**, 3146-55 (2004).
61. Wang, J. et al. Artemis deficiency confers a DNA double-strand break repair defect and Artemis phosphorylation status is altered by DNA damage and cell cycle progression. *DNA repair* **4**, 556-70 (2005).
62. Zhang, X. et al. Artemis is a phosphorylation target of ATM and ATR and is involved in the G2/M DNA damage checkpoint response. *Molecular and cellular biology* **24**, 9207-20 (2004).
63. Paull, T.T. Saving the ends for last: the role of pol mu in DNA end joining. *Molecular cell* **19**, 294-6 (2005).
64. Bernstein, N.K. et al. Polynucleotide kinase as a potential target for enhancing cytotoxicity by ionizing radiation and topoisomerase I inhibitors. *Anti-cancer agents in medicinal chemistry* **8**, 358-67 (2008).
65. Bekker-Jensen, S. et al. Human Xip1 (C2orf13) is a novel regulator of cellular responses to DNA strand breaks. *The Journal of biological chemistry* **282**, 19638-43 (2007).
66. Rasouli-Nia, A., Karimi-Busheri, F. & Weinfeld, M. Stable down-regulation of human polynucleotide kinase enhances spontaneous mutation frequency and sensitizes cells to genotoxic agents. *Proceedings of the National Academy of Sciences of the United States of America* **101**, 6905-10 (2004).
67. Gu, J. et al. XRCC4:DNA ligase IV can ligate incompatible DNA ends and can ligate across gaps. *The EMBO journal* **26**, 1010-23 (2007).
68. Ahnesorg, P., Smith, P. & Jackson, S.P. XLF interacts with the XRCC4-DNA ligase IV complex to promote DNA nonhomologous end-joining. *Cell* **124**, 301-13 (2006).
69. Sekiguchi, J.M. & Ferguson, D.O. DNA double-strand break repair: a relentless hunt uncovers new prey. *Cell* **124**, 260-2 (2006).
70. Mahaney, B.L., Meek, K. & Lees-Miller, S.P. Repair of ionizing radiation-induced DNA double-strand breaks by non-homologous end-joining. *The Biochemical journal* **417**, 639-50 (2009).
71. Guirouilh-Barbat, J., Rass, E., Plo, I., Bertrand, P. & Lopez, B.S. Defects in XRCC4 and KU80 differentially affect the joining of distal nonhomologous ends.

Proceedings of the National Academy of Sciences of the United States of America **104**, 20902-7 (2007).

72. Soulas-Sprauel, P. et al. Role for DNA repair factor XRCC4 in immunoglobulin class switch recombination. *The Journal of experimental medicine* **204**, 1717-27 (2007).
73. Lee, K. & Lee, S.E. Saccharomyces cerevisiae Sae2- and Tel1-dependent single-strand DNA formation at DNA break promotes microhomology-mediated end joining. *Genetics* **176**, 2003-14 (2007).
74. Ma, J.L., Kim, E.M., Haber, J.E. & Lee, S.E. Yeast Mre11 and Rad1 proteins define a Ku-independent mechanism to repair double-strand breaks lacking overlapping end sequences. *Molecular and cellular biology* **23**, 8820-8 (2003).
75. Aylon, Y., Liefshitz, B. & Kupiec, M. The CDK regulates repair of double-strand breaks by homologous recombination during the cell cycle. *The EMBO journal* **23**, 4868-75 (2004).
76. Ira, G. et al. DNA end resection, homologous recombination and DNA damage checkpoint activation require CDK1. *Nature* **431**, 1011-7 (2004).
77. Ahmad, A. et al. ERCC1-XPF endonuclease facilitates DNA double-strand break repair. *Molecular and cellular biology* **28**, 5082-92 (2008).
78. Daley, J.M. & Wilson, T.E. Rejoining of DNA double-strand breaks as a function of overhang length. *Molecular and cellular biology* **25**, 896-906 (2005).
79. Liang, L. et al. Human DNA ligases I and III, but not ligase IV, are required for microhomology-mediated end joining of DNA double-strand breaks. *Nucleic acids research* **36**, 3297-310 (2008).
80. Perrault, R., Wang, H., Wang, M., Rosidi, B. & Iliakis, G. Backup pathways of NHEJ are suppressed by DNA-PK. *Journal of cellular biochemistry* **92**, 781-94 (2004).
81. Lichten, M. & de Massy, B. The impressionistic landscape of meiotic recombination. *Cell* **147**, 267-70 (2011).
82. Aguilera, A. & Gomez-Gonzalez, B. Genome instability: a mechanistic view of its causes and consequences. *Nature reviews. Genetics* **9**, 204-17 (2008).
83. Nagaraju, G. & Scully, R. Minding the gap: the underground functions of BRCA1 and BRCA2 at stalled replication forks. *DNA repair* **6**, 1018-31 (2007).
84. Kinoshita, E., van der Linden, E., Sanchez, H. & Wyman, C. RAD50, an SMC family member with multiple roles in DNA break repair: how does ATP affect function? *Chromosome research : an international journal on the molecular, supramolecular and evolutionary aspects of chromosome biology* **17**, 277-88 (2009).
85. Feeney, K.M., Wasson, C.W. & Parish, J.L. Cohesin: a regulator of genome integrity and gene expression. *The Biochemical journal* **428**, 147-61 (2010).
86. Williams, R.S., Williams, J.S. & Tainer, J.A. Mre11-Rad50-Nbs1 is a keystone complex connecting DNA repair machinery, double-strand break signaling, and the chromatin template. *Biochemistry and cell biology = Biochimie et biologie cellulaire* **85**, 509-20 (2007).
87. Yeeles, J.T. & Dillingham, M.S. The processing of double-stranded DNA breaks for recombinational repair by helicase-nuclease complexes. *DNA repair* **9**, 276-85 (2010).

88. Mimitou, E.P. & Symington, L.S. DNA end resection: many nucleases make light work. *DNA repair* **8**, 983-95 (2009).
89. Mimitou, E.P. & Symington, L.S. Nucleases and helicases take center stage in homologous recombination. *Trends in biochemical sciences* **34**, 264-72 (2009).
90. Sartori, A.A. et al. Human CtIP promotes DNA end resection. *Nature* **450**, 509-14 (2007).
91. D'Amours, D. & Jackson, S.P. The Mre11 complex: at the crossroads of dna repair and checkpoint signalling. *Nature reviews. Molecular cell biology* **3**, 317-27 (2002).
92. Gravel, S., Chapman, J.R., Magill, C. & Jackson, S.P. DNA helicases Sgs1 and BLM promote DNA double-strand break resection. *Genes & development* **22**, 2767-72 (2008).
93. Nimonkar, A.V. et al. BLM-DNA2-RPA-MRN and EXO1-BLM-RPA-MRN constitute two DNA end resection machineries for human DNA break repair. *Genes & development* **25**, 350-62 (2011).
94. Garcia, V., Phelps, S.E., Gray, S. & Neale, M.J. Bidirectional resection of DNA double-strand breaks by Mre11 and Exo1. *Nature* **479**, 241-4 (2011).
95. Falck, J., Coates, J. & Jackson, S.P. Conserved modes of recruitment of ATM, ATR and DNA-PKcs to sites of DNA damage. *Nature* **434**, 605-11 (2005).
96. Stucki, M. et al. MDC1 directly binds phosphorylated histone H2AX to regulate cellular responses to DNA double-strand breaks. *Cell* **123**, 1213-26 (2005).
97. Stucki, M. & Jackson, S.P. gammaH2AX and MDC1: anchoring the DNA-damage-response machinery to broken chromosomes. *DNA repair* **5**, 534-43 (2006).
98. Bekker-Jensen, S. et al. Spatial organization of the mammalian genome surveillance machinery in response to DNA strand breaks. *The Journal of cell biology* **173**, 195-206 (2006).
99. Bekker-Jensen, S., Lukas, C., Melander, F., Bartek, J. & Lukas, J. Dynamic assembly and sustained retention of 53BP1 at the sites of DNA damage are controlled by Mdc1/NFBD1. *The Journal of cell biology* **170**, 201-11 (2005).
100. Wold, M.S. Replication protein A: a heterotrimeric, single-stranded DNA-binding protein required for eukaryotic DNA metabolism. *Annual review of biochemistry* **66**, 61-92 (1997).
101. Zou, L., Liu, D. & Elledge, S.J. Replication protein A-mediated recruitment and activation of Rad17 complexes. *Proceedings of the National Academy of Sciences of the United States of America* **100**, 13827-32 (2003).
102. Mordes, D.A., Glick, G.G., Zhao, R. & Cortez, D. TopBP1 activates ATR through ATRIP and a PIKK regulatory domain. *Genes & development* **22**, 1478-89 (2008).
103. Motycka, T.A., Bessho, T., Post, S.M., Sung, P. & Tomkinson, A.E. Physical and functional interaction between the XPF/ERCC1 endonuclease and hRad52. *The Journal of biological chemistry* **279**, 13634-9 (2004).
104. Sy, S.M., Huen, M.S. & Chen, J. PALB2 is an integral component of the BRCA complex required for homologous recombination repair. *Proceedings of the National Academy of Sciences of the United States of America* **106**, 7155-60 (2009).

105. Zhang, F. et al. PALB2 links BRCA1 and BRCA2 in the DNA-damage response. *Current biology : CB* **19**, 524-9 (2009).
106. McIlwraith, M.J. et al. Human DNA polymerase eta promotes DNA synthesis from strand invasion intermediates of homologous recombination. *Molecular cell* **20**, 783-92 (2005).
107. Johnson, R.D. & Jasin, M. Sister chromatid gene conversion is a prominent double-strand break repair pathway in mammalian cells. *The EMBO journal* **19**, 3398-407 (2000).
108. Nagaraju, G., Odate, S., Xie, A. & Scully, R. Differential regulation of short- and long-tract gene conversion between sister chromatids by Rad51C. *Molecular and cellular biology* **26**, 8075-86 (2006).
109. Bugreev, D.V., Mazina, O.M. & Mazin, A.V. Rad54 protein promotes branch migration of Holliday junctions. *Nature* **442**, 590-3 (2006).
110. Bohr, V.A. Rising from the RecQ-age: the role of human RecQ helicases in genome maintenance. *Trends in biochemical sciences* **33**, 609-20 (2008).
111. Wu, L. & Hickson, I.D. The Bloom's syndrome helicase suppresses crossing over during homologous recombination. *Nature* **426**, 870-4 (2003).
112. Ip, S.C. et al. Identification of Holliday junction resolvases from humans and yeast. *Nature* **456**, 357-61 (2008).
113. Svendsen, J.M. et al. Mammalian BTBD12/SLX4 assembles a Holliday junction resolvase and is required for DNA repair. *Cell* **138**, 63-77 (2009).
114. Fekairi, S. et al. Human SLX4 is a Holliday junction resolvase subunit that binds multiple DNA repair/recombination endonucleases. *Cell* **138**, 78-89 (2009).
115. Delacote, F., Han, M., Stamato, T.D., Jasin, M. & Lopez, B.S. An xrcc4 defect or Wortmannin stimulates homologous recombination specifically induced by double-strand breaks in mammalian cells. *Nucleic acids research* **30**, 3454-63 (2002).
116. Wu, D., Topper, L.M. & Wilson, T.E. Recruitment and dissociation of nonhomologous end joining proteins at a DNA double-strand break in Saccharomyces cerevisiae. *Genetics* **178**, 1237-49 (2008).
117. Shim, E.Y. et al. Saccharomyces cerevisiae Mre11/Rad50/Xrs2 and Ku proteins regulate association of Exo1 and Dna2 with DNA breaks. *The EMBO journal* **29**, 3370-80 (2010).
118. Yu, X. & Baer, R. Nuclear localization and cell cycle-specific expression of CtIP, a protein that associates with the BRCA1 tumor suppressor. *The Journal of biological chemistry* **275**, 18541-9 (2000).
119. Huertas, P., Cortes-Ledesma, F., Sartori, A.A., Aguilera, A. & Jackson, S.P. CDK targets Sae2 to control DNA-end resection and homologous recombination. *Nature* **455**, 689-92 (2008).
120. Huertas, P. & Jackson, S.P. Human CtIP mediates cell cycle control of DNA end resection and double strand break repair. *The Journal of biological chemistry* **284**, 9558-65 (2009).
121. Yun, M.H. & Hiom, K. CtIP-BRCA1 modulates the choice of DNA double-strand-break repair pathway throughout the cell cycle. *Nature* **459**, 460-3 (2009).

122. Ubersax, J.A. et al. Targets of the cyclin-dependent kinase Cdk1. *Nature* **425**, 859-64 (2003).
123. Kosugi, S., Hasebe, M., Tomita, M. & Yanagawa, H. Systematic identification of cell cycle-dependent yeast nucleocytoplasmic shuttling proteins by prediction of composite motifs. *Proceedings of the National Academy of Sciences of the United States of America* **106**, 10171-6 (2009).
124. Grenon, M. et al. Docking onto chromatin via the Saccharomyces cerevisiae Rad9 Tudor domain. *Yeast* **24**, 105-19 (2007).
125. Linding, R. et al. Systematic discovery of in vivo phosphorylation networks. *Cell* **129**, 1415-26 (2007).
126. Lazzaro, F. et al. Histone methyltransferase Dot1 and Rad9 inhibit single-stranded DNA accumulation at DSBs and uncapped telomeres. *The EMBO journal* **27**, 1502-12 (2008).
127. Lukas, J., Lukas, C. & Bartek, J. More than just a focus: The chromatin response to DNA damage and its role in genome integrity maintenance. *Nature cell biology* **13**, 1161-9 (2011).
128. Shakya, R. et al. BRCA1 tumor suppression depends on BRCT phosphoprotein binding, but not its E3 ligase activity. *Science* **334**, 525-8 (2011).
129. Bouwman, P. et al. 53BP1 loss rescues BRCA1 deficiency and is associated with triple-negative and BRCA-mutated breast cancers. *Nature structural & molecular biology* **17**, 688-95 (2010).
130. Bunting, S.F. et al. 53BP1 inhibits homologous recombination in Brca1-deficient cells by blocking resection of DNA breaks. *Cell* **141**, 243-54 (2010).
131. Postow, L. et al. Ku80 removal from DNA through double strand break-induced ubiquitylation. *The Journal of cell biology* **182**, 467-79 (2008).
132. Watanabe, K. et al. RAD18 promotes DNA double-strand break repair during G1 phase through chromatin retention of 53BP1. *Nucleic acids research* **37**, 2176-93 (2009).
133. Mailand, N. et al. RNF8 ubiquitylates histones at DNA double-strand breaks and promotes assembly of repair proteins. *Cell* **131**, 887-900 (2007).
134. Bekker-Jensen, S. et al. HERC2 coordinates ubiquitin-dependent assembly of DNA repair factors on damaged chromosomes. *Nature cell biology* **12**, 80-6; sup pp 1-12 (2010).
135. Doil, C. et al. RNF168 binds and amplifies ubiquitin conjugates on damaged chromosomes to allow accumulation of repair proteins. *Cell* **136**, 435-46 (2009).
136. Galanty, Y. et al. Mammalian SUMO E3-ligases PIAS1 and PIAS4 promote responses to DNA double-strand breaks. *Nature* **462**, 935-9 (2009).
137. Galanty, Y., Belotserkovskaya, R., Coates, J. & Jackson, S.P. RNF4, a SUMO-targeted ubiquitin E3 ligase, promotes DNA double-strand break repair. *Genes & development* **26**, 1179-95 (2012).
138. Chun, H.H. & Gatti, R.A. Ataxia-telangiectasia, an evolving phenotype. *DNA repair* **3**, 1187-96 (2004).

139. Peterson, R.D., Funkhouser, J.D., Tuck-Muller, C.M. & Gatti, R.A. Cancer susceptibility in ataxia-telangiectasia. *Leukemia : official journal of the Leukemia Society of America, Leukemia Research Fund, U.K* **6 Suppl 1**, 8-13 (1992).
140. Shiloh, Y. Ataxia-telangiectasia and the Nijmegen breakage syndrome: related disorders but genes apart. *Annual review of genetics* **31**, 635-62 (1997).
141. Difilippantonio, S. et al. Role of Nbs1 in the activation of the Atm kinase revealed in humanized mouse models. *Nature cell biology* **7**, 675-85 (2005).
142. Sallmyr, A., Tomkinson, A.E. & Rassool, F.V. Up-regulation of WRN and DNA ligase IIIalpha in chronic myeloid leukemia: consequences for the repair of DNA double-strand breaks. *Blood* **112**, 1413-23 (2008).
143. Gaymes, T.J., Mufti, G.J. & Rassool, F.V. Myeloid leukemias have increased activity of the nonhomologous end-joining pathway and concomitant DNA misrepair that is dependent on the Ku70/86 heterodimer. *Cancer research* **62**, 2791-7 (2002).
144. Friedberg, E.C. Out of the shadows and into the light: the emergence of DNA repair. *Trends in biochemical sciences* **20**, 381 (1995).
145. Hickson, I. et al. Identification and characterization of a novel and specific inhibitor of the ataxia-telangiectasia mutated kinase ATM. *Cancer research* **64**, 9152-9 (2004).
146. Kennedy, R.D. et al. Fanconi anemia pathway-deficient tumor cells are hypersensitive to inhibition of ataxia telangiectasia mutated. *The Journal of clinical investigation* **117**, 1440-9 (2007).
147. Hine, C.M., Seluanov, A. & Gorbunova, V. Use of the Rad51 promoter for targeted anti-cancer therapy. *Proceedings of the National Academy of Sciences of the United States of America* **105**, 20810-5 (2008).
148. Okano, S., Lan, L., Caldecott, K.W., Mori, T. & Yasui, A. Spatial and temporal cellular responses to single-strand breaks in human cells. *Molecular and cellular biology* **23**, 3974-81 (2003).
149. Wang, M. et al. PARP-1 and Ku compete for repair of DNA double strand breaks by distinct NHEJ pathways. *Nucleic acids research* **34**, 6170-82 (2006).
150. Vilenchik, M.M. & Knudson, A.G. Endogenous DNA double-strand breaks: production, fidelity of repair, and induction of cancer. *Proceedings of the National Academy of Sciences of the United States of America* **100**, 12871-6 (2003).
151. Bryant, H.E. et al. Specific killing of BRCA2-deficient tumours with inhibitors of poly(ADP-ribose) polymerase. *Nature* **434**, 913-7 (2005).
152. Farmer, H. et al. Targeting the DNA repair defect in BRCA mutant cells as a therapeutic strategy. *Nature* **434**, 917-21 (2005).
153. Lord, C.J. & Ashworth, A. Targeted therapy for cancer using PARP inhibitors. *Current opinion in pharmacology* **8**, 363-9 (2008).
154. Fong, P.C. et al. Inhibition of poly(ADP-ribose) polymerase in tumors from BRCA mutation carriers. *The New England journal of medicine* **361**, 123-34 (2009).
155. Hartwell, L.H., Szankasi, P., Roberts, C.J., Murray, A.W. & Friend, S.H. Integrating genetic approaches into the discovery of anticancer drugs. *Science* **278**, 1064-8 (1997).

156. Rosenzweig, K.E., Youmell, M.B., Palayoor, S.T. & Price, B.D. Radiosensitization of human tumor cells by the phosphatidylinositol3-kinase inhibitors wortmannin and LY294002 correlates with inhibition of DNA-dependent protein kinase and prolonged G2-M delay. *Clinical cancer research : an official journal of the American Association for Cancer Research* **3**, 1149-56 (1997).
157. Schaeper, U., Subramanian, T., Lim, L., Boyd, J.M. & Chinnadurai, G. Interaction between a cellular protein that binds to the C-terminal region of adenovirus E1A (CtBP) and a novel cellular protein is disrupted by E1A through a conserved PLDLS motif. *The Journal of biological chemistry* **273**, 8549-52 (1998).
158. Molloy, D.P., Barral, P.M., Bremner, K.H., Gallimore, P.H. & Grand, R.J. Structural determinants outside the PXDLS sequence affect the interaction of adenovirus E1A, C-terminal interacting protein and Drosophila repressors with C-terminal binding protein. *Biochimica et biophysica acta* **1546**, 55-70 (2001).
159. Fusco, C., Reymond, A. & Zervos, A.S. Molecular cloning and characterization of a novel retinoblastoma-binding protein. *Genomics* **51**, 351-8 (1998).
160. Yu, X., Wu, L.C., Bowcock, A.M., Aronheim, A. & Baer, R. The C-terminal (BRCT) domains of BRCA1 interact in vivo with CtIP, a protein implicated in the CtBP pathway of transcriptional repression. *The Journal of biological chemistry* **273**, 25388-92 (1998).
161. Koipally, J. & Georgopoulos, K. Ikaros-CtIP interactions do not require C-terminal binding protein and participate in a deacetylase-independent mode of repression. *The Journal of biological chemistry* **277**, 23143-9 (2002).
162. Rebollo, A. & Schmitt, C. Ikaros, Aiolos and Helios: transcription regulators and lymphoid malignancies. *Immunology and cell biology* **81**, 171-5 (2003).
163. Chen, P.L. et al. Inactivation of CtIP leads to early embryonic lethality mediated by G1 restraint and to tumorigenesis by haploid insufficiency. *Molecular and cellular biology* **25**, 3535-42 (2005).
164. Liu, F. & Lee, W.H. CtIP activates its own and cyclin D1 promoters via the E2F/RB pathway during G1/S progression. *Molecular and cellular biology* **26**, 3124-34 (2006).
165. Wong, A.K. et al. Characterization of a carboxy-terminal BRCA1 interacting protein. *Oncogene* **17**, 2279-85 (1998).
166. Dubin, M.J. et al. Dimerization of CtIP, a BRCA1- and CtBP-interacting protein, is mediated by an N-terminal coiled-coil motif. *The Journal of biological chemistry* **279**, 26932-8 (2004).
167. Wang, H. et al. CtIP Protein Dimerization Is Critical for Its Recruitment to Chromosomal DNA Double-stranded Breaks. *The Journal of biological chemistry* **287**, 21471-80 (2012).
168. Qvist, P. et al. CtIP Mutations Cause Seckel and Jawad Syndromes. *PLoS genetics* **7**, e1002310 (2011).
169. Gu, B. & Chen, P.L. Expression of PCNA-binding domain of CtIP, a motif required for CtIP localization at DNA replication foci, causes DNA damage and activation of DNA damage checkpoint. *Cell cycle* **8**, 1409-20 (2009).

170. You, Z. et al. CtIP links DNA double-strand break sensing to resection. *Molecular cell* **36**, 954-69 (2009).
171. Miki, Y. et al. A strong candidate for the breast and ovarian cancer susceptibility gene BRCA1. *Science* **266**, 66-71 (1994).
172. Shinohara, A. et al. Cloning of human, mouse and fission yeast recombination genes homologous to RAD51 and recA. *Nature genetics* **4**, 239-43 (1993).
173. Langerak, P., Mejia-Ramirez, E., Limbo, O. & Russell, P. Release of Ku and MRN from DNA ends by Mre11 nuclease activity and Ctp1 is required for homologous recombination repair of double-strand breaks. *PLoS genetics* **7**, e1002271 (2011).
174. Yu, X. & Chen, J. DNA damage-induced cell cycle checkpoint control requires CtIP, a phosphorylation-dependent binding partner of BRCA1 C-terminal domains. *Molecular and cellular biology* **24**, 9478-86 (2004).
175. Nakamura, K. et al. Collaborative action of Brca1 and CtIP in elimination of covalent modifications from double-strand breaks to facilitate subsequent break repair. *PLoS genetics* **6**, e1000828 (2010).
176. Li, S. et al. Functional link of BRCA1 and ataxia telangiectasia gene product in DNA damage response. *Nature* **406**, 210-5 (2000).
177. Matsuoka, S. et al. ATM and ATR substrate analysis reveals extensive protein networks responsive to DNA damage. *Science* **316**, 1160-6 (2007).
178. Greenberg, R.A. et al. Multifactorial contributions to an acute DNA damage response by BRCA1/BARD1-containing complexes. *Genes & development* **20**, 34-46 (2006).
179. Takeda, S., Nakamura, K., Taniguchi, Y. & Paull, T.T. Ctp1/CtIP and the MRN complex collaborate in the initial steps of homologous recombination. *Molecular cell* **28**, 351-2 (2007).
180. Lee-Theilen, M., Matthews, A.J., Kelly, D., Zheng, S. & Chaudhuri, J. CtIP promotes microhomology-mediated alternative end joining during class-switch recombination. *Nature structural & molecular biology* **18**, 75-9 (2011).
181. You, Z. & Bailis, J.M. DNA damage and decisions: CtIP coordinates DNA repair and cell cycle checkpoints. *Trends in cell biology* **20**, 402-9 (2010).
182. Germani, A. et al. SIAH-1 interacts with CtIP and promotes its degradation by the proteasome pathway. *Oncogene* **22**, 8845-51 (2003).
183. Buis, J., Stoneham, T., Spehalski, E. & Ferguson, D.O. Mre11 regulates CtIP-dependent double-strand break repair by interaction with CDK2. *Nature structural & molecular biology* **19**, 246-52 (2012).
184. Pawson, T. & Scott, J.D. Protein phosphorylation in signaling--50 years and counting. *Trends in biochemical sciences* **30**, 286-90 (2005).
185. Blume-Jensen, P. & Hunter, T. Oncogenic kinase signalling. *Nature* **411**, 355-65 (2001).
186. Lee, M.S. & Tsai, L.H. Cdk5: one of the links between senile plaques and neurofibrillary tangles? *Journal of Alzheimer's disease : JAD* **5**, 127-37 (2003).
187. Pal, D. & Chakrabarti, P. Cis peptide bonds in proteins: residues involved, their conformations, interactions and locations. *Journal of molecular biology* **294**, 271-88 (1999).

188. Pahlke, D., Leitner, D., Wiedemann, U. & Labudde, D. COPS--cis/trans peptide bond conformation prediction of amino acids on the basis of secondary structure information. *Bioinformatics* **21**, 685-6 (2005).
189. Dolinski, K., Muir, S., Cardenas, M. & Heitman, J. All cyclophilins and FK506 binding proteins are, individually and collectively, dispensable for viability in Saccharomyces cerevisiae. *Proceedings of the National Academy of Sciences of the United States of America* **94**, 13093-8 (1997).
190. Lu, K.P., Hanes, S.D. & Hunter, T. A human peptidyl-prolyl isomerase essential for regulation of mitosis. *Nature* **380**, 544-7 (1996).
191. Lu, P.J., Zhou, X.Z., Shen, M. & Lu, K.P. Function of WW domains as phosphoserine- or phosphothreonine-binding modules. *Science* **283**, 1325-8 (1999).
192. Ranganathan, R., Lu, K.P., Hunter, T. & Noel, J.P. Structural and functional analysis of the mitotic rotamase Pin1 suggests substrate recognition is phosphorylation dependent. *Cell* **89**, 875-86 (1997).
193. Yaffe, M.B. et al. Sequence-specific and phosphorylation-dependent proline isomerization: a potential mitotic regulatory mechanism. *Science* **278**, 1957-60 (1997).
194. Zhou, X.Z., Lu, P.J., Wulf, G. & Lu, K.P. Phosphorylation-dependent prolyl isomerization: a novel signaling regulatory mechanism. *Cellular and molecular life sciences : CMLS* **56**, 788-806 (1999).
195. Werner-Allen, J.W. et al. cis-Proline-mediated Ser(P)5 dephosphorylation by the RNA polymerase II C-terminal domain phosphatase Ssu72. *The Journal of biological chemistry* **286**, 5717-26 (2011).
196. Zhou, X.Z. et al. Pin1-dependent prolyl isomerization regulates dephosphorylation of Cdc25C and tau proteins. *Molecular cell* **6**, 873-83 (2000).
197. Lu, K.P., Finn, G., Lee, T.H. & Nicholson, L.K. Prolyl cis-trans isomerization as a molecular timer. *Nature chemical biology* **3**, 619-29 (2007).
198. Lee, T.H. et al. Death-associated protein kinase 1 phosphorylates Pin1 and inhibits its prolyl isomerase activity and cellular function. *Molecular cell* **42**, 147-59 (2011).
199. Lee, T.H., Pastorino, L. & Lu, K.P. Peptidyl-prolyl cis-trans isomerase Pin1 in ageing, cancer and Alzheimer disease. *Expert reviews in molecular medicine* **13**, e21 (2011).
200. Ryo, A. et al. PIN1 is an E2F target gene essential for Neu/Ras-induced transformation of mammary epithelial cells. *Molecular and cellular biology* **22**, 5281-95 (2002).
201. Wulf, G.M. et al. Pin1 is overexpressed in breast cancer and cooperates with Ras signaling in increasing the transcriptional activity of c-Jun towards cyclin D1. *The EMBO journal* **20**, 3459-72 (2001).
202. Orlicky, S., Tang, X., Willems, A., Tyers, M. & Sicheri, F. Structural basis for phosphodependent substrate selection and orientation by the SCFCdc4 ubiquitin ligase. *Cell* **112**, 243-56 (2003).

203. Jentsch, S. & Siepe, D. Pin1, a novel switch in the ubiquitin pathway. *Cell cycle* **8**, 3800-1 (2009).
204. Siepe, D. & Jentsch, S. Prolyl isomerase Pin1 acts as a switch to control the degree of substrate ubiquitylation. *Nature cell biology* **11**, 967-72 (2009).
205. Liou, Y.C. et al. Loss of Pin1 function in the mouse causes phenotypes resembling cyclin D1-null phenotypes. *Proceedings of the National Academy of Sciences of the United States of America* **99**, 1335-40 (2002).
206. Ryo, A., Nakamura, M., Wulf, G., Liou, Y.C. & Lu, K.P. Pin1 regulates turnover and subcellular localization of beta-catenin by inhibiting its interaction with APC. *Nature cell biology* **3**, 793-801 (2001).
207. Zacchi, P. et al. The prolyl isomerase Pin1 reveals a mechanism to control p53 functions after genotoxic insults. *Nature* **419**, 853-7 (2002).
208. Zhou, W. et al. Pin1 catalyzes conformational changes of Thr-187 in p27Kip1 and mediates its stability through a polyubiquitination process. *The Journal of biological chemistry* **284**, 23980-8 (2009).
209. Lu, K.P. & Zhou, X.Z. The prolyl isomerase PIN1: a pivotal new twist in phosphorylation signalling and disease. *Nature reviews. Molecular cell biology* **8**, 904-16 (2007).
210. Bao, L. et al. Prevalent overexpression of prolyl isomerase Pin1 in human cancers. *The American journal of pathology* **164**, 1727-37 (2004).
211. Tan, X. et al. Pin1 expression contributes to lung cancer: Prognosis and carcinogenesis. *Cancer biology & therapy* **9**, 111-9 (2010).
212. Lu, K.P. et al. Targeting carcinogenesis: a role for the prolyl isomerase Pin1? *Molecular carcinogenesis* **45**, 397-402 (2006).
213. Fukuchi, M. et al. Prolyl isomerase Pin1 expression predicts prognosis in patients with esophageal squamous cell carcinoma and correlates with cyclinD1 expression. *International journal of oncology* **29**, 329-34 (2006).
214. Kuramochi, J. et al. High Pin1 expression is associated with tumor progression in colorectal cancer. *Journal of surgical oncology* **94**, 155-60 (2006).
215. Sasaki, T. et al. An immunohistochemical scoring system of prolyl isomerase Pin1 for predicting relapse of prostate carcinoma after radical prostatectomy. *Pathology, research and practice* **202**, 357-64 (2006).
216. Basu, A. et al. Proteasomal degradation of human peptidyl prolyl isomerase pin1-pointing phospho Bcl2 toward dephosphorylation. *Neoplasia* **4**, 218-27 (2002).
217. Liao, Y. et al. Peptidyl-prolyl cis/trans isomerase Pin1 is critical for the regulation of PKB/Akt stability and activation phosphorylation. *Oncogene* **28**, 2436-45 (2009).
218. Zheng, H. et al. The prolyl isomerase Pin1 is a regulator of p53 in genotoxic response. *Nature* **419**, 849-53 (2002).
219. Ryo, A. et al. Regulation of NF-kappaB signaling by Pin1-dependent prolyl isomerization and ubiquitin-mediated proteolysis of p65/RelA. *Molecular cell* **12**, 1413-26 (2003).

220. Li, H.Y. et al. [Expression and clinical significance of Pin1 and Cyclin D1 in cervical cancer cell lines and cervical epithelial tissues]. *Ai zheng = Aizheng = Chinese journal of cancer* **25**, 367-72 (2006).
221. Miyashita, H., Uchida, T., Mori, S., Echigo, S. & Motegi, K. Expression status of Pin1 and cyclins in oral squamous cell carcinoma: Pin1 correlates with Cyclin D1 mRNA expression and clinical significance of cyclins. *Oncology reports* **10**, 1045-8 (2003).
222. Miyashita, H., Mori, S., Motegi, K., Fukumoto, M. & Uchida, T. Pin1 is overexpressed in oral squamous cell carcinoma and its levels correlate with cyclin D1 overexpression. *Oncology reports* **10**, 455-61 (2003).
223. Kim, C.J. et al. Pin1 overexpression in colorectal cancer and its correlation with aberrant beta-catenin expression. *World journal of gastroenterology : WJG* **11**, 5006-9 (2005).
224. Wulf, G., Garg, P., Liou, Y.C., Iglehart, D. & Lu, K.P. Modeling breast cancer in vivo and ex vivo reveals an essential role of Pin1 in tumorigenesis. *The EMBO journal* **23**, 3397-407 (2004).
225. Fujimori, F., Takahashi, K., Uchida, C. & Uchida, T. Mice lacking Pin1 develop normally, but are defective in entering cell cycle from G(0) arrest. *Biochemical and biophysical research communications* **265**, 658-63 (1999).
226. Atchison, F.W., Capel, B. & Means, A.R. Pin1 regulates the timing of mammalian primordial germ cell proliferation. *Development* **130**, 3579-86 (2003).
227. van Drogen, F. et al. Ubiquitylation of cyclin E requires the sequential function of SCF complexes containing distinct hCdc4 isoforms. *Molecular cell* **23**, 37-48 (2006).
228. Yeh, E. et al. A signalling pathway controlling c-Myc degradation that impacts oncogenic transformation of human cells. *Nature cell biology* **6**, 308-18 (2004).
229. Akli, S. et al. Tumor-specific low molecular weight forms of cyclin E induce genomic instability and resistance to p21, p27, and antiestrogens in breast cancer. *Cancer research* **64**, 3198-208 (2004).
230. Naaz, A. et al. Loss of cyclin-dependent kinase inhibitors produces adipocyte hyperplasia and obesity. *FASEB journal : official publication of the Federation of American Societies for Experimental Biology* **18**, 1925-7 (2004).
231. Yeh, E.S., Lew, B.O. & Means, A.R. The loss of PIN1 deregulates cyclin E and sensitizes mouse embryo fibroblasts to genomic instability. *The Journal of biological chemistry* **281**, 241-51 (2006).
232. Wiegand, S. et al. The rotamase Pin1 is up-regulated, hypophosphorylated and required for cell cycle progression in head and neck squamous cell carcinomas. *Oral oncology* **45**, e140-9 (2009).
233. Williams, R.S. et al. Nbs1 flexibly tethers Ctp1 and Mre11-Rad50 to coordinate DNA double-strand break processing and repair. *Cell* **139**, 87-99 (2009).
234. Lengsfeld, B.M., Rattray, A.J., Bhaskara, V., Ghirlando, R. & Paull, T.T. Sae2 is an endonuclease that processes hairpin DNA cooperatively with the Mre11/Rad50/Xrs2 complex. *Molecular cell* **28**, 638-51 (2007).

235. Ivanov, E.L., Sugawara, N., White, C.I., Fabre, F. & Haber, J.E. Mutations in XRS2 and RAD50 delay but do not prevent mating-type switching in Saccharomyces cerevisiae. *Molecular and cellular biology* **14**, 3414-25 (1994).
236. Mimitou, E.P. & Symington, L.S. Sae2, Exo1 and Sgs1 collaborate in DNA double-strand break processing. *Nature* **455**, 770-4 (2008).
237. Zhu, Z., Chung, W.H., Shim, E.Y., Lee, S.E. & Ira, G. Sgs1 helicase and two nucleases Dna2 and Exo1 resect DNA double-strand break ends. *Cell* **134**, 981-94 (2008).
238. McKee, A.H. & Kleckner, N. A general method for identifying recessive diploid-specific mutations in Saccharomyces cerevisiae, its application to the isolation of mutants blocked at intermediate stages of meiotic prophase and characterization of a new gene SAE2. *Genetics* **146**, 797-816 (1997).
239. Moreau, S., Ferguson, J.R. & Symington, L.S. The nuclease activity of Mre11 is required for meiosis but not for mating type switching, end joining, or telomere maintenance. *Molecular and cellular biology* **19**, 556-66 (1999).
240. Butch, A.W., Chun, H.H., Nahas, S.A. & Gatti, R.A. Immunoassay to measure ataxia-telangiectasia mutated protein in cellular lysates. *Clinical chemistry* **50**, 2302-8 (2004).
241. Cejka, P. et al. DNA end resection by Dna2-Sgs1-RPA and its stimulation by Top3-Rmi1 and Mre11-Rad50-Xrs2. *Nature* **467**, 112-6 (2010).
242. Niu, H. et al. Mechanism of the ATP-dependent DNA end-resection machinery from Saccharomyces cerevisiae. *Nature* **467**, 108-11 (2010).
243. Nicolette, M.L. et al. Mre11-Rad50-Xrs2 and Sae2 promote 5' strand resection of DNA double-strand breaks. *Nature structural & molecular biology* **17**, 1478-85 (2010).
244. Limbo, O. et al. Ctp1 is a cell-cycle-regulated protein that functions with Mre11 complex to control double-strand break repair by homologous recombination. *Molecular cell* **28**, 134-46 (2007).
245. Williams, R.S. et al. Mre11 dimers coordinate DNA end bridging and nuclease processing in double-strand-break repair. *Cell* **135**, 97-109 (2008).
246. Liou, Y.C., Zhou, X.Z. & Lu, K.P. Prolyl isomerase Pin1 as a molecular switch to determine the fate of phosphoproteins. *Trends in biochemical sciences* **36**, 501-14 (2011).
247. Bennardo, N., Cheng, A., Huang, N. & Stark, J.M. Alternative-NHEJ is a mechanistically distinct pathway of mammalian chromosome break repair. *PLoS genetics* **4**, e1000110 (2008).
248. Wang, Y., Liu, C., Yang, D., Yu, H. & Liou, Y.C. Pin1At encoding a peptidyl-prolyl cis/trans isomerase regulates flowering time in Arabidopsis. *Molecular cell* **37**, 112-22 (2010).
249. Lippens, G., Landrieu, I. & Smet, C. Molecular mechanisms of the phospho-dependent prolyl cis/trans isomerase Pin1. *The FEBS journal* **274**, 5211-22 (2007).
250. Smet, C., Wieruszeski, J.M., Buee, L., Landrieu, I. & Lippens, G. Regulation of Pin1 peptidyl-prolyl cis/trans isomerase activity by its WW binding module on a multi-phosphorylated peptide of Tau protein. *FEBS letters* **579**, 4159-64 (2005).

251. Nakamura, K. et al. Proline isomer-specific antibodies reveal the early pathogenic tau conformation in Alzheimer's disease. *Cell* **149**, 232-44 (2012).
252. Khalil, A. et al. ATM-dependent ERK signaling via AKT in response to DNA double-strand breaks. *Cell cycle* **10**, 481-91 (2011).
253. Reinhardt, H.C., Cannell, I.G., Morandell, S. & Yaffe, M.B. Is post-transcriptional stabilization, splicing and translation of selective mRNAs a key to the DNA damage response? *Cell cycle* **10**, 23-7 (2011).
254. Arnold, H.K. et al. The Axin1 scaffold protein promotes formation of a degradation complex for c-Myc. *The EMBO journal* **28**, 500-12 (2009).
255. Kousholt, A.N. et al. CtIP-dependent DNA resection is required for DNA damage checkpoint maintenance but not initiation. *The Journal of cell biology* **197**, 869-76 (2012).
256. Uchida, T. et al. Pin1 and Par14 peptidyl prolyl isomerase inhibitors block cell proliferation. *Chemistry & biology* **10**, 15-24 (2003).
257. Joseph, J.D., Daigle, S.N. & Means, A.R. PINA is essential for growth and positively influences NIMA function in Aspergillus nidulans. *The Journal of biological chemistry* **279**, 32373-84 (2004).
258. Gemmill, T.R., Wu, X. & Hanes, S.D. Vanishingly low levels of Ess1 prolyl-isomerase activity are sufficient for growth in Saccharomyces cerevisiae. *The Journal of biological chemistry* **280**, 15510-7 (2005).

7. ACKNOWLEDGEMENTS

I would like to thank all my colleagues and friends who helped and supported me during my time as PhD student.

First of all I am very grateful to Prof. Alessandro A. Sartori for accepting me as PhD Student in his laboratory and for the great supervision during my studies. Moreover, I would like to thank all the present and past Sartori lab members, especially our technician Christine who contributed significantly to my work. Thanks also to Hella for proofreading parts of my thesis and changing the summary to understandable german. Special thanks also to Olga for support, helpful discussions and for constantly sparing cells. I also thank Daniela, Kay and Lorenzo who contributed to the PIN1 manuscript.

Further I acknowledge my thesis committee members Prof. Josef Jiricny, Prof. Giannino del Sal and Dr. Manuel Stucki for critical discussions and helpful suggestions as well as for sharing reagents.

Moreover, I would like to thank all the collaborators who have supported my work including Prof. Oliver Zerbe and Dr. Reto Walser (Organic Chemistry Institute, University of Zurich), present and past members of the Functional Genomic Center Zurich (FGCZ) including Bertran, Doro and Paolo. Moreover I'm grateful to Dr. Urs Ziegler (Center for Microscopy and Image Analysis, University of Zurich) for help in confocal microscopy and image analysis.

I also thank all the present and past IMCR members, particularly Dr. Stefano Ferrari, who helped me in optimizing experiments and gave a lot of helpful scientific inputs. I also thank Shreya for performing and helping in optimizing GFP-based reporter assays. Thanks also to Kai for help with flow cytometry.

Further I thank the Cancer biology PhD program of the Life Science Graduate School Zurich for providing such an exceptional atmosphere and network.

I also want to thank all my friends, at and outside IMCR, who supported me in one way or in another.

I am also very grateful to my family and to my girlfriend Medini who supported me constantly over last years.

8. CURRICULUM VITAE

PERSONAL DETAILS

Name:	Martin Steger
Date of birth:	31st October 1982
Nationality:	Italian

EDUCATION AND TRAINING

09/2008-to date	**University of Zurich, Institute of Molecular Cancer Research** employed as PhD student in the group of Prof. Alessandro A. Sartori PhD Thesis: PIN1-mediated isomerisation of CtIP determines double-strand break repair pathway choice
01/2008-08/2008	**University of Bologna (Bologna, Italy), Institute of General and Human Physiology** Research assistant in the laboratory of Molecular Neurobiology directed by Dr. Elisabetta Ciani
12/2007	**University of Bologna (Bologna, Italy), Institute of General and Human Physiology** Master Thesis: CB1 cannabinoid receptors increase neuronal precursor proliferation through AKT/glycogen synthase kinase-3beta/beta-catenin signaling
2005-2007	**University of Bologna (Bologna, Italy)** Master of Science (MSc) in Molecular and Cell Biology
07/2005	**University of Bologna (Bologna, Italy), Institute of Plant Biology** Bachelor Thesis: Redox regulation of a novel plastid-targeted beta-amylase of Arabidopsis thaliana
2002-2005	**University of Bologna (Bologna, Italy)** Bachelor of Science (BSc) in Molecular and Cell Biology
1997-2002	**Gewerbeoberschule Bruneck (Italy)** High school diploma (Matura)
1988-1997	Primary school education

PUBLICATIONS:

Trazzi S*, **Steger M***, Mitrugno VM, Bartesaghi R, Ciani E: CB1 cannabinoid receptors increase neuronal precursor proliferation through AKT/glycogen synthase kinase-3beta/beta-catenin signaling. *J Biol Chem.* 2010; 285(13): 10098-109.

Eid W*, **Steger M***, El-Shemerly M, Ferretti LP, Peña-Diaz J, König C, Valtorta E, Sartori AA, Ferrari S: DNA end resection by CtIP and exonuclease 1 prevents genomic instability. *EMBO Rep.* 2010; 12: 962-8.

Toller IM*, Neelsen KJ*, **Steger M**, Hartung ML, Hottiger MO, Stucki M, Kalali B, Gerhard M, Sartori AA, Lopes M, Müller A: Carcinogenic bacterial pathogen Helicobacter pylori triggers DNA double-strand breaks and a DNA damage response in its host cells. *Proc Natl Acad Sci* U S A. 2011; 108(36): 14944-9.

Steger M, Murina O, Huehn D, Walser R, Paliwal S, Haenggi K, Lafranchi L, Neugebauer C, Gerrits B, Janscak P, Zerbe O and Sartori AA: PIN1-mediated isomerisation of CtIP determines DNA double-strand break repair pathway choice. *Manuscript in preparation.*

*equal contribution

9. APPENDIX

Carcinogenic bacterial pathogen Helicobacter pylori triggers DNA double-strand breaks and a DNA damage response in its host cells

article published in PNAS, 2011

authors: Toller IM, Neelsen KJ, Steger M, Hartung ML, Hottiger MO, Stucki M, Kalali B, Gerhard M, Sartori AA, Lopes M and Müller A

contributions: I contributed the figures 1F-G and helped optimizing experiments of figure 2A. IMT, KJN and MLH contributed the other figures.

Carcinogenic bacterial pathogen *Helicobacter pylori* triggers DNA double-strand breaks and a DNA damage response in its host cells

Isabella M. Toller[a,1], Kai J. Neelsen[a,1], Martin Steger[a], Mara L. Hartung[a], Michael O. Hottiger[b], Manuel Stucki[b], Behnam Kalali[c], Markus Gerhard[c], Alessandro A. Sartori[a], Massimo Lopes[a,2], and Anne Müller[a,2]

[a]Institute of Molecular Cancer Research and [b]Institute of Veterinary Biochemistry and Molecular Biology, University of Zürich, 8057 Zürich, Switzerland; and [c]Department of Medicine, Technical University Munich, 81675 Munich, Germany

Edited by Jeffrey W. Roberts, Cornell University, Ithaca, NY, and approved July 28, 2011 (received for review January 24, 2011)

The bacterial pathogen *Helicobacter pylori* chronically infects the human gastric mucosa and is the leading risk factor for the development of gastric cancer. The molecular mechanisms of *H. pylori*-associated gastric carcinogenesis remain ill defined. In this study, we examined the possibility that *H. pylori* directly compromises the genomic integrity of its host cells. We provide evidence that the infection introduces DNA double-strand breaks (DSBs) in primary and transformed murine and human epithelial and mesenchymal cells. The induction of DSBs depends on the direct contact of live bacteria with mammalian cells. The infection-associated DNA damage is evident upon separation of nuclear DNA by pulse field gel electrophoresis and by high-magnification microscopy of metaphase chromosomes. Bacterial adhesion (e.g., via blood group antigen-binding adhesin) is required to induce DSBs; in contrast, the *H. pylori* virulence factors vacuolating cytotoxin A, γ-glutamyl transpeptidase, and the cytotoxin-associated gene (Cag) pathogenicity island are dispensable for DSB induction. The DNA discontinuities trigger a damage-signaling and repair response involving the sequential ataxia telangiectasia mutated (ATM)-dependent recruitment of repair factors—p53-binding protein (53BP1) and mediator of DNA damage checkpoint protein 1 (MDC1)—and histone H2A variant X (H2AX) phosphorylation. Although most breaks are repaired efficiently upon termination of the infection, we observe that prolonged active infection leads to saturation of cellular repair capabilities. In summary, we conclude that DNA damage followed by potentially imprecise repair is consistent with the carcinogenic properties of *H. pylori* and with its mutagenic properties in vitro and in vivo and may contribute to the genetic instability and frequent chromosomal aberrations that are a hallmark of gastric cancer.

DNA damage signaling | genomic instability | gastric tumorigenesis | chromosome breaks

Chronic infection with the human bacterial pathogen *Helicobacter pylori* causes gastritis and peptic ulceration (1) and increases the carrier's risk of developing gastric cancer (2) or gastric mucosa-associated lymphoid tissue lymphoma (3). The epidemiological association between *H. pylori* infection and gastric adenocarcinoma has been confirmed experimentally in rodent models using Mongolian gerbils (4) and C57BL/6 mice (5–7). Both epidemiological and experimental data suggest that bacterial virulence factors, host genetic traits, and environmental influences determine whether *Helicobacter*-induced gastritis will progress to gastric cancer (6, 8). In particular, *H. pylori*'s cytotoxin-associated gene (Cag) pathogenicity island (PAI), certain proinflammatory cytokine promoter polymorphisms, and a high-salt diet have been identified as cofactors affecting gastric cancer risk (2, 4, 5, 9). We have shown previously that gastric cancer precursor lesions induced by *Helicobacter felis* or *H. pylori* infection in C57BL/6 mice (which manifest histologically as atrophic gastritis, hyperplasia, and metaplasia) arise as a consequence of a T-helper type 1 cell-driven immunopathological response to the infection (10, 11). Mice lacking functional α/β^+ T cells are protected from precancerous lesions, and the adoptive transfer of $CD4^+CD25^-$ effector T cells is sufficient to sensitize mice to *Helicobacter*-induced preneoplasia (10).

In addition to the pathological effects of the *Helicobacter*-specific immune response on the gastric mucosa, several lines of evidence indicate that the bacteria may promote gastric carcinogenesis by jeopardizing the integrity and stability of their host's genome (12). *H. pylori* infection of cultured gastric epithelial cells down-regulates the components of the mismatch repair (MMR) and base excision repair machineries at the RNA and protein levels and impairs the efficiency of DNA repair as judged by MMR activity assay (13, 14). The down-regulation of MMR proteins was confirmed in experimentally infected murine gastric mucosa (14) and can be reversed by *Helicobacter* eradication in patients (15), suggesting that impaired DNA repair also is a hallmark of *H. pylori* infection in vivo. Touati et al. (16) reported an infection-induced increase in gastric mutation frequencies in the Big Blue transgenic model. The genotoxicity of *H. pylori* in this model has been attributed to oxidative damage of the DNA by reactive oxygen species (ROS) based on a high frequency of AT → CG and GC → TA transversions (16). Furthermore, mice deficient for the repair enzyme alkyladenine DNA glycosylase are more sensitive than wild-type animals to *H. pylori*-induced gastric preneoplasia (17).

Interestingly, early precancerous lesions in patient samples, as well as specific oncogene activation in different tumor models, have been linked to the formation of DNA double-strand breaks (DSBs) and the activation of DNA-damage checkpoints (18, 19). Thus, in this study, we examined the possibility that *H. pylori* directly damages DNA and triggers a DNA-damage response (DDR) in infected cells. We find that DSBs accumulate in various cell lines and in primary gastric epithelial cells upon infection with *H. pylori* in a time- and dose-dependent manner. The fragmentation of host nuclear DNA requires direct contact of live bacteria with their host cells, is independent of the *H. pylori* virulence determinants vacuolating cytotoxin A (VacA) and the Cag PAI, and does not require ROS-mediated DNA damage. Furthermore, infected cells display ataxia telangiectasia mutated-dependent phosporylated histone H2A variant X (γ-H2AX), mediator of DNA damage checkpoint protein 1

Author contributions: I.M.T., K.J.N., M.O.H., M.L., and A.M. designed research; I.M.T., K.J.N., M. Steger, M.L.H., and B.K. performed research; K.J.N., M. Steger, M. Stucki, B.K., M.G., and A.A.S. contributed new reagents/analytic tools; I.M.T., K.J.N., M. Steger, M.O.H., A.A.S., M.L., and A.M. analyzed data; and A.M. wrote the paper.

The authors declare no conflict of interest.

This article is a PNAS Direct Submission.

[1]I.M.T. and K.J.N. contributed equally to this work.

[2]To whom correspondence may be addressed. E-mail: lopes@imcr.uzh.ch or mueller@imcr.uzh.ch.

This article contains supporting information online at www.pnas.org/lookup/suppl/doi:10.1073/pnas.1100959108/-/DCSupplemental.

(MDC1), and p53-binding protein 1 (53BP1) nuclear foci indicative of *H. pylori*-induced DNA-damage signaling. Efficient repair of *H. pylori*-induced DSBs is apparent upon antibiotic killing of the bacteria, but prolonged infections lead to residual unrepaired breaks and negatively affect cell viability. In conclusion, we show here that *H. pylori* has the unique ability to induce host cellular DNA damage directly, providing a mechanistic explanation for the carcinogenic properties of this bacterial pathogen.

Results

***H. pylori* Infection of Cultured Cells Induces DSBs in Nuclear DNA That Trigger a DNA-Damage and Repair Response.** To assess a possible effect of *H. pylori* infection on the integrity of host cellular DNA, we subjected cultured gastric adenocarcinoma cells (AGS) to a pulse field gel electrophoresis (PFGE) approach that visualizes fragmented DNA ranging in size from 0.5–2.5 Mb (20). Infection of AGS cells with *H. pylori* G27 for 6 h results in a dose-dependent fragmentation of the DNA that is consistent with DSB induction (Fig. 1*A*). DSB induction leads to the recruitment of the early repair factor 53BP1 (21) to microscopically visible nuclear foci that form at the sites of DSBs in approximately one-third of infected AGS cells at 6 h postinfection as well as in all γ-irradiated cells at 1 h postirradiation (Fig. 1*B*). To assess whether this effect is restricted to cancer cells, we cultured murine primary gastric epithelial cells and infected them with *H. pylori*. Indeed, 53BP1 foci also could be detected readily in primary cells (Fig. 1*C*). Finally, we tested U2OS osteosarcoma cells, a convenient and commonly used system for DDR studies (18). *H. pylori* adheres well to these cells despite their fibroblastic origin and induces DNA fragmentation and 53BP1 foci to a similar extent as in gastric epithelial cells (Fig. 1*D* and Fig. S1*A*). *H. pylori*-induced foci also contain MDC1 (Fig. S1*B*), which binds to phosphorylated H2AX and directs the recruitment of DDR factors to damaged chromatin (22). The utility of U2OS cells as target cells of *H. pylori* allowed us to determine the kinetics of foci formation in U2OS cells stably expressing MDC1 as an EGFP fusion protein; EGFP-MDC1 is recruited rapidly to the sites of DSBs (Fig. S1*C*) and is retained in DSB-induced foci for at least 16 h as determined by time-lapse video microscopy (Fig. S1*D*). Indeed, the proportion of cells with clearly discernible repair foci increases over time and is greater than 50% after 48 h of infection (Fig. 1*E* and Fig. S2*A*). To determine whether 53BP1 foci form as the result of a physiological response to DSBs, which is known to be mediated by the activation of the ATM kinase at broken DNA (23), we treated U2OS cells with the ATM inhibitor KU-55933 during the 6-h time course of *H. pylori* infection. ATM inhibition strongly reduced the number of γH2AX/53BP1$^+$ cells, indicating that *H. pylori*-induced DSBs elicit a canonical DDR including the activation of the ATM kinase signaling pathway (Fig. 1 *F* and *G*).

The colocalization of 53BP1 and γH2AX foci in *H. pylori*-infected cells suggests strongly that the fragmented DNA observed by PFGE analysis results from DSBs formed in the host cells. To rule out that the "fragmented DNA" is of bacterial origin (the *H. pylori* genome is 1.6 Mb in size and should migrate in the same band), we performed Southern blots using a probe hybridizing to *H. pylori* 16S rRNA (Fig. S2*B*). Southern detection of 16S rRNA revealed that the bacterial genome indeed migrates similarly as broken DNA under the PFGE conditions used; however, the amount of bacterial DNA present in our infected cell cultures is not sufficient to be detected by ethidium bromide staining (or Southern hybridization; Fig. S2*B*). Therefore, we can rule out the possibility that the band corresponding to broken DNA in the pulse field gels is of bacterial rather than host cell origin. Another concern was related to the viability of the infected cells; therefore we checked parameters of apoptotic cell death by Western blotting for activated caspase-3 and cleaved poly-(ADP-ribose) polymerase 1 (PARP-1) and by flow cytometric analysis. No indication of apoptotic cell death was obtained at 6 and 16 h postinfection, confirming that the infected cells are viable despite sustaining considerable DNA damage (Fig. S2 *C* and *D*). In conclusion, *H. pylori* acts as an efficient inducer of DSBs in the nuclear DNA of its host cells, thereby triggering the recruitment of DDR factors to DSB sites in various primary and transformed mammalian cells.

***H. pylori*-Induced DSBs Appear at Mitosis as Chromosomal Breaks and Depend on Direct Host–Pathogen Contact but Not on the Cag PAI or VacA.** To detect DSBs microscopically and quantify them in the chromosomes of infected cells, we examined their condensed metaphase chromosomes (Fig. 2*A*). Although control cells with more than one broken chromatid were observed only rarely, ∼30% of infected cells exhibited two or more breaks (Fig. 2 *A* and *B* and Fig. S3*A*). In fact, we found a substantial proportion of infected cells in which at least three and up to seven chromosomes had sustained microscopically evident chromatid breaks; such severely damaged cells were not detectable in the absence of *H. pylori* infection (Fig. *2 A* and *B*). To examine whether the ability to induce DSBs is specific to (live) *H. pylori*, we compared live and dead bacteria and also included a laboratory strain of *Escherichia coli*. Only live *H. pylori* efficiently induced DSBs in AGS cells as determined by PFGE; *E. coli* or *H. pylori* bacteria killed by ethanol had no discernible effects (Fig. 2*C*). Inhibition of bacterial protein synthesis by chloramphenicol or gentamycin during the coculture with AGS cells also reduced DSB induction (Fig. S3*B*). DSB induction further required the direct interaction between the bacteria and their host cells and was abolished by their separation with a Transwell filter (Fig. 2*D*). We also assessed the effects of preconditioned medium (i.e., supernatants of AGS cells that had been infected for 16 h) with respect to DSB induction in fresh cells. No breaks were detected (Fig. 2*D*), ruling out the possibility that DSBs are induced by secreted bacterial or host cell factors.

Having obtained evidence that direct binding of *H. pylori* is a prerequisite for DSB induction, we next examined the dependence of DSB induction on the *H. pylori* blood-group antigen-binding adhesin BabA, which targets human Lewis (b) surface epitopes and has been tightly associated with duodenal ulcers and gastric cancer (24). We took advantage of the Kato III gastric epithelial cell infection model, in which we found *H. pylori* adhesion and *H. pylori*-specific IL-8 induction to be mediated predominantly by BabA (Fig. S4 *A*–*C*). Kato III cells were infected with either wild-type *H. pylori* or an isogenic Δ*babA* mutant and were assessed for DSB induction by PFGE. The Δ*babA* mutant was clearly less capable of inducing DSBs than the corresponding parental strain; this result was obtained with two different *H. pylori* strain backgrounds, J99 and G27 (Fig. 2*E* and Fig. S4*D*). Interestingly, preincubation of wild-type bacteria with increasing amounts of soluble Lewis (b) reduced DSB induction by *H. pylori* in a dose-dependent manner (Fig. S4*E*). The results confirm that tight attachment of the bacteria to their host cells, e.g., through the BabA/Lewis (b) interaction, is a prerequisite for infection-induced DNA damage. We next sought to determine whether well-known *H. pylori* virulence factors such as Cag PAI or VacA contribute to DSB induction. Isogenic Δ*PAI* or Δ*vacA* mutants induced DSBs to a similar extent as wild-type bacteria (Fig. 2 *F*–*H*), suggesting that neither VacA nor the PAI-encoded type IV secretion system of *H. pylori* is essential for DSB induction. Finally, we assessed whether a suspected *H. pylori* virulence factor that previously was reported to induce oxidative DNA damage (25), the γ-glutamyl transferase (γGT), is involved in DSB induction. This clearly was not the case; furthermore, a double mutant lacking both γGT and VacA also did not differ in this respect from the corresponding wild-type bacteria (strain P12) (Fig. S5). In summary, *H. pylori*, but not *E. coli*, induces DSBs in

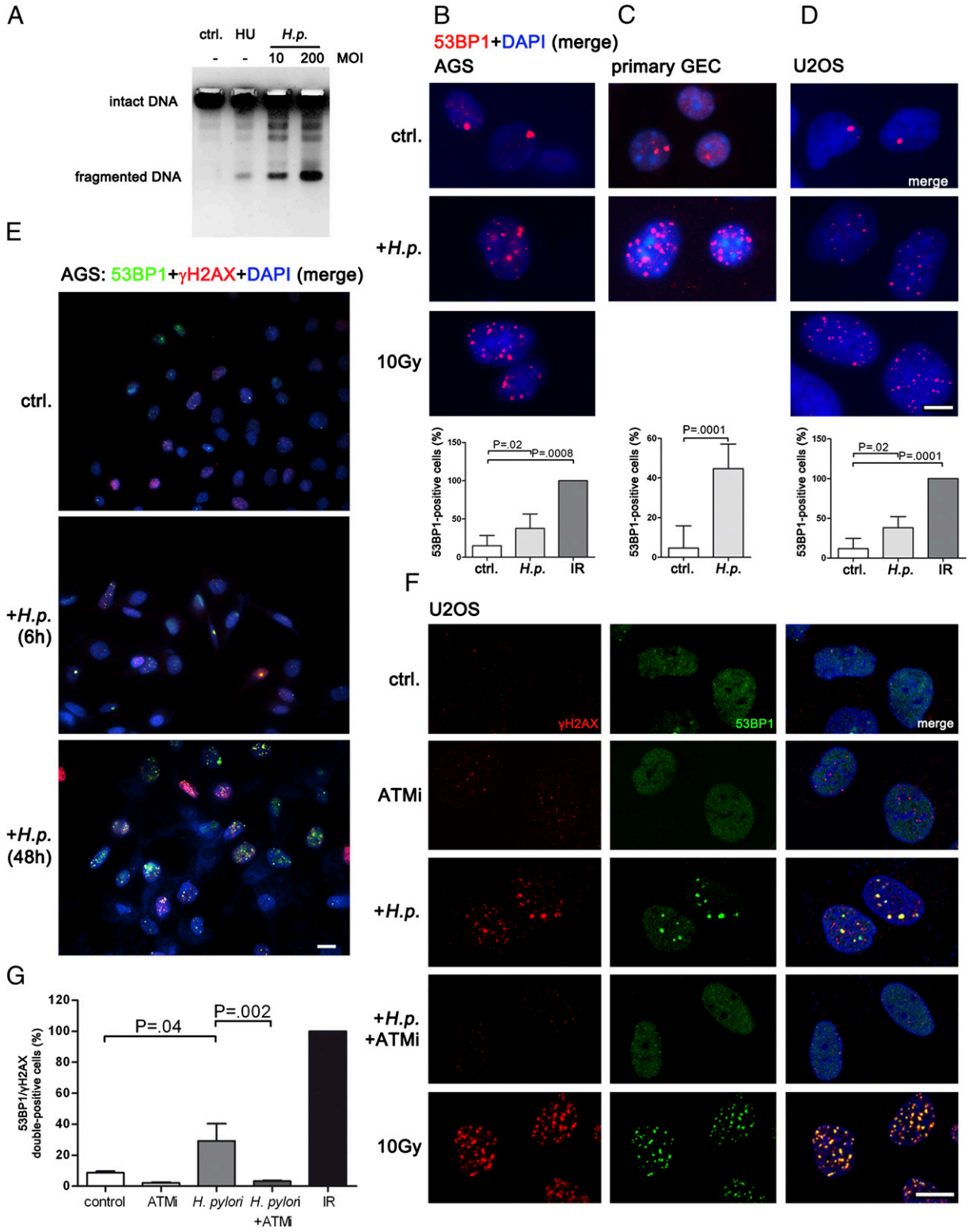

Fig. 1. *H. pylori* infection of cultured cells induces DSBs and DNA damage-response pathways. (*A*) AGS cells were infected with *H. pylori* strain G27 for 6 h at MOIs of 10 and 200. Hydroxyurea (HU) treatment (5 mM) served as positive control. DNA integrity was assessed by PFGE. (*B–D*) AGS cells (*B*), primary murine gastric epithelial cells (GEC) (*C*), and U2OS cells (*D*) were infected with *H. pylori* strain G27 (MOI 200) for 6 h and immunostained for 53BP1 and stained with DAPI for nuclear DNA. Cells irradiated with 10 Gy served as positive control as indicated. (*E*) AGS cells were infected for 6 or 48 h with G27 and stained for 53BP1, γH2AX, and nuclear DNA. (*F* and *G*) U2OS cells were infected with *H. pylori* G27 (MOI 200) for 6 h and/or treated with the ATM inhibitor KU-55922 before staining for 53BP1 and γH2AX. (Scale bars: 10 μm.) In *B*, *C*, *D*, and *G*, cells with more than four foci per nucleus were scored as positive; 150 cells were scored per condition. SEM and *P* values (Student's two-tailed *t* test) were calculated from three independent experiments.

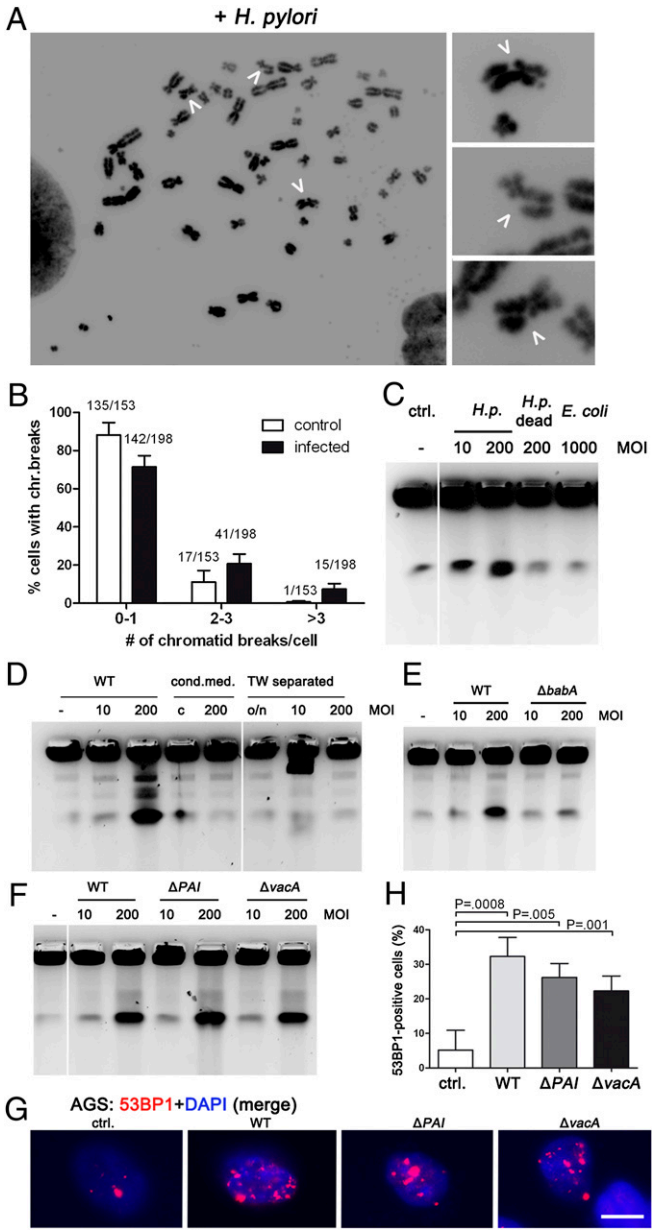

Fig. 2. DSB induction is *H. pylori* specific and depends on the direct contact of live bacteria with their host cells. (*A* and *B*) U2OS cells were infected with *H. pylori* strain G27 (MOI 200) followed by visualization of chromatid breaks by chromosome spreading. The integrity of chromatids was assessed by visual inspection of the chromosome spreads of 153 control cells and 198 infected cells in three independent experiments. The number of chromatid breaks per cell and number of cells with chromatid breaks (%) is indicated in *B*; error bars indicate the variation within the three experiments. (*C*) AGS cells were cocultured with live *H. pylori* G27, ethanol-killed bacteria, or live *E. coli* DH10B at the indicated MOIs for 16 h. DNA fragmentation was assessed by PFGE. (*D*) AGS cells were infected with *H. pylori* G27 for 6 h at the indicated MOIs (lanes 1–3). In lanes 4 and 5, cells were treated with sterile-filtered cell-culture supernatants obtained from 16-h control- or *H. pylori*-infected (MOI 200) AGS cells. In lanes 6–8, Transwell filters were used to separate AGS cells physically from a concentrated overnight *H. pylori* culture supernatant (lane 6) or from living bacteria at MOIs of 10 (lane 7) or 200 (lane 8). DNA fragmentation was assessed by PFGE. (*E*) Kato III cells were infected with *H. pylori* J99 or the isogenic mutant Δ*babA* for 6 h at the indicated MOIs. DNA integrity was assessed by PFGE. (*F–H*) AGS cells were infected with wild-type G27 or Δ*PAI* or Δ*vacA* isogenic mutants and assessed by PFGE (*F*) or staining for 53BP1 (*G* and *H*). In *H*, cells with more than four foci per nucleus were scored as positive; SEM and *P* values were calculated from three independent experiments.

a contact/BabA-dependent but VacA-, Cag PAI-, and γGT-independent manner.

Neither DNA Synthesis nor Oxidative Damage Is Required for *H. pylori*-Induced DSBs. Only a fraction of infected cells exhibits nuclear foci and chromatid aberrations (Figs. 1 and 2 *A* and *B*), suggesting a cell-cycle dependence of DSB induction. Because oncogene-induced DSBs have been attributed to DNA replication stress, and most spontaneous DSBs are caused by collapsed replication forks (18, 19), a possible explanation would be that cells are sensitive only in S-phase. To determine whether DNA replication is required for DNA fragmentation, we synchronized U2OS cells in G2/M by nocodazole treatment before infection with *H. pylori*. Cells were infected for 6 h at 2 h after release from G2/M arrest. Their DNA integrity was assessed by PFGE at the end point 8 h after release, i.e., at a time when the cells had not yet reentered S-phase (as documented by flow cytometric cell-cycle analysis; Fig. S6). As shown in Fig. 3*A*, synchronized cells sustained a level of DSBs similar to that in asynchronous cultures infected in parallel for the same period. Thus, unlike DSBs that are caused by alkylating agents, intrastrand crosslinking, and topoisomerase I inhibitors, *Helicobacter*-induced DSBs do not require bulk DNA replication.

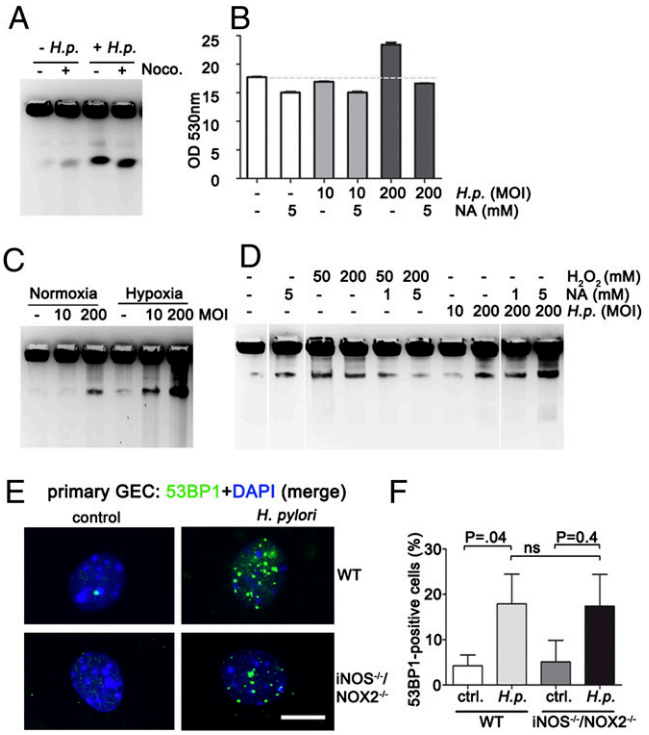

Fig. 3. *H. pylori*-associated DSBs occur independently of cell-cycle phase and oxidative DNA damage. (*A*) U2OS cells were arrested in G2/M by 12-h treatment with 250 ng/mL nocodazole, released for 2 h, and infected with *H. pylori* G27 for 6 h. DNA integrity was assessed by PFGE. (*B*) AGS cells were left untreated, were treated with 5 mM *N*-acetyl-cysteine (NA), and/or were infected with *H. pylori* G27 at MOIs of 10 and 200. Relative induction of ROS was assessed by oxidation of 2,7-dichlorofluorescein diacetate (DCF-DA) to fluorescent DCF. (*C*) AGS cells were infected with *H. pylori* G27 for 6 h at the indicated MOIs in 20% oxygen (normoxia) or 1% oxygen (hypoxia). (*D*) AGS cells were infected at the indicated MOIs for 6 h. *N*-acetyl-cysteine (NA) was added at 1 or 5 mM as indicated. H_2O_2 treatment for 1 h served as positive control. In *C* and *D*, DNA fragmentation was visualized by PFGE. (*E* and *F*) Primary gastric epithelial cells explanted from wild-type C57BL/6 or iNOS$^{-/-}$/NOX2$^{-/-}$ mice were infected with *H. pylori* for 6 h and immunostained for 53BP1. Cells with more than four 53BP1 foci per nucleus were graded as positive; SEM and *P* values were calculated from three independent experiments.

The mutations detected in the chronically *H. pylori*-infected stomach are predominantly AT > CG and GC > TA transversions indicative of oxidative DNA damage (16). *H. pylori* efficiently induces reactive oxygen and nitrogen species (RONS) in AGS cells, which can be scavenged by *N*-acetyl-cysteine (Fig. 3*B*). To determine whether *H. pylori*-associated DSB induction is dependent on RONS, we used three complementary approaches in which the production of RONS was minimized by growth under hypoxic conditions, pharmacological scavenging of RONS, or a combined targeted deletion of the genes encoding inducible nitric oxide synthase (iNOS) and NADPH oxidase 2 (NOX2). Remarkably, AGS cells grown under hypoxic conditions (1% oxygen) suffered more, rather than fewer, DSBs upon infection with *H. pylori*, arguing against the idea that *H. pylori*-induced DSBs are mediated by RONS (Fig. 3*C*). Similarly, addition of the RONS scavenger *N*-acetyl-cysteine to infected cells aggravated *H. pylori*-induced DSBs rather than preventing them (Fig. 3*D*); in contrast, the same scavenger concentrations efficiently reduced H_2O_2-induced DSBs (Fig. 3*D*). Finally, infection of primary gastric epithelial cells isolated from iNOS/NOX2$^{-/-}$ mice induced DSBs with a similar efficiency as infection of wild-type cells (Fig. 3 *E* and *F*), suggesting that the RONS produced through the combined activity of both enzymes are not essential for DSB induction. In summary, the results suggest that RONS produced by gastric epithelial cells upon *H. pylori* infection are not mechanistically involved in DSB induction despite a temporal correlation of RONS production and DSB induction.

Infection-Induced DSBs Are Continuously Repaired. We next assessed whether DSBs accumulate during infection and/or whether they are resolved continuously by the cellular DNA repair machinery. We observed no PFGE-detectable difference in DSB levels comparing short (6-h) and prolonged (54-h) infections (Fig. 4*A*), suggesting that infected cells may reach an equilibrium in which DSBs are repaired continuously even as new breaks are incurred. Indeed, we find that the PFGE band corresponding to fragmented DNA persists for at least 48–54 h in the continuous presence of live bacteria in two independent cell types tested (Fig. S7). To test whether cells are capable of efficient DSB repair, we infected AGS cells for 6 h, eradicated the bacteria by antibiotic therapy, and allowed the cells to recover for 48 h. Antibiotic eradication resulted in the subsequent efficient repair of DSBs as judged by the disappearance of fragmented DNA (Fig. 4*A*) as well as by the disappearance of 53BP1/MDC1 foci (Fig. 4 *B* and *C*). However, in the presence of continuous infection for 48 h or longer, ~70% of the cells lose their proliferative capacity (i.e., fail to form colonies in a clonogenic assay) (Fig. 4*D*). We conclude from these results that *H. pylori*-induced DSBs are addressed efficiently by the host cell repair machinery, with the results of the repair process being evident only after the de novo induction of DSBs is prevented by inactivation of the bacteria. However, prolonged continuous infection at high multiplicities of infection (MOIs) may saturate the repair mechanisms, lead to unrepaired breaks, and cause cell lethality.

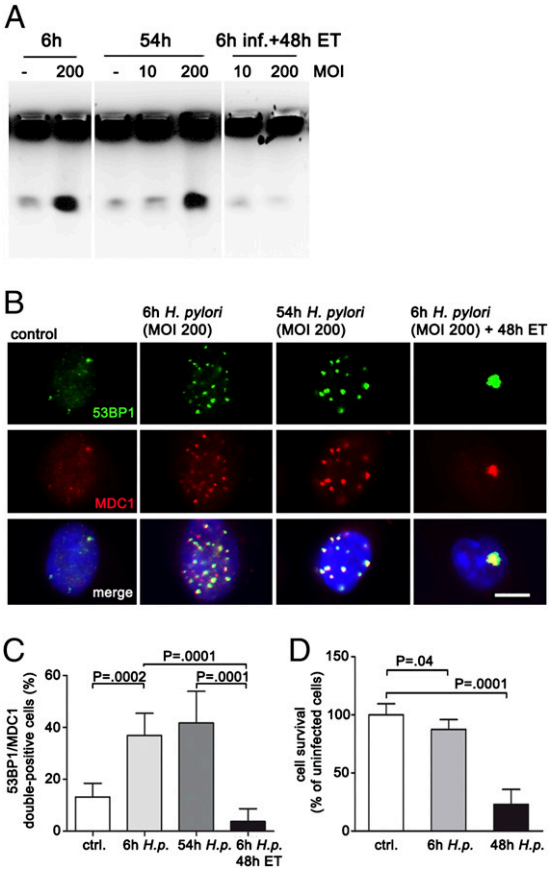

Fig. 4. *H. pylori*-induced breaks are repaired only after bacterial killing. (*A*–*C*) AGS cells were infected with *H. pylori* G27 at the indicated MOIs for 6 h before antibiotic killing of the bacteria (eradication therapy, ET). Cells then were grown in full medium containing penicillin/streptomycin for 48 h to allow DNA repair to occur, were harvested, and were subjected to PFGE (*A*) or to immunostaining for 53BP1 and MDC1 (*B*) and compared with control cells that had been infected either for 6 h or continuously for 54 h. In *C*, cells with more than four foci per nucleus were graded as positive; SEM and *P* values were calculated from three independent experiments. (*D*) Cells were infected with *H. pylori* G27 for 6 and 48 h, subjected to *H. pylori* eradication, and cultured for another 10 d. Proliferative capacity was assessed by clonogenic assay; the survival and clonogenic capacity of never-infected (ctrl) cells is set at 100%.

Discussion

We describe here the phenomenon of chromosomal DSB induction in mammalian cells upon infection with the carcinogenic bacterium *H. pylori*. This process requires viable bacteria in close contact with their host cells. We provide evidence that bacterial adhesion, for instance via the BabA adhesin, is required for DSB induction; in contrast, the *H. pylori* virulence factors VacA, γGT, and the Cag PAI are dispensable for DSB induction. Host cellular ROS and reactive nitrogen species production is triggered by the infection but appears to not contribute to DSB formation. The ability to induce DSBs is shared by the three *H. pylori* isolates examined in the course of our studies (G27, J99, and P12) and occurs with similar kinetics and efficiency in primary and transformed, murine and human, epithelial and mesenchymal cells. *H. pylori*-induced DSBs are evident upon separation of nuclear DNA by PFGE and by high-magnification microscopy of metaphase chromosomes. The damaged DNA triggers a damage-signaling and repair response involving the sequential ATM-dependent recruitment of repair factors (53BP1, MDC1) and the phosphorylation of histone H2AX. *H. pylori*-induced DSBs can be repaired efficiently by the damaged cells, but prolonged bacterial infection at high MOIs saturates cellular repair mechanisms and impairs proliferation.

Very few reports are available on bacterially induced DNA damage of host cell nuclear DNA. Interestingly, most bacterial species with demonstrated genotoxic properties are gastrointestinal pathogens. In pathogenic strains of *E. coli*, a genomic island encoding modular nonribosomal peptide and polyketide synthases has been linked to DSB induction and DNA-damage checkpoint activation (26). The hybrid peptide/polyketide genotoxin produced by these enzymes arrests the DNA-damaged cells at the G2/M transition; the decelerated self-renewal of the intestinal epithelium resulting from cell-cycle arrest has been

proposed to benefit the bacteria by facilitating their persistence (26). The only other bacterial virulence factor known to affect the integrity of the host genome is produced by the enteropathogenic species *Helicobacter hepaticus* and *Campylobacter jejuni*, close relatives of *H. pylori*. The so-called "cytolethal distending toxins" (CDTs) exhibit structural and functional homology to mammalian phosphodiesterases such as DNase I (21) and cause cell-cycle arrest and cell death in intestinal epithelial cells (27). In murine models of *H. hepaticus* infection, CDT triggers the development of chronic intestinal inflammation mimicking inflammatory bowel disease in humans (28) and promotes hepatocellular dysplasia (29). Similarly, CDT is required for the induction of gastroenteritis by *C. jejuni* (30). No orthologs of CDT are present in any of the *H. pylori* genomes sequenced to date, including the genome of G27, which we predominantly used here.

DNA DSBs are the most harmful lesions a cell can encounter, and efficient DSB repair is crucial for the maintenance of genomic integrity and viability (31). Cells have evolved mechanistically distinct strategies for DSB repair (32). These strategies include minor mutagenic pathways that recently have generated great interest in the field as a possible source of the chromosomal aberrations observed in many cancers (33). Induction of DSBs followed by imprecise repair would be consistent with the carcinogenic properties of *H. pylori* (as well as those of other enteropathogenic species capable of inducing DSBs, such as *H. hepaticus*) and with its mutagenic properties in vitro and in vivo (16). Importantly, we observe that prolonged bacterial infection leads to saturation of the repair capabilities of the host cells, possibly leading to ineffective and mutagenic DSB repair attempts. We consider a comprehensive analysis of the DSB repair pathways activated by *H. pylori* infection to be an important challenge for future studies. In conclusion, we propose here that DSB induction contributes to the genetic instability and frequent chromosomal aberrations that are a hallmark of gastric cancer, indicating that as yet unidentified *H. pylori*-derived oncoproteins encoded outside the Cag PAI must be considered to gain a better understanding of *H. pylori*-induced gastric carcinogenesis.

Materials and Methods

Mouse and Bacterial Strains, Cell Lines, Infection Conditions, and Pharmacological Treatments. C57BL/6 (Charles River Laboratories) and iNOS$^{-/-}$/NOX2$^{-/-}$ mice (generously provided by Wolf-Dietrich Hardt, Eidgenössische Technische Hochschule, Zurich) were used to generate primary gastric epithelial cells as described (10). *H. pylori* was grown as described (10). AGS cells (ATCC CRL 1739, a human gastric adenocarcinoma cell line), immortalized murine primary gastric epithelial cells (IMPGE) (10), U2OS cells, and a stable U2OS line expressing EGFP-MDC1 were grown and infected with *E. coli* DH10B or *H. pylori* strains as specified in *SI Materials and Methods*.

PFGE, Chromosome Spreads, Quantification of RONS, Cell-Cycle Analysis, and Clonogenic Assays. Chromosome spreads, PFGE experiments, quantification of RONS, cell-cycle analysis, clonogenic assays are specified in *SI Materials and Methods*.

Immunofluorescence Microscopy, Western and Southern Blotting. For immunostaining, cells were fixed in methanol, stained with 53BP1 (sc-22760; Santa Cruz), MDC1 (3835), or γH2AX (05-636; Upstate), quantified and analyzed as specified in *SI Materials and Methods*. Western and Southern blotting protocols are specified in *SI Materials and Methods*.

ACKNOWLEDGMENTS. We thank Wolf-Dietrich Hardt for providing iNOS$^{-/-}$/NOX2$^{-/-}$ mice and Johannes Kusters and Thomas Boren for providing G27Δ*vacA* and J99Δ*babA* mutants, respectively. We thank Esther Kohler for expert technical assistance. This work was supported by grants from the Swiss National Science Foundation (to A.M. and M.L.), the Swiss Cancer League and the Zurich Cantonal Cancer League (to A.M.), the Vontobel-Foundation and a Swiss National Science Foundation Ambizione fellowship (to A.A.S.), and the Forschungskredit from the University of Zurich (to M.S.).

1. Marshall BJ, Warren JR (1984) Unidentified curved bacilli in the stomach of patients with gastritis and peptic ulceration. *Lancet* 1:1311–1315.
2. Parsonnet J, Friedman GD, Orentreich N, Vogelman H (1997) Risk for gastric cancer in people with CagA positive or CagA negative *Helicobacter pylori* infection. *Gut* 40: 297–301.
3. Parsonnet J, Isaacson PG (2004) Bacterial infection and MALT lymphoma. *N Engl J Med* 350:213–215.
4. Rieder G, Merchant JL, Haas R (2005) *Helicobacter pylori* cag-type IV secretion system facilitates corpus colonization to induce precancerous conditions in Mongolian gerbils. *Gastroenterology* 128:1229–1242.
5. Fox JG, et al. (2003) *Helicobacter pylori*-associated gastric cancer in INS-GAS mice is gender specific. *Cancer Res* 63:942–950.
6. Fox JG, Wang TC (2007) Inflammation, atrophy, and gastric cancer. *J Clin Invest* 117:60–69.
7. Fox JG, et al. (2003) Host and microbial constituents influence *Helicobacter pylori*-induced cancer in a murine model of hypergastrinemia. *Gastroenterology* 124: 1879–1890.
8. Pritchard DM, Crabtree JE (2006) *Helicobacter pylori* and gastric cancer. *Curr Opin Gastroenterol* 22:620–625.
9. El-Omar EM, et al. (2000) Interleukin-1 polymorphisms associated with increased risk of gastric cancer. *Nature* 404:398–402.
10. Sayi A, et al. (2009) The CD4+ T cell-mediated IFN-gamma response to Helicobacter infection is essential for clearance and determines gastric cancer risk. *J Immunol* 182: 7085–7101.
11. Toller IM, Altmeyer M, Kohler E, Hottiger MO, Müller A (2010) Inhibition of ADP ribosylation prevents and cures helicobacter-induced gastric preneoplasia. *Cancer Res* 70:5912–5922.
12. Machado AM, Figueiredo C, Seruca R, Rasmussen LJ (2010) *Helicobacter pylori* infection generates genetic instability in gastric cells. *Biochim Biophys Acta* 1806:58–65.
13. Machado AM, et al. (2009) *Helicobacter pylori* infection induces genetic instability of nuclear and mitochondrial DNA in gastric cells. *Clin Cancer Res* 15:2995–3002.
14. Kim JJ, et al. (2002) *Helicobacter pylori* impairs DNA mismatch repair in gastric epithelial cells. *Gastroenterology* 123:542–553.
15. Park DI, et al. (2005) Effect of *Helicobacter pylori* infection on the expression of DNA mismatch repair protein. *Helicobacter* 10:179–184.
16. Touati E, et al. (2003) Chronic *Helicobacter pylori* infections induce gastric mutations in mice. *Gastroenterology* 124:1408–1419.
17. Meira LB, et al. (2008) DNA damage induced by chronic inflammation contributes to colon carcinogenesis in mice. *J Clin Invest* 118:2516–2525.
18. Bartkova J, et al. (2005) DNA damage response as a candidate anti-cancer barrier in early human tumorigenesis. *Nature* 434:864–870.
19. Gorgoulis VG, et al. (2005) Activation of the DNA damage checkpoint and genomic instability in human precancerous lesions. *Nature* 434:907–913.
20. Hanada K, et al. (2007) The structure-specific endonuclease Mus81 contributes to replication restart by generating double-strand DNA breaks. *Nat Struct Mol Biol* 14: 1096–1104.
21. Lara-Tejero M, Galán JE (2000) A bacterial toxin that controls cell cycle progression as a deoxyribonuclease I-like protein. *Science* 290:354–357.
22. Stucki M, et al. (2005) MDC1 directly binds phosphorylated histone H2AX to regulate cellular responses to DNA double-strand breaks. *Cell* 123:1213–1226.
23. Ciccia A, Elledge SJ (2010) The DNA damage response: Making it safe to play with knives. *Mol Cell* 40:179–204.
24. Gerhard M, et al. (1999) Clinical relevance of the *Helicobacter pylori* gene for blood-group antigen-binding adhesin. *Proc Natl Acad Sci USA* 96:12778–12783.
25. Gong M, Ling SS, Lui SY, Yeoh KG, Ho B (2010) *Helicobacter pylori* gamma-glutamyl transpeptidase is a pathogenic factor in the development of peptic ulcer disease. *Gastroenterology* 139:564–573.
26. Nougayrède JP, et al. (2006) *Escherichia coli* induces DNA double-strand breaks in eukaryotic cells. *Science* 313:848–851.
27. Liyanage NP, et al. (2010) *Helicobacter hepaticus* cytolethal distending toxin causes cell death in intestinal epithelial cells via mitochondrial apoptotic pathway. *Helicobacter* 15:98–107.
28. Young VB, et al. (2004) In vitro and in vivo characterization of Helicobacter hepaticus cytolethal distending toxin mutants. *Infect Immun* 72:2521–2527.
29. Ge Z, et al. (2007) Bacterial cytolethal distending toxin promotes the development of dysplasia in a model of microbially induced hepatocarcinogenesis. *Cell Microbiol* 9: 2070–2080.
30. Fox JG, et al. (2004) Gastroenteritis in NF-kappaB-deficient mice is produced with wild-type *Camplyobacter jejuni* but not with *C. jejuni* lacking cytolethal distending toxin despite persistent colonization with both strains. *Infect Immun* 72:1116–1125.
31. Hakem R (2008) DNA-damage repair; the good, the bad, and the ugly. *EMBO J* 27: 589–605.
32. Pardo B, Gómez-González B, Aguilera A (2009) DNA repair in mammalian cells: DNA double-strand break repair: How to fix a broken relationship. *Cell Mol Life Sci* 66: 1039–1056.
33. Zhang Y, et al. (2010) The role of mechanistic factors in promoting chromosomal translocations found in lymphoid and other cancers. *Adv Immunol* 106:93–133.

Supporting Information

Toller et al. 10.1073/pnas.1100959108

SI Materials and Methods

Cell Lines, Bacterial Strains, and Infection Conditions. Cell lines were grown in the following media: AGS, U2OS, stable U2OS line expressing EGFP-MDC1 (DMEM/10% FCS), and immortalized primary gastric epithelial cells (IMPG) DMEM/ F12 (1:1) (Gibco).

The following previously published or newly generated strains of H. pylori were used: G27 (1); G27Δ*PAI* [deficient for the Cag PAI (1)]; G27Δ*vacA* (deficient for VacA; generously provided by J. Kusters, Department of Medical Microbiology, University Medical Center Utrecht, Utrecht, The Netherlands); G27ΔbabA (2); G27Δγgt (2); J99 (3); J99Δ*babA* (3); P12 (4); and P12Δ*γgt*/ΔvacA (lacking both γ-GT and VacA; obtained by replacing a P12Δ*vacA* mutant's γgt gene by a kanamycin resistance cassette and subsequent selection on chloramphenicol and kanamycin plates) (4). The G27Δ*babA* mutant was generated by transformation of J99Δ*babA* genomic DNA into G27 wild-type bacteria. Infections were performed for 6 to 54 h. Experiments under hypoxic conditions (1% oxygen) were performed in a gas-controlled glove box (InVivO2 400; Ruskinn Technologies). Pharmacological Treatments. U2OS cells were synchronized in G1 by 12 h of nocodazole treatment (250 ng/mL), followed by a 2-h release before infection. The ATM inhibitor KU-55933 (Tocris) was used at 10 μM. Transwell filters (0.4 μm, Falcon 353493) were used to separate bacteria and cells. Hydroxy urea was used at 5 mM, N-acetyl cysteine at 1 mM and 5 mM, and staurosporine at 5 μM (all from Sigma). Lewis (b) human serum albumin glycoconjugate was obtained from IsoSep. Bacteria were killed by incubation in 100% ethanol; protein synthesis was inhibited by 10 or 80 μg/mL chloramphenicol. Bacteria in co-culture with host cells were killed with penicillin/streptomycin combined with 15 μg/mL metronidazole, 30 μg/mL tetracycline hydrochloride (both from Sigma), and 4 μg/mL bismuth subcitrate (Park-Davis).

PFGE, Chromosome Spreads, Quantification of RONS, Cell-Cycle Analysis, and Clonogenic Assay. For PFGE, cells were harvested, embedded in 1% agarose plugs (5 × 105 cells per plug), digested in lysis buffer [100 mM EDTA, 1% (wt/vol) sodium lauryl sarcosyne, 0.2% (wt/vol) sodium deoxycholate, 1 mg/mL proteinase K] at 37 °C for 48 h, and washed in 10 mM Tris-HCl (pH 8.0), 100mM EDTA. Electrophoresis was performed for 23 h at 14 °C in 0.9% (wt/vol) pulse field-certified agarose (BioRad) containing Tris-borate/EDTA buffer according to the conditions described in ref. 5 and adapted to a BioRad CHEF DR III apparatus. Gels were stained with ethidium bromide and imagedon an Alpha Innotech Imager. The chromosome-spread protocol was performed as previously published (6). In brief, for the generation of chromosome/meta- phase spreads, cells were infected for 48 h, and 0.1 μg/mL colcemid was added for the final 3 h. Cells were harvested by trypsinization and treated with hypotonic 75 mM KCl before fixation with methanol/acetic acid (3:1) and staining with DAPI. The number of chromatid breaks per metaphase spread was quantified by visual inspection. For the quantitative detection of RONS, cells were incubated with 5 μM 2,7-dichlorofluorescein (DCF) diacetate in the dark for 30 min at 37 °C. The oxidation-induced deesterification of DCF was detected at 530 nm. For cell-cycle analysis, cells were fixed in 70% ethanol followed by RNase treatment (100 μg/mL) and staining with 25μg/mL propidium iodide. Cell-cycle distribution was recorded on a Cyan9 instrument and analyzed using Summit Software (both from Beckman Coulter). For clonogenic assays, 300 cells per well were seeded in full medium containing all eradication antibiotics to eliminate residual bacteria. After 10 d in culture, colonies were stained with 0.1% Coomassie blue (in 50% methanol/7% acetic acid) and were counted.

Immunofluorescence Microscopy, Western and Southern Blotting. For immunostaining, cells were fixed in methanol, stained with 53BP1 (sc-22760; Santa Cruz), MDC1 (3835), or γH2AX (05-636; Upstate) mAbs and appropriate secondary antibodies (Molecular Probes) and mounted with VECTASHIELD (Vector Laboratories). Cells were imaged in a Leica DM RB microscope equipped with a Leica DFC 360 FX camera. Images were taken at 60–100× magnification using Leica Application Suite 3.3.0 software. One hundred fifty nuclei were assessed per condition; positive cells had more than four foci per nucleus. PARP1 (sc7150) and activated caspase-3 were assessed by Western blotting as markers of apoptosis. For Southern blotting, a deoxycytidine triphosphate (α[32P])-labeled 1,200-bp Helicobacter spp-specific 16S probe was generated using the primers (forward) GCTATGACGGGTATCC and (reverse) ACTTCACCCCAGTCGCTG. A pulse field gel was stained, UV cross-linked with 150 mJ, transferred to a Zeta-Probe GT nylon membrane for 12 h, detected with radiolabeled 16S probe, and exposed on a Typhoon 9400 PhosphoImager.

1. Censini S, et al. (1996) Cag, a pathogenicity island of Helicobacter pylori, encodes type I-specific and disease-associated virulence factors. *Proc Natl Acad Sci USA* 93: 14648–14653.
2. Schmees C, et al. (2007) Inhibition of T-cell proliferation by Helicobacter pylori gamma-glutamyl transpeptidase. *Gastroenterology* 132:1820–1833.
3. Mahdavi J, et al. (2002) Helicobacter pylori SabA adhesin in persistent infection and chronic inflammation. *Science* 297:573–578.
4. Fassi Fehri L, et al. (2010) Helicobacter pylori induces miR-155 in T cells in a cAMPFoxp3-dependent manner. *PLoS ONE* 5:e9500.
5. Hanada K, et al. (2007) The structure-specific endonuclease Mus81 contributes to replication restart by generating double-strand DNA breaks. *Nat Struct Mol Biol* 14: 1096–1104.
6. Eid W, Steger M, et al. (2010) DNA end resection by CtIP and exonuclease 1 prevents genomic instability. *EMBO Rep* 11(12):962–968.

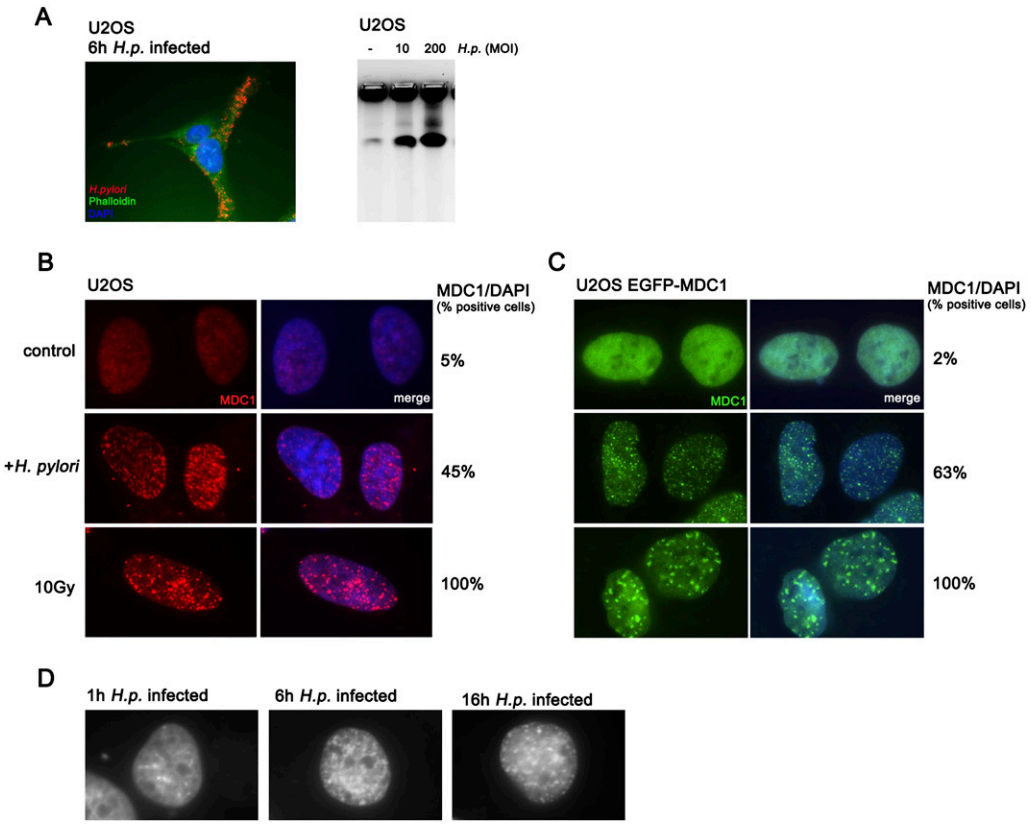

Fig. S1. U2OS cells are a convenient model for *Helicobacter pylori*-induced double-stranded breaks (DSBs). (*A* and *B*) U2OS cells were infected with *H. pylori* G27 for 6 h and were immunostained for *H. pylori* (red), phalloidin (green), and nuclei (blue) or subjected to pulse field gel electrophoresis (PFGE) (*A*) or were stained for mediator of DNA damage checkpoint 1 (MDC1) (*B*). (*C*) U2OS EGFP-MDC1 cells were infected with *H. pylori* G27 for 6 h; EGFP fluorescence is shown alone (*Left*) and merged with DAPI staining (*Right*). As a positive control, cells irradiated with 10 Gy are included in *B* and *C*. (*D*) U2OS EGFP-MDC1 cells were infected with *H. pylori* G27, and EGFP-MDC1 foci formation was monitored by time-lapse video microscopy over a period of 16 h. Still images of a single cell are shown at 1 h, 6 h, and 16 h postinfection.

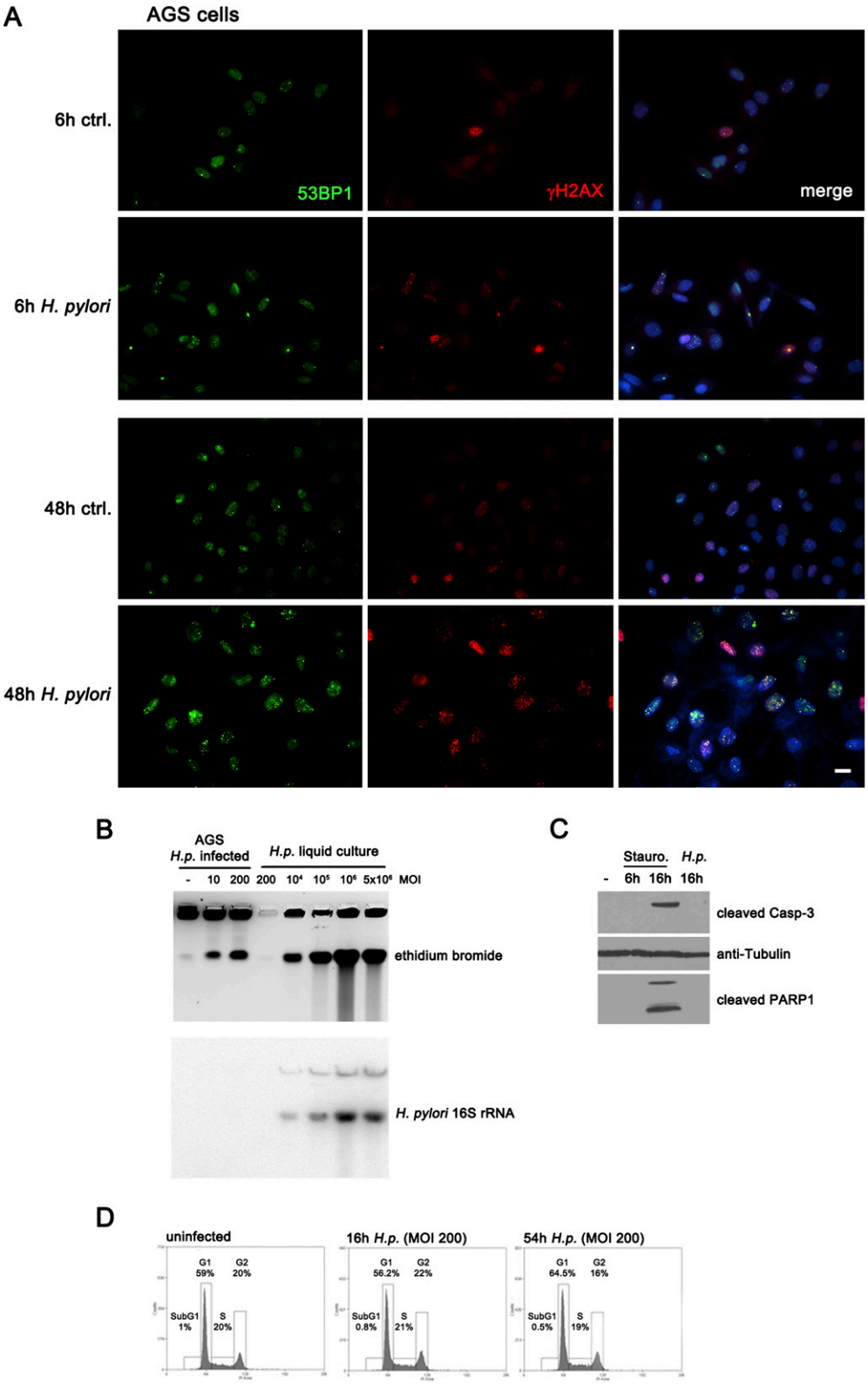

Fig. S2. The proportion of repair foci-positive cells increases over time; the fragmented DNA of infected cells corresponds neither to bacterial DNA nor to apoptotic debris. (*A*) AGS cells were infected for 6 or 48 h with *H. pylori* G27 and were stained for p53-binding protein 1 (53BP1), phosphorylated histone H2A variant X (γH2AX), and nuclear DNA. Individual and merged images are shown for every condition. (*B*) AGS cells were infected with *H. pylori* for 6 h at the indicated multiplicities of infection (MOIs). In addition, host cell-free bacterial pellets corresponding to MOIs 200, 10^4, 10^5, 10^6, and 5×10^6 were loaded. All samples were subjected to PFGE. The gel was stained with ethidium bromide (*Upper*); then the DNA was transferred to a Zeta membrane, UV cross-linked, and probed with a deoxycytidine triphosphate ($\alpha[^{32}P]$)-labeled probe detecting *H. pylori* 16S rRNA (*Lower*). (*C*) AGS cells were infected with *H. pylori* G27 for 16 h or were treated for 6 or 16 h with 5 μM staurosporine, a global tyrosine kinase inhibitor known to induce apoptosis. Immunoblots are shown for the cleavage products of poly-(ADP-ribose) polymerase 1 (PARP1) and caspase-3. Tubulin served as loading control. (*D*) AGS cells were infected with *H. pylori* G27 for 16 or 54 h. Cell-cycle distribution was assessed by propidium iodide staining. Percentages of cells in the respective cell-cycle phases are indicated. (Scale bar: 10 μm.)

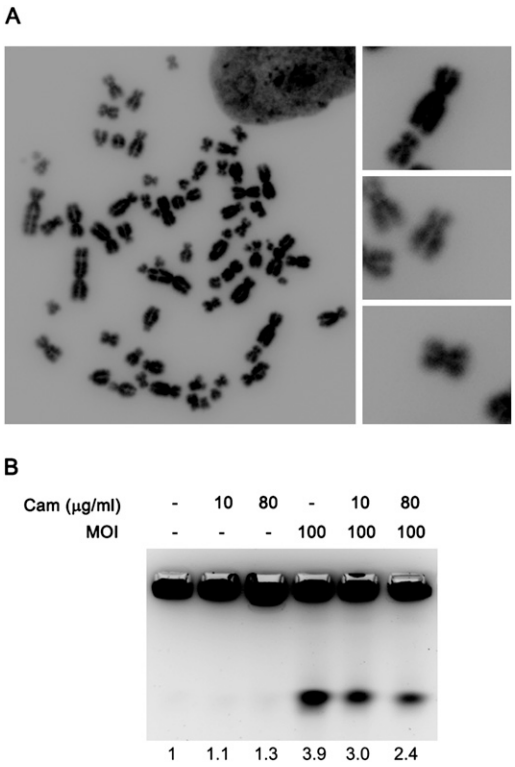

Fig. S3. Chromosome spreads from uninfected cells do not show chromatid breaks; inhibition of protein synthesis abrogates DSB induction. (*A*) Uninfected U2OS cells were processed as described in the legend to Fig. 2 *A* and *B*. A representative uninfected cell in metaphase without chromatid breaks is shown here. (*B*) AGS cells were infected for 6 h with *H. pylori* G27 at MOI 100 in the presence or absence of 10 or 80 μg/mL chloramphenicol, respectively. DSB induction was determined by PFGE. Gentamycin treatment produced similar effects. The signal intensity of the bands corresponding to fragmented DNA is indicated below the respective lanes with the untreated control set as 1.

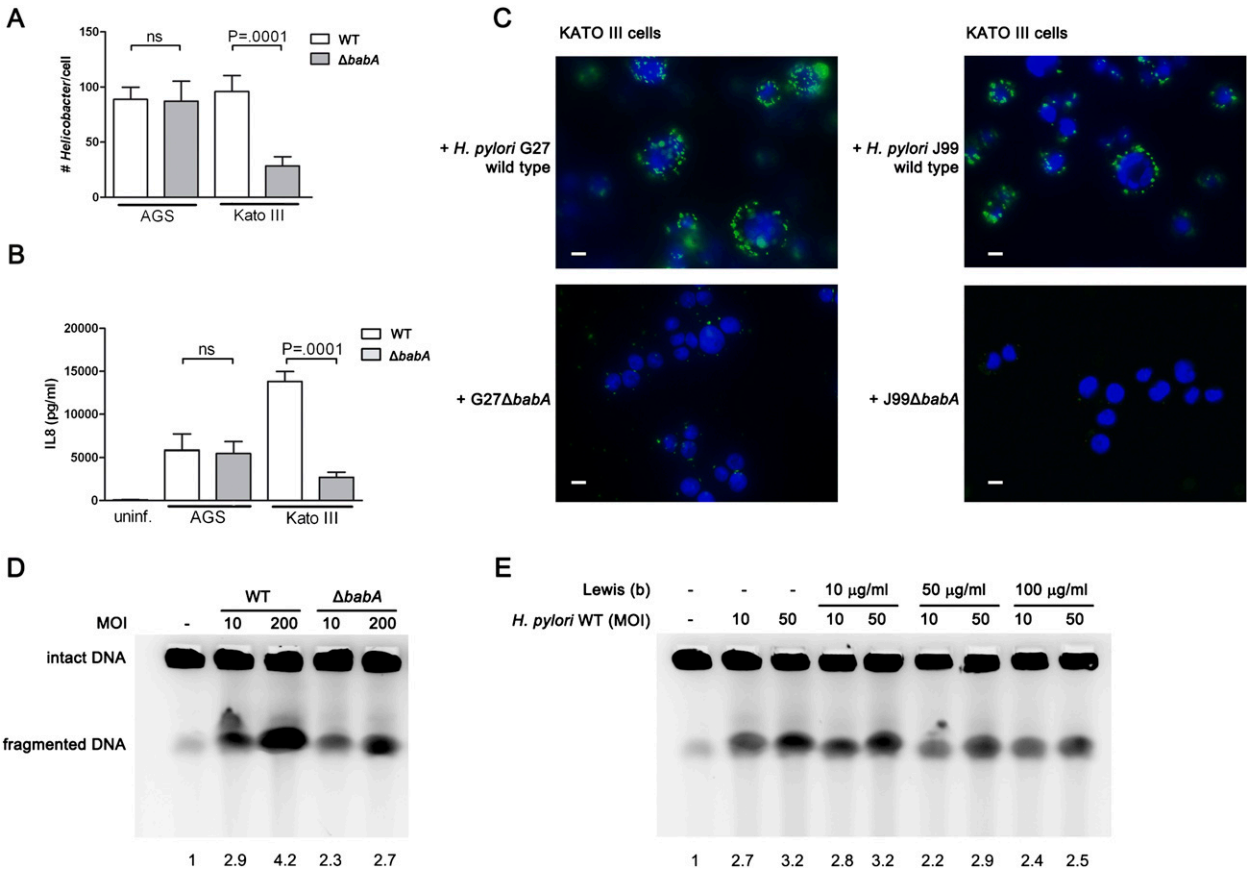

Fig. S4. *H. pylori* adheres to Kato III cells but not to AGS cells, predominantly via the blood group antigen-binding adhesin (BabA)/Lewis (b) interaction. (*A* and *B*) The gastric epithelial cell lines AGS and Kato III were infected (MOI 200) for 6 h with wild-type *H. pylori* J99 and its isogenic Δ*babA* mutant. (*A*) Adherent bacteria per cell were counted microscopically. (*B*) The culture supernatants were assessed for IL-8 production by ELISA, because IL-8 induction is an accepted readout for the biological consequences of virulent *H. pylori* infection of gastric epithelial cells. (*C*) Kato III cells were incubated with FITC-labeled bacteria of the indicated strains (wild-type G27 or J99 and their respective Δ*babA* mutants) at MOI 200; nonadherent bacteria were washed away before microscopic analysis. (*D*) Kato III cells were infected with wild-type *H. pylori* G27 or G27Δ*babA* mutant bacteria for 6 h at the indicated MOIs; DSBs were determined by PFGE. (*E*) G27 wild-type bacteria were incubated for 2 h with 0, 10, 50, or 100 μg/mL Lewis (b) in *Brucella* broth before thorough washing. Preincubated bacteria were added to the cells at the indicated MOIs; DSB induction was determined by PFGE at 6 h postinfection. In *D* and *E*, the signal intensity of the bands corresponding to fragmented DNA is indicated below the respective lanes with the untreated control set as 1. (Scale bar: 10 μm.)

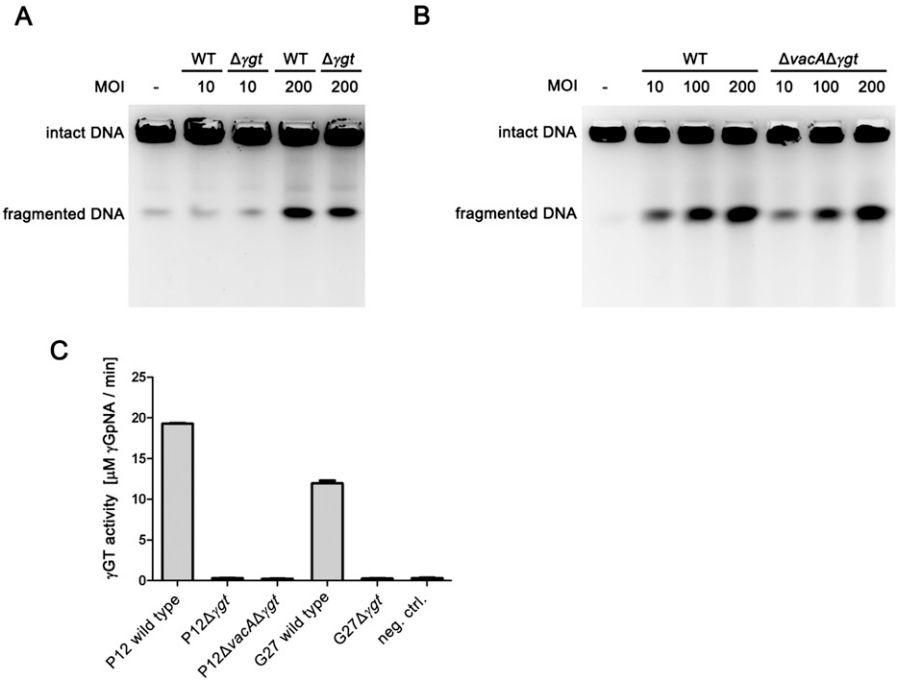

Fig. S5. The putative *H. pylori* virulence factor γ-glutamyl transpeptidase (γGT) is not required for *H. pylori*-induced DSBs. (*A*) AGS cells were infected with wild-type *H. pylori* G27 or its isogenic mutant lacking γGT (Δγ*gt*) for 6 h at the indicated MOIs. DNA integrity was assessed by PFGE. (*B*) AGS cells were infected with wild-type *H. pylori* P12 or an isogenic Δ*vacA*Δγ*gt* double mutant for 6 h at the indicated MOIs. DNA integrity was assessed by PFGE. (*C*) To quantify the enzymatic γGT activity of the four strains used in *A* and *B*, 10^9 bacteria were suspended in 500 μL PBS and incubated at 37 °C for 4 h. After centrifugation, the supernatant containing secreted *H. pylori* proteins was diluted 1:4 in reaction buffer containing 2.5 mM of L-γ-glutamyl-p-nitroanilide (γGpNA). To determine the exchange rate of the substrate to 4-p-nitroaniline, the reaction was monitored at 405 nm, and the exchange rate was calculated by using the reported extinction coefficient of 8,800 $M^{-1} \cdot cm^{-1}$. Enzymatic activity was measured in 0.1 M Tris HCl (pH 8.0), 20 mM glycyl-glycine, and 2.5 mM γGpNA. The experiments were carried out at 37 °C for 30 min using a Mithras LB940 Well-Reader. The results for a P12Δγ*gt* single mutant are shown as well.

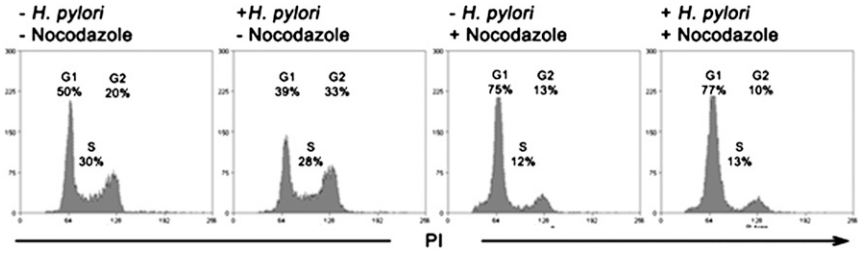

Fig. S6. Nocodazole-synchronized cells have not reentered S-phase 8 h after release from G2/M arrest. U2OS cells were arrested in G2/M by 12-h treatment with 250 ng/mL nocodazole, released for 2 h, and infected with *H. pylori* G27 for 6 h. Their cell-cycle distribution was assessed at 8 h after release from G2/M arrest, i.e., at the time when parallel wells of identically treated cells were subjected to PFGE (Fig. 3*A*). Most nocodazole-treated cells have reached G1 at 8 h after release but have not yet reentered S-phase. Asynchronous cells (infected, uninfected) are shown for comparison.

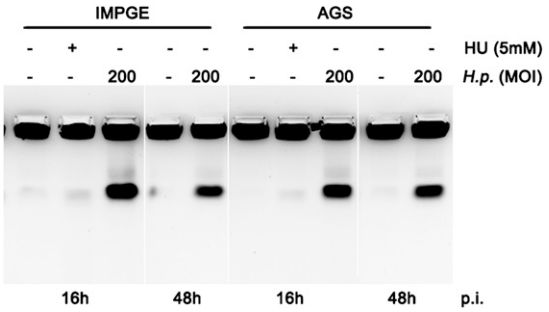

Fig. S7. *H. pylori*-induced DSBs persist for at least 48 h. Immortalized gastric epithelial cells (IMPGE) and AGS cells were infected for 16 or 48 h with *H. pylori* G27 at MOI 200. Hydroxyurea (HU) treatment (5 mM) for 16 h served as positive control. DNA fragmentation was visualized by PFGE.